A NATURALLY VENTILATED CROP PROTECTION STRUCTURE FOR TROPICAL CONDITIONS

by

REZUWAN KAMARUDDIN

Thesis Submitted in Fulfilment of the Requirements
for the Degree of Doctor of Philosophy in the
Silsoe College, Cranfield University

June 1999

Acknowledgements

The author wishes to express his sincere appreciation to his thesis committee chairman Mr. B.C. Stenning and supervisors Mr. M.P. Douglass and Dr. B.J. Bailey for their guidance, helpful advice and constructive criticisms throughout the course of this thesis and during the preparation of this manuscript.

Gratitude is also expressed to all lecturers at Silsoe College; Dr R.P. Hoxey and Mr R.P. White at Silsoe Research Institute; Dr J.I. Montero at Institut de Recerca I Technologia Agroalimentàries (IRTA), Spain; Dr P. Linden and Dr G. Hunt at DAPMT, Cambridge University who have imparted valuable knowledge to the author throughout the graduate studies.

The author is indebted to Mr. A. Hilton, Mr. D.J. Wilkinson, Mr. A.G.T. Lockwood and Mr. N.P. Teer for their help throughout the work at the Silsoe College and Silsoe Research Institute. His sincere thanks are also offered to all the organisations and individuals who directly or indirectly helped the author in carrying out this project successfully

His sincere appreciation also goes to Silsoe College, Cranfield University for offering his study and Silsoe Research Institute for providing experimental facilities. Special mention is made to the Board of Directors of Malaysian Agricultural Research and Development Institute (MARDI) for their kindness in employing him as a Research Officer and funding his studies.

Finally, the author wishes to express his utmost appreciation and love to his parents, Kamaruddin Tamat and Sarini Aseh (Allahyarhamah), his wife Siti Rukiah Ikhsan, His children M. A. Hifzuddin, H. Athirah, M. N. Aliuddin, M H. Taqiuddin, M.F. Wahiduddin and M.F. Wajihuddin, his brothers and sisters for their profound

encouragement and guidance through his course at Silsoe College, Cranfield University and Silsoe Research Institute, England.

Abstract of thesis submitted to the Senate of Silsoe College, Cranfield University as fulfilment of the requirement for the degree of Doctor of Philosophy

A Naturally Ventilated Crop Protection Structure For Tropical Conditions

by
Rezuwan Kamaruddin

Chairman: Mr. B.C. Stenning
Supervisors: Mr. M.P. Douglass and Dr. B. J. Bailey

This study presents the theoretical and experimental results of natural ventilation rates induced by stack, wind and the combination of both stack and wind effects for a typical crop protection structure suitable for the tropics. The structure consists of simple structural frame, transparent roofing and insect screen side walls. It was found the relative importance of the stack and wind effects is dependent on the ratio between wind speed and the square root of the inside-outside temperature difference ($u/\Delta T^{0.5}$). In this study, the wind effect dominates over the stack effect when the ratio $u/\Delta T^{0.5}$ becomes greater than 0.5.

Ventilation rate induced by the stack effect was found to increase with increasing temperature difference between inside and outside of the crop protection structure according to a power law, with an index of 0.5. The wind effect ventilation rate was found to increase linearly with increasing outside wind speed measured at eaves level. In addition, the combination of the stack and wind effects could be represented as the vectorial sum of two the independent effects ($\Phi_{SW} = [\Phi_{stack}^2 + \Phi_{wind}^2]^{0.5}$). However, the result of the wind effect in the combined effects was insignificant when the ratio of ventilator opening to the total wall area is higher than 20 %.

Different methods have been used to determine the natural ventilation rates. The dynamic tracer gas was used as the control; direct airspeed measurement, energy

balance and neutral plane methods were used to quantify ventilation induced by the stack effect. Pressure field measurements were used to quantify ventilation by wind effect. In addition, the dynamic tracer gas, energy balance, and stack and wind methods were used to quantify ventilation induced by the combined effects. However, these methods have their constraints and limitations because of statistically significant differences in the comparison between the methods.

The tracer gas method was found very difficult to use in the highly porous structure. In addition, the ventilation rate measured by this method was 30-40 % less than the other methods. The energy balance method has the advantage that it estimates many important climatic and crop parameters, however, the errors were found to be the highest. The neutral plane method was suitable for measuring ventilation induced by stack effect, the simplest method, requiring only the measurement of the inside and outside temperatures. The direct airspeed measurement method was much easier to handle and the result was comparable to other methods suitable for determining the ventilation induced by the wind effect.

The physical properties of the covering materials, namely light transmission, coefficient of discharge and airflow characteristics were also determined in this study. It was found that the light transmissions of transparent polythene film and insect screens were close to each other. The coefficient of discharge and light transmission were dominant parameters in the ventilation rate calculation. It was found that when air flows through a screen, the pressure drop increases linearly with the square of approach airspeed. Airflow distributions inside the crop protection structure induced by the stack and wind effects are also presented in this study. Finally, this study presents information on natural ventilation for tropical greenhouses that was not previously available.

Table of contents

List of tables

List of figures

List of plates

Nomenclature

Φ_{STG} Ventilation rate using static gas method [$m^3 s^{-1}$]

M_g Injection rate of tracer gas [$kg s^{-1}$]

C_i Internal concentration of tracer gas [ppm]

C_o External concentration of tracer gas [ppm]

C_i^1 Internal tracer gas concentration for the previous measurement [ppm]

C_o^1 External tracer gas concentration for the previous measurement [ppm]

V Volume of the greenhouse [m^3]

ρ Density of tracer gas [$kg m^{-3}$]

Φ_{DTG} Ventilation rate using dynamic tracer gas method [$m^3 s^{-1}$]

h Distance above the datum to the neutral plane [m]

Φ_{NP} Ventilation rate by neutral plane method [$m^3 m^{-2} s^{-1}$]

ΔT Temperature difference between inside and outside [K]

T_i Inside air temperature [K]

T_o Outside air temperature [K]

C_d Coefficient of discharge [no unit]

A_R Area of side ventilator [m^2]

A_S Area of roof ventilator [m^2]

P_e External wind pressure [Pa]

C_{pe} External wind pressure coefficient [no unit]

ρ_e External air density [$kg m^{-3}$]

v External wind speed at eaves height [$m s^{-1}$]

V_x Wind speed at height h_x [$m s^{-1}$]

V_o Wind speed at standard height h_o [$m s^{-1}$]

a	Exponent depends on the upward terrain [no unit]
P_i	Internal wind pressure [Pa]
C_{pi}	Internal wind pressure coefficient [no unit]
Δ_{Cp}	Pressure coefficient difference [no unit]
ΔP	Pressure difference [Pa]
m	Slope of gradient [$m^2\ s^{-2}\ Pa^{-1}$]
C_D	Coefficient of drag [no unit]
F	Force on the screen [N]
ρ	air density [$kg\ m^{-3}$]
F_o	Friction factor [no unit]
μ	Dynamic viscosity [Pa s]
ε	Porosity [no unit]
u	Superficial fluid velocity [$m\ s^{-1}$]
p	Pressure [Pa]
Y	Inertial factor [no unit]
K	Permeability [m^2]
A_T	Total area [m^2]
Φ_{WS}	Ventilation rate caused by the wind effect [$m^3\ m^{-2}\ s^{-1}$]
Φ_{SW}	Ventilation rate induced by the stack and wind effects [$m^3\ m^{-2}\ s^{-1}$]
Φ_{STACK}	Ventilation rate induced by the stack effect [$m^3\ m^{-2}\ s^{-1}$]
Φ_{WIND}	Ventilation rate induced by the wind effect [$m^3\ m^{-2}\ s^{-1}$]
g	Gravitational acceleration [$m\ s^{-2}$]
C_w	Global wind pressure coefficient [no unit]
E_V	Energy removed from the greenhouse by ventilation process [$W\ m^{-2}$]
E_S	Solar energy collected in the greenhouse [$W\ m^{-2}$]

E_C Thermal energy loss through the cover [W m^{-2}]

E_{SEN} Ventilation by sensible heat [m^3 m^{-2} s^{-1}]

E_{LAT} Ventilation by latent heat [m^3 m^{-2} s^{-1}]

L Latent heat of vaporisation of water [Jk g^{-1}]

E_{EST} Stored energy in the greenhouse [W m^{-2}]

Φ_{EB} Ventilation rate by energy balance method [m^3 m^{-2} s^{-1}]

Φ_{AS} Ventilation rate by airspeed measurement method [m^3 m^{-2} s^{-1}]

Φ_{TG} Ventilation rate by tracer gas method [m^3 m^{-2} s^{-1}]

Φ_{NP} Ventilation rate by neutral plane method [m^3 m^{-2} s^{-1}]

A_g Area of ground [m^2]

τ Light transmission of the greenhouse [W m^{-2}]

p Average reflectivity of the greenhouse contents [%]

I Total solar radiation [W m^{-2}]

U Thermal transmittance of covering materials [W m^{-2} K^{-1}]

θi Inside air temperature [K]

θo Outside air temperature [K]

M Mass per unit greenhouse area [kg m^{-2}]

θ_B External temperature [K]

θ_E Internal temperature [K]

t_E Start time [s]

t_B End time [s]

λ Latent heat of vaporisation of water [J kg^{-1}]

Wi Internal absolute humidity [kg kg^{-1}]

Wo External absolute humidity [kg kg^{-1}]

A_{CL} Area of cladding [m^2]

K_o Thermal exchange with outside air [W m^{-2} K^{-1}]

K_s Thermal exchange with the sky [W m^{-2} K^{-1}]

q_s Coefficient for the influence of the sky temperature [no unit]

$G_{CL\text{-}in}$ Thermal coupling coefficients between cladding and inside air [W K^{-1}]

$G_{CL\text{-}out}$ Thermal coupling coefficients between cladding and outside air [WK^{-1}]

$G_{CL\text{-}sky}$ Thermal coupling coefficients between cladding and sky [W K^{-1}]

Φ_o Internal air temperature [K]

Φ_s Sky temperature [K]

Φ_i Internal air temperature [K]

$F_{cl\text{-}sky}$ Fraction of sky seen from the cladding [no unit]

ϵ_{CL} Cladding emissivity for long wave radiation [no unit]

P_i Pressure inside the structure [Pa]

P_o Pressure outside the structure [Pa]

P Pressure at the neutral plane [Pa]

L Length of the structure [m]

X Integral value from ventilator opening [no unit]

C Ventilation coefficient [no unit]

λ Power law index [no unit]

n Number of samples [no unit]

σ_{n-1} Refinement standard deviation [no unit]

R^2 Coefficient of determination [no unit]

Adj.R^2 Adjusted coefficient of determination [no unit]

% Percentage [no unit]

S.E. Standard of error [no unit]

s	Variance [no unit]
$\overline{x}$	mean [no unit]
Max	Maximum value [no unit]
Min	Minimum value [no unit]
$S.E._C$	Standard error of ventilation coefficient [no unit]
$S.E._\lambda$	Standard error of power index [no unit]

Chapter 1

Introduction

1.1 Background

High value crop production in the tropics is facing high risk if conventional agricultural practices are applied. The main problems in the tropics are extreme solar radiation, uniformly high temperature, high humidity, and high rains which fall throughout the year. The mean of a typical tropical climate is shown in Table 1.1. In addition weeds, pests and diseases are also very serious problems.

Table 1.1 The mean annual of a typical tropical climate (Malaysian Meteorological Services, 1995)

Climate	**Quantity/Unit**
Temperature	21-37 °C
Rainfall	2392 mm
Humidity	55.7-97.5 %
Surface wind	1.86-21.65 m s^{-1}
Surface level pressure	1010 mb
Daily global radiation	12.17-19.23 MJ m^{-2}
Daily sunshine hour	6.3 hour
Daily evaporation	6.4 4.41 mm

Selected temperate vegetables, flowers and fruits can be grown in the hot and humid lowlands. However, the yields are generally low, poor quality and the crops are sometimes totally destroyed if conventional open farming methods are applied. In addition, the requirements for usage of pesticides, fungicides, herbicides and labour are increased. (Illias *et al.* 1992,1994 and Hawa *et al.* 1990, 1992).

Insects and diseases are the most serious problems faced by vegetable growers in Malaysia. It is estimated that 30% of vegetables are damaged by insects and 30-

40% by diseases. Losses ranging from 50-100% have been reported if infestation levels are high (Hawa *et. al.* 1990). The intensive spraying of pesticides results in high residual levels in many vegetables and causes many vegetables to be rejected after harvest as unfit for human consumption.

Heavy rainfall throughout the year will cause crop damage, difficulty of working in wet conditions, susceptibility to diseases, fertiliser loss by surface runoff and there are adverse effects of continuous cropping. In addition, hot and humid weather seem not to be conducive to crop growth and production. These conditions are more pronounced in enclosed greenhouse structures. Thus requirements of ventilation are increased.

In order to address the above problems, Crop Protection Structures have been developed in Malaysia by Malaysian Agricultural Research and Development Institute (MARDI) and other greenhouses in the tropical countries. MARDI structures are the rainshelter, the insect-proof structure and a combination of rainshelter and insect-proof structures, which are shown in plates 1, 2, 3 and 4. These structures are widely being used to solve problems and replace the temperate greenhouses which are not suitable in the tropical conditions. However, studies on the effects of the structures in producing a suitable indoor climate have not been carried out. (Yeoh 1992 and Rezuwan 1995).

Plate 1. Rainshelter structure

Plate 2. Insect-proof structure

Plate 3. Insect-proof rainshelter structure (wooden frame)

Plate 4. Insect-proof rainshelter structure (Steel frame)

Rainshelters consist of structural frames, open side walls and transparent polyethylene film roofing, while the insect-proof structure is entirely covered with polyethylene insect screen and the combination of both is called the insect-proof rainshelter (IPRS). Usually, the standard dimension and geometry of the structures are varied according to particular requirements. Improvised studies have shown that the differences between inside and outside average air temperature (min-max), soil temperature, relative humidity (8.30 a.m. - 2.30 p.m.) and shade under IPRS are 1.0-3.0 °C, 1.0 °C, 2.1-3.2% and 30-43% respectively. However, the temperature differences for temperate glasshouses and polytunnels that have been tested in the tropics is 10 - 15 °C. Consequently, these types of crop protection structures, especially the IPRS is increasingly in demand in Malaysia. (Yeoh 1992 and Rezuwan 1995)

In general high value vegetables that have been grown under those structures give 2-4 times higher yield than those grown in the open field, and the produce is of much higher quality. Plates 5, 6, 7, 8, 9 and 10 show crop production under those structures in the tropical lowlands. The use of rainshelters reduces production costs and gives growers a better income. Weed control is much easier under rainshelters and reduces weeding operations by 80-90%. Fertiliser applications are reduced by 25-30%, since the applied fertiliser is not leached away by rain. The use of foliar application of fertiliser rather than powdered or granular form in the soil doubles the yield for the same nutrient input. Under rainshelters the crops are protected from rainfall, therefore production can continue throughout the year. The incidence of insects and diseases is low so that only very minimal use of pesticides is required. In the case of insect-proof rainshelters, no chemical sprays at all are needed, so that vegetables can safely be eaten raw. Protected cultivation also enables growers to

select their planting times and crop varieties to suit market demand (Hawa *et al.* 1992).

Hence, crop production inside the insect-proof rainshelter or crop protection structure has been proven technically feasible and economically viable. However, there is little knowledge of the relationships between the structure, crop and internal climate and this needs to be known. This present study is to develop the ability to predict natural ventilation in relation to the structure and crop requirements for crop production in the tropics.

Plate 5. Capsicum grown using hydroponics system

Plate 6. Celery production

Plate 7. Chinese cabbage production

Plate 8. Tomato production

Plate 9. Cabbage production

Plate 10. Cauliflower production

1.2 Natural ventilation

Ventilation is defined as the amount of air exchange between inside and outside the greenhouse through the openings per unit time and floor area. Air exchange can be driven either by natural or forced ventilation systems. Usually, natural ventilation is induced by the stack or wind effects or a combination of both, while forced ventilation is driven by electrical fans or other mechanical means. Natural ventilation systems generally required less energy and maintenance and are quieter than forced ventilation methods.

Air exchange occurs if there is a pressure difference across the openings. Pressure differences can be created by interaction of wind with the greenhouse (wind effect) or the density difference between interior and exterior air generated by

temperature difference (stack effect). In general both the wind and stack effect occur together, but depending on the condition, one may dominate.

Ventilation is necessary to provide air exchange and good climate control in the greenhouse. It limits the temperature rise on hot days, controls excessive humidity caused by transpiration and prevents excessive depletion of the carbon dioxide concentration. Therefore, an understanding of air exchange rate is necessary because it directly effects the development and production of crops.

1.3 Scope and objective

The objective of this study is to develop an understanding of how to predict natural ventilation induced by the stack, wind and combined stack and wind effects, for the crop protection structure in tropical conditions. The important effects of ventilator area, insect screen mesh size and airflow characteristics on natural ventilation are also investigated.

The crop protection structure (insect-proof rainshelter structure) has straight side walls and tunnel roof shape with jack-roof, which has been developed by the author at Malaysian Agricultural Research and Development Institute, Malaysia. The structure is shown in the Plate 4. It is a typical single span greenhouse which is considered suitable for use in the tropics. It consists of a steel tube frame, transparent polyethylene film roofing and polyethylene insect screen cladding. Different insect screens are used in different trials as openings of air inlets and outlets.

The opening size depends on the area of insect screen that covers the structural frame, while the screen mesh in this study is the number of holes per inch. Three types of screen are used namely N50, N32 and N24. N50 means there are 50 holes per inch. In addition, the airflow characteristics across the insect screen and

airflow patterns inside the structure due to stack effect, wind effect and the combined effects are also investigated.

1.4 Outline of the thesis

Chapter 2 of this thesis presents an overview of previous investigations on natural ventilation in different types of greenhouses. It also covers theoretical considerations of various methods used to predict ventilation rate by measurement and calculation. Consideration is given to theories which can be applied in tropical conditions. A review of different measuring techniques is also presented with the description of the principle, response time, measurement range and accuracy associated with each technique.

Chapter 3 presents the measurements of physical properties of covering materials that have been used in the Crop Protection Structure. These are the transparent polyethylene sheet and three polyethylene insect screens. Parameters such as diffuse and direct light transmission at different incidence angles, material thickness, single hole area of screen mesh, coefficient of discharge and the relationship between pressure difference across the screens and the air speed are considered. In addition air flow patterns due to stack and wind effects inside the crop protection structure are also presented. Comparisons of results within the study and with other findings are also made. Some parameters from this chapter are required in ventilation rate calculations.

The contribution of the stack effect to natural ventilation is discussed in Chapter 4. Different approaches to predict natural ventilation rates by direct measurement and calculation are presented. The findings reveal which approach gives consistent and reliable results. Some important discussion is presented on the

comparison of the different methods. Improvement of equations, introduction of coefficients and constants enable the designer to predict ventilation rate by the stack effect in the tropics.

Natural ventilation induced by wind is discussed in Chapter 5. Ventilation rate as a function of the wind pressure coefficient, screen opening area, wind speed and direction are presented. Some useful information on the relationship between screened structure and natural ventilation is discussed.

Natural ventilation induced by the combination of wind and stack effects is detailed in Chapter 6. Different methods are used to quantify ventilation rate and they are compared. Important equations, coefficients and constants are revealed. The methods which give reliable and consistent results are also identified.

Finally, Chapter 7 presents the conclusions and recommendations for future research. The findings from each chapter are inter-related and contribute knowledge to predict natural ventilation for crop protection structure in the tropics.

Chapter 2

Literature review

2.1 Properties of covering materials

Optimum ventilation for crop production is essential in naturally ventilated crop protection structures. Apart from the surrounding environment, ventilation performance is also affected by properties of the covering materials. Light transmission is one important property of transparent polyethylene sheet and insect screens. However, hole area, coefficient of discharge, pressure difference and air flow characteristics are equally important for screens which cover greenhouse ventilators.

Light transmission studies on different covering materials have been conducted by many researchers. The main objectives of their studies were to develop reliable measurement methods and estimate the quantity of light received inside greenhouses, Stone (1913), Lawrence (1948) and Whittle *et al.* (1959). Boon (1973) has studied some aspects of light transmission on glass and acrylic greenhouses. He estimated the amount of specularly reflected radiation within the greenhouse. Furthermore Russell (1985) presented a mathematical analysis on light transmission through twin-walled materials. His analysis yielded general expressions for the average transmittance for light incident at any angles.

Another study on radiation transfer through covering materials, solar and thermal screens in greenhouses has been presented by Nijskens *et al.* (1985). They highlighted radiometric property measurement and calculation for the materials and then adapted them to the agronomic needs.

Kittas *et al.* (1998) have studied the spectral radiometric properties of various greenhouse covering materials in the laboratory. They used a spectroradiometer equipped with an integrating sphere. In addition, studies on fluorescent materials under natural daylight were also made. They concluded that the accurate determination of some specific parameters such as ratio of the photon flux rate, effective photosynthetic transmission and quantum transmission of materials is necessary to assess their influence on plant growth and development under greenhouse conditions.

Most of the above studies are concentrated on light transmission of transparent covering materials. No studies have been made on insect screens. In the present studies, light transmission through transparent polyethylene sheet and polypropylene screens is investigated in the laboratory to facilitate the natural ventilation calculations.

Screens reduce airspeed and so cause an air flow reduction. Knowledge of the flow reduction is important to predict screen behaviour for a specific application such as a natural ventilation system. Studies on flow reduction, such as coefficient of discharge, permeability, porosity and coefficient of drag through the screens have been conducted by some researchers. Carpenter *et al.* (1973) have presented pressure drop and air velocity curves from forty-five different permeable materials. They explained the properties of materials by fitting the data taken from a simple wind tunnel in formulated equations. Air flow through permeable materials was also studied by Bailey (1978, 1981) using a tracer gas technique. He found that the permeability of materials increased with increasing temperature difference across them.

Sakurai *et al.* (1985) have found the loss coefficients did not vary directly with the free area ratio, but implied that other factors, such as the screen construction had a significant effect on drag. Coefficient of discharge studies for screening materials have been made by Sase *et. al.* (1990). Two types of coefficients of various screens were presented; one relating pressure drop to the square of the approach velocity and the second relating the approach velocity to the square root of the imposed pressure. They claimed that the coefficient of discharge has a significant effect on the design and performance of natural ventilation systems.

The force on and static pressure drop across a screen created by airflow have been determined by Kosmos *et al.* (1993) in a wind tunnel. They found wind pressure on the screen and static pressure drop across the screen increased exponentially with increases in apparent air velocity. The properties of the screen greatly affected wind pressure and static pressure drops.

Miguel *et al.* (1997) have conducted experiments to examine the airflow characteristics of greenhouse screens and the ability to predict airflow through them. They defined the permeability and porosity of those screens based on the Forcheimer's equation.

Investigations of hole area of mesh, thickness, coefficient of discharge, pressure drop and air velocity across screens are made in the present studies. These parameters will be used to calculate ventilation rate by stack effect, wind effect and the combined effects in the next chapters.

2.2 Natural ventilation of glasshouses

Natural ventilation is considered to be one of the most important components in residential, greenhouse, animal and industrial buildings. It regulates air exchange

between inside and outside of the building environment. However, the actual quantification of the air exchange is still difficult even after a long period of study.

Ventilation studies in greenhouses started in the middle fifties. Direct measurement of air exchange in the greenhouses was made by Morris and Neale (1954). They published ventilation rates of two relatively small greenhouses with both side and roof windows. The measurements were made by the tracer gas method. However, their data had no relationship with weather conditions. Whittle and Lawrence (1960) applied the same tracer gas technique to describe a relationship between ventilation rate and wind speed in a greenhouse equipped with side and roof windows. Okada and Takakura (1973) have derived theoretical principles for the air exchange in a small greenhouse. They showed that the air infiltration rate is a sum of two terms, one proportional to the outside wind speed and the other to the square root of the temperature difference between interior and exterior air. However, the effect of wind direction was not considered in their calculation.

The first theoretical model for predicting greenhouse ventilation rate was initiated by Kozai and Sase (1978). They used physical and mathematical models to demonstrate the influence of wind speed and direction, temperature difference and opening angles of windows on natural ventilation rates. However, their studies were limited to greenhouses which had both side and roof ventilators. In large multi-span greenhouses, Bot (1983) introduced a general approach to describe the ventilation through the types of windows, opening angles and environmental factors such as temperature difference, wind speed and direction. He proposed a non-dimensional ventilation function, which gives the ventilation flux per unit ventilator area and wind speed, as a function of the opening angle. However, many empirical relations were based on model studies and full scale measurements were only carried out in a small

compartment by means of the static tracer gas technique. This technique takes a long time to reach an equilibrium. Ventilation in Bot's compartment with a small window opening was remeasured by Nedehoff *et al.* (1985) by mean of a dynamic tracer gas technique. Their experimental results agreed with Bot's findings.

Ruther (1985) studied natural ventilation rates of closed greenhouses using CO_2 and N_2O tracer gas. Results before and after sealing the greenhouse were compared and linear dependencies on wind speed and temperature difference were exhibited. No effect of wind direction on the leakage seemed to be present.

De Jong (1990) studied natural ventilation on large multi-span greenhouses. He made a series of measurements in some larger compartments and studied separately the effects of temperature difference and wind, and also the flow characteristic through the openings. In addition, Fernandez and Bailey (1992) have proposed regression models of the dimensionless ventilation function for a small Venlo greenhouse, based on full scale measurements using the dynamic tracer gas and static energy balance equation. The advantage of the energy balance model is that the energy lost and gained through structure, the plants and the air are taken into consideration.

Most of the above studies concentrated on ventilation under steady state conditions. However, the wind creates a fluctuating pressure field over the greenhouse surface. The effect of such fluctuations has been studied extensively by Robertson and Hoxey (1992). Their studies concentrated on the ability of the structure to withstand wind loads that forms one of the main requirements in a greenhouse design. They presented wind pressure coefficients of most common shapes and sizes of greenhouses. Generally the wind produces a positive pressure on the windward side and a negative pressure over the roof and lee-ward surfaces.

Sonic anemometers have been used by Boulard *et al.* (1997) for measuring internal air speeds and the speed in the window openings of several greenhouses. The same technique has also been used by Wang (1997) to measure the airflow pattern in a Venlo glasshouse. He found that the air entering occurred predominantly in the leeward part of the greenhouse, while the air exhausting occurred in the windward part. It seemed that the general internal air movement exist against the external wind direction

An innovative experimental technique using transparent scale models in a transparent water flume and a tank was carried out by Hunt and Linden (1997a, 1997b). They studied the flows in the models driven by stack and wind forces. Static salt solution in the tank and flowing fresh water in flume were used to study stack and wind effect respectively. In addition, a CCD camera and computer software were also used to digitise the images and analyse the particle tracks.

Miguel *et al.* (1998) have presented experimental and theoretical studies to predict air exchange through porous screens and window openings in glasshouses. They installed the thermal screens horizontally at the ceiling level and roof windows were opened; they showed that the theoretically predicted airflow through the screens agreed reasonably well with experimental values.

2.3 Natural ventilation of plastic houses

Natural ventilation studies on plastic houses started in the early nineties. This type of greenhouse is widely used in Mediterranean and arid regions. Seginer *et al.* (1993) have shown that a neural network can be trained to describe air exchange rates from two quite different greenhouses, a two-span, curved roof film plastic greenhouse

with continuous gutter level ventilators and a four-span pitched roof glasshouse with staggered ridge-hinged ventilators.

Ventilation studies on tunnel plastic houses have been carried out by Feuilloley *et al.* (1994). They tried to understand the problems of ventilation in Mediterranean climates and suggested a simple way to determine the dimension of the openings.

Boulard and Draoui (1995) have measured natural ventilation of a twin-span plastic houses with continuous roof vents. Then was followed by Boulard and Baille (1995) who did the same studies by simulation. Kittas *et al.* (1995-96) have again studied the ventilation in the greenhouse used by Boulard and Daroui (1995) and presented a non-dimensional ventilation function per unit of window area and per unit ground area. Measurement and analysis of air exchange in a plastic house with both continuous roof and side openings was carried out by Papadakis *et al.* (1996).

An application of Computational Fluid Dynamics to ventilation studies was presented by Mistriotis *et al.* (1997). They found that this technique has some problems related to establishing the boundary conditions and requires experimental knowledge on the flow to support the calculation. They claimed that this technique consumes time and the CFD software is expensive. More recent studies were made by Oca *et al.* (1998) on tunnel plastic houses using the same technique as Hunt and Linden (1997a, 1997b).

2.4 Natural ventilation of tropical greenhouses

Little knowledge is available on natural ventilation in the tropical greenhouses. Most of the greenhouses in the tropics are imported from the temperate

latitudes. These greenhouses are very expensive, not suitable in hot and humid tropical weather and their use is limited in research and teaching.

Commercial tunnel plastichouses have been used in the tropical lowland climate by Rault (1990) at Institut de Recherches Agronomiques Tropicales, Martinique, French Guyana. His studies was focused on reducing the temperature difference and on the structural stability under intense cyclones. He has also developed a two span wooden greenhouse. The structures have open side wall and transparent plastic roofing and can be classified as rain shelter structures. Temperature difference and light transmission were reported in his study. However, no study was been made on natural ventilation.

Some modification to temperate greenhouses and tropical version greenhouses have been made to suit local conditions by Yeoh (1992) and Rezuwan (1995) at Malaysian Agricultural Research and Development Institute. They are known as naturally ventilated crop protection structures; rainshelter, insect-proof and insect-proof rainshelter structures. Typical structures are shown in Plates 1, 2, 3, 4, 11 and 12. The main functions of these structures are to reduce temperature difference between inside and outside environment, to protect the cultivation area from heavy rainfall, insects and diseases, and as well as providing an appropriate indoor environment for high value crop production. An improvised study has shown that these structures give a better internal environment compared to those in the imported ones. However, a specific study on natural ventilation has still not been made.

Plate 11. Modified glasshouse structure

Plate 12. Modified plastic tunnel greenhouse

Crop production using soil and hydroponics cultures under the crop protection structures are increasingly in demand in Malaysia. Rainshelter structures have been used in commercial production since early eighties in the highlands and research on lowland structures was begun in 1985. From 1990 to 1995 about 20 hectare of structures were built for crop production in the low land by the author.

From the preceding review, most of the greenhouse research on natural ventilation is confined to the temperate, Mediterranean and sub-tropical regions. Very little information is available in tropical conditions. Therefore, the present studies highlight some information on natural ventilation for typical insect-proof rainshelter or crop protection structures for tropical conditions.

Natural ventilation can be quantified by using existing experimental techniques. These are direct measurements such as tracer gas decay method, pressure field and wind speed measurement or theoretical calculations. Application of these techniques must be within the budget and time constraints, however the other hand reliability of the result must not be jeopardised. Some of the experimental techniques, that are related to the present studies are presented here in term of principles, reliability and limitations.

2.5 Ventilation by tracer gas method

The use of the tracer gas technique to measure natural ventilation rate is well known and widely used. There are two main methods of measuring ventilation rate using tracer gases. These are the continuous injection method or static method, and the pulse injection method or dynamic method. For the static method, gas is injected into the greenhouse at constant rate until an equilibrium state is reached. According to Geodhart *et al.* (1984), the gas supply and sampling system system must be

branched in order to obtain good dispersion of the gas and uniform sampling of air. The ventilation rate is calculated from Bailey *et al.* (1993).

$$\Phi_{STG} = \frac{M_g}{\rho(C_i - C_o) - \left(\frac{V}{dt}\right)\left[\ln\frac{(C_i^1 - C_o^1)}{C_i - C_o}\right]} \tag{2.1}$$

where Φ_{STG} is the ventilation rate using static tracer gas method ($m^3\ s^{-1}$), M_g is injection rate of tracer gas (kg s^{-1}), ρ is the density of tracer gas (kg m^{-3}), C_i is the internal concentration of tracer gas (ppm), C_o is the external concentration of tracer gas (ppm), C_i^1 is the internal concentration of tracer gas for the pervious measurement (ppm), C_o^1 is the external concentration of tracer gas for pervious measurement (ppm), V is the volume of the greenhouse (m^3) and dt is the time interval between measurement (s).

In the dynamic tracer gas method, the tracer gas is injected and distributed uniformly in the greenhouse until a certain predetermined concentration is reached and then stopped. The decay of the concentration of the tracer gas is then measured. When the concentration has decreased to 80-90 % of the initial value, another pulse of gas is injected and then the decay is again measured. This method is the most common one and requires the simplest apparatus, and has been used by many researchers such as Okada and Takakura (1973), Geodhart *et al.*, (1984), Ruther (1985), Nederhoff *et al.* (1985), De Jong (1990), and Fernandez and Bailey (1993). The ventilation rate can be calculated using a simplified continuity equation as given by;

$$\Phi_{DTG} = \frac{V}{dt} \ln \frac{C_i(t) - C_o}{C_i(t_o) - C_o} \qquad (2.2)$$

where Φ_{DTG} is the ventilation rate using dynamic tracer gas method ($m^3 s^{-1}$), C_i (t) is the internal concentration of tracer gas at any time t (ppm), C_o is the external concentration of tracer gas (ppm), C_i (t_o) is the internal concentration of tracer gas at the initial time (ppm), V is the volume of the greenhouse (m^3) and dt is the time interval between measurement (s).

A plot of concentration versus the logarithm of time gives a straight line if the tracer gas is uniformly distributed throughout the volume and the air exchange is constant during the measurement. The air exchange rate is obtained from the gradient of the linear regression. The advantage relative to the continuous method is that the decay method uses less tracer gas and can be used to measure over a wide range of ventilation rates while the continuous method requires an appropriate flow meter.

Selection of the tracer gas for the two methods is very important. Many gases have been used as a tracer gas like sulphur hexafluride (SF_6), methane (CH_4), carbon dioxide (CO_2), nitrous oxide (N_2O), argon 41 and krypton 85.

Geodhart *et al.* (1984) have suggested that the tracer gas has to meet the following requirements; easy to measure at low concentration, inert, not toxic, not flammable, not a natural component of air and a molecular weight close to the average weight of air. If the tracer used is not inert a correction factor in the formula had to be included.

In order to measure the tracer gas decay, the measuring system must have a system for supplying and sampling the tracer gas, an infra-red gas analyser to measure the gas concentration, sensors to measure the external factors that influence ventilation and a data logging system to record data. According to Dufton *et al.*

(1942), Hitchin *et al.* (1967) and Ducarme *et al.* (1994), air exchange measured by tracer gas is not the real one, it based on the assumption of a perfect proportionality between the flows of air and gas. They noted that if the mixing is 'perfect', one air change changes about 60 - 70 % of the room air.

2.6 Ventilation by stack effect

Natural ventilation is the movement of air through greenhouse openings by natural pressures produced by temperature difference, wind force or combination of both effects. According to Bot (1983) and Wang (1998), if there is no wind or the wind speed less than 1 - 2 ms^{-1}, temperature difference (stack or buoyancy effect) will dominate the natural ventilation. In addition, the combined effects dominate natural ventilation when wind speed is less than 4 ms^{-1}.

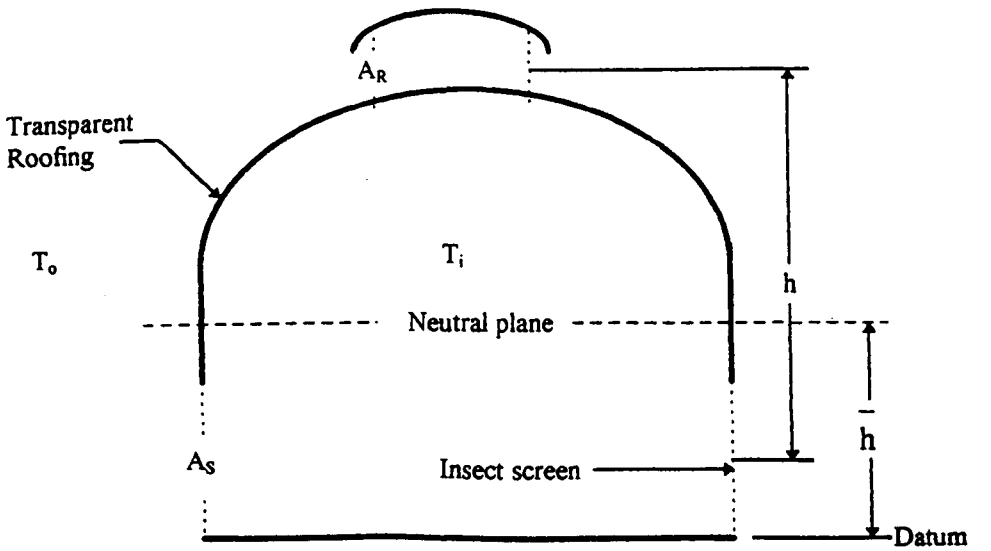

Figure 2.1 Cross-section of a crop protection structure

A general theory of natural ventilation by temperature difference or the stack effect was published by Bruce (1978). His theory can be applied to any openings in any enclosure and any building geometry. It assumes that the air is an ideal gas, that

there are no density difference between the inside and outside of the enclosure, and that the density difference between the inside and outside of the enclosure is small. For every enclosure with one or more openings and with a lower density inside than outside, there will be a neutral plane, such that the air below the neutral plane will be drawn in and the air above will be exhausted. The position of the neutral plane for any enclosure with n openings can be predicted by solving the following equation for $\bar{h}$;

$$\sum_{i=1}^{n} \int_{A_i} \frac{|\bar{h} - h|^{\frac{3}{2}}}{\bar{h} - h} dA = 0 \qquad (2.3)$$

where $\bar{h}$ is the distance above the datum to the neutral plane (m) and h is the distance above a reference datum plane (m). After the position of the neutral plane has been calculated, the ventilation rate can be determined by solving the equation;

$$\phi_{NP} = C_d \left(\frac{2g\Delta T}{T_o} \right)^{\frac{1}{2}} \sum_{i=1}^{n} \int_{A_i(\bar{h})} \frac{|\bar{h} - h|^{\frac{3}{2}}}{\bar{h} - h} dA \qquad (2.4)$$

where ϕ_{NP} is ventilation rate by neutral plane approach ($m^3 s^{-1}$), g is the gravitational constant (9.81 m s^{-2}), ΔT is difference between inside and outside air temperature (K) and T_o is outside air temperature (K). If the greenhouse has roof and side opening as shown in Figure 2.1, then integrating equation 2.4 gives;

$$\Phi_{NP} = C_d \left(\frac{A_R A_S}{\sqrt{A_R^2 + A_S^2}} \right) \left(2g \frac{\Delta T}{T_o} h \right)^{\frac{1}{2}} \quad (2.5)$$

where A_S and A_R are the area of side and roof openings respectively (m^2) and h is the vertical distance between the midpoint of side and roof openings (m). The advantage of the temperature effect approach in predicting natural ventilation by measuring temperature difference inside and outside of the greenhouse is simplicity and cheapness.

2.7 Ventilation by wind effect

When wind flows around a building, its creates pressure on the building. Generally, positive pressures (relative to atmospheric pressure in the undisturbed flow) arise wherever the wind must decelerate and negative pressure (suction) arises wherever the air must accelerate or the flow separates. The constantly changing nature of wind (gustiness) causes an ever changing pressure field to exist around a building. However, for analysis purposes, constant and steady wind pressures are usually assumed.

The pressure distribution may be represented as a distribution of the pressure coefficient, which is defined as the ratio of actual gauge pressure at a point on a building, divided by the stagnation pressure of the wind, where the stagnation pressure is determined using the Bernoulli equation,

$$P_e = C_{pe} \frac{1}{2} \rho_e v^2 \quad (2.6)$$

where P_e is the external wind pressure relative to the undisturbed flow (Pa), ρ_e is the external air density (kg m^{-3}), C_{pe} is the external wind pressure coefficient (dimensionless) and V is the windspeed at eaves height (m s^{-1}). Pressure coefficients for wind effects are generally determined based on the wind velocity at eaves height. If the wind is not at the eaves height, a correction can be made by;

$$V_x = V_o\left[\frac{h_x}{h_o}\right]^a \tag{2.7}$$

where V_x is the windspeed at height h_x (m), Vo is the wind speed at the standard height (h_o) and a is the exponent whose value depends on the upwind terrain. According to Albright (1990), for most agricultural applications, values of a between 0.20 and 0.28 are appropriate. When wind flows across a building which has a number of vents, the internal air pressure can be expressed as equation 2.8;

$$P_i = C_{pi}\frac{1}{2}\rho_i v^2 \tag{2.8}$$

The indoor wind pressure coefficient C_{pi} is defined in a manner parallel to C_{pe}, as the ratio between the existing indoor gauge and the wind stagnation pressures and is affected by the external pressure coefficients and the sizes of the openings. Bruce (1974,1975) and Albright (1990) derived the velocity equation for air moving through an inlet opening, based on the definitions of the pressure coefficients, Bernoulli's equation and the two pressure differences;

$$V_n = V \frac{(C_{pe} - C_{pi})}{\sqrt{|(C_{pe} - C_{pi})|}} \qquad (2.9)$$

Finally, the flow rate through the inlet openings ($m^3 s^{-1}$)is given by;

$$\Phi_w = \sum_{i=1}^{n} V_n A_n \qquad (2.10)$$

Natural ventilation rates can be calculated by measuring wind at eaves level and pressure difference between inside and outside the greenhouse. Wind is usually defined by two magnitudes that are the direction from which it blows and its speed. The devices to be selected for wind measurement depend upon the experimental objectives. Above the greenhouse structure, various types of cup or windmill (propeller) anemometers are commonly used, while in close proximity the hot wire anemometer is often selected.

Hot wire anemometers can measure the variables occurring in turbulent flows, such as mean and fluctuating air speed. According to Tanner (1963) most mechanical anemometers can measure wind speed above a low starting threshold in the range of 0.15 to 0.7 m s^{-1}. However, Simmons (1949), Benseman *et al.* (1959) and Krishnaswamy (1963) have used thermal hot wire anemometers that can measure low airspeed down to 0.003 to 0.03 m s^{-1}.

Natural ventilation rate calculations by wind effect also require the pressure difference between the inside and outside of the greenhouse. Pressure tappings connected to the transducers have been used to get the external surface pressure of the greenhouse and the internal pressure coefficients. Generally, this pressure is a

function of wind speed, direction and time. Pressure difference can also be measured using a pitot tube. Since it lacks the sensitivity for very small pressure drops, it is now largely replaced by electronic transducers, which are small, sensitive, portable and cheap.

2.8 Ventilation by stack and wind effects

In the previous studies, theories are well developed for cases in which only thermal buoyancy or only wind exist. When there is no wind, buoyancy provides the minimum ventilation rate which is critical in the design of naturally ventilated greenhouses. For cases when the wind speed is relatively large, the contribution of thermal buoyancy to the total ventilation rate can usually be neglected compared to that of the wind effect. However when both contributions are comparable with each other (for example, when wind speed is low), both must be considered for calculating the ventilation rate and inside temperature.

ASHRAE (1989) has recommended a simple method for estimating the total airflow due to the combined stack and wind effects by square root of the sum of the square of stack effect and the square of the wind effect (add through quadrature). Brockett *et al.* (1987) developed a theoretical description of combined natural ventilation. They used their description to calculate airflow rates in a natural ventilation control model for adjusting sidewall openings. Zhang *et al.* (1989) presented a model of natural ventilation by combining wind and thermal buoyancy effects based on established theoretical work. He found that his model gave good agreement with measured data for the inside temperature of a swine barn.

The above studies are confined to animal buildings and few have been made on greenhouses. Kittas *et al.* (1996) have developed an air exchange rate model by

combining stack and wind effects on the greenhouse with ridge and side openings. Their model was validated by comparison with experimental data. They concluded that both effects are dependent on the total area of openings, but the temperature effect depends also on the ratio of ridge to side openings and the wind effect is related to the global wind effect coefficient. However, the wind effect dominates the stack effect in their experiment when the ratio between wind velocity and the square root of the inside-outside temperature difference is more than one.

Boulard *et al.* (1995) have combined the stack and wind effects as the algebraic sum which implies the hypothesis that the resulting flux is the sum of two independent fluxes;

$$\Phi_{SW} = \Phi_{STACK} + \Phi_{WIND} \qquad (2.11)$$

where Φ_{STACK} and Φ_{WIND} is ventilation flux by stack and wind effects respectively ($m^3 s^{-1}$). When the flow is driven by the pressure field equal to the sum of the two independent (stack and wind) pressure fields, Zhang *et al.* (1989) have suggested the vectorial sum as;

$$\Phi_{SW} = \sqrt{\Phi^2_{STACK} + \Phi^2_{WIND}} \qquad (2.12)$$

Based on steady wind pressure, ventilation rate by stack and wind effects can be calculated from combination of equation 2.5, 2.9 and 2.12 and we have;

$$\Phi_{sw} = C_d \left[\left(\frac{A_R A_S}{\sqrt{A_R^2 + A_S^2}} \right)^2 \left(2g \frac{\Delta T}{T_o} h \right) + \left(\frac{A_T}{2} \right)^2 \frac{C_{pe} - C_{pi}}{\sqrt{|(C_{pe} - C_{pi})|}} V^2 \right]^{\frac{1}{2}} \quad (2.13)$$

However, wind turbulence in the wind effect was considered by Kittas *et al.* (1997). He calculated a global wind pressure coefficient C_w by fitting measured data (tracer gas technique) in the model equation. He included the turbulence effect in the equations 2.5, 2.9 and 2.12 as follows;

$$\Phi_{sw} = C_d \left[\left(\frac{A_R A_S}{\sqrt{A_R^2 + A_S^2}} \right)^2 \left(2g \frac{\Delta T}{T_o} h \right) + \left(\frac{A_T}{2} \right)^2 C_w V^2 \right]^{\frac{1}{2}} \quad (2.14)$$

The procedures and instruments that have been used to measure climatic parameters in calculating ventilation rates by stack and wind effect as in the sections 2.7 and 2.8 can be applied in this section.

2.9 Ventilation by energy balance method

The energy balance method can be used to calculate natural ventilation rate. Ventilation removes energy and water vapour from the greenhouse and contributes to its energy and water balance. The flow of energy through a greenhouse is illustrated in Figure 2.2.

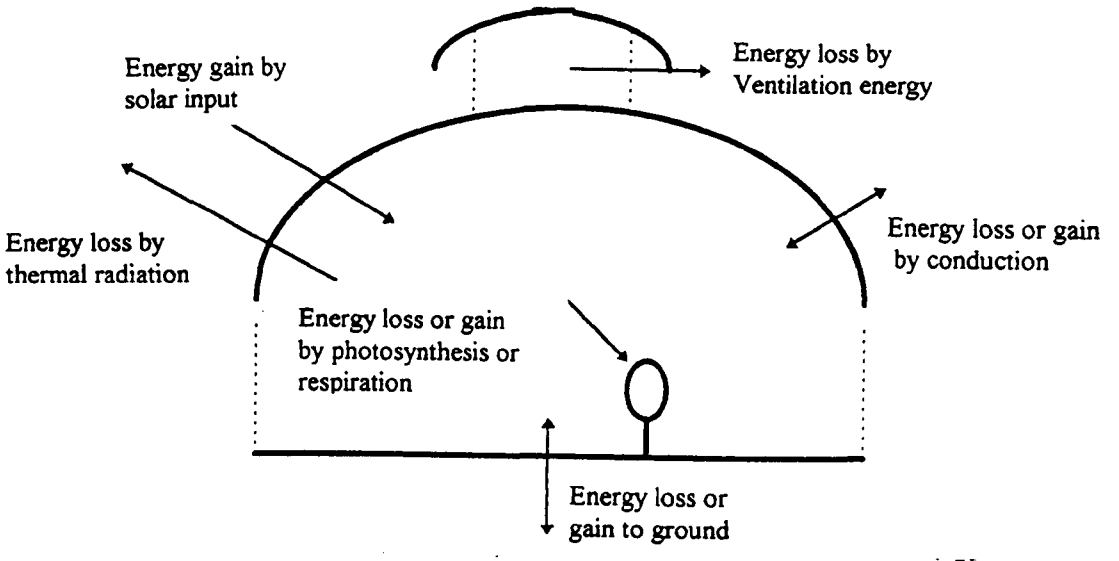

Figure 2.2 Energy losses and gain in a ventilated greenhouse

The energy balance method uses either a static or a dynamic model to calculate the air exchange rate. Morris (1964) and Chiapale *et al.* (1981) have presented the basic static models to estimate energy consumption from the total thermal losses. Then, the improved version of this basic static model was presented by Hurd *et al.* (1981) and Breuur *et al.* (1985). They included solar contributions but the precision was very limited. A recent improved static model was revealed by Fernandez and Bailey (1992) to estimate the ventilation rate of a greenhouse that interacted thermally with air, plants, soil and roof. Its energy balance equation, expressed per unit floor area, is given by;

$$E_v = E_s - E_c - E_{sr} \qquad (2.15)$$

where E_V is the energy removed from the greenhouse by the process of ventilation (W m^{-2}), E_S is the solar energy collected in the greenhouse (W m^{-2}), E_C is the thermal losses through the cover of the greenhouse (W m^{-2}) and E_{ST} is the stored energy in the greenhouse (W m^{-2}). These individual energy fluxes can each be formulated by its own equation. Fernandez and Bailey (1992), and Bot *et al.* (1995) have presented the final equation for ventilation rate calculation by energy balance as follows;

$$\Phi_{EB} = \frac{A_g}{\rho} \cdot \frac{\left[(\tau(1-p)I) - \left(U\frac{A_{CL}}{A_g}(\theta_i - \theta_o)\right) - \left(\frac{MC_P(\theta_B - \theta_E)}{t_E - t_B}\right)\right]}{\left[\lambda(W_i - W_o) + C_P(\theta_i - \theta_o)\right]} \qquad (2.16)$$

where Φ_{EB} is the natural ventilation by the energy balance method (m^3 m^{-2} s^{-1}), A_g is the ground area (m^2), τ is the light transmission of the greenhouse (W m^{-2}), ρ is the density of air (kg m^{-3}), p is the average reflectivity of the green house contents, I is the total solar radiation (W m^{-2}), U is the thermal transmittance of the covering materials (W m^{-2} K^{-1}), A_{CL} is the covering area (m^2), θ_i and θ_o are inside and outside temperatures respectively (K), M is the mass per unit greenhouse area (kg m^{-2}), θ_B and θ_E are the temperatures (K) of the component at the beginning and at the end of the experiment respectively, t_B and t_E are the start and end times of the experiment respectively (s), C_p is the specific heat of air (J kg^{-1} K^{-1}), λ is the latent heat of vaporisation of water (J kg^{-1}) and W_i and W_o are the absolute humidity of internal and external air (kg kg^{-1}).

Due to their simplicity and suitability for use over long periods, the static models have been chosen in these present studies. The advantages of this method, its include many parameters such as light transmission, absolute humidity, temperature

difference, covering properties, etc., in the ventilation rate calculation. The instrumentation such as pyranometer, pyrradiometer, capacity hygrometer, thermisitor, radiation thermometer and condensation hygrometer can be used to measure solar radiation, total radiation, relative humidity, soil temperature, cover temperature and dew point respectively. In addition, data logging computer system is also needed.

Dynamic models were introduced by Businger (1963) and Walker (1965), and then improvement were made by Takakura *et al.* (1971), Kindelan (1980), Van Bavel *et al.* (1981), Bot (1983), Deltour *et al.* (1985), De Halleux *et al.* (1989) and Wang *et al.* (1990, 1993). Generally, they have developed a dynamic climate model that can predict energy needs and also give details of the greenhouse interior climate.

2.10 Conclusions

From the above review, it was found that no specific study has been made on naturally ventilated crop protection structures in the tropics. The tropical greenhouse is a heat dissipation type, while temperate greenhouses conserve heat in the cold weather. Natural ventilation studies on greenhouses in the temperate and Mediterranean regions have been conducted by many authors. Little information has been provided on screened greenhouses. Thermal or shade screens are normally used in temperate climates for heat conservation as well as to protect the crop from extreme solar radiation and insects. Usually, these screens are horizontally spread at ceiling level in the glasshouses. The difference between the present study and the previous studies are; the specific insect screen entirely covers the vertical side walls, the height between side and roof openings is high, and this provides a highly porous

structure in which it is very difficult to measure the ventilation rate by stack, wind or the combined effects.

Ventilation rates can be quantified by measurement or calculation. Even though the existing methods have some constraints and limitations, they can be used in the tropics with some improvement or modifications. Tracer gas, energy balance, neutral plane, direct airspeed and wind speed methods have been identified to be used in the present studies. These methods will provide ventilation rates due to stack effect, wind effect and the combination of both effects.

The properties of covering materials such as light transmission, coefficient of discharge, coefficient of drag, air flow characteristics and air exchange through the screens have also been studied by many authors. However, only light transmission, coefficient of discharge and air flow characteristics are stressed in this study to facilitate the ventilation calculations. In addition, some information on reliability and accuracy of the instrumentation which can be used is given in this study.

Chapter 3

Properties of covering materials

3.1 Introduction

Crop protection structures in the tropics consist of structural frames and covering materials. Transparent polyethylene films and polyethylene insect screens are frequently used for the roofing and side wall cladding respectively. The function of the film is to provide solar radiation transmission and to protect the crop from rainfall. The insect screen permits ventilation and will exclude the pests and insects from entering.

The covering material properties are needed in the greenhouse structural design and to quantify the natural ventilation rate induced by different effects. However, these properties are always not available by the manufacturers and in the standard code of practices. Therefore, measurements of the covering material properties are essential.

The aims of the present studies are to determine some of the important properties of the transparent polyethylene film and polyethylene insect screens. Emphasis is given to the properties that can be used to predict the natural ventilation rate caused by the stack effect, wind effect and the combination of stack and wind effects described in the preceding chapters.

3.1.1 Light transmission

High light transmission through greenhouse covers is one of the important parameters required for crop photosynthesis. Studies of light transmittance through the covering materials have been made in the laboratory and also on greenhouses by

many researchers. Stone (1913) measured light transmission in the glasshouses using a photo-chemical method. He found that about 82% light transmission was received by the floor of that glasshouse.

Lawrence (1948) used photo-voltaic type photometers to measured light intensity in twelve research and commercial glasshouses. He found that luminuous flux density in the average glasshouse was often only 50 % of that outside. A study on natural illumination in glasshouses that differed in size and orientation was made by Whittle *et al.* (1959). They used photometers to measure light transmittance and concluded that the transmission was affected by the orientation of the glasshouse. In winter the east-west orientation gave higher light transmision compared to a north-south one.

Some aspects of light transmission of glass and acrylic greenhouses were studied by Boon (1973). He developed a theory for the computation of spectral reflection within a greenhouse of radiation from the sun. Another study for twin-walled materials was presented by Russell (1985). He produced a general expression for calculating the average of light transmittance at any incident angle.

Determination of the spectral properties of several greenhouse cover materials and evaluation of specific parameters related to plant response have been made by Kittas *et al.* (1998). They measured spectral radiometric properties in the laboratory using a spectroradiometer equipped with an integrating sphere and for fluorescent materials, the transmission was determined outdoors, under natural daylight. They concluded that the accurate determination of some specific parameters such as the ratio of the photon flux rate, effective photosynthetic transmission or quantum transmission for selective or fluorescent materials is necessary to assess their influence on plant growth and development under greenhouse conditions.

Thermal screens used in glasshouses at night can reduce the heat loss by between 35 and 60 %. Bailey (1981) and Nijskens *et al.* (1985) have studied radiation transfer through thermal screens in greenhouses. They described the methods used to measure transmittance, absorptance and transmittance of the screens, and presented results for potential thermal screen materials.

3.1.2 Coefficient of discharge

Screens have been reported to be an efficient method for reducing the entry of pests into greenhouses, and hence for reducing the number of pesticide treatments (Berlinger *et al.*, 1991; Baker and Shearin, 1994; Roberts *et al.*, Ross and Gill, 1994). Several commercial insect screens are available for this purpose. According to Ross *et el.* (1994) greenhouse whitefly and thrips require screens with holes smaller than 288 μm and 192 μm respectively for their exclusion.

To decide which screen to apply to a greenhouse, it is necessary to know the maximum size of opening that can be tolerated in the screen to exclude the target insects. In addition the screen should not restrict the area necessary to obtain the desired air exchange rates. Baker *et al.* (1994) revealed that the size of the mesh affects the pressure drop across the screen, the air exchange rate, energy consumption by fans and temperature in the greenhouse.

As air flows through the screen a static pressure drop occurs across it. Brundrett, 1993 and Teitel *et al.* (1998) have studied the pressure drop across the insect-proof screens. They found that the pressure drop was a function of the upstream velocity, the air density and a pressure loss coefficient. The latter is a function of the screen porosity and the Reynolds number.

Several studies have been made on the flow through the different screens for agricultural activities. Bailey (1978) has investigated the air flow through glasshouse thermal screens. He found that the permeability of all screens increased with increasing temperature difference across them, the dependence being greater the higher the material permeability.

Kosmos *et al.* (1993) tested screens used in agriculture to determine the force on them and the static pressure drop across them. They found that the wind pressure on a screen and the pressure drop across it increased exponentially with increasing apparent air velocity. In addition, the fabric density and configuration greatly affected the pressure drop.

Sase *et al.* (1990) determined the coefficient of discharge for several selected screen materials for use in greenhouse applications. They found that for all the materials tested the pressure drop varied linearly with the square of the approach velocity. Kosmos *et al.* (1993) determined the force and static pressure resulting from airflow through screens. They found the wind pressure on screens and static pressure drops across screens increased exponentially with increasing approach air velocity. The coefficient of drag was unstable at lower approach air velocities but tended to stabilise to a constant value for the higher velocities through each screen.

Miguel *et al.* (1997) used porous media flow analysis to characterise airflow through thermal, shading and insect screens. Instead of using the discharge coefficient for characterising the screens, they used porosity and inertial factors, and concluded that the use of a discharge coefficient is appropriate only when $Re > 150$.

Experiments on a small scale greenhouse model were carried out by Montero *et al.* (1997), who measured the discharge coefficients of screens installed on continuous roof openings. Three types of screens with different hole sizes were tested.

They found that the discharge coefficients decreased as the hole size decreased and that windows equipped with anti-thrips screens had a discharge coefficient approximately half those of the same windows without screens. In this study, coefficient of discharge was measured to facilitate natural ventilation rate calculation in the preceding chapters.

3.1.3 Airflow patterns

Airflow patterns in ventilated enclosures have been derived a variety of ways. Four relevant approaches have been used by many authors to determine the airflow distribution inside buildings. There were studies of air jets in both free and confined space, using of air or water with models, measurements made in full scale buildings and using Computational Fluid Dynamics (CFD).

Duncan and Hamilton (1969) described the direction of airflow in the vents of glasshouse. Air flow patterns with artificial heating and a low level of ventilation of a full scale glasshouse have been reported by Dufton *et al.* (1942). In addition, the patterns in a number of greenhouses with various fan ventilation systems were made by Wolfe *et al.* (1972). They found that the air flow was influenced by air inlet and outlet configuration, roof shape, and presence of crop or other resistance.

Hunt and Linden (1997) observed air flow pattern induced by combined stack and wind effects at small scale in laboratory models of room buildings. They claimed that the results obtained from small-scale were similar to those at full-scale. Mistriotis *et al.* (1997) used CFD to observe air flow patterns of single span greenhouse. They claimed that airflow pattern generated by CFD programme had reasonably good correlation and concluded that CFD can be used to provide a good representation of reality.

3.2 Principal considerations

3.2.1 Direct and diffuse light transmission

Global solar radiation comprises beam radiation received directly from the sun and diffuse radiation from the hemispherical sky vault. The radiation received at the surface of the earth varies with latitude, the times of the year and day. Not all the radiation incident on a greenhouse is transmitted to its interior, some is reflected and absorbed by the cover and structure. The ratio of the solar irradiances on horizontal surfaces inside and outside the greenhouse is known as the light transmission of the greenhouse. This depends on the detailed design of the greenhouse and on the covering material, but it is also influenced by latitude, the orientation of the greenhouse and it varies through the day and over the year (Bot, 1983).

Radiation emitted by the sun is commonly used to indicate energy transfer by electromagnetic waves. Two wave length regions are important for the greenhouse climate; first the shortwave, solar irridiation with wavelengths between about 400 to 700 nm and the second that of the longwave, thermal radiation with wavelengths between about 5.0 and 60 μm. The shortwave irridiation is called photosynthetically active radiation (PAR) which is important for photosynthesis for greenhouse production. However, the long wavelength radiation is not required by plants and has to be shielded by an opaque covering materials.

When the radiation strikes a body, it can be absorbed, reflected or transmitted through the body. The fractions of the radiation absorbed, reflected and transmitted are as follow;

$$\alpha + \rho + \tau = 1 \qquad (3.1)$$

where α is the absorptivity, ρ is the reflectivity, and τ is the transsmissivity. A real body absorbs less radiation than a black body at the same temperature and it also emits less radiation. A black body is a perfect emitter and absorber of thermal radiation. Kirchoff's law states that the emissivity (ε) of a real surface is equal to the absorbtivity for radiation of same wavelength. The values of emissivity, transmissivity and reflectivity depend on the material and the wavelength of radiation. For example, the transmissivity of glass is close to 0.9 for photosynthetically active radiation, but is almost zero for infrared radiation. The emissivity of a material depends on its temperature and surface finish.

Greenhouse covering materials must favour the penetration of sun radiation and counteract inner thermal radiation loss. The incident energy comes both from direct sun radiation and from sky vaults diffused radiation. According to Nijskens *et al.* (1985), the transmittances and reflectances are monochromatic biangular or angular hemispherical. The angular hemispherical transmittances and reflectances for a precise radiation source can be defined by integrating the angular hemispherical monochromatic results of the primary measurements on the characteristic spectral density of the same source.

$$\tau_{x,\phi} = \frac{\sum_{\lambda} \tau_{\lambda,\phi} E_x(\lambda) \Delta\lambda}{\sum_{\lambda} E_x(\lambda) \Delta\lambda} \tag{3.2}$$

$$\rho_{x,\phi} = \frac{\sum_{\lambda} \rho_{\lambda,\phi} E_x(\lambda) \Delta\lambda}{\sum_{\lambda} E_x(\lambda) \Delta\lambda} \tag{3.3}$$

where τ is the transmittance (%), ρ is the reflectance (%), E is the spectral density of a black body (W m^{-2} μm^{-1}), λ is the wave length (μm), x stands for the type of radiation considered (direct or diffuse) and ϕ specifies the angle of incidence.

3.2.2 Coefficient of discharge

When air moves through a screen, the screen creates a resistance to the flow and a static pressure drop develops across the screen. These phenomena make the actual airflow reduce and can be expressed in the ventilation equation as a coefficient of discharge. The coefficient of discharge is the product of the coefficients of velocity and contraction: both of which are 1.0 or less in value. It is also a function of inlet type and design. It can be expressed in the form of Euler-like relation,

$$\Delta P = \frac{1}{2} F_o \rho V^2 \tag{3.4}$$

and

$$C_d = \frac{1}{\sqrt{F_o}} \tag{3.5}$$

where ΔP is the static pressure drop across the screen (Pa), F_o is the friction factor (dimensionless), ρ is the air density (kg m^{-3}), V is average air velocity through screen (m s^{-1}). Sakurai *et al.* (1991) and Kosmos *et al.* (1993) have formulated the coefficient of drag (C_D) which allows the calculation of force applied on screen at any flow given by;

$$C_D = \frac{2F}{\rho A V_a^2} \tag{3.6}$$

where F is the force on the screen (N), ρ is the air density (kg m^{-3}), A is the total area occupied by screen material (m^2), V_a is approach air velocity through screen ($m^3 m^{-2} s^{-1}$) and C_D is dimensionless number that depends on the shape of the object in the fluid stream and the Reynolds number.

3.2.3 Air flow characteristics through a screen

Miguel *et al.* (1998) derived the motion equation for one-dimensional mass transfer through a permeable material that can be expressed as;

$$\left(\frac{\rho}{\varepsilon}\right)\frac{\partial u}{\partial t}+\left(\frac{\rho}{\varepsilon^2}\right)u\left(\frac{\partial u}{\partial x}\right)=\frac{\partial p}{\partial x}-\left(\frac{\mu}{K}\right)u-\rho\left(\frac{Y}{K^{\frac{1}{2}}}\right)|u|u+\left(\frac{\mu}{\varepsilon}\right)\left(\frac{\partial^2 u}{\partial x^2}\right) \qquad (3.7)$$

with $u=\varepsilon u_j$

where u is the superficial fluid velocity (m s^{-1}), u_j is the velocity through the material in direction y (m s^{-1}), ρ is the density (kg m^{-3}), p is the pressure (Pa), μ is the dynamic viscosity (Pa s), Y is the inertial factor and x is the direction of flow, ε is the porosity and K is the permeability of the screen (m^2).

Lebon and Cloot (1986) stated that the permeability is related to the reciprocal of the collision frequency of diffusing particles and the kinematic fluid viscosity. Then according to Bear and Bachment (1990), for a Reynolds number (Re) smaller than 150 the flow is incompressible. Therefore, equation 3.7 can be expressed in term of quadratic law or the Forchheimer equation as;

$$\left(\frac{\mu}{K}\right)u+\rho\frac{Y}{K^{\frac{1}{2}}}|u|u=\frac{\partial p}{\partial x} \qquad (3.8)$$

where u is the superficial fluid velocity (m s^{-1}), u is the velocity through the material in direction y (m s^{-1}), |u| is the absolute velocity through the material (m s^{-1}), ρ is the density (kg m^{-3}), p is the pressure (Pa), μ is the dynamic viscosity (Pa s) and Y is the inertial factor and x is the direction of flow.

3.3 Physical dimensions

3.3.1 Experimental design

Samples of transparent polyethylene film and polyethylene insect screens were prepared according to the requirements of the physical properties to be measured. Three screens N50, N32 and N50 were used in these studies. N50 means there are 50 holes per inch. Polyethylene film and insect screens were supplied by Fordingbridge Limited and Tildenet Limited respectively. The test programme is shown in Table 3.1.

Table 3.1 Experimental programme for measuring the physical properties of polyethylene film and screens

Material	Thickness (m)	Hole area (m^2)	Coefficient of discharge (dimensionless)	Direct light transmission (%)	Diffuse light transmission (%)
Polyethylene sheet	√	x	x	√	√
Insect screens;					
Screen N50	√	√	√	√	√
Screen N32	√	√	√	√	√
Screen N24	√	√	√	√	√

A fluorescence microscope with CCD camera was used to measure the individual screen hole size. The image from the camera was sent to a computer that had image analysis software programme to process the data. This measurement system gave the desired accuracy and the results could be obtained from the computer print out. Plate 13. shows the apparatus for measuring the hole size at Silsoe College, Cranfield University. The specifications of the image analysis instruments are as follows;

1. Optomax V image analysis computer : 256 grey levels, 704 x 560 pixels, image editing
2. Leitz flourescence microscope : 1.6 - 100x objectives, 3 narrow band filters
3. Optical bench/macro-stand
4. Newvicon, videcon and CCD cameras
5. Custom Software

The thickness of both film and screens were measured using a micrometer gauge.

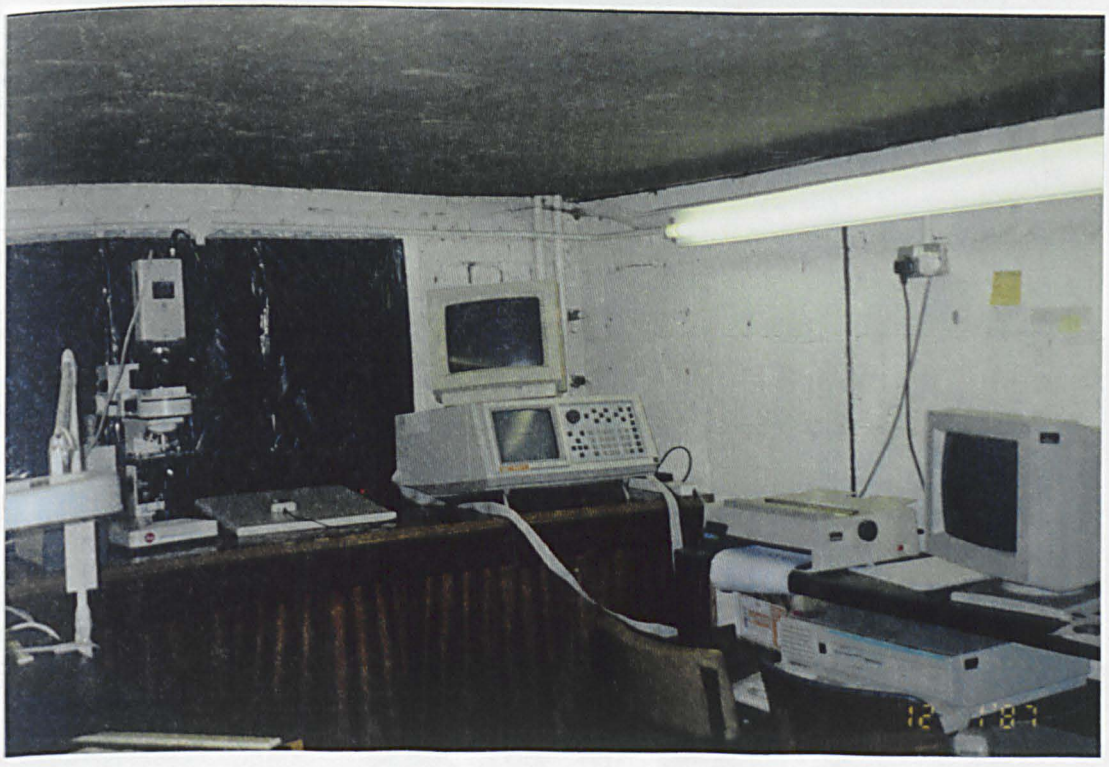

Plate 13. Apparatus for screen hole measurement

3.3.2 Results and discussion

3.3.2.1 Area of screen hole

The mean hole areas for screens N50, N32 and N24 are shown in Table 3.2. The area was measured between the edges of the threads that separate the hole. Screen N50 had the smallest hole area and screen N24 had the biggest hole area. If the openings are considered in relation to the actual area of the screens, the ratios are 53%, 66% and 68% for screens N50, N32 and N24 respectively.

Table 3.2. Area of single holes in the different sizes of insect screen (mm^2).

Screen	n	$\bar{x}$	max	min	S.E.	σ_{n-1}
Screen N50	117	0.133	0.160	0.100	0.001	0.011
Screen N32	113	0.401	0.580	0.270	0.005	0.058
Screen N24	149	0.732	0.850	0.600	0.003	0.035

3.3.2.2 Thickness of materials

The thickness of transparent polyethylene sheet and polyethylene insect screens are shown in Table 3.3. The means of the sheet thickness are 0.178 mm, 0.372 mm, 0.348 mm and 0.351 mm for polyethylene, screen N50, N32 and N50 respectively.

Table 3.3. Thickness of transparent polyethylene film and polyethylene insect screens (mm).

Material	n	$\bar{x}$	max	min	S.E.	σ_{n-1}
Polyethylene	100	0.178	0.198	0.155	0.0010	0.008
Insect Screens;						
Screen N50	50	0.372	0.385	0.358	0.0010	0.006
Screen N32	50	0.348	0.363	0.340	0.0010	0.004
Screen N24	50	0.351	0.355	0.348	0.0002	0.002

3.4 Light transmission

3.4.1 Experimental design

3.4.1.1 Diffuse light transmission

The diffuse light transmissions of the samples were measured using a diffuse light transmission goniometer. This is shown in Figure 3.1 and Plate 14. The specifications of the diffuse light transmission are as follows;

Hemisphere	:	2.0 m diameter semi hemispherical dome with an Eastman White Reflectance Coating on the internal surface.
Light source	:	120 units of 8 W fluorescent lamps.
Spectroradiometer	:	Bentham Instruments Ltd. Monochromator - M300 Detector - photomultiplier, Hamatsu R446 185-87 nm Diffraction grating - 1200 line/mm, 0.1 μm Light guide - Macam UV, 100 μm fibre, 500 mm long
Integrating sphere	:	600 mm diameter, 2 port copper sphere with an Eastman White reflectance Coating on the internal surface
Sphere aperture	:	200 diameter aperture on top of the sphere
Accuracy	:	± 1%

Measurement was made by placing the sample on top of the sphere aperture and then measurement was made. A second measurement was made when the top aperture was left open. The transmittance was calculated as the ratio of the first measurement to the second.

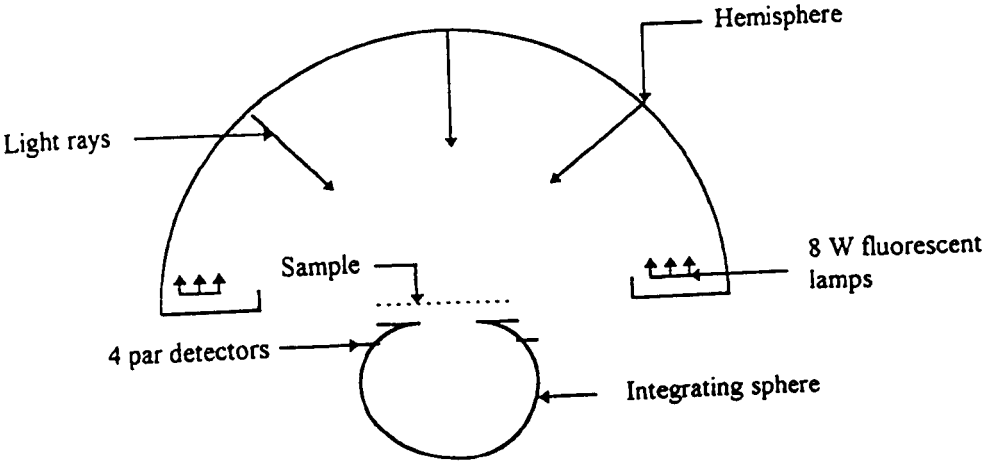

Figure 3.1 Diffuse light transmission measurement

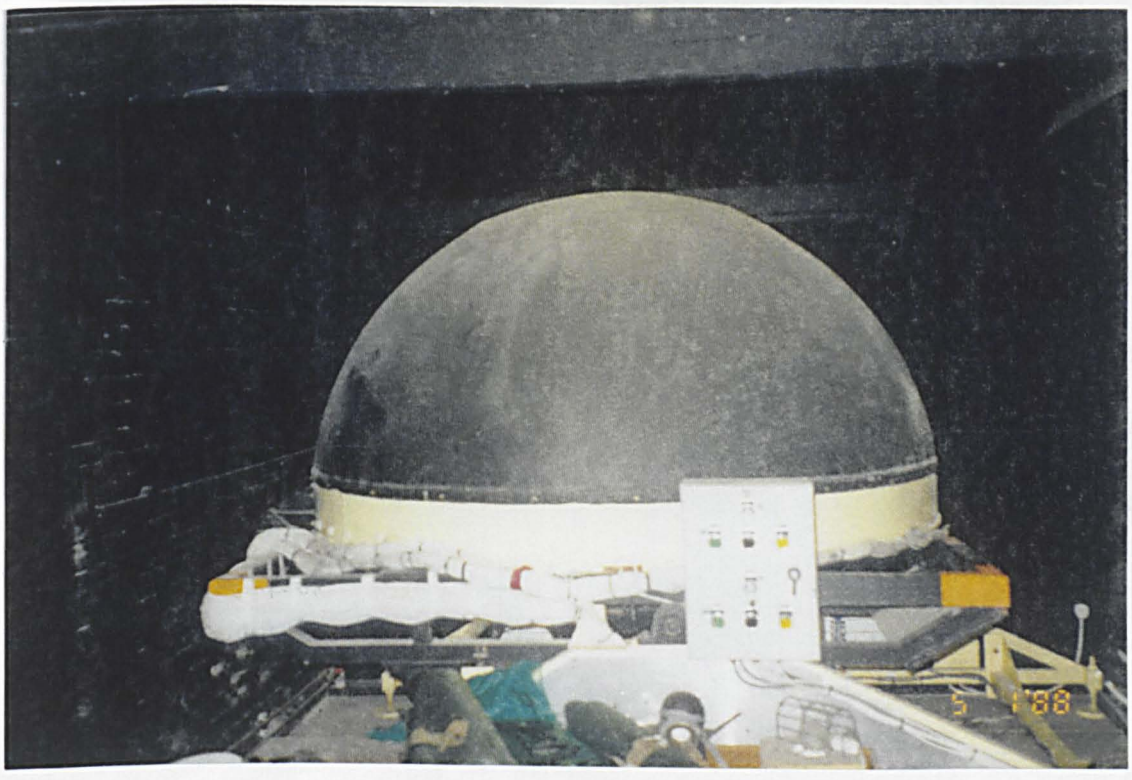

Plate 14. Diffuse light transmission goniometer

3.4.1.2 Direct light transmission

Direct light transmission of the samples was measured using a direct light transmission goniometer. This machine was developed by Silsoe Research Institute as shown in Figure 3.2 and Plate 15. The specifications of the machine are as follows;

Light source	:	600 w tungsten-halogen overhead projector lamp
Collimator	:	Spherical mirror and Fresnel lens to produce a horizontal light beam
Mirror	:	Two planes mirrors mounted in a ring which can rotate through 360 degrees about the horizontal axis of the light beam and rotate the beam through 360 degrees in a vertical plane
Spectroradiometer	:	Bentham Instruments Ltd Monochromator - M300 Detector - photomultipler, Hammatsu R446 185-87 nm Diffraction grating - 1200 line/mm, 0.1 μm Light guide - Macam UV, 100 μm fibre, 500 mm long

Integrating sphere	:	400 mm diameter, 2 port copper sphere with an Eastman White Reflectance Coating on the internal surface
Sphere aperture	:	100 mm diameter aperture on top of sphere with a second identical aperture inclined at 45 degrees
Accuracy	:	± 1%

Measurements were made by allowing the light source to reach a constant operating temperature and its light output to become stable. The mirror assembly was rotated so the light beam was vertical and centred over the horizontal aperture in the top of the integrating sphere. The test sample was placed over the top aperture and inclined aperture left opened but shielded from stray light.

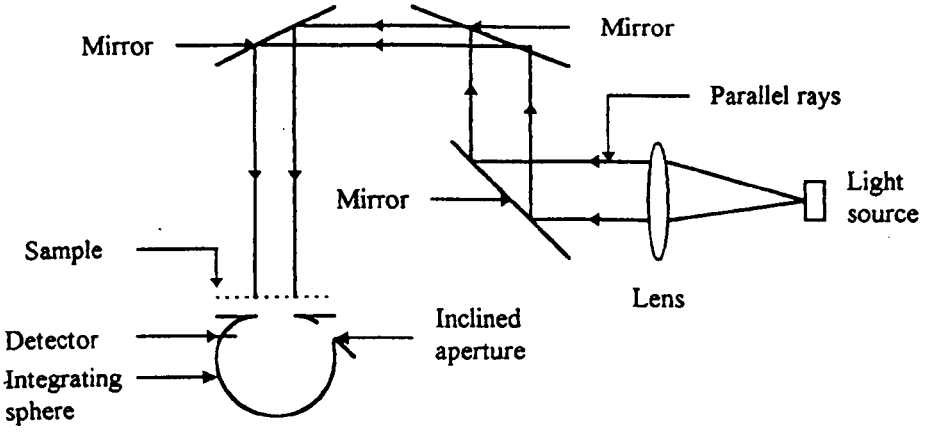

Figure 3.2 Direct light transmission measurement

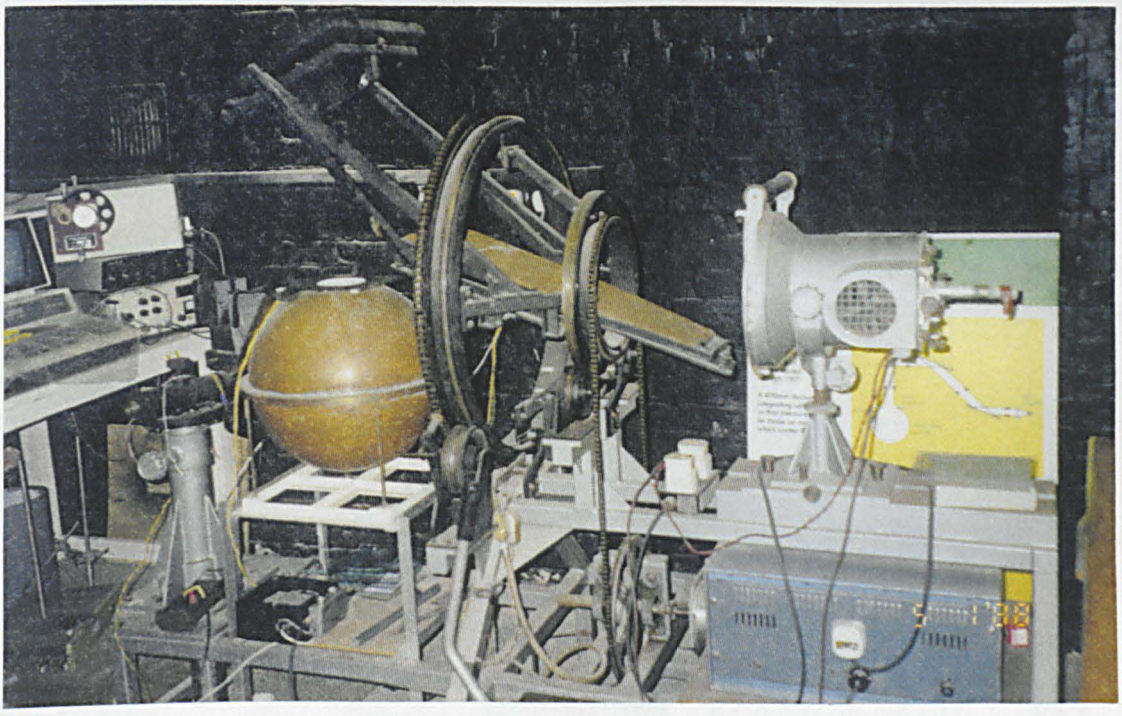

Plate 15. Direct light transmission goniometer

The test sample was placed over the inclined aperture and shielded from stray light and the top aperture was left open. A second measurement was then made. The transmittance was calculated as the ratio of the first measurement to the second. With this method of measurement the reflectivity of the sphere remains constant and the transmission value was not influenced by the reflectivity of the sample.

3.4.2 Results and discussion

3.4.2.1 Diffuse light transmission

The diffuse light transmission of the transparent polyethylene sheet and the polyethylene insect screens are shown in Table 3.4. The means of the diffuse light transmission of the polyethylene film and screens N50, N32 and N24 are 82.0 %, 75.0 %, 78.9 % and 83.2 % respectively. Screen N50 gives the lowest light transmission of

the three screens. This is because screen N50 had the smallest hole area to transmit light. The diffuse light transmission of the polyethylene film lies between screen N32 and screen N24. Therefore, the polyethylene film and screens are suitable for cladding the crop protection structure.

Table 3.4 Diffuse light transmission of polyethylene film and polyethylene insect screens (%).

Material	**n**	$\bar{x}$	**max**	**min**	**S.E.**	σ_{n-1}
Polyethylene film	100	82.0	86.1	71.3	0.20	2.01
Insect Screens;						
Screen N50	50	75.0	76.1	73.7	0.07	0.51
Screen N32	50	78.9	79.7	77.6	0.06	0.46
Screen N24	50	83.2	84.0	82.1	0.07	0.49

3.4.2.2 Direct light transmission

The results of direct light transmission at different incidence angles are presented in Table 3.5. The angle of incidence was measured relative to the perpendicular to the sheet surface. An angle of 0^{o} means light perpendicular to the sheet surface. The effect of incidence angle on the direct light transmission is presented in Figure 3.3.

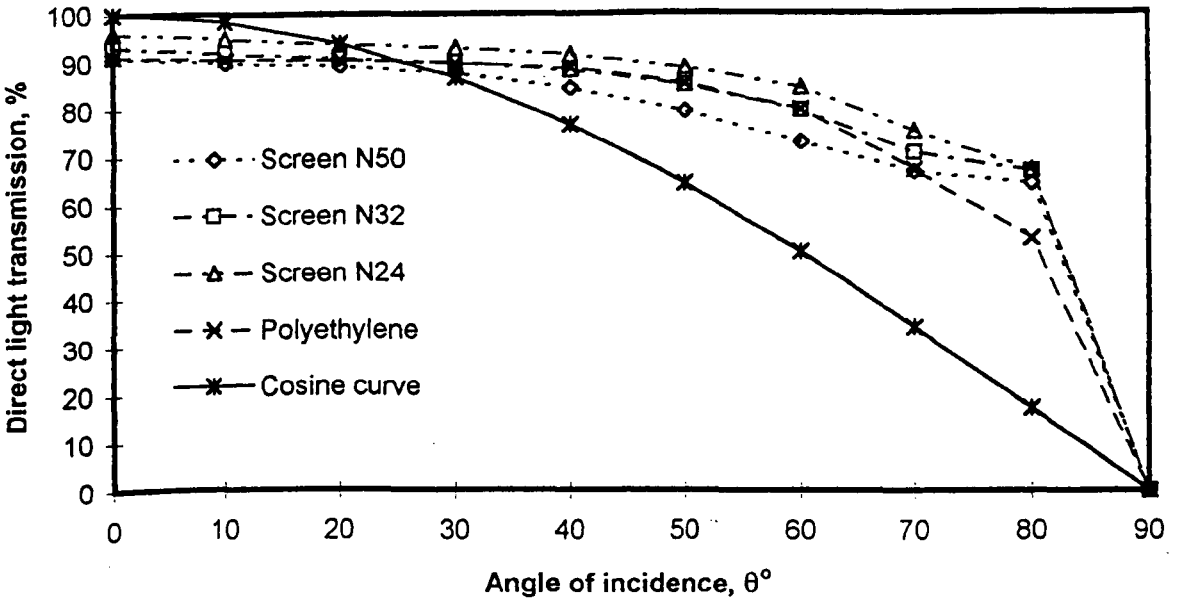

Figure 3.3 Relationship between direct light transmission and angle of incidence for polyethylene film and insect screens

The figure shows that screen N50 gave the lowest light transmission compared to screen N32 and screen N24. This is due to the screen N50 having the smallest hole area to transmit light. However, the polyethylene film transmission fell within the range of the three screens. Therefore, the capabilities of the polyethylene film and screens to transmit solar radiation into the crop protection structure is similar. In addition, the effect of rough screen surface to scatter the light transmission at different incidence angles was insignificant if compared to the film surface.

The figure also shows that light transmission is highest for light incident perpendicular to the sheet surface. The transmission gradually reduces when the angle of incidence increases. The effect of the material surface on the

Theoretically, light transmission of transparent materials follows the cosine curve law where light transmission decreases when the angle of incidence increases. The figure also shows all screens and polyethylene curves do not follow the cosine curve. Light transmission curves of materials are lower than the theoretical curve at angles 0°-25° and will be higher when angle more than 25°. In general light transmission is sufficient for crop production when angle of incidence is less than 30°. However, the light transmission for angle more than 80° is difficult to be measured.

Table 3.5 Direct light transmission of polyethylene film and polyethylene insect screens (%)

Material	n	$\bar{x}$	max	min	S.E.	σ_{n-1}
Polyethylene sheet;						
Angle 00°	100	91.3	92.0	90.9	0.02	0.20
Angle 10°	100	90.7	96.0	90.0	0.06	0.59
Angle 20°	100	90.6	91.1	89.9	0.02	0.20
Angle 30°	100	89.8	90.3	89.1	0.02	0.24
Angle 40°	100	88.6	89.2	87.8	0.03	0.30
Angle 50°	100	85.2	86.3	83.2	0.06	0.57
Angle 60°	100	79.8	81.7	77.3	0.09	0.90
Angle 70°	100	67.2	69.3	64.9	0.10	0.96
Angle 80°	100	52.9	56.6	50.3	0.16	1.58
Insect Screens;						
Screen N50						
Angle 00°	50	91.0	91.6	90.0	0.06	0.42
Angle 10°	50	89.9	90.6	88.9	0.05	0.37
Angle 20°	50	89.2	90.3	88.1	0.05	0.37
Angle 30°	50	87.6	88.5	86.1	0.07	0.48
Angle 40°	50	84.4	85.3	83.1	0.08	0.57
Angle 50°	50	79.4	80.9	78.0	0.10	0.68
Angle 60°	50	73.0	74.6	71.4	0.10	0.73
Angle 70°	50	66.7	70.0	64.1	0.19	1.37
Angle 80°	50	64.4	69.6	59.5	0.42	2.93
Screen N32						
Angle 00°	50	93.3	94.1	92.3	0.06	0.44
Angle 10°	50	91.9	92.5	91.2	0.05	0.32
Angle 20°	50	90.9	91.5	90.0	0.05	0.37
Angle 30°	50	89.9	90.5	88.9	0.05	0.38
Angle 40°	50	88.0	89.2	87.0	0.08	0.54
Angle 50°	50	84.9	86.0	83.4	0.09	0.60
Angle 60°	50	79.6	81.2	77.4	0.13	0.89
Angle 70°	50	70.7	71.9	69.3	0.09	0.60
Angle 80°	50	66.9	69.8	65.4	0.15	1.08
Screen N24						
Angle 00°	50	96.0	96.7	95.2	0.05	0.36
Angle 10°	50	95.0	95.7	94.4	0.05	0.36
Angle 20°	50	93.7	94.6	91.4	0.08	0.57
Angle 30°	50	92.9	94.1	92.3	0.06	0.40
Angle 40°	50	91.4	92.2	90.4	0.06	0.43
Angle 50°	50	88.6	90.0	87.6	0.07	0.47
Angle 60°	50	84.4	85.7	83.5	0.08	0.56
Angle 70°	50	75.2	77.2	73.6	0.11	0.77
Angle 80°	50	67.2	71.5	63.9	0.24	1.73

3.5 Coefficient of discharge

3.5.1 Experimental design

The static pressure difference and air velocity across the insect screens were measured using a fan test rig according to BS 848. The rig consisted of a fan to supply air at different air speeds, diffusing screens for straightening the air flow, a louvered shutter to regulate the air flow direction and the test material frame mounted at the outlet. In order to measure the related parameters, the instrumentation such Type FC014 manometers by Furness Controls Ltd., platinum resistance thermometer by H. Tinsley & Co. Ltd., DOL 14 hygrometer by Skov Bros., barometer series 8190 by KDG Instruments Ltd. and the computer logging system were incorporated with the test rig. The fan test rig used in these studies was developed by Silsoe Research Institute is shown in Figure 3.4 and Plates 16, 17 and 18. In addition, the details of the fan test rig specifications were reported by Mousley *et al.* (1987).

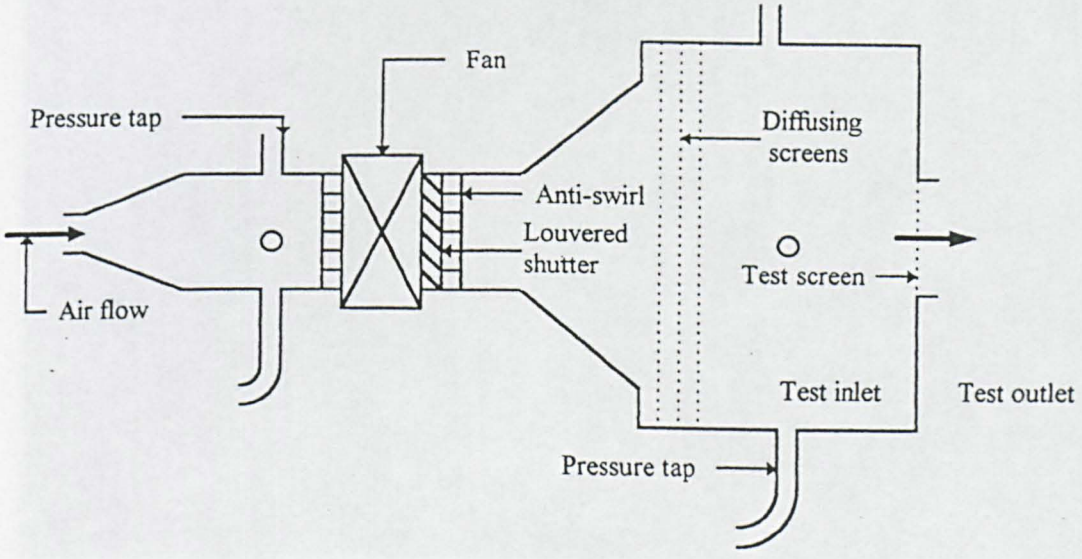

Figure 3.4 Lay-out of fan test rig

Plate 16. Fan test facility for measuring coefficient of discharge

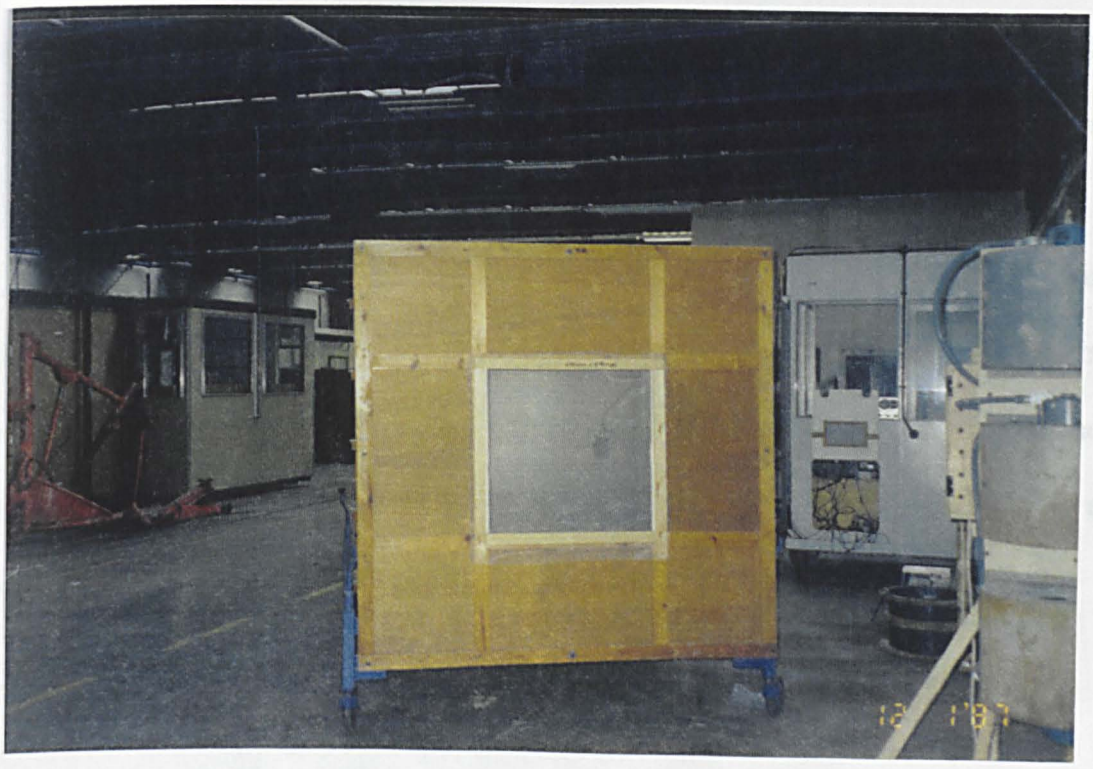

Plate 17. Front view of fan test facility

Plate 18. Fan test logging system

In the experiment, the screens were mounted in the frame at the outlet of the rig and the approach air speed was controlled by the fan. The approach air speed through the screen is defined as the airflow rate through the screen divided by the total area occupied by the screen.

Measurement was made by regulating the fan for different approach air speeds. Once the desired air speed across the screen sample was made, parameters such as approach airspeed, air pressure, air temperature and relative humidity at the test inlet and outlet were measured by the sensors. Then, the data was recorded by a data logger and could be produced graphically on the computer screen.

3.5.2 Results and discussion

3.5.2.1 Coefficient of discharge

The coefficients of discharge of the insect screens are presented in Table 3.6. The means of the coefficients of discharge for screen N50, screen N32 and screen N24 are 0.411, 0.520 and 0.547 respectively. Screen N50 gives the lowest coefficient of discharge compared to other screens. This is due to the screen N50 having the smallest holes that created the highest pressure drop and the lowest airspeed through the screen. The importance of these coefficients is significant as shown in the equations 2.5, 2.13 and 2.14 and will be widely used in the preceding chapters.

Table 3.6 Coefficient of discharge of polyethylene insect screens (dimensionless)

Screen	n	$\bar{x}$	max	min	S.E.	σ_{n-1}
Insect Screens;						
Screen N50	52	0.411	0.412	0.411	0.00004	0.0003
Screen N32	65	0.520	0.521	0.519	0.00008	0.0006
Screen N24	50	0.547	0.548	0.547	0.00003	0.0002

The linear relationships between the pressure drop and the square of the airspeed across screens N50, N32 and N24 are presented in Figure 3.5. This relationship is in good agreement with the findings of Sase (1990), Baker (1995) and Brundrett (1995). The figure also shows that the pressure drop increases with decreasing screen hole and with the square of the approach airspeed. The linear regression equations and coefficients of determinations derived from Figure 3.5 are summarised in Table 3.7.

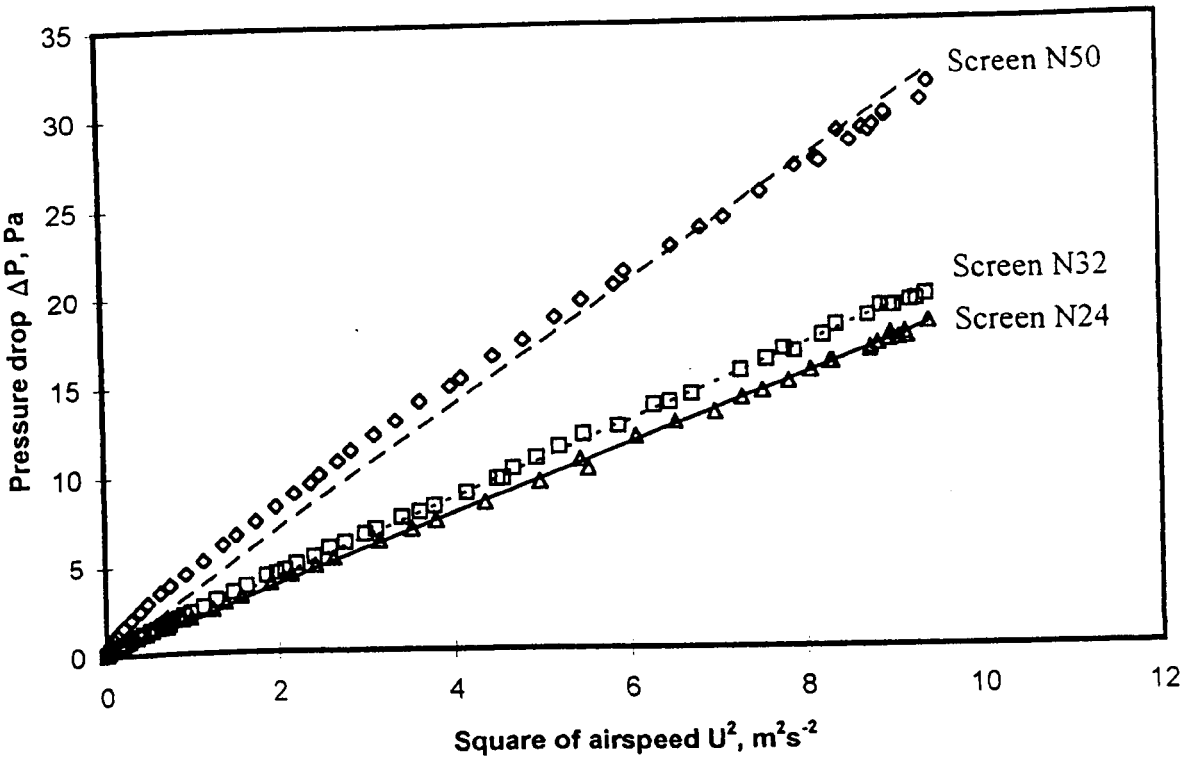

Figure 3.5 Relationship between pressure drop and square of airspeed through the insect screens.

Table 3.7. The linear regression equations and coefficients of determination derived from Figure 3.5

Screen	n	Equation	Adjusted R^2	S.E.
Screen N50	52	$\Delta P = 3.412U^2$	0.971	0.028
Screen N32	65	$\Delta P = 2.120U^2$	0.983	0.006
Screen N24	50	$\Delta P = 1.908U^2$	0.979	0.006

The relationship between pressure drop and airspeed for the three screens according to Forchheimer's flow regime is presented in Figure 3.6. This relationship is in agreement with the finding of Miguel (1988), where the pressure drop across the screen increases with increasing apparent airspeed according to a quadratic law. The

figure also shows that the smallest screen hole gives the highest pressure drop. This is because the smallest opening has the smallest value of the discharge coefficient. The regression equations and coefficients of determination for the screen are summarised in Table 3.8.

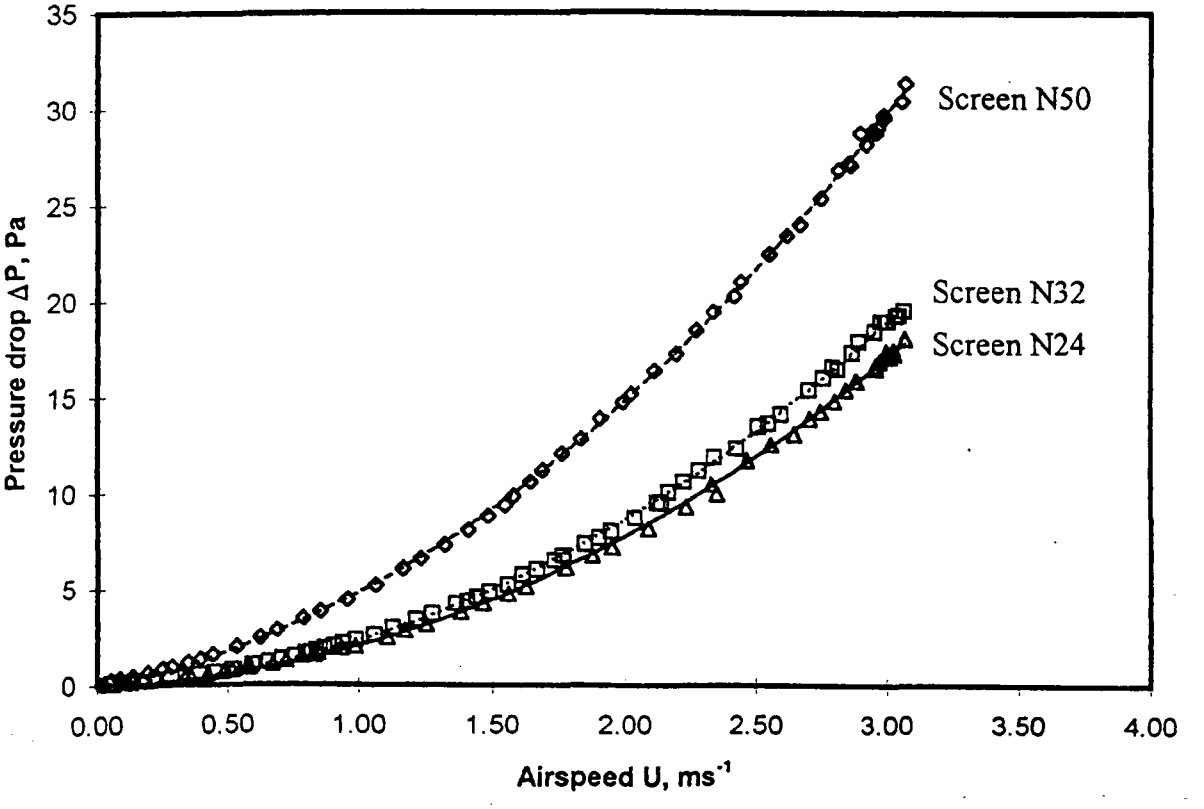

Figure 3.6 Relationship between pressure drop and airspeed through the insect screens

Table 3.8 The summary of quadratic regression equations and coefficients of discharge of screens derived from Figure 3.6

Screen	n	Equation	R^2
Screen N50	52	$\Delta P = 2.536U^2 + 2.324U$	0.9997
Screen N32	65	$\Delta P = 1.962U^2 + 0.410U$	0.9997
Screen N24	50	$\Delta P = 1.794U^2 + 0.309U$	0.9994

The results of airflow across the screens in the forms of linear relationship are useful to quantify natural ventilation rate according to equation 2.13, while the quadratic can be used to fit ventilation equation according to Miguel (1988).

3.6 Airflow patterns

3.6.1 Experimental design

3.6.1.1 Scale model airflow pattern by stack effect

Airflow pattern inside the crop protection structure was observed by using transparent 1:15 scale models (Plate19) in the two separated experiments. First, the airflow due to the stack effect that was made by staff of IRTA Spain, using a static transparent water tank 2 m long x 0.25 m high x 0.40 m deep as shown in Figure 3.7. The tank was filled with water and model placed upside down in the tank. Then a coloured salt solution that had a higher density than water was injected at the floor of the model using an adjustable flow piston pump. Descent of the saline solution in the tank simulates the airflow due to buoyancy or stack effect. A CCD Hi8-format video camera with shutter speed and exposure manually controlled recorded the tests. Images were digitised by a monochrome video card with 256 grey levels (Data Translation DT3851) installed in a personal computer. By using a software package (Global Lab) the images were processed to produce plots of the airflow pattern inside the crop protection model.

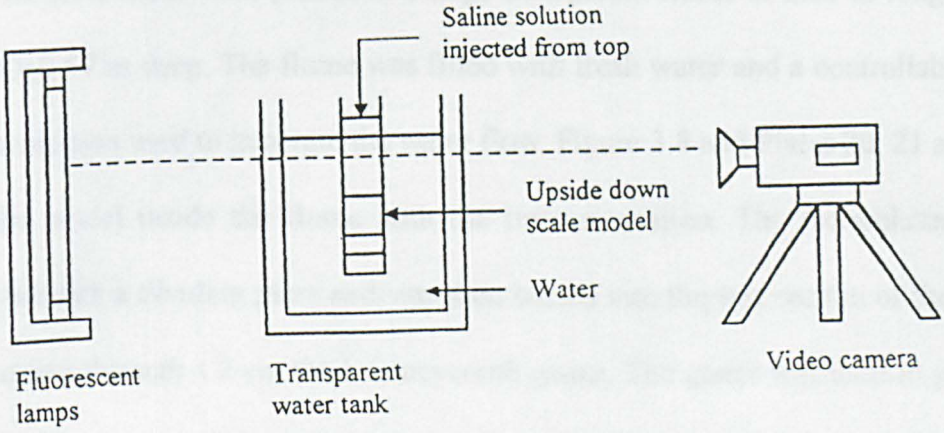

Figure 3.7 Visualisation of airflow pattern by stack effect

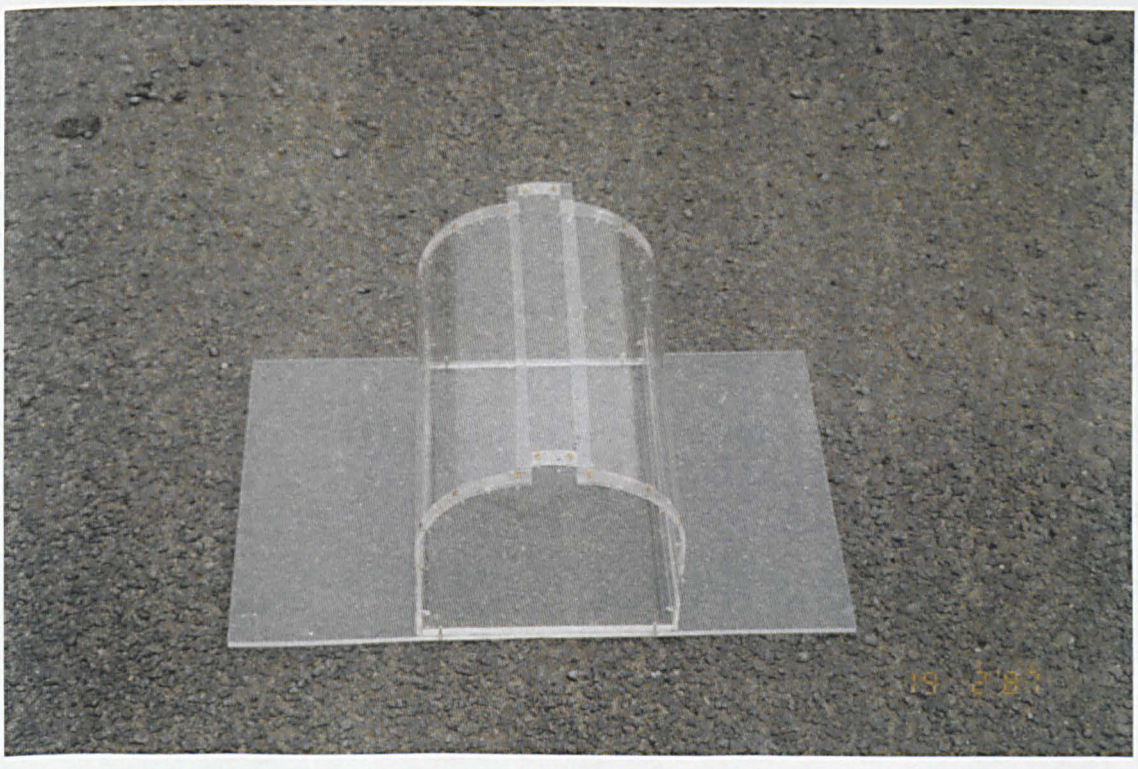

Plate 19. Crop protection structure scale model

3.6.1.2 Scale model airflow pattern by wind effect

The second observation was made at the Department of Applied Mathematics and Theoretical Physics, University of Cambridge. This observation was carried out with the guidance of Dr. Juan Montero from IRTA Spain and Cambridge University's staff. The scale model was placed in a large transparent flume of 2.65 m long x 0.30 m wide x 0.57 m deep. The flume was filled with fresh water and a controllable 4 hp water pump was used to generate the water flow. Figure 3.8 and Plates 20, 21 and 22., show the model inside the flume with the instrumentation. The recirculating flow passed beneath a dividing plate and was then turned into the test section of the flume after passing through a 2 cm thick honeycomb gauze. The gauze was used to produce a more uniform water flow. The horizontal flow in the test section was used to model the wind. This flow was controlled by means of a valve on the bypass circuit and was measured using a flow meter attached to the inlet pipe of the flume.

In order to visualise the airflow pattern inside the flume, white particles that had same density as water were mixed in the flowing water. The model was illuminated in the test section using diffuse back lighting and the moving particles were recorded by using a CCD Hi8-format video camera. The camera has a shutter speed and manually controlled exposure to record the experiments onto video tape. Each frame of the recording was then digitised in a false-colour format using the image analysis DigImage (Dalziel, 1993) By using this software package the images were processed to produce plots of the airflow patterns graphically inside the crop protection model.

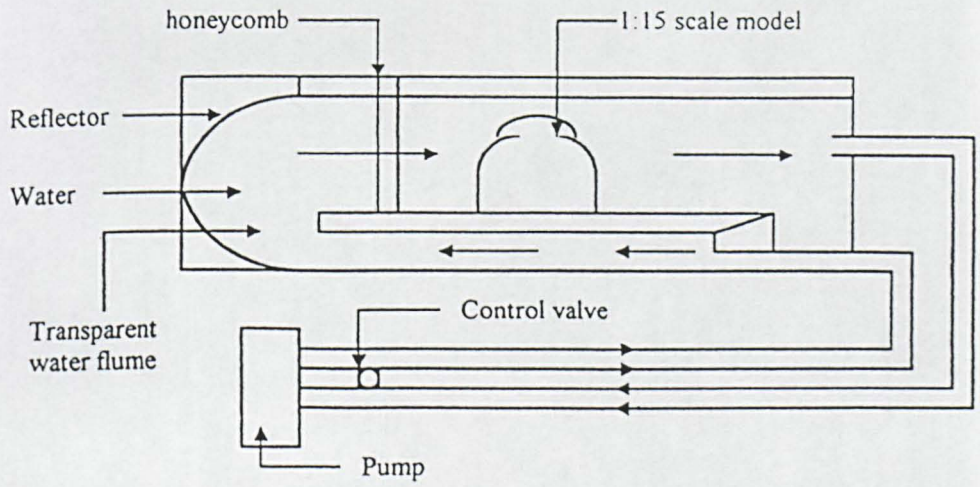

Figure 3.8 Visualisation of airflow pattern by wind effect

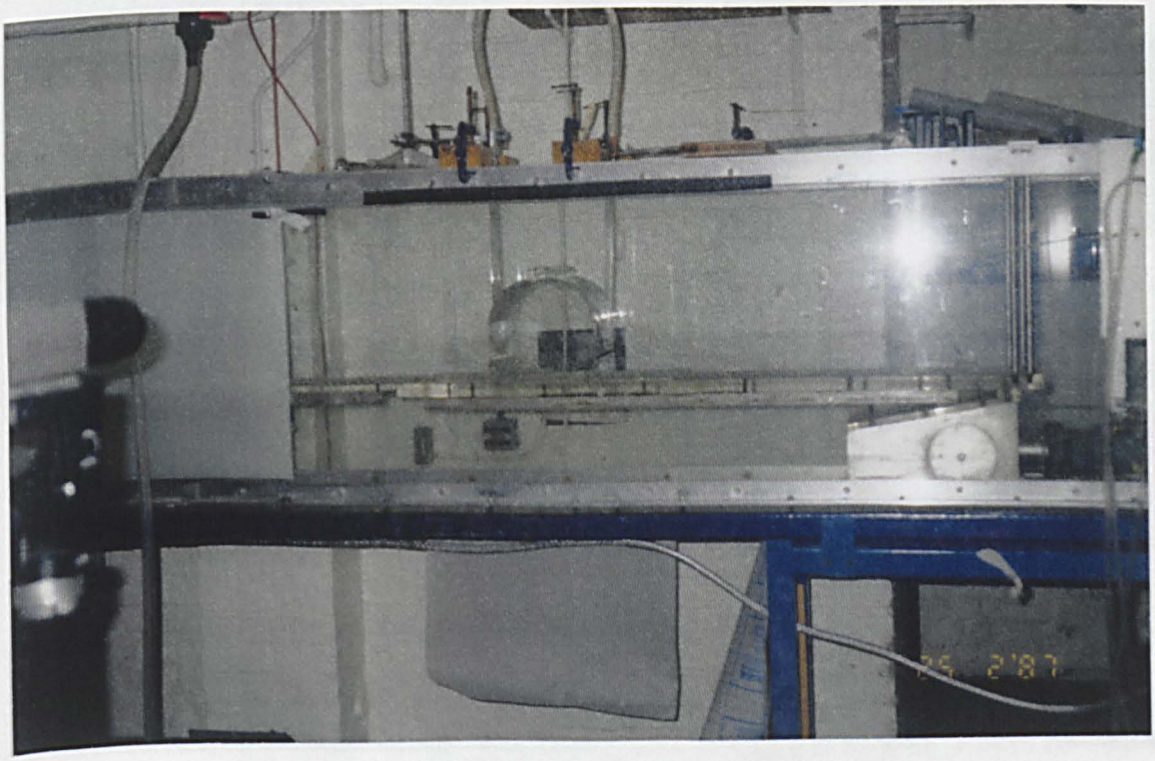

Plate 20. Apparatus for airflow pattern induced by the wind effect

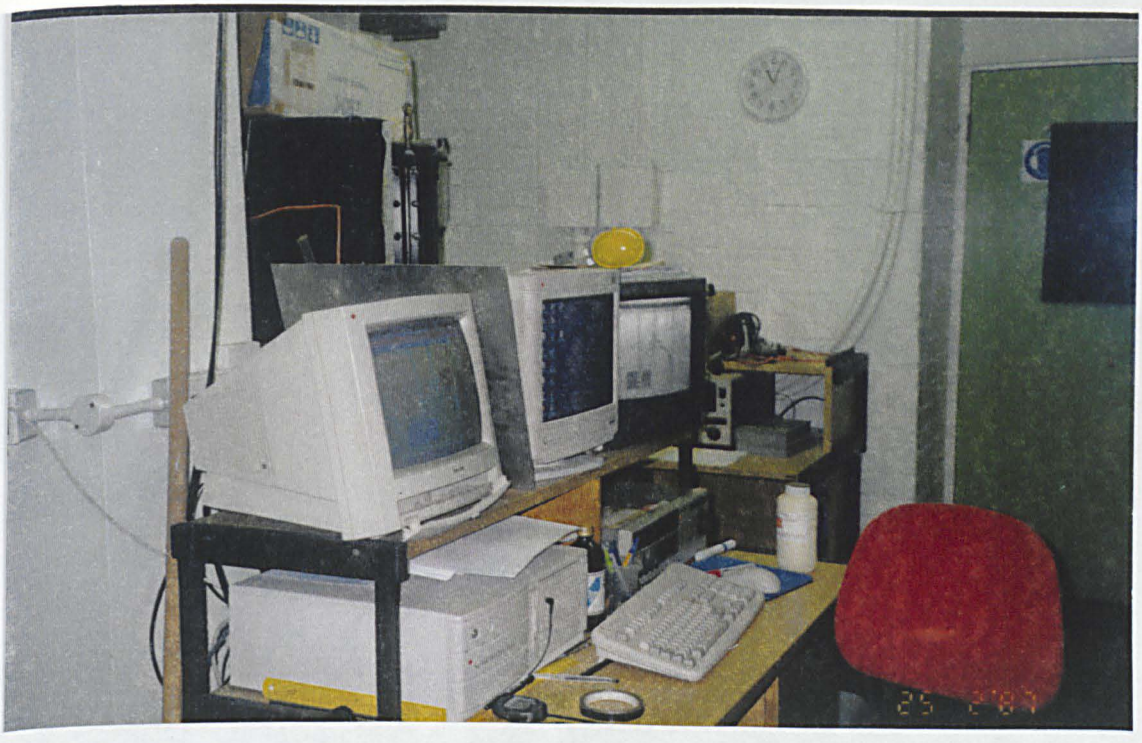

Plate 21. Logging system for airflow pattern by the wind effect

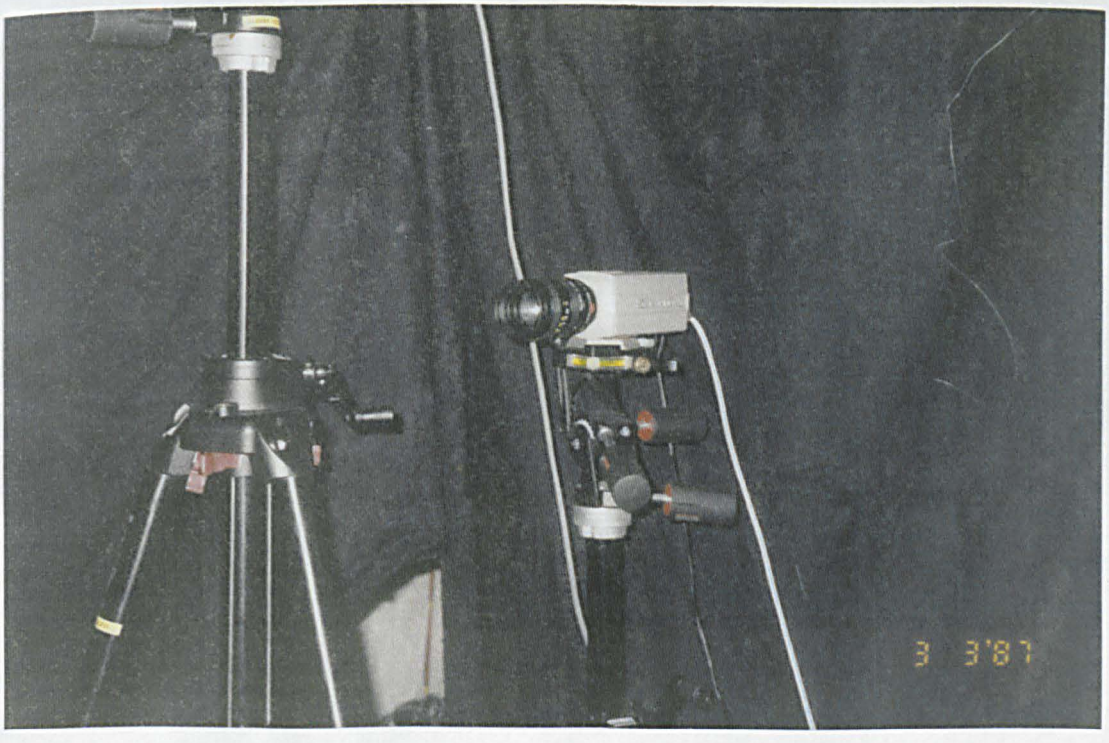

Plate 22. CCD camera for airflow pattern induced by the wind effect

3.6.1.3 Full scale airflow patterns

Airflow patterns were also visualised by using smoke as a tracer in the full scale crop protection structure. The airflow patterns induced by stack and wind effects were observed when the structure was placed in the large glasshouse and at the open field respectively. These observations were made concurrently with the experiments described in the preceding chapters. The experiments for airflow patterns caused by thermal buoyancy and wind effects in the full scale crop protection structure are shown in Plates 23 and Plate 24 respectively.

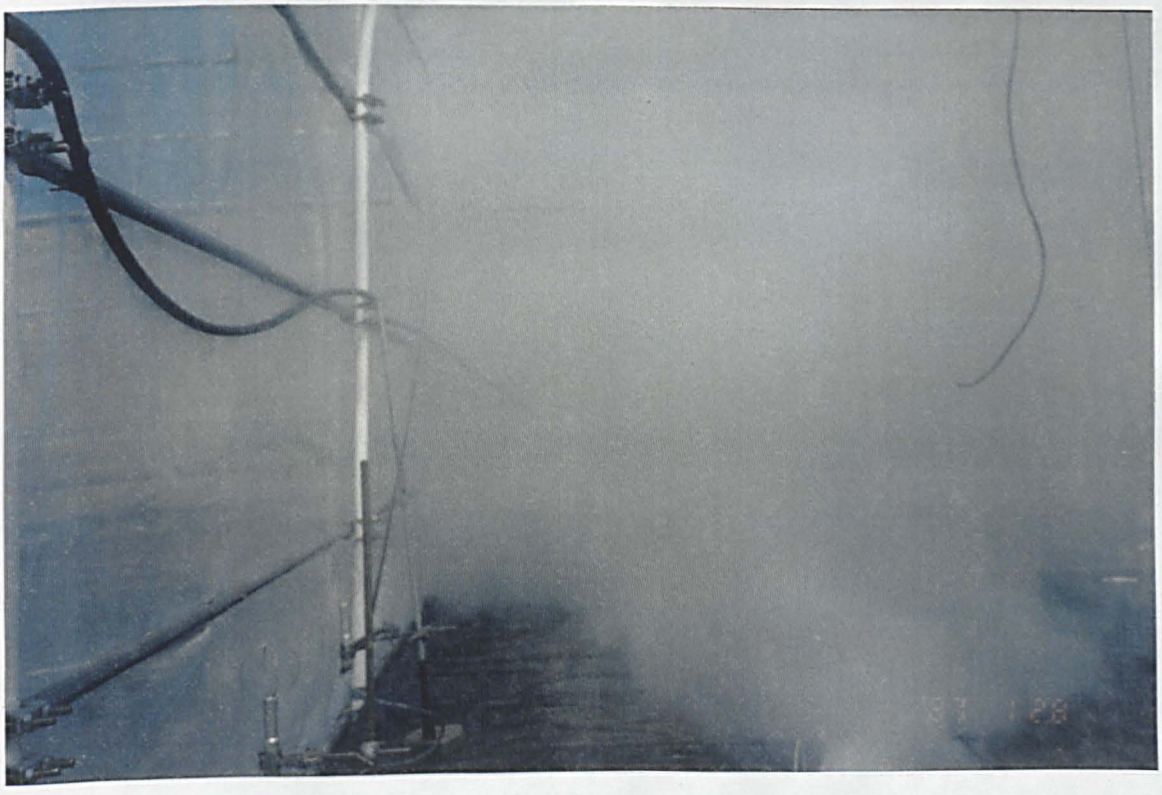

Plate 23. Full scale airflow pattern induced by the stack effect

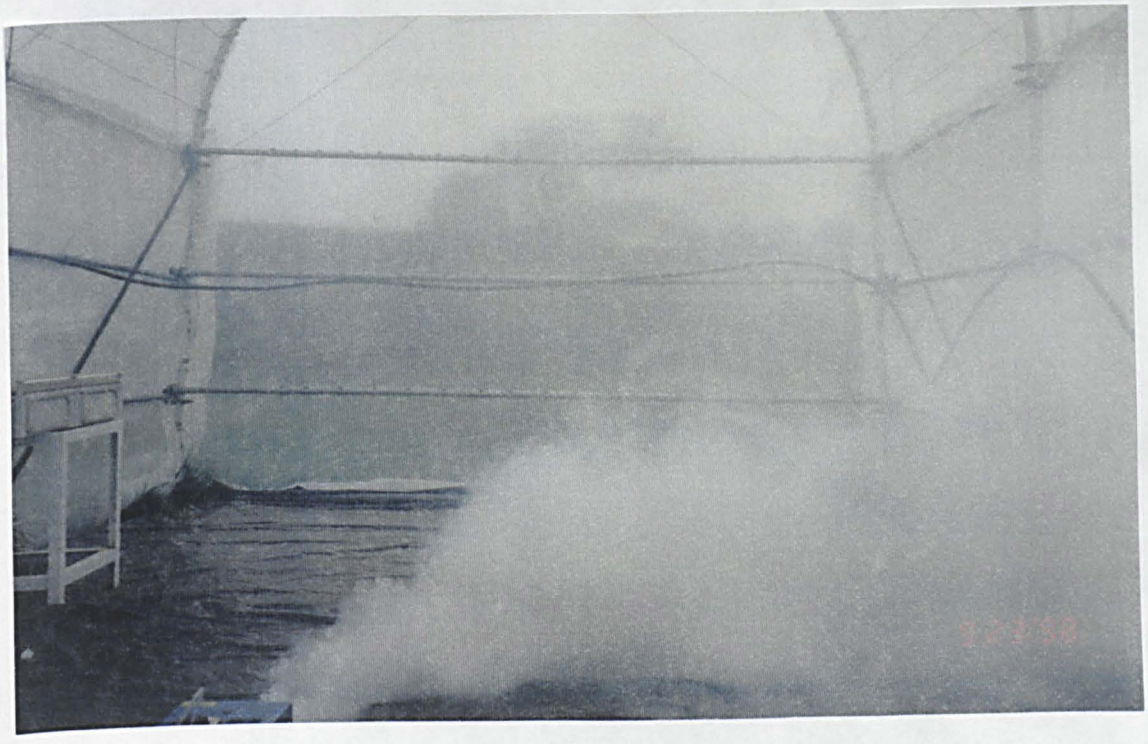

Plate 24. Full scale airflow pattern induced by the wind effect

3.6.2 Results and discussion

3.6.2.1 Scale model airflow pattern by stack effect

A typical air flow pattern inside the scale crop protection structure model induced by the stack effect is shown in Figure 3.9. This shows that air enters through the side openings and exhausts through the roof openings. This pattern is in good agreement with the actual air flow pattern that was visualised in the full scale crop protection structure shown in Plate 23. It was also observed that some of the exhaust flow occurred in side openings if the neutral plane intersected the side openings.

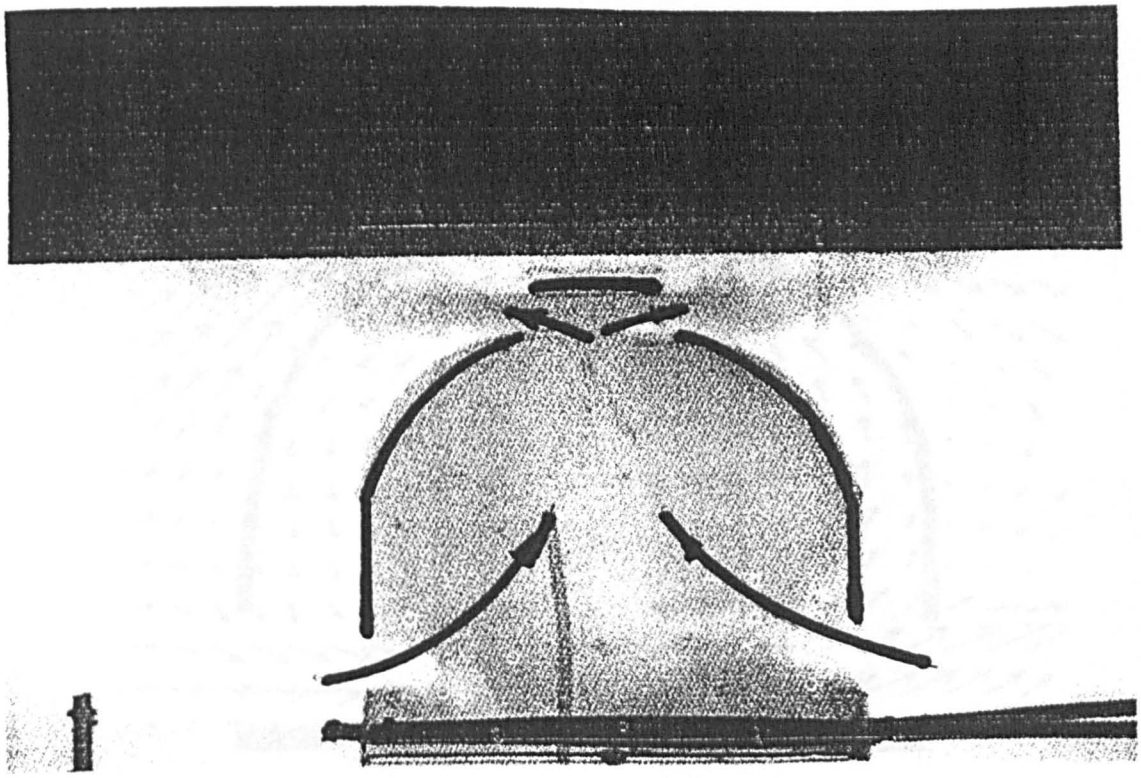

Figure 3.9 Airflow pattern caused by the stack effect (Montero, 1998)

3.6.2.2 Scale model airflow pattern by wind effect

Airflow pattern caused by the wind effect inside the scale model is shown in Figure 3.10. It shows that when the wind direction was perpendicular to the model, the openings on the windward and leeward sides of the model become the inlet and outlet respectively. In the roof and side openings the air flows directly from inlet to outlet. In addition, an anti clockwise air circulation was observed at the space between the roof and side openings. These patterns are in good agreement with the actual full scale airflow patterns shown in Plate 24.

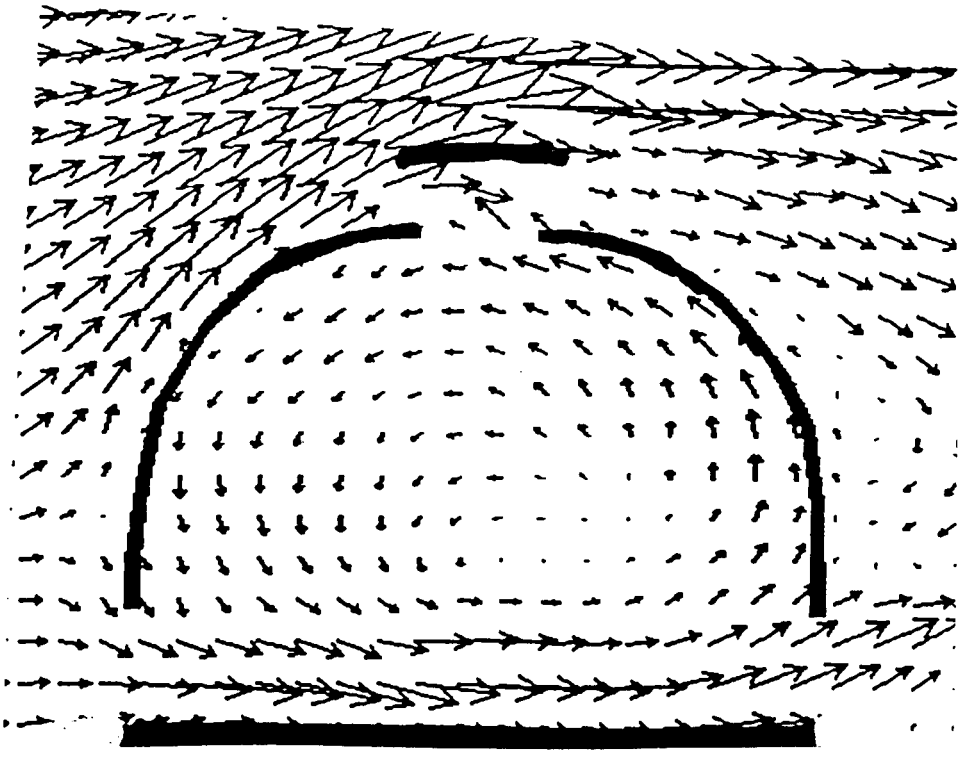

Figure 3.10 Airflow pattern caused by the wind effect

The airflow patterns for different ventilator openings and locations are presented in Figure 3.11 (a) - (d). The figures show the airflow patterns of the model that had ventilators in the roof (windward and leeward), roof (windward) and side (leeward), side (windward) and roof (leeward), and side (windward) and roof (leeward). In general, they show that when the wind direction was perpendicular to the model, the openings on the windward and leeward sides of the model became the inlet and outlet respectively. The air flows from inlet to outlet and also air circulation was observed at the space between the openings.

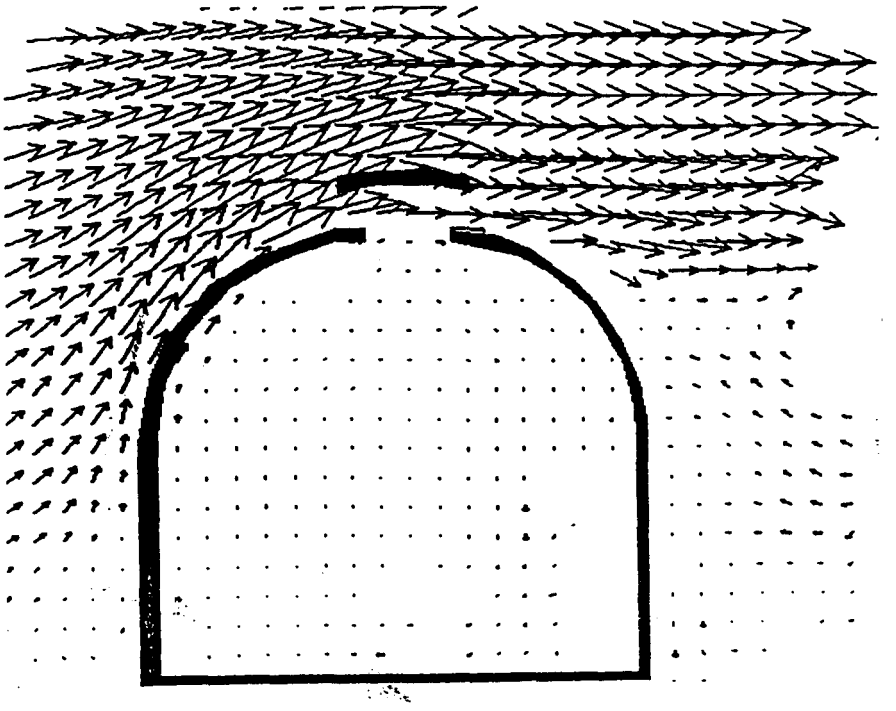

Figure 3.11 (a) Roof ventilators at windward and leeward
(Montero and Bailey, 1998)

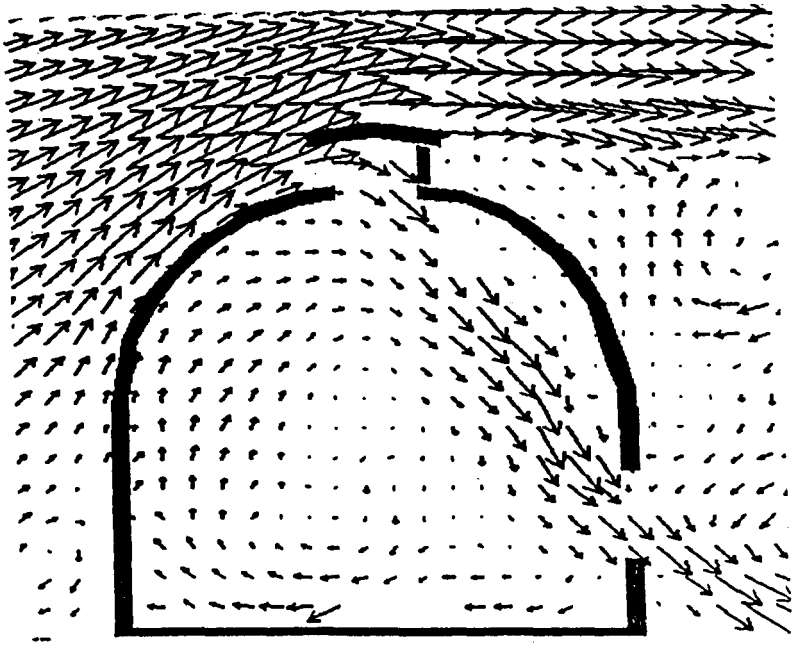

Figure 3.11 (b) Roof ventilator at windward and side ventilator at leeward
(Montero and Bailey, 1998)

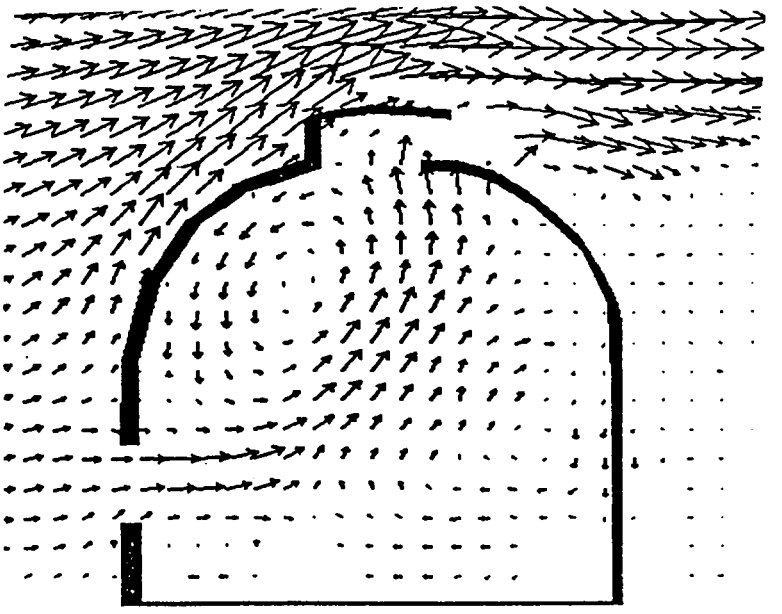

Figure 3.11 (c) Side ventilator at windward and roof ventilator at leeward
(Montero and Bailey, 1998)

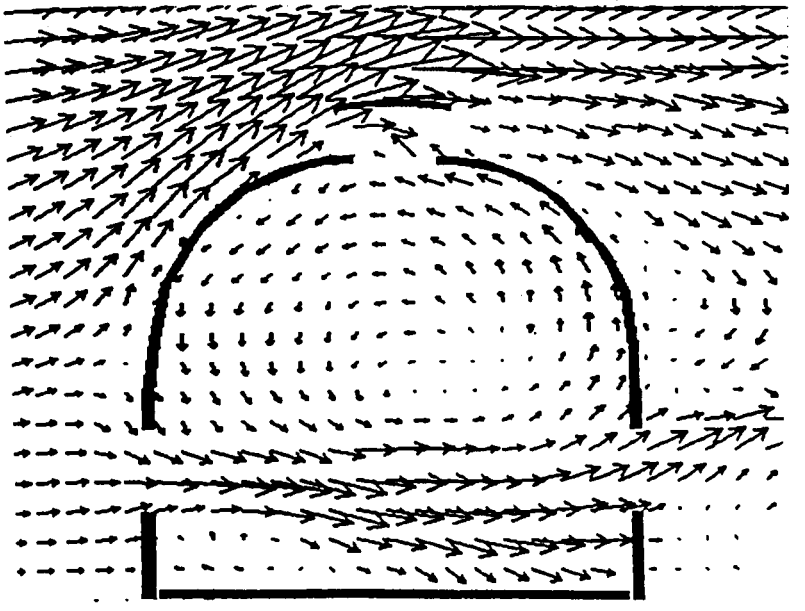

Figure 3.11 (d) Side and roof ventilators at windward and leeward
(Montero and Bailey, 1998)

3.6.2.3 Full scale airflow patterns

For the stack effect, airflow in the form of a stream was formed when air is entering through the screens into the enclosure at the two side openings. Then the air was moving upward and exhausting at both roof openings. When the neutral plane intersected at side openings, some of the airflow was turning down under the roof curve and then exhausting at the side openings above the neutral plane. This airflow pattern is shown in Plate 23.

The airflow pattern induced by wind effect is shown in Plate 24. It shows that the airflow pattern caused by wind effect could be seen clearly, if there was a minimum external airspeed available. When the wind direction was perpendicular to the model, the openings on the windward and leeward screen ventilators of the model became the inlet and outlet respectively. In the roof and side openings the air flows directly from inlet to outlet. Somewhere at the middle, an anticlockwise air circulation was observed at the space between the roof and side openings. However, when the wind direction was diagonal to the structure, the airflow pattern inside the structure showed similar pattern to the perpendicular ones, but it followed the outside diagonally direction.

Both stack and wind effect on the airflow patterns are important when making a decision on where to place the measurement sensors in studying natural ventilation by the stack effect, wind effect and the combination of both which are described in the preceding chapters. In addition, the airflow patterns contribute some useful information for the design of crop protection structures for the tropics

3.7 Conclusion

The physical properties of covering materials varied according to the nature of materials. Diffuse and direct light transmission of transparent polyethylene sheet and insect screens are relatively close to each other and so do not have much effect on the overall light transmission of the crop protection structure. Direct light transmission decreases when the angle of incidence is closer to the sheet or screen surface. In general, the direct and diffuse light transmission of both polyethylene film and screens is more than 90 % and 75 % respectively. However, the direct light transmission does not follow the theoretical cosine law.

The coefficients of discharges for screen N50, screen N32 and screen N24 are 0.411, 0.520 and 0.547 respectively. The smallest screen gives the smallest value of the coefficient of discharge. When air flows through the screen, it was found that there was a linear relationship between pressure drop and the square of approach air speed. In addition, the relationship between the pressure drop and apparent airspeed is in accordance of Forchheimer's flow regime, where the pressure drop increases with airspeed according to a quadratic law. Finally, laboratory observation of the airflow patterns caused by the stack and wind effects exhibit similar patterns as formed in the full scale structure. The patterns show the actual air movements inside and outside of the structure that is useful information for the greenhouse designer and grower in dealing with natural ventilation.

Chapter 4

Natural ventilation by stack effect

4.1 Introduction

Natural ventilation induced by temperature difference is called buoyancy or stack effect driven ventilation. It takes place when the outside environment has static or low wind speed. At the same time the temperature difference between the inside and outside of the crop protection structure needs to be high enough. Wind speed can be absent if the area is not in the prevailing wind direction or the area is surrounded by wind obstructions.

The temperature difference depends on global solar radiation, structural geometry, vent openings and the vertical height between the openings. Usually, the internal temperature is higher than the external temperature. If the enclosed structures have openings, fresh air will enter from bottom openings and move out through the upper openings. This is due to chimney or buoyancy effect, where air density inside the structure is less than the outside. Somewhere between them is a pressure neutral plane where the lateral air movement is static.

Solar radiation received by the structure is one of the main causes of the temperature difference, which can vary through the day. Rault (1990) has shown that the differences increased in the morning, reached the peak in the afternoon and decreased in the evening under a rain shelter structure in the tropics. He claimed that the internal temperature can be 4-5 °C higher than the external temperature, which is high enough for crop production.

The author has modified the temperate plastic tunnel and developed insect-proof rainshelter structures known as crop protection structures. These were built

from steel tubes or wooden frames, with transparent roofing and insect screen side walls. The structures are shown in Plates 3, 4, 11 and 12. Different structural geometries have also been developed and tested. The improvised design approach was taken to reduce internal temperature and provide a suitable environment for crop production. However, studies on natural ventilation on these structures have not been made.

Ventilation studies by natural convection or the stack effect have been done by many authors in different applications. Brown and Solvason (1962) have presented theoretical considerations for natural convection. Brown (1962) presented a theory for openings in horizontal partitions. In both studies, the same test unit was used to measure the natural convection through mainly square openings, with varying ratios of the partition thickness to the dimension of the opening. Shaw (1971) and Shaw *et al.* (1974) have measured the natural convection through doorways in a more practical situation.

A theoretical analysis of natural ventilation of buildings by the natural stack effect was published by Bruce (1978). His general theory can be applied to any building geometry. He compared the theoretical stack effect equation with experimentally measured data in a small-scale laboratory experiment. He presented the results that, when plotted graphically, fall on a straight line, consistent with the theory for the simplified geometry.

Timmons and Baughman (1981) have conducted experiments on a half-scale model open-ridge and side opening livestock building to establish empirical relationships between the temperature difference in a livestock building and the ventilating air speed at the ridge opening. He revealed that the ventilation rate is

proportional to the ridge vent opening for a given temperature difference and fixed ridge height.

The above studies have been made on small model and animal buildings. However there are very obvious differences between animal buildings and greenhouses. Animal buildings are totally shaded from sun light, but greenhouses transmit solar radiation for the photosynthesis process. Stack effect studies in the glasshouses have been made by De Jong (1990), Kittas *et al.* (1996) and Miguel *et al.* (1998). Their studies were conducted in the open with the assumption that the wind speed was relatively low and the temperature difference high. However, in reality their assumption did not represent pure natural convection because of environment fluctuations through out the measurements.

De Jong (1990) has also studied natural convection through the roof windows of a small greenhouse model. The model was heated by convector and tested using a tracer gas in the enclosed room. He found that the experimental results and the predicted ventilation were in fairly good agreement. The ventilation rate increased with the increasing window opening angle and temperature difference.

Until now, there have been no studies made on predicting natural ventilation through the porous side walls of tropical greenhouses. In the present study a full scale tropical greenhouse was tested in a natural environment with no wind disturbances. It was intended to contribute knowledge on how to predict actual natural ventilation by the stack effect. Different methods have been used to calculate ventilation rates. The hypothesis of the study was that the different methods gave similar results either by measurement or calculation.

4.2 Principal considerations

Natural ventilation induced by the stack effect can be quantified by different methods. In these studies the dynamic tracer gas, direct airspeed measurement, energy balance and neutral plane methods have been used to quantify ventilation rates. In order to verify the results, the tracer gas measurement is treated as the control.

4.2.1 Dynamic tracer gas

The dynamic tracer gas or pulse injection technique is one of the important methods for quantifying natural ventilation rate. This technique is based on a mass balance of the tracer gas in the building air. Many researchers have used this technique as a control method in residential houses, animal buildings and greenhouses studies. Greenhouse studies have been made by Okada and Takakura, (1973), Bot (1983), Geodhart *et al.*, (1984), Ruther, (1985), Nederhoff *et al.*, (1985), De Jong (1990), Fernandez and Bailey (1992, 1993), and Boulard *et al.* (1993).

In this method the tracer gas is injected and distributed uniformly in the building structure until a pre-determined concentration is reached and then stopped. The decay of the concentration of the tracer gas is the measured. Ventilation rate is defined as the number of air changes between the building interior and the outside environment per hour;

$$\Phi_g = \frac{R \times V}{3600 \times A_g} \qquad (4.1)$$

where Φ_g is the ventilation rate by tracer gas method ($m^3\ m^{-2}\ s^{-1}$), R is the hourly air exchange rate (h^{-1}), V is the volume of greenhouse (m^3), and A_g is the area of the ground (m^2). The method assumes that the tracer gas concentration is uniformly distributed inside (C_i, ppm) and outside (C_o, ppm), and there is a perfect proportionality between the flow of air and the flow of gas. The decay rate is given by;

$$V\frac{dc_i}{dt} = -\Phi_g\left(C_i(t) - C_o\right) \tag{4.2}$$

Integration of equation (4.2) between times t_o and t yields;

$$\ln\frac{C_i(t) - C_o}{C_i(t_o) - C_o} = -\frac{\Phi_g}{V}\left(t - t_o\right) \tag{4.3}$$

where $C_i(t)$ is the inside gas concentration at time t, C_o is the outside gas concentration that is constant, and $C_i(t_o)$ is the gas concentration at the initial time. Monitoring the gas concentration decay inside the greenhouse allows computation of the air exchange rate in equation (4.2). Nevertheless it should be kept in mind that this value of ventilation is not a real value of air flux but a virtual one based on assumption of a perfect proportionality between the flows of air and gas.

4.2.2 Direct airspeed measurement

Natural ventilation occurs through the structures' screened openings. The air exchange through the openings can be estimated by measuring the actual air flow through each of the openings. This technique has been used by many researchers like

Suomi (1957), Kaimal and Businger (1963), Mitsuta (1966), and Campbell and Unsworth (1979) to measure surface layer winds with sonic anemometers. Wind speed measurement and turbulence research using sonic anemometers were conducted by Izumi and Barad (1970), Smith (1980), Wyngaard (1981), Coppin and Taylor (1983) and Wang (1998). However, their studies were carried out in the open and no measurements were made on the stack effect.

In the present study, hot-wire anemometers were used to measure direct airspeed through the screen in the enclosed transparent environment. Air movement was observed to be less than 1.0 ms^{-1} and the air flow was uniformly laminar created by the screen. The volume flow rate through the nth opening is given by;

$$V_n = A_n U_n \tag{4.4}$$

and the natural ventilation rate by the stack effect for the structure is expressed by;

$$\Phi_{AS} = \frac{1}{2A_g} \sum_{i=1}^{n} V_n \tag{4.5}$$

where, U_n is the airspeed through the opening (m s^{-1}), V_n is the ventilation rate (m^3 s^{-1}), A_n is the opening area (m^2), A_g is the ground area (m^2) and Φ_{AS} is the ventilation rate (m^3 m^{-2} s^{-1}).

4.2.3 Energy Balance

Good ventilation is necessary in the crop protection structure to promote good growth of plants. It can limit the greenhouse temperature, removing water vapour transpired by the plants and replacing the CO_2 used in photosynthesis. Another

method to calculate the ventilation is by an energy balance model. The advantage of this method is many components in the structure that interact thermally, including the air, plants, soil and roof are taken into consideration. Each energy balance consists of its own equation that describes the gains and losses of energy in the structure. The flow of energy through a crop protection structure illustrated in Figure 4.1.

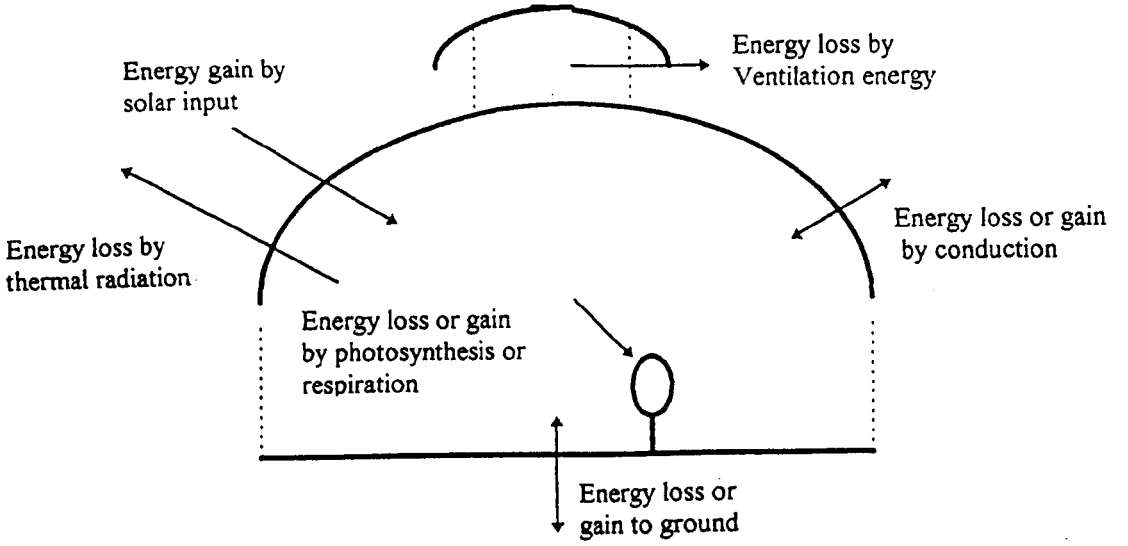

Figure 4.1. Energy transfer in the crop protection structure.

The energy balance equations are formulated with temperatures of the interacting components, which are obtained when the equations are solved. The individual heat flows can then be calculated. The first energy balance model for greenhouses was developed by Businger (1963) and then later by many researchers like Walker (1965), Winspear (1967), Garzoli and Blackwell (1981), Jolliet *et al.* (1985), Seginer and Kantz (1989). Fernandez and Bailey (1992) have also developed an energy balance model on naturally ventilated greenhouse as given by;

$$E_V = E_S - E_C - E_{ST} \tag{4.6}$$

where E_V is the energy removed from the greenhouse by the process of ventilation (W m^{-2}), E_S is the solar energy collected in the greenhouse (W m^{-2}), E_C is the thermal losses through the cover of the greenhouse (W m^{-2}), and E_{ST} is the stored energy in the greenhouse (W m^{-2}).The energy lost by ventilation has two components, one component due to sensible heat, and the other component due to latent heat. Therefore,

$$E_V = E_{SEN} + E_{LAT} \tag{4.7}$$

The energy removed by the process of ventilation consists of sensible and latent heat fluxes as;

$$E_{SEN} = \frac{\phi_v}{A_g} \rho C_p (\theta_i - \theta_o) \tag{4.8}$$

$$E_{LAT} = \frac{\phi_v}{A_g} \rho L (w_i - w_o) \tag{4.9}$$

where E_{SEN} is the sensible heat flux (W m^{-2}), E_{LAT} is the latent heat flux (W m^{-2}), ρ is the density of the air (kg m^{-3}), C_P is the specific heat of the air (Jk g^{-1} K^{-1}), L is the latent heat of vaporisation of water (Jk g^{-1}), θ is temperature of the air (K), w is absolute humidity of air (kg kg^{-1}), and A_g is the ground area (m^{-2}). The solar energy collected in the greenhouse depends on the coefficient of absorption of solar radiation by;

$$E_s = \tau(1-\rho)I \tag{4.10}$$

where τ is the light transmission of the greenhouse, ρ is the reflectivity of the greenhouse contents, that is crop, soil, etc., and I is the total solar radiation (W m^{-2}). The thermal losses through the cover have also given by Fernandez and Bailey (1992) as;

$$E_C = U\frac{A_{cl}}{A_g}(\phi_i - \phi_o) \tag{4.11}$$

where A_{cl} is the cladding area (m^2), U is the thermal transmittance of the cladding (W m^{-2} K^{-1}) was calculated by using the following equations developed by Jolliet (1991).

$$U = K_o + K_s + K_s q_s \tag{4.12}$$

This equation considers separately thermal exchange with the sky (K_S) and,

$$K_o = \frac{1}{A_g}\left(\frac{G_{CL-in}\ G_{CL-out}}{G_{CL-in} + G_{CL-out} + G_{CL-sky}}\right) \tag{4.13}$$

$$K_s = \frac{1}{A_g}\left(\frac{G_{CL-in}\ G_{CL-sky}}{G_{CL-in} + G_{CL-out} + G_{CL-sky}}\right) \tag{4.14}$$

$$q_s = \frac{\Phi_o - \Phi_s}{\Phi_i - \Phi_o} \tag{4.15}$$

where K_o is the thermal exchange with the outside air (W m^{-2} K^{-1}), K_s is the thermal exchange with the sky (W m^{-2} K^{-1}), q_s is the coefficient for the influence of the sky temperature, G are the thermal coupling coefficients between the cladding and inside air, outside air and sky (W K^{-1}). These coefficients have been calculated with the equations given by Jolliet (1991).

The sky temperature (Φ_S) was calculated from the atmospheric longwave radiation assuming unit emissivity. The longwave radiation flux was obtained as the difference between the total radiation flux, measured by pyradiometer, and solar radiation, measured by pyranometer. The influence of the sky temperature is characterised by the ratio q_S. Jolliet, (1991) has also given the thermal coupling coefficients as follows;

Exchange between cladding and sky;

$$G_{CL-SKY} = F_{CL-SKY} A_{CL} R_{RAD} \tag{4.16}$$

with,

$$R_{rad} = 4\varepsilon_{CL} 5.67 \times 10^{-8} \theta_O^3 \tag{4.17}$$

where A_{CL} is the cladding area (m^2), F_{CL-SKY} is the fraction of sky seen from the cladding (0.5 for vertical and 0.8 for roof), ϵ_{CL} is the cladding emissivity for long wave radiation (0.90), and θ^o is outside temperature (K).

Exchange between cladding and outside air is as follow;

$$G_{CL-OUT} = A_{CL}\left[2.8 + 1.2v + \left(1 - F_{CL-SKY}\right)R_{RAD}\right] \tag{4.18}$$

where v is the wind speed (m s^{-1}). Exchange between cladding and inside air is given by;

$$G_{CL-IN} = \left[\frac{1}{A_{CL}\left(\frac{1}{U_{CL}} - \frac{1}{\alpha_{OUT}} \right)^{-1}} \right]^{-1} \tag{4.19}$$

where U_{CL} is the U-factor (thermal load coefficient per unit area) of the cladding (7.40 W m^{-2} K^{-1}) and α_{OUT} is 23 (W m^{-2} K^{-1}). The transfer of stored energy inside the crop protection structure involves the cover, inside air, crop and soil,

$$E_{ST} = E_{ST}^{COVER} + E_{ST}^{AIR} + E_{ST}^{SOIL} \tag{4.20}$$

Fernandez and Bailey (1992), and Bot and Van de Braak (1995) give in each case, the transfer of stored energy with the following equation;

$$E_{ST} = \frac{MC_p\left(\Phi_B - \Phi_E\right)}{t_E - t_B} \tag{4.21}$$

where M is the mass per unit greenhouse area (kg m^{-2}), Φ_B and Φ_E are the temperature (K) of the component at the beginning and at the end of the experiment respectively and t_B and t_E are the start and end times of the experiment respectively. Fernandez and Bailey (1992), Boulard and Baille (1994) and Bot and Van de Braak (1995) have combined equation 4.8, 4.9, 4.10, 4.11 and 4.21 to give the final ventilation rate by the energy balance (Φ_{EB}, $m^3m^{-2}s^{-1}$) as follow;

$$\Phi_{EB} = \frac{A_g}{\rho} \cdot \frac{\left[\left(\tau(1-p)I\right) - \left(U\frac{A_{cl}}{A_g}\left(\theta_i - \theta_o\right)\right) - \left(\frac{MC_p\left(\theta_B - \theta_E\right)}{t_E - t_B}\right)\right]}{\left[\lambda\left(W_i - W_o\right) + C_p\left(\theta_i - \theta_o\right)\right]} \qquad (4.22)$$

4.2.4 Neutral Plane

The theory of the stack effect by the neutral plane approach has been developed by many authors, such as Emswiler (1962), Brown and Solvason (1962), Bruce (1978), Timmons et al. (1984), Albright (1990), and Down *et al.* (1990). If the air inside the structure has a lower density than the outside air and outside wind speed is low, then air exchange by the stack effect will dominate through any suitable openings. Air will move into the structure through the lower openings and out through the higher ones. At a certain height $\bar{h}$, the pressures inside and outside the structure will be equal, and there will be no lateral air flow. The plane at this height is defined as the neutral plane.

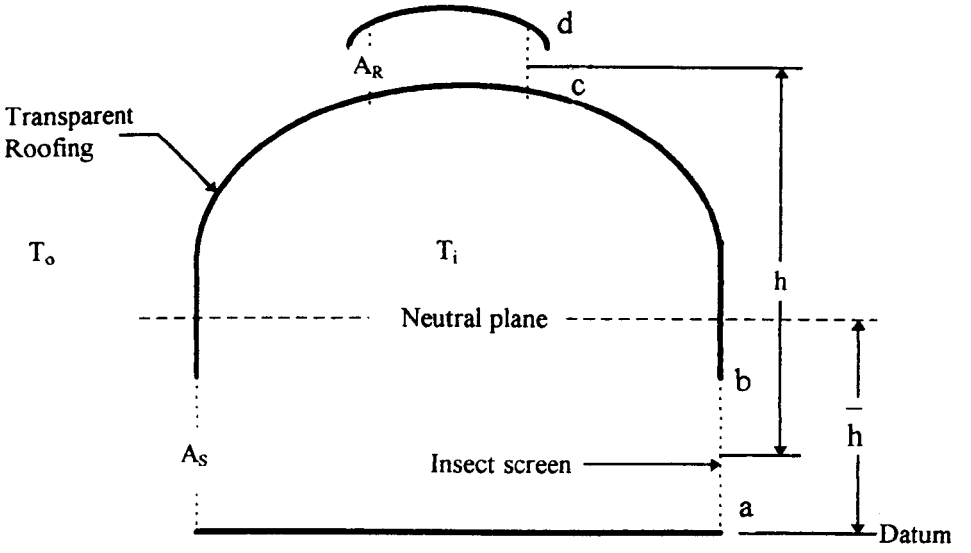

Figure 4.2. Schematic diagram of the crop protection structure showing the position of the neutral plane

Consider an opening area A in enclosure as shown in Figure 4.2. According to Bruce (1978), if the fluid densities on each side of the opening are different then natural convection take place through the opening due to differences in hydrostatic pressure. The fluid will move through the lower opening in one direction and at the upper opening the flow will be in the opposite direction. Somewhere at a height $\bar{h}$,

$$P_i(\bar{h}) = P_o(\bar{h}) = \bar{P} \tag{4.23}$$

where P_i and P_o are the pressure of inside and outside the room respectively, (Pa) and $\bar{P}$ is the pressure at the neutral plane (Pa). At the height $\bar{h}$, the lateral air is stagnant because both the pressures on both sides of the opening are equal. The pressures on each side of the opening at any height are given by;

$$P_i(h) = \bar{P} + \rho_i g(\bar{h} - h) \tag{4.24}$$

and,

$$P_o(h) = \bar{P} + \rho_o g(\bar{h} - h) \tag{4.25}$$

where ρ_i and ρ_o are the inside and outside air densities respectively (kg m^{-3}) and h is the variable height (m). The pressure difference across the opening at a height h is therefore given by;

$$P_i(h) - P_o(h) = g(\rho_i - \rho_2)(\bar{h} - h) \tag{4.26}$$

Applying Bernoulli's theorem which assumes that the pressure difference is converted to kinetic head with negligible loss then the velocity at a height h is found from

$$\frac{1}{2}\rho V^2 = g\Delta\rho(\bar{h} - h) \tag{4.27}$$

where V is the air velocity (m s^{-1}), g is the acceleration due to gravity (m s^{-2}) and $\Delta\rho$ is density difference (kg m^{-3}). It is assumed that no vertical density gradients exist and that $\rho \approx \rho_I \approx \rho_o$. The velocity of the fluid flow from the dense to the less dense side of the opening takes the same sign as ($\bar{h}$ - h) so that after taking the square root of equation (4.27) and re-arranging, the velocity at h is given by;

$$V = \frac{|\bar{h} - h|}{\bar{h} - h}\left[2g\frac{\Delta\rho}{\rho}|\bar{h} - h|\right]^{\frac{1}{2}} \tag{4.28}$$

where $|\bar{h} - h|$ is the modulus of $(\bar{h} - h)$. If the confined structure has a number of openings. The height of the neutral plane can be expressed as

$$\sum_{i=1}^{n}\int_{A_i}\frac{|\bar{h} - h|^{\frac{3}{2}}}{\bar{h} - h}\,dA = 0 \tag{4.29}$$

Once the height of the neutral plane is found from equation (4.29), and if there is no net flow across the opening area, the ventilation rate is determined by;

$$C_d\int_A V dA = 0 \tag{4.30}$$

where, C_d is the coefficient of discharge. By treating air is a perfect gas ($\Delta\rho/\rho \approx \Delta T/T$) and if we combined equation (4.28), (4.29), and (4.30) we have the neutral plane ventilation rate (Φ_{NP}, $m^3 s^{-1}$)

$$\Phi_{NP} = C_d\left[2g\frac{\Delta T}{T_o}\right]^{\frac{1}{2}}\sum_{i=1}^{n}\int_{A_i}\frac{|\bar{h} - h|^{\frac{3}{2}}}{\bar{h} - h}dA \tag{4.31}$$

For the typical crop protection structure shown in Figure 4.2, the neutral plane expression is;

$$\int_a^b \frac{|\bar{h}-h|^{\frac{3}{2}}}{\bar{h}-h} L_1 dh + \int_c^d \frac{|\bar{h}-h|^{\frac{3}{2}}}{\bar{h}-h} L_2 dh = 0 \qquad (4.32)$$

where L_1 and L_2 is the length of the side and roof openings respectively (m), subscripts a, b, c, and d are the height of the openings from the ground. According to Bruce (1978), equation (4.32) is a continuous modulus function and therefore is integrable. The following results are stated without proof;

$$\int |y|^n y^m dy = \frac{1}{n+m+1} |y|^n y^{m+1} \qquad \text{for } n+m \neq -1 \qquad (4.33)$$

$$\int |y|^n y^m dy = \left(\frac{|y|}{y}\right)^n \ln y \qquad \text{for } n+m = -1 \qquad (4.34)$$

from which,

$$\int |a-y|^n (a-y)^m dy = -\frac{1}{n+m+1} |a-y|^n (a-y)^{m+1} \qquad \text{for } n+m \neq -1 \qquad (4.35)$$

$$\int |a-y|^n (a-y)^m dy = -\left(\frac{|a-y|}{a-y}\right)^n \ln(a-y) \qquad \text{for } n+m = -1 \qquad (4.36)$$

Integration of equation (4.32) by application of equation (4.35), gives the neutral plane expression for the typical crop protection structure;

$$|\bar{h}-b|^{\frac{3}{2}} - |\bar{h}-a|^{\frac{3}{2}} + |\bar{h}-d|^{\frac{3}{2}} - |\bar{h}-c|^{\frac{3}{2}} = 0 \qquad (4.36)$$

According to the mass flow equation the total inflow $\Phi_{NP\text{-}in}$ ($m^3 s^{-1}$) is equal to the total outflow $\Phi_{NP\text{-}out}$ ($m^3 s^{-1}$). In the case of the crop protection structure shown in Figure 4.2,

$$2\Phi_{NP-IN} + 2\Phi_{NP-OUT} = 0 \tag{4.37}$$

Where,

$$\Phi_{NP-IN} = C_d\left[2g\frac{\Delta T}{T_o}\right]^{\frac{1}{2}}\int_a^b \frac{|\bar{h}-h|^{\frac{3}{2}}}{\bar{h}-h}Ldh \tag{4.38}$$

$$\Phi_{NP-out} = C_d\left[2g\frac{\Delta T}{T_o}\right]^{\frac{1}{2}}\int_a^b \frac{|\bar{h}-h|^{\frac{3}{2}}}{\bar{h}-h}Ldh \tag{4.39}$$

Theoretically the inlet air flow is equal to outlet air flow. Therefore, for inlet ventilation rate by the stack effect h can be substituted from equation (4.36) into equation (4.38). This then gives the general equation Φ_{NP} ($m^3\ m^{-2}\ s^{-1}$) as;

$$\Phi_{NP} = \frac{4}{3A_g}C_dLX\left[2g\frac{\Delta T}{T_o}\right]^{\frac{1}{2}} \tag{4.40}$$

where L is the length (m) and X is obtained from the integral (m) of openings at the typical crop protection structure. The heights of the side openings from the ground of the 1st, 2nd and 3rd level openings are 0.5, 1.0 and 1.5 m respectively. However, the height of the roof opening is constant at 0.3 m. The integral values of X are as follow;

First level, x = 0.637, if the neutral plane is above the side openings

Second level, x = 0.739, if the neutral plane intersects the openings

Third level, x = 0.993 if the neutral plane intersects the openings

4.3 Experimental design

Studies on natural ventilation by the stack effect have been conducted with the crop protection structure inside a four span Venlo glasshouse at Silsoe Research Institute, England. This empty large glasshouse (60 m x 12 m x 4 m) was chosen to simulate a natural hot environment with no disturbance from wind during the measurement period. The far end windows of the glasshouse were opened to facilitate minimal ventilation of the glasshouse and the internal airspeed was monitored and found to be less than 1.0 ms^{-1} throughout the studies. This is to satisfy the theory of the stack effect.

Plate 25. Crop protection structure inside the glasshouse

The crop protection structure, shown in Plate 25 was made full scale 5.8 m long, 3.0 m wide and 3.3 m high and is similar to the insect-proof rainshelter that has been developed in Malaysia. This pre-fabricated structure can be erected, dismantled

and transferred with minimal labour requirements. The structure was made of galvanised steel tubes, transparent polyethylene film, different insect screens and high tensile clips. Furthermore, the ground was covered with polyethylene sheet, 50 mm thick polycarbonate panels and black plastic sheet. This was to reduce CO_2 emission from the ground and insulate the ground from the heat absorbed.

In order to investigate the effect on ventilation rate, three different insect screens were chosen for the present studies. They were screens N50, N32 and N24 that are usually used in the tropics. N50 means the insect screen has 50 holes per inch. N50 has the smallest mesh and N24 the biggest. The effects of the screen mesh and ventilator opening size on natural ventilation were determined in nine sets of experiments shown in Table 4.1. For each experiment, the same screen was used to clad the continuous side and roof openings. Each side opening was 5.8 m long with heights of 0.5 m (level 1), 1.0 m (level 2) and 1.5 m (level 3) from the ground. However the fixed roof opening was 5.8 m long and 0.3 m high. Screen replacement was organised in the simple way by clamping them to the frames using high tensile clips. While each level was changed by covering the screen using the transparent polyethylene films from the roof eaves to the ground. The schematic of opening levels is presented in the Figure 4.3.

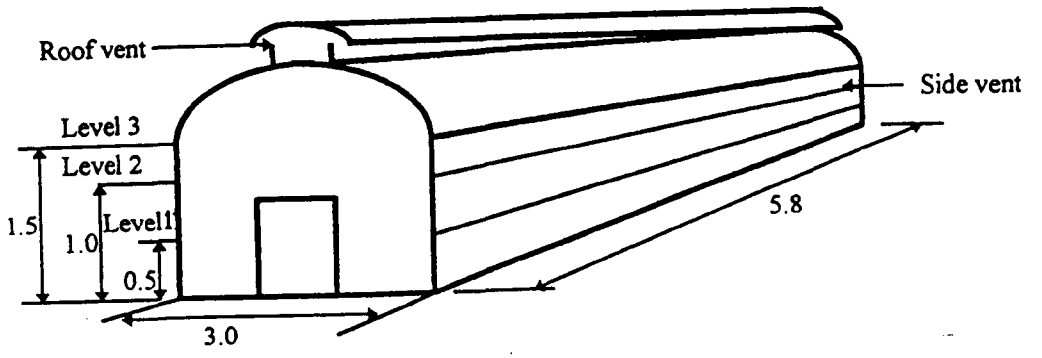

Figure 4.3 Schematic diagram of the roof and side ventilator openings.

Four methods for determining ventilation rates have been compared in these studies. They are the dynamic tracer gas, direct airspeed measurement, energy balance and neutral plane. The first is the control method. Data collection for all methods was carried out simultaneously for each set, for example screen N50 and level 1 and so on. The required parameters of each method are presented in Table 4.1.

Table 4.1 Experimental programme for stack effect studies

Screen	N50			N32			N24		
Method/Level	L1	L2	L3	L1	L2	L3	L1	L2	L3
1. Tracer gas	a,b	a,b	a,b	a,b	a,b	a,b	a,b	a,b	a,b
2. Airspeed	a,c	a,c	a,c	a,c	a,c	a,c	a,c	a,c	a,c
3. Energy balance	a,c,d,e	a,c,d,e	a,c,d,e	a,c,d,e	a,c,d,e	a,c,d,e	a,c,d,e	a,c,d,e	a,c,d,e
4. Neutral plane	a	a	a	a	a	a	a	a	a

Note : N50 means insect screen N50 and L1 means one vent openings on both sides. a = inside and outside temperature, b = gas decay and time , c = inside and outside airspeed, d = inside and outside solar radiation, d = inside and outside relative humidity.

Sensors to measure the required environmental variables were installed in the crop protection structure, the glasshouse and outside of glasshouse. Table 4.2 gives a list of the sensors and measured variables. The readings of all sensors and instruments were recorded every 1.0 minute using a data logging computer system (Data Measurement Software Package). All the sensors had been tested and calibrated by Silsoe Research Institute. However, another calibration was made before they were used.

Table 4.2 Variables measured during the experiments and sensors

Parameters	**Sensors**
Solar radiation	Pyranometer, PAR sensor
Total radiation	Pyrradiometer
Air temperature	Aspirated platinum resistance thermometer
Relative humidity	Electronic hygrometer
Dry and wet bulb temperature	Aspirated platinum resistance thermometer
Airspeed	Hot wire anemometer
CO_2 concentration	Infra red gas analyser

Temperature and humidity sensors inside an aspirated screen were placed inside and outside the crop protection structure. The aspirated screen was hung in the middle of the structure and outside. Solar radiation sensors were placed on the structure's floor and outside the glasshouse. Hot wire anemometers were also placed inside and outside the structure. The inside sensors were placed at the middle of the ventilation openings near the screens.

CO_2 gas was used as a tracer gas and was injected through a perforated pipe. To ensure the gas was uniformly distributed, many holes at different angles were punched in the pipe which lay around inside the structure. A fan was not used for mixing because the structure is highly porous at the side walls and it would also disturb the buoyancy force. When the desired concentration (1500 ppm) was reached, the supply of CO_2 was stopped and then the inside and outside air was sampled during the period of decreasing concentrated. The air from the 3 positions was mixed and pumped through an infra red gas analyser to measure the CO_2 concentration. These positions were at the middle, under the roof curvature and under the roof top, where there was a prevailing airflow as described in Chapter 3. In addition, the outside CO_2 concentrations were also determined. Plates 25, 26 and 27 show some of the sensors that were installed inside and outside the crop protection structure.

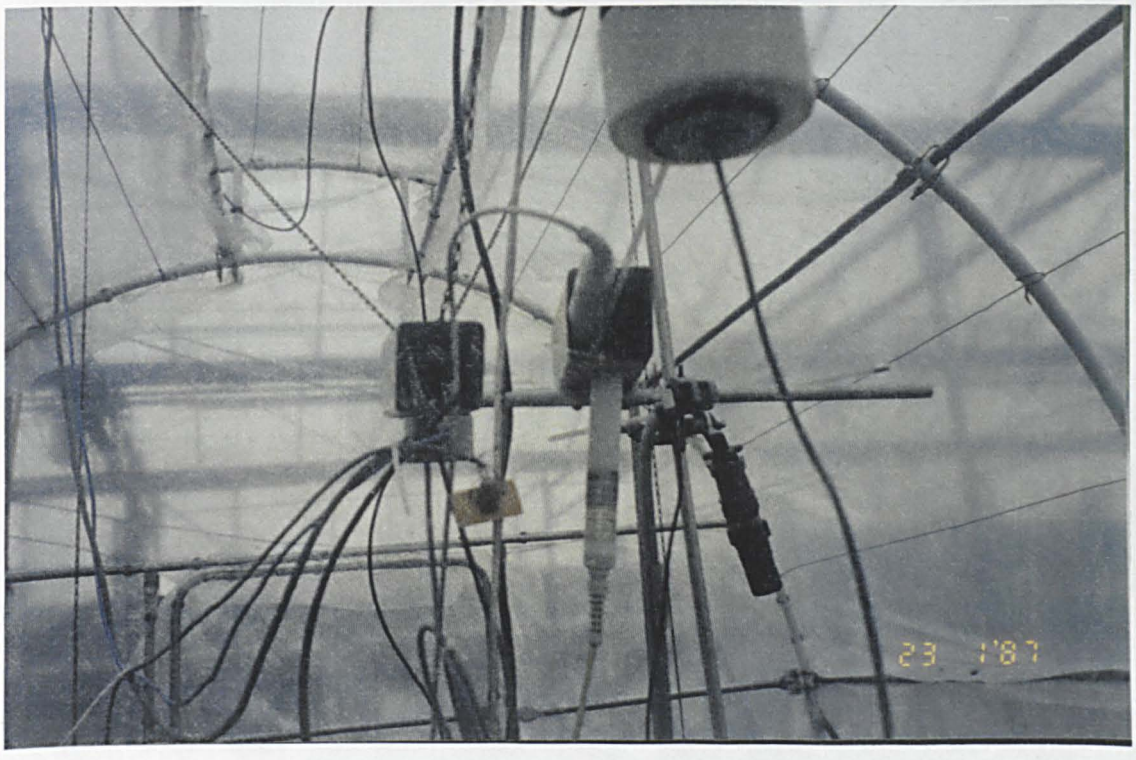

Plate 26. Instrumentation for climatic parameter measurement

Plate 27. Logging system for climatic parameter measurement

4.4 Results and discussion

4.4.1 Ventilation by tracer gas

There were 662 tracer gas decay measurements made in this study. A typical relationship between gas decay and time taken in the crop protection structure is presented in Figure 4.4. It was found that all measurements followed an exponential decay regression line that is in good agreement with the theory in section 4.2. In addition, the mean of coefficient of determination (R^2) is 0.9202. This shows a very strong correlation between gas decay and time. Therefore, about 96% of the data are accounted in the calculation and 4 % is not accounted due to the errors in the measurements. Errors could occur due to the external gas concentration which is assumed constant for equation 4.3, but in a real situation the external gas concentration is always fluctuating, but only the average concentration is taken in the calculation. Errors may be also due to the tracer gas not being perfectly mixed in the structure. The average times for the gas decay in these measurements were 8 to 15 minutes.

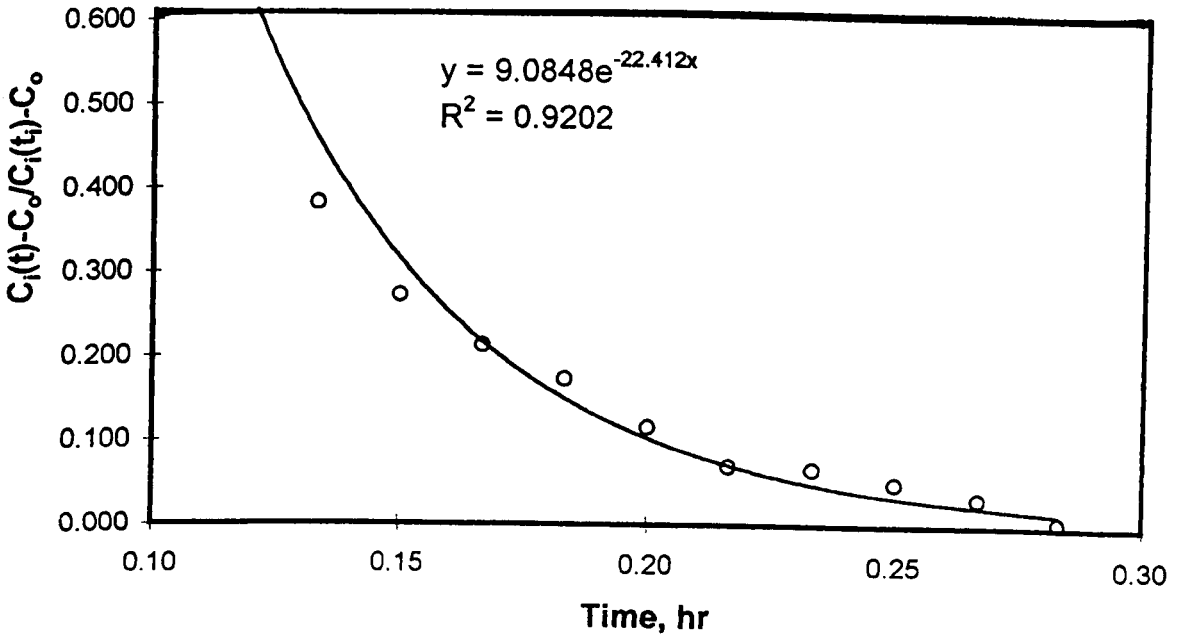

Figure 4.4 Relationship between tracer gas concentration and time

Natural ventilation rates determined by the tracer gas method are shown as a function of temperature difference in Figure 4.5 (a) - (c). They show that the measured ventilation rates increase with increasing temperature differences according to a power law. This shows the measured ventilation rates are in good agreement with the theoretical power curve in equation 4.40. The biggest opening areas exhibit the highest ventilation rates (Level 3 > Level 2 > Level 1). A similar trend in ventilation rates are also exhibited by the insect screen meshes (screen N24 > screen N32 > screen N50). Therefore, ventilation rates increase with the temperature difference and the size of ventilator openings which agrees with the findings of De Jong (1990) . In addition, the exchange rate is a function of the temperature difference and screen opening area which agrees with the findings of Bailey (1978).

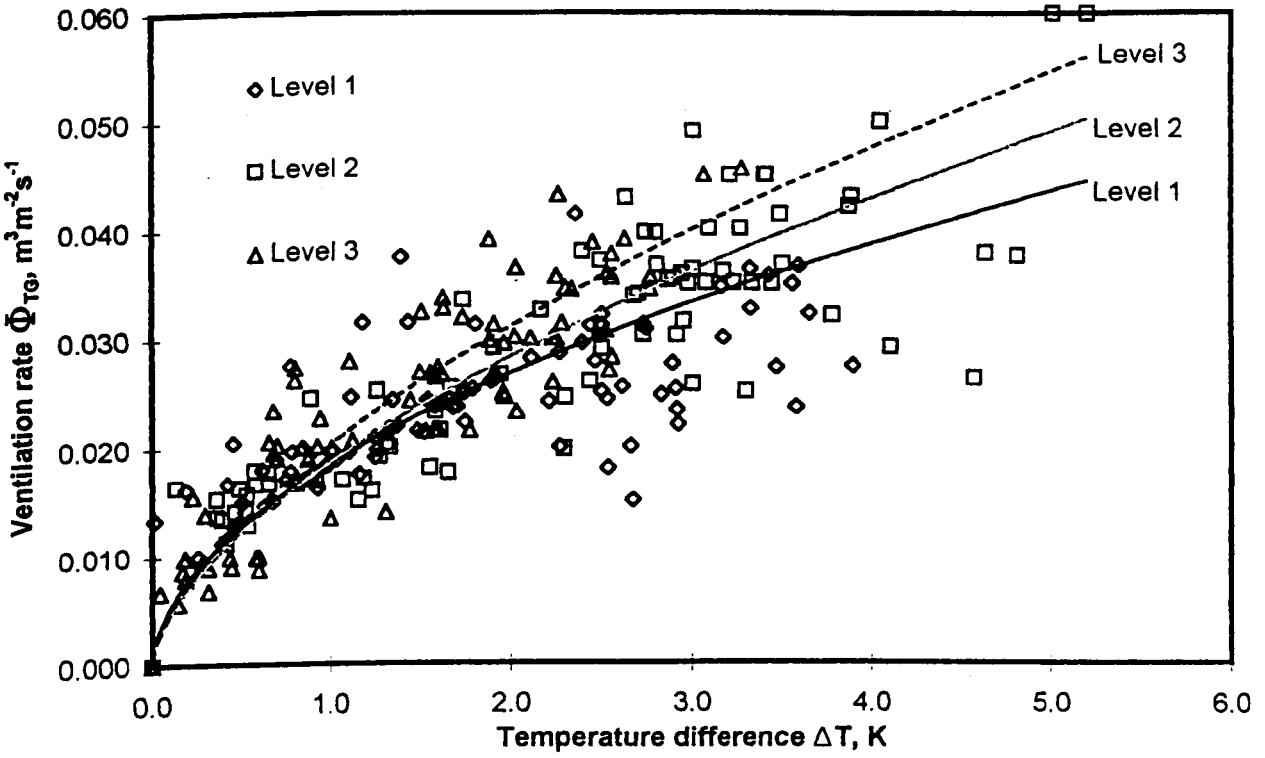

Figure 4.5 (a) Effect of opening levels covered with screen N50 on natural ventilation rate by stack effect using tracer gas method.

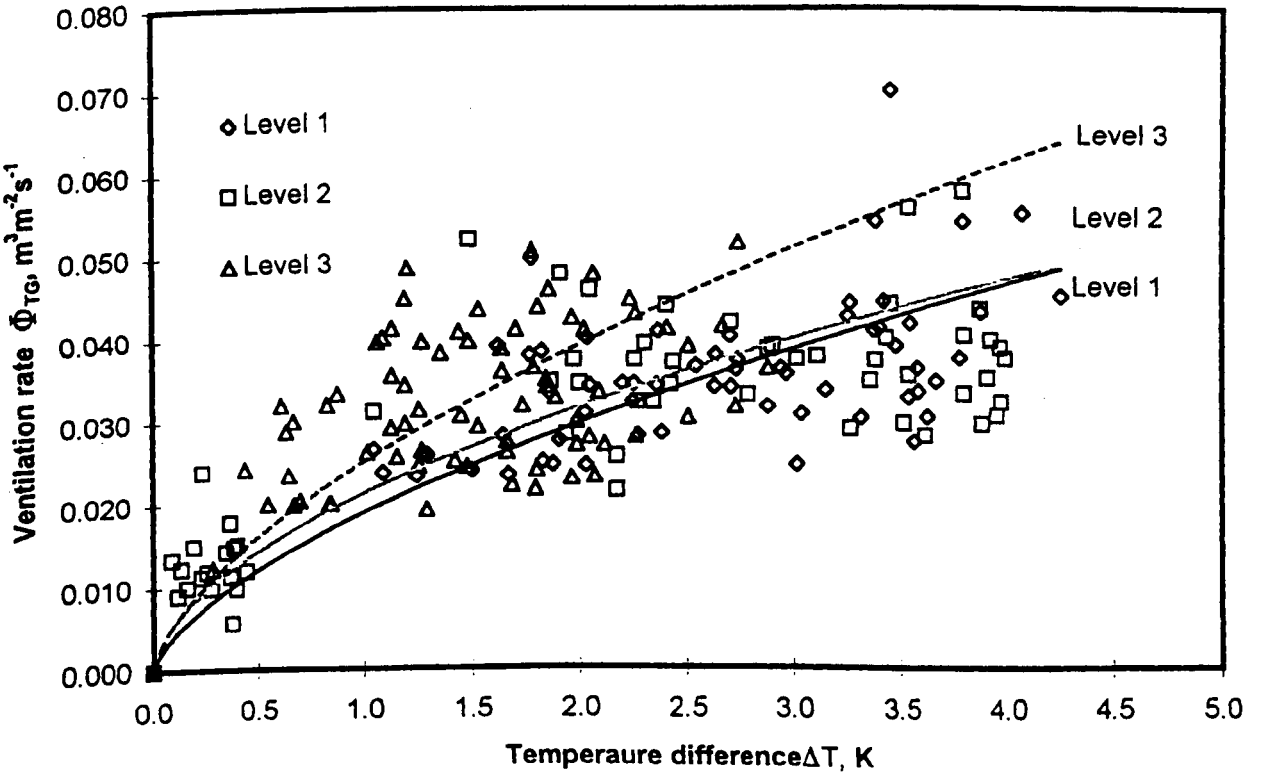

Figure 4.5 (b) Effect of opening levels covered with screen N32 on natural ventilation rate by stack effect using tracer gas method

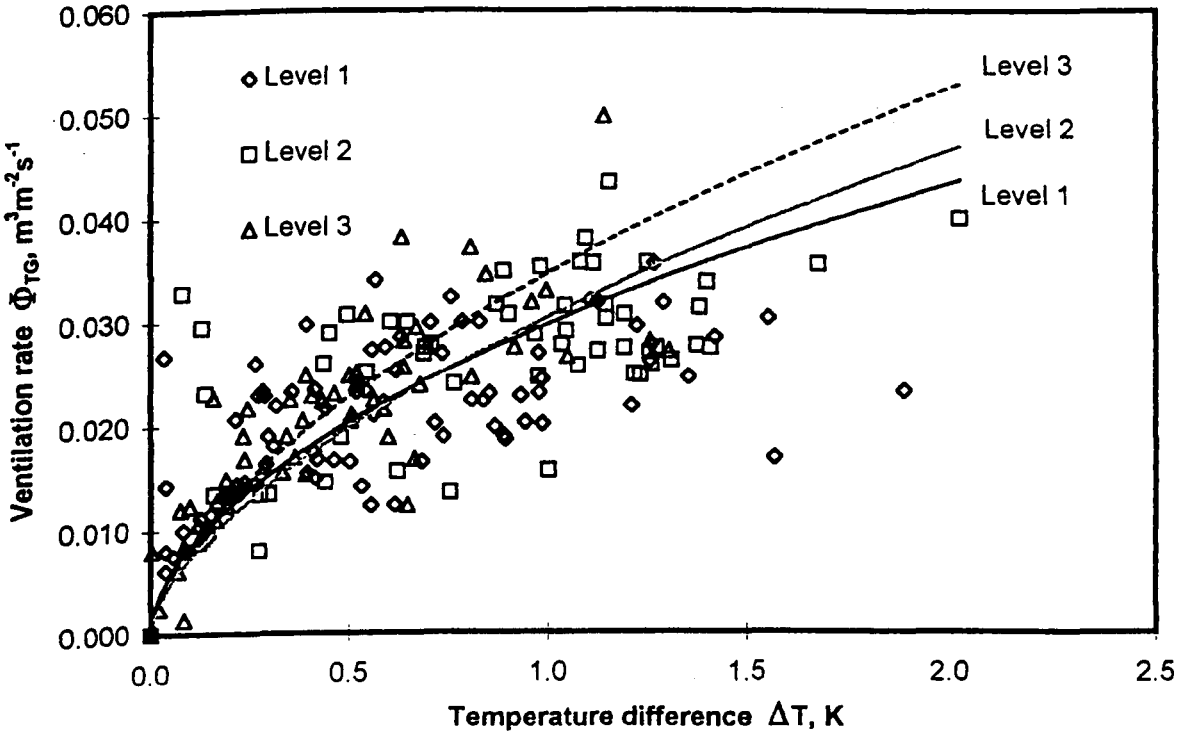

Figure 4.5 (c) Effect of opening levels covered with screen N24 on natural ventilation rate by stack effect using tracer gas method

The temperature differences are significantly affected by the size of the screen. Figure 4.5 shows screen N50 gives the higher temperature difference, followed by screen N32 and screen N24. This is due to fact that the smallest screen gives the lowest ventilation rate which results in a high temperature inside the structure. The summaries of the regression equations of the ventilation rates from Figure 4.5 are presented in Table 4.3.

Table 4.3 Regression equations of natural ventilation rates by the stack effect for the Crop Protection Structure. The equations are extracted from tracer gas decay method.

Screen/level	Level 1	Level 2	Level 3
Screen N24	$\Phi_{TG} = 0.0298\ \Delta T^{0.5447}$ Adj. R^2=0.7964 n = 82 S.E.$_C$ = 0.00070 S.E.$_\lambda$ = 0.03006	$\Phi_{TG} = 0.0304\ \Delta T^{0.6046}$ Adj. R^2=0.856 n = 56 S.E.$_C$ = 0.00077 S.E.$_\lambda$ = 0.03404	$\Phi_{TG} = 0.3460\ \Delta T^{0.6046}$ Adj. R^2=0.85595 n = 63 S.E.$_C$ = 0.00110 S.E.$_\lambda$ = 0.03146
Screen N32	$\Phi_{TG} = 0.0190\ \Delta T^{0.6431}$ Adj. R^2=0.95998 n = 61 S.E.$_C$ = 0.00025 S.E.$_\lambda$ = 0.01700	$\Phi_{TG} = 0.0213\ \Delta T^{0.5699}$ Adj. R^2=0.89783 n = 62 S.E.$_C$ = 0.00043 S.E.$_\lambda$ = 0.02460	$\Phi_{TG} = 0.0252\ \Delta T^{0.6415}$ Adj. R^2=0.90913 n = 74 S.E.$_C$ = 0.00038 S.E.$_\lambda$ = 0.02372
Screen N50	$\Phi_{TG} = 0.0186$ $\Delta T^{0..5299}$ Adj. R^2=0.84572 n = 97 S.E.$_C$ = 0.00028 S.E.$_\lambda$ = 0.02320	$\Phi_{TG} = 0.0187\Delta T^{0.6009}$ Adj. R^2=0.93509 n = 80 S.E.$_C$ = 0.00024 S.E.$_\lambda$ = 0.01780	$\Phi_{TG} = 0.0203\Delta T^{0.6152}$ Adj. R^2=0.93156 n = 87 S.E.$_C$ = 0.00024 S.E.$_\lambda$ = 0.01797

Note: Φ_{TG} is the ventilation rate by tracer gas method, ΔT is the temperature difference between inside and outside, n is the number of observation, Adj. R^2 is the adjusted coefficient of determination , S.E.$_C$ and S.E. λ are the standard of error of the ventilation coefficient (C) and power law index (λ) respectively.

All the regression equations in Table 4.3 satisfy the theoretical power curve as shown in equation 4.40. The very strong correlation between natural ventilation and temperature difference is exhibited by the high adjusted coefficients of determination (Adj. R^2). The adjusted R^2 is defined in section 6.4.1. In addition, the series of results show consistently increasing values of ventilation coefficient and uniformly values of power curves. The ventilation coefficient increases with increasing screen size and ventilator opening.

The statistical test on regression equations shows that the values of standard error for the ventilation coefficient ($S.E_C$) and power law index (S.E $_\lambda$) are small. In addition, their probability values are less than 5% level of significance. Therefore, the

tracer gas method can be used to quantify natural ventilation rate in crop protection structure. In general the regression equations can be formulated as;

$$\Phi_{TG} = C\Delta T^{\lambda} \tag{4.41}$$

where Φ_{TG} is the tracer gas ventilation rate ($m^3\ m^{-2}\ s^{-1}$), C is the ventilation coefficient (dimensionless), ΔT is the temperature difference (K) and λ is the power law index (dimensionless).

The power law indices are almost constant between 0.530 to 0.643 for the nine sets of data. Table 4.4 summarises the power law indices and the correlation between ventilation rate and temperature difference. The mean value of the power law index is 0.596 which is close to the theoretical value 0.5. Therefore, the general power equation proposed by Bruce (1978) for any geometry and openings can be used in this study.

Table 4.4 Ventilation power law index value by tracer gas method

Descriptive statistics	**n**	$\bar{X}$	**max**	**min**	**s**	σ_{n-1}
Value of power, λ	9	0.596	0.643	0.530	0.002	0.040
Adjusted coefficient of determination, Adj. R^2	9	0.889	0.960	0.799	0.003	0.052

Moreover, the ventilation coefficients increase with increasing screen size and opening area. They follow the power decay curve that shows very strong correlation between ventilation coefficient and screen size. This can be clearly seen in Figure 4.6. The figure is also shows the standard error for each ventilation coefficient.

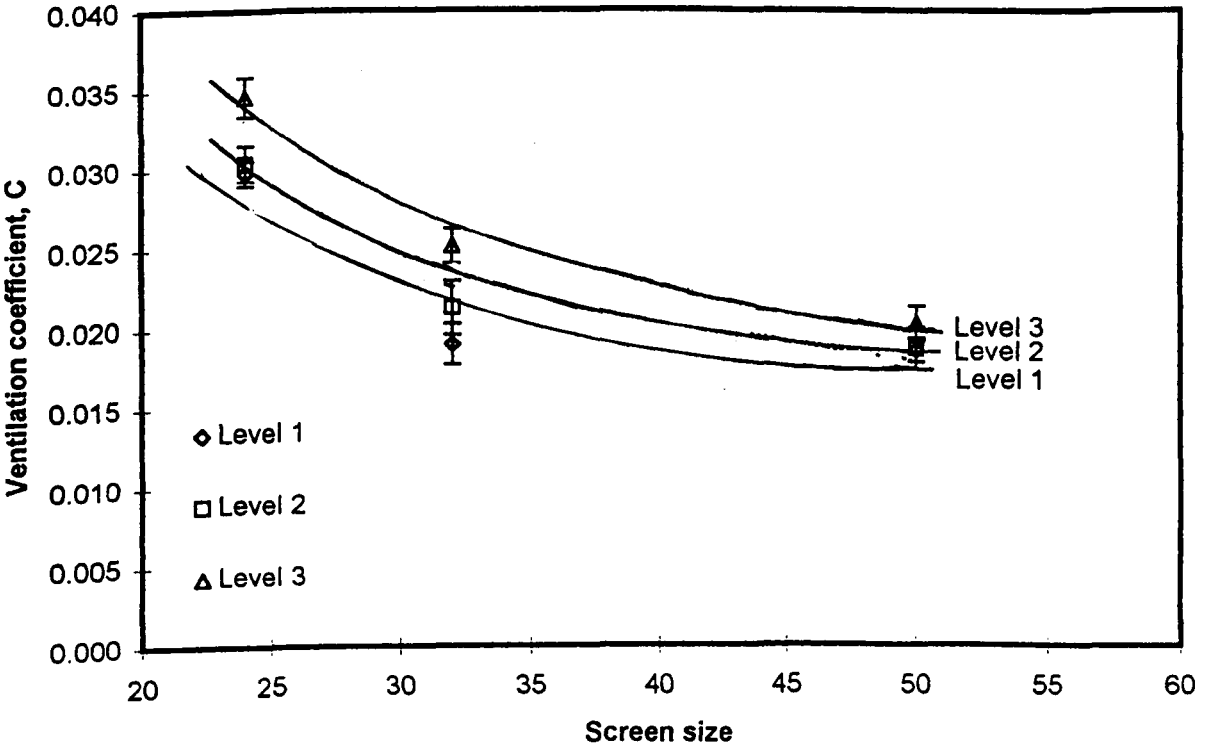

Figure 4.6 Effect of screen size and ventilator opening on ventilation coefficient

4.4.2 Ventilation by direct air measurement

Direct airspeed measurement is also one of the method used in these studies. It was found that all airspeed data lay between 0.05 and 0.5 ms^{-1}. These airspeeds are within the measurement accuracy of the instrument (54N10 Multi channel Flow Analyser). Typical airspeed data for screen N32 at level 1 is presented in Table 4.5. The mean of the airspeeds measurement outside the model but inside the glasshouse is 0.266 ms^{-1}. This airspeed is lower than the wind speeds of 1.5 - 2.0 ms^{-1}, which satisfies the stack effect requirement proposed by Bot (1983), De Jong (1990), Kittas *et al.* (1997) and Miguel *et al.* (1998).

Table 4.5. Typical air speed data for screen N32 at level1

Measured airspeed (ms^{-1})	n	$\overline{x}$	max	min	s	σ_{n-1}
Outside of the structure	45	0.266	0.372	0.141	0.002	0.047
Inside near the side screen	45	0.169	0.236	0.093	0.001	0.028
Inside near the roof screen	45	0.340	0.447	0.096	0.006	0.077

The relationship between ventilation rate and temperature difference by direct airspeed measurement method is shown in Figure 4.7 (a) - (c). These show the measured ventilation rates increase with increasing temperature difference according to the power law. This trend is similar to the tracer gas method and in good agreement with theoretical equation 4.40. Similar trends are also exhibited where the biggest ventilator opening (Level 3 > Level 2 > Level 1) and the biggest screen size (screen N24 > screen N32 > screen N50) gives the highest ventilation rate.

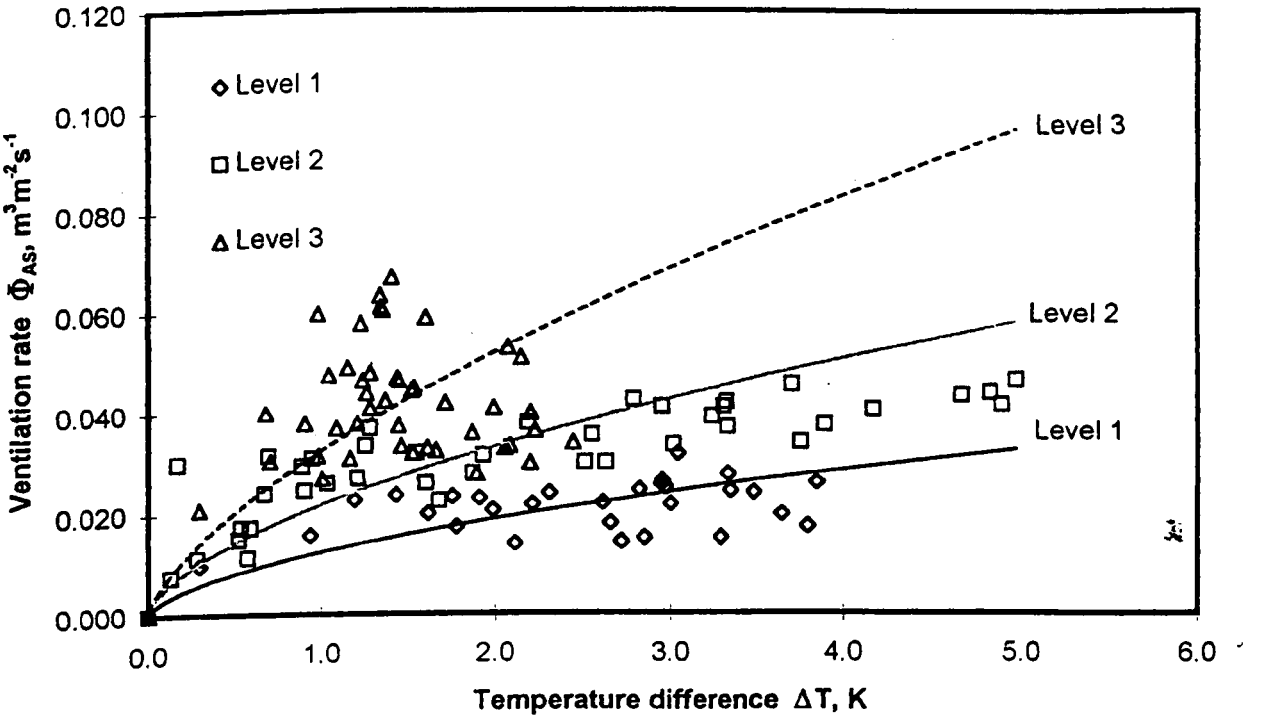

Figure 4.7 (a). Effect of ventilator opening and screen N50 on natural ventilation rate by the stack effect using the direct airspeed measurement method

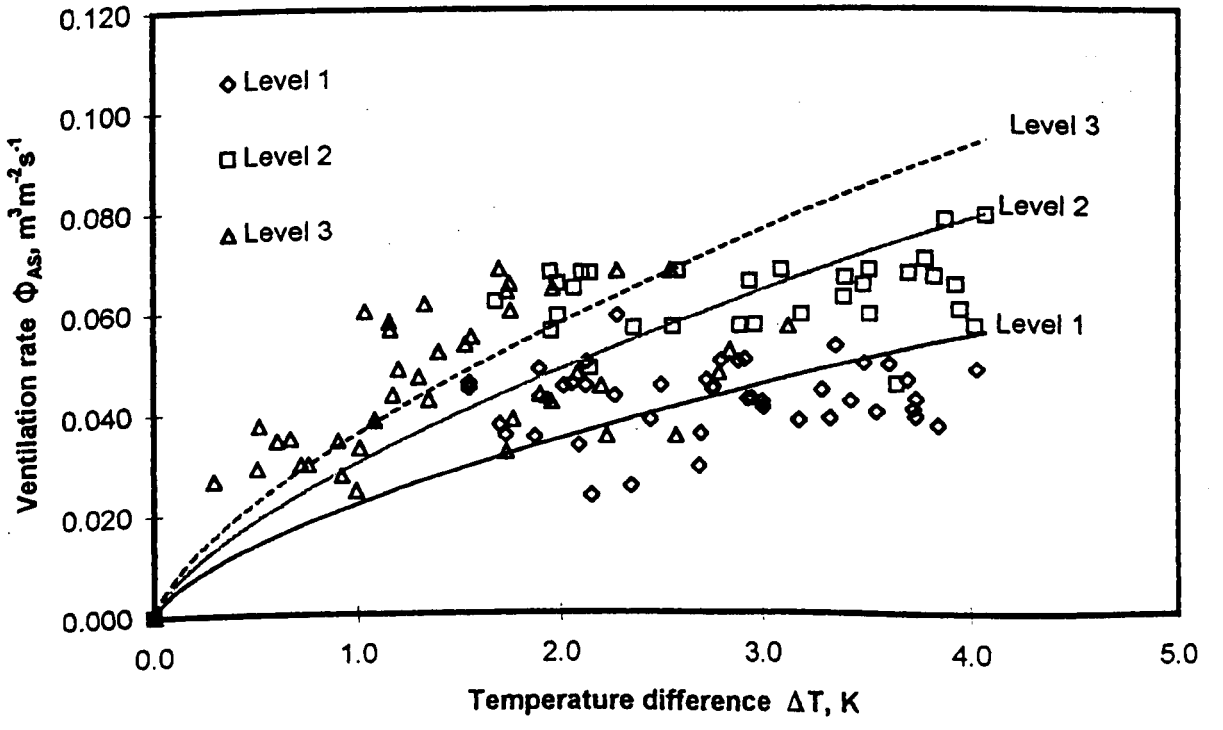

Figure 4.7 (b). Effect of ventilator opening and screen N32 on natural ventilation rate by the stack effect using the direct airspeed measurement method

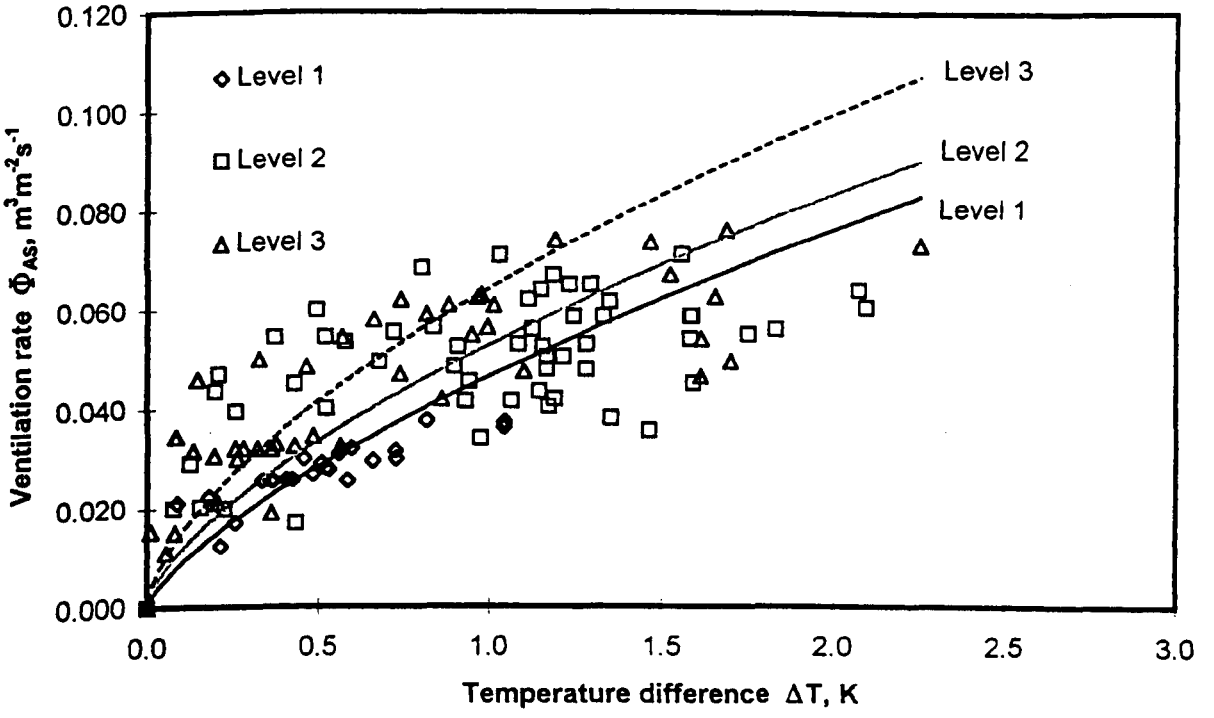

Figure 4.7 (c). Effect of ventilator opening and screen N24 on natural ventilation rate by the stack effect using the direct airspeed measurement method

Typical ventilation rates for side ventilator (lower) and roof ventilator (upper) openings are shown in Figure 4.8 (a)-(c). They show the relationship between air inlet and outlet with reference the neutral plane proposed by Bruce (1978). The inlet and outlet ventilation rates are close to each other which means that they are in accordance with the mass flow law. In addition, they show that the predicted neutral plane position agrees with the position calculated in equation 4.29.

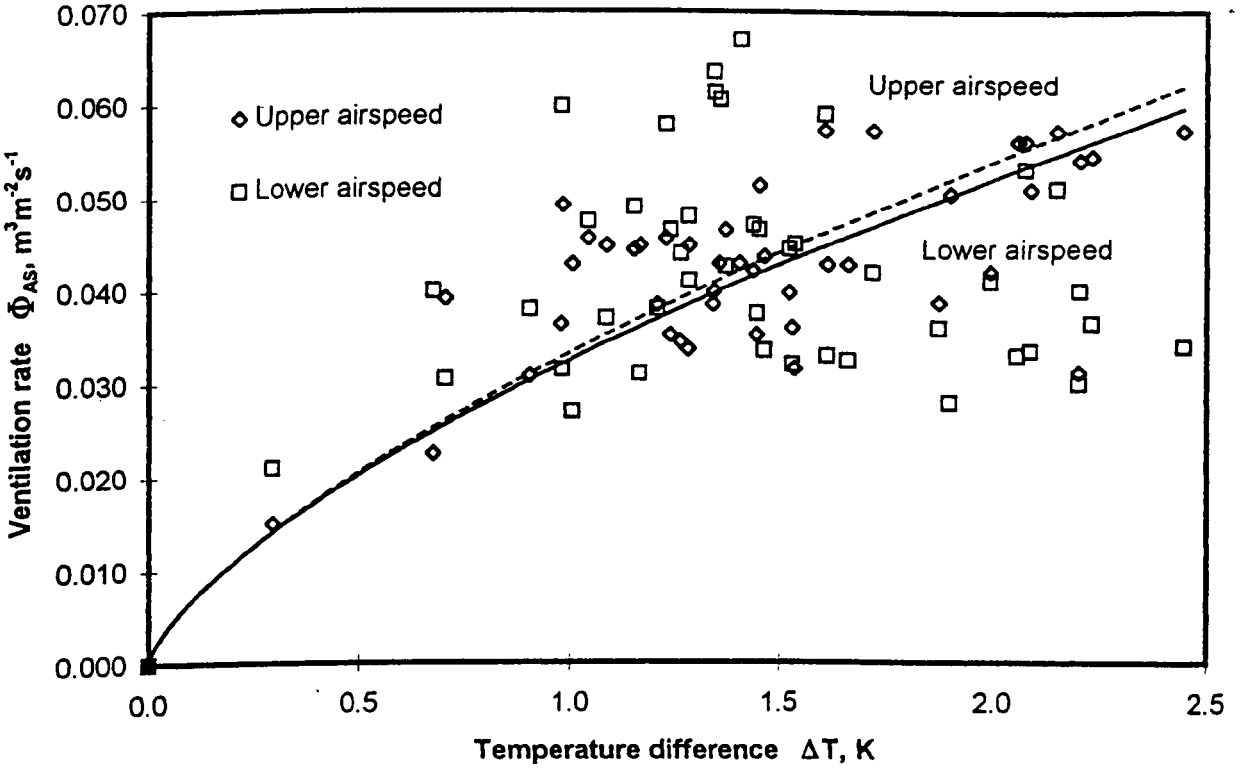

Figure 4.8 (a). Relationship between side and roof opening ventilation rates for screen N50 at level 3 using the direct airspeed measurement method

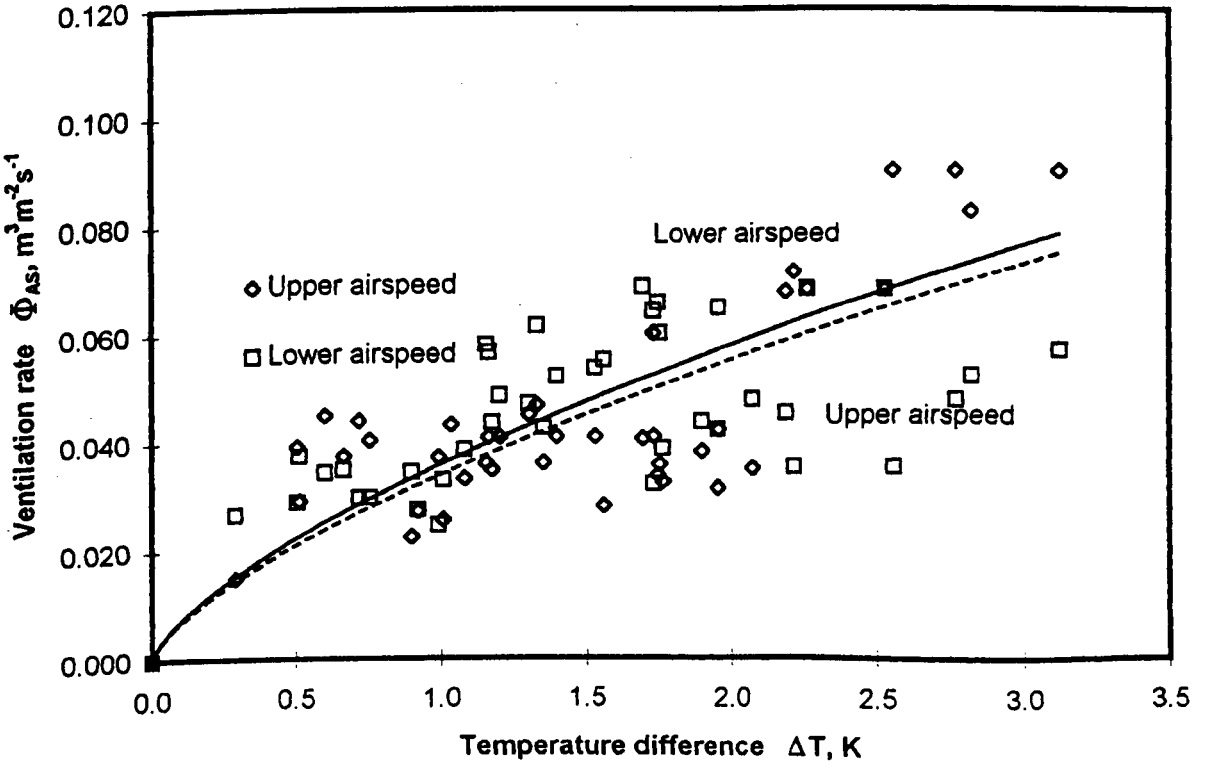

Figure 4.8 (b). Relationship between side and roof opening ventilation rates for screen N32 at level 3 using the direct airspeed measurement method

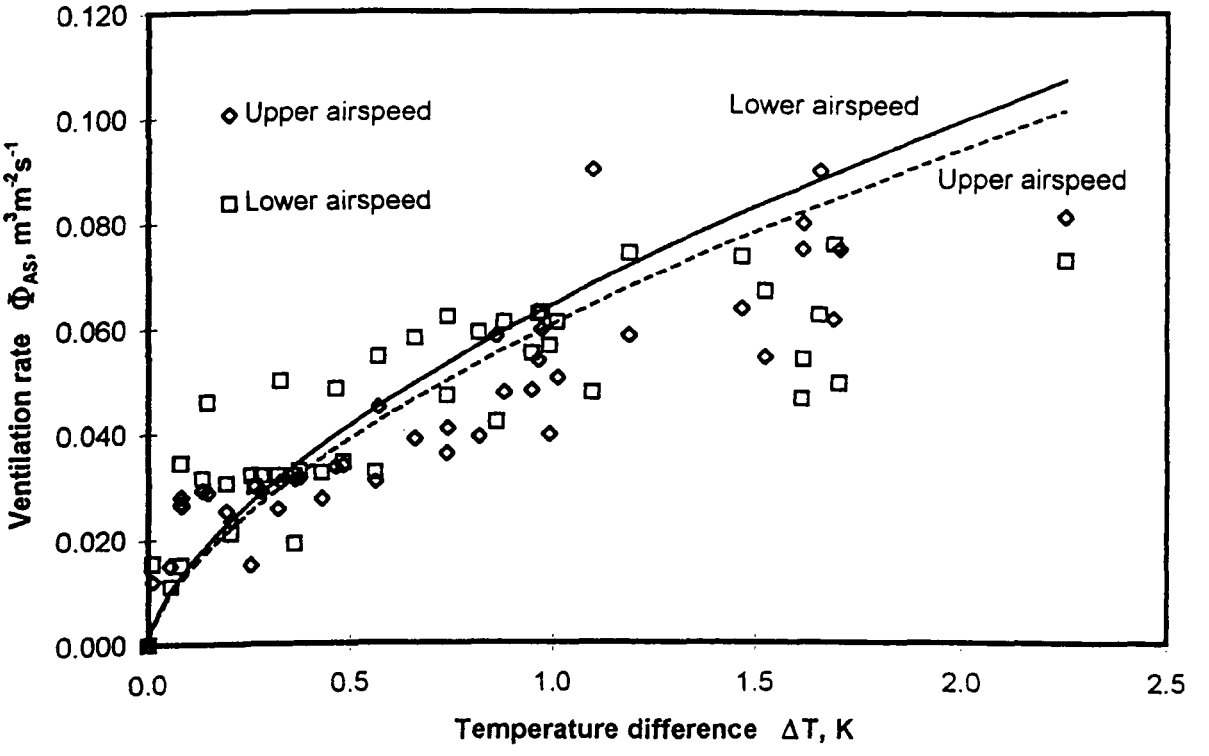

Figure 4.8 (c). Relationship between side and roof opening ventilation rates for screen N24 at level 3 using the direct airspeed measurement method

The effect of screen size is highly significant on the temperature difference between inside and outside the structure. Figure 4.7(a) - (c) also shows that screen N50 gives the highest temperature difference, followed by screen N32 and screen N24. This follows the trend that the smaller ventilator opening reduces the ventilation rate which consequently increases the internal sensible heat and water vapour pressure. A summary of regression the equations is presented in Table 4.6.

Table 4.6 Regression equations of natural ventilation rate by the stack effect for Crop Protection Structure. These results are extracted from the inlet airspeed method.

Screen/level	Level 1	Level 2	Level 3
Screen N24	$\Phi_{AS} = 0.0466\ \Delta T^{0.7113}$ Adj. $R^2 = 0.97176$ n = 24 S.E.C = 0.00130 S.E.λ = 0.02527	$\Phi_{AS} = 0.0529\ \Delta T^{0.6574}$ Adj. $R^2 = 0.88429$ n = 56 S.E.C = 0.00126 S.E.λ = 0.03203	$\Phi_{AS} = 0.0644\ \Delta T^{0.6300}$ Adj. $R^2 = 0.86389$ n = 44 S.E.C = 0.00233 S.E.λ = 0.03806
Screen N32	$\Phi_{AS} = 0.0022\ \Delta T^{0.6431}$ Adj. $R^2 = 0.96380$ n = 46 S.E.C = 0.00036 S.E.λ = 0.01894	$\Phi_{AS} = 0.0302\ \Delta T^{0.6861}$ Adj. $R^2 = 0.98229$ n = 32 S.E.C = 0.00050 S.E.λ = 0.01654	$\Phi_{AS} = 0.0360\ \Delta T^{0.682}$ Adj. $R^2 = 0.94594$ n = 42 S.E.C = 0.00075 S.E.λ = 0.02545
Screen N50	$\Phi_{AS} = 0.0125\ \Delta T^{0.6000}$ Adj. $R^2 = 0.96036$ n = 30 S.E.C = 0.00029 S.E.λ = 0.02304	$\Phi_{AS} = 0.0218\Delta T^{0.6083}$ Adj. $R^2 = 0.93073$ n = 41 S.E.C = 0.00051 S.E.λ = 0.02621	$\Phi_{AS} = 0.0326\Delta T^{0.6770}$ Adj. $R^2 = 0.93049$ n = 45 S.E.C = 0.00070 S.E.λ = 0.02787

Note : Φ_{AS} is the ventilation rate by direct airspeed measurement, ΔT is the temperature difference between inside and outside, n is the number of observation, Adj. R^2 is the adjusted of coefficient of determination respectively, S.E.C and S.E. λ are the standard of error of the ventilation coefficient (C) and power law index (λ) respectively.

The regression equations obtained from the direct airspeed measurements are found to be good in agreement those of the tracer gas method. They follow the same best power curve law and have very strong correlation values. Table 4.7 shows the mean value of power law index that is 0.657 and Adjusted R^2 is 0.944. Two samples for variance F-test shows that the power curve law indices from the direct air speed measurement and the tracer gas method have no statistically different at the 5% level of significance. That means the direct airspeed measurement method is closer to tracer gas method. Therefore, the direct airspeed measurement can be used in predicting natural ventilation rate.

Table 4.7 Ventilation power curve values by direct airspeed measurement method taken at the side and roof openings

Descriptive statistics	n	$\bar{x}$	max	min	s	σ_{n-1}
Value of power, λ	18	0.657	0.7113	0.600	0.001	0.035
Adjusted coefficient of determination, Adj. R^2	18	0.944	0.987	0.867	0.002	0.037

A similar trend of ventilation coefficient is also observed in this method. The coefficients increase with the increasing screen size and opening area. They follow the power decay curve that shows very strong correlation between ventilation coefficient and screen size. This can be clearly seen in Figure 4.9., which also shows the standard error for the ventilation coefficients.

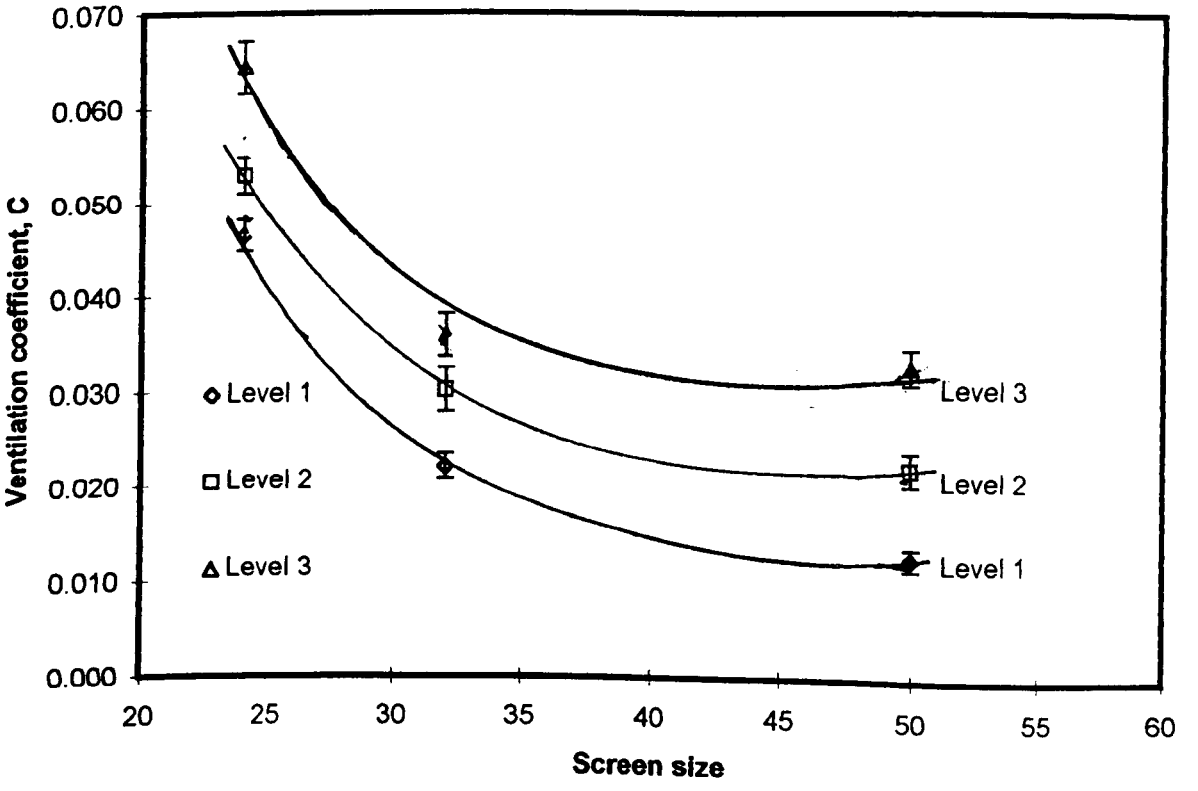

Figure 4.9 Effect of screen size and ventilator opening on ventilation coefficient by the direct airspeed measurement method

4.4.3 Ventilation by energy balance

The energy balance method considers a number of factors such as the solar intensity, solar radiation transmittance, ambient temperature, humidity, covering material properties and crop physical process in the natural ventilation calculation. However, the effect of crop on natural ventilation in this study was excluded because of small temperature difference was observed. Sometimes the internal temperature of crop protection structure was higher than the external. This was due to the transpiration of crop and higher humidity inside the structure. The lower internal temperature than the external is not the critical issue in the tropic greenhouses. Energy losses and gains in the crop protection structure have been calculated according to equation 4.22 and the results are presented in Figure 4.10 (a)-(c).

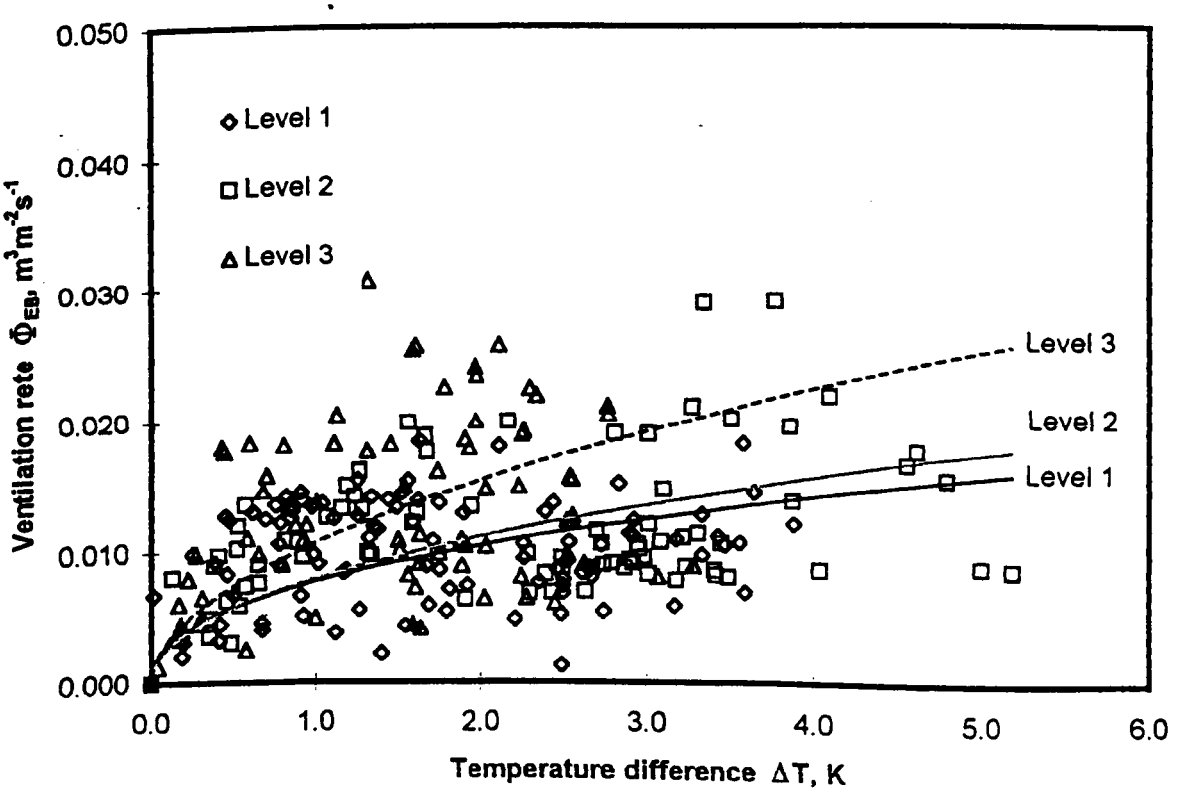

Figure 4.10 (a) Effect of opening level and screen N50 on natural ventilation rate by the stack effect using the energy balance method.

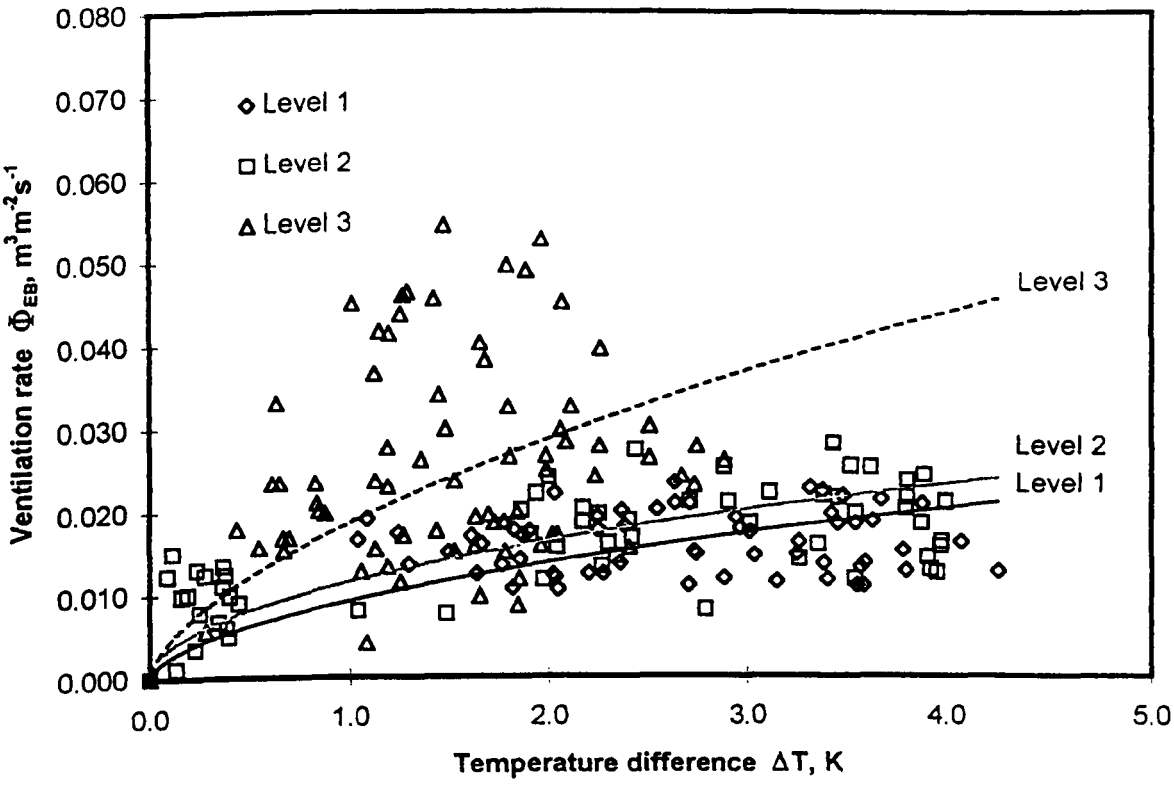

Figure 4.10 (b) Effect of opening level and screen N32 on natural ventilation rate by the stack effect using the energy balance method

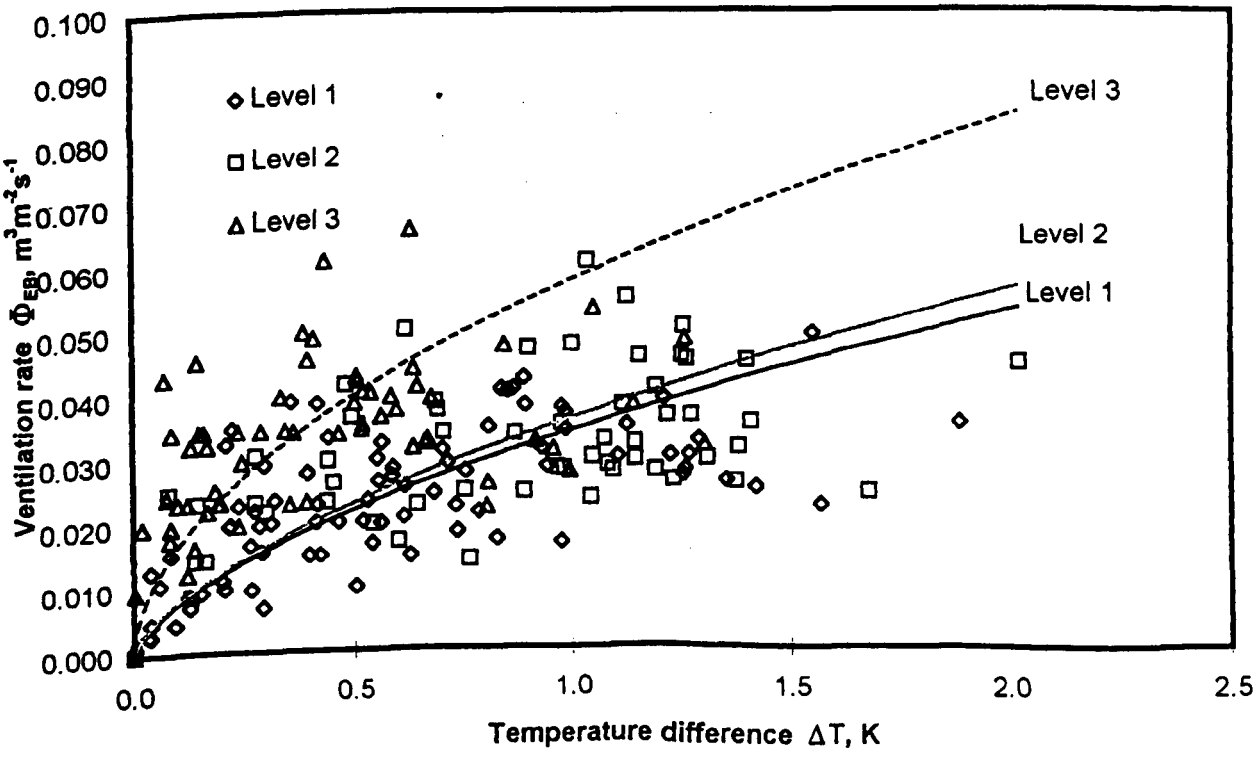

Figure 4.10 (c) Effect of opening level and screen N24 on natural ventilation rate by the stack effect using the energy balance method

Figure 4.10 shows that the ventilation rate is a function of temperature difference that follows the power curve shown by the tracer gas method. Ventilation rates substantially increase with increasing of temperature difference according to power curve law. This is in good agreement with the theory and curve produced by Walker *et al.* (1983). Ventilation rates also increase with increasing of ventilator opening (Level 3 > Level 2 > Level 1) and screen size (screen N24 > screen N32 > screen N50). This trend is clearly seen in that screen N50 and screen N24 at level 3 give ventilation rates at a temperature difference of 1 K of 0.0107 and 0.0577 $m^3 m^{-2} s^{-1}$ respectively. In general these results are in agreement with the findings of Fernandez and Bailey (1992), and Bot *et al.* (1995) A summary of the regression equations of the ventilation rates from Figure 4.10 (a)-(c) are presented in Table 4.8.

Table 4.8 Regression equations of natural ventilation rates by stack effect for the Crop Protection Structure using energy balance method.

Screen/level	Level 1	Level 2	Level 3
Screen N24	$\Phi_{EB} = 0.0342\Delta T^{0.6240}$ Adj. $R^2 = 0.8340$ n = 82 $S.E._C = 0.00081$ $S.E._\lambda = 0.03090$	$\Phi_{EB} = 0.0361\ \Delta T^{0.5288}$ Adj. $R^2 = 0.86830$ n = 56 $S.E._C = 0.00090$ $S.E._\lambda = 0.03338$	$\Phi_{EB} = 0.0577\ \Delta T^{0.5288}$ Adj. $R^2 = 0.73243$ n = 63 $S.E._C = 0.00235$ $S.E._\lambda = 0.04047$
Screen N32	$\Phi_{EB} = 0.0093$ $\Delta T^{0.5664}$ Adj. $R^2 = 0.90550$ n = 61 $S.E._C = 0.00017$ $S.E._\lambda = 0.02360$	$\Phi_{EB} = 0.0116\ \Delta T^{0.5031}$ Adj. $R^2 = 0.78435$ n = 62 $S.E._C = 0.00319$ $S.E._\lambda = 0.03370$	$\Phi_{EB} = 0.0187\ \Delta T^{0.6175}$ Adj. $R^2 = 0.75385$ n = 74 $S.E._C = 0.00049$ $S.E._\lambda = 0.04121$
Screen N50	$\Phi_{EB} = 0.0077$ $\Delta T^{0.4302}$ Adj. $R^2 = 0.54339$ n = 97 $S.E._C = 0.00020$ $S.E._\lambda = 0.04003$	$\Phi_{EB} = 0.0079\Delta T^{0.4821}$ Adj. $R^2 = 0.72848$ n = 80 $S.E._C = 0.00018$ $S.E._\lambda = 0.03303$	$\Phi_{EB} = 0.0107\Delta T^{0.5308}$ Adj. $R^2 = 0.6908$ n = 87 $S.E._C = 0.00027$ $S.E._\lambda = 0.03819$

Note: Φ_{EB} is the ventilation rate by tracer gas method, ΔT is the temperature difference between inside and outside, n is the number of observation, Adj. R^2 is the adjusted coefficient of determination, $S.E._C$ and $S.E._\lambda$ are the standard of error of the ventilation coefficient (C) and power curve (λ) respectively.

All regression equations in the table 4.8 satisfy the theoretical power curve law of equation 4.40. The strong correlation between natural ventilation and temperature difference is exhibited by the high adjusted coefficients of determination (Adj. R^2). The mean of adjusted R^2 and power law index are 0.763 and 0.535 respectively. This index is not statistically different to that obtained with the tracer gas method, at the 5% level of significance. In addition, the series of results show consistency of the ventilation coefficient (C) and similar power law indices (λ). The ventilation coefficient increases with increasing size of screen and ventilator opening. The smallest range of temperature difference was observed for the biggest ventilator opening and screen size. This is due to the higher ventilation rates that reduced the internal temperature of the structure.

4.4.4 Ventilation by neutral plane

Ventilation rates obtained as a function of temperature difference, ventilator opening and screen size are presented in Figure 4.11 (a) - (c). These ventilation rates were calculated from equation 4.40 and coefficient of discharge from Table 3.6. The figures show that all the regression equations are in good agreement with the theoretical law index 0.5 that is proposed by Bruce (1978), Bot (1983), De Jong (1990) and Wang (1998). Ventilation rates increase with increasing ventilator openings (Level 3 > Level 2 > Level 1) and screen size (screen N24 > screen N32 > screen N50).

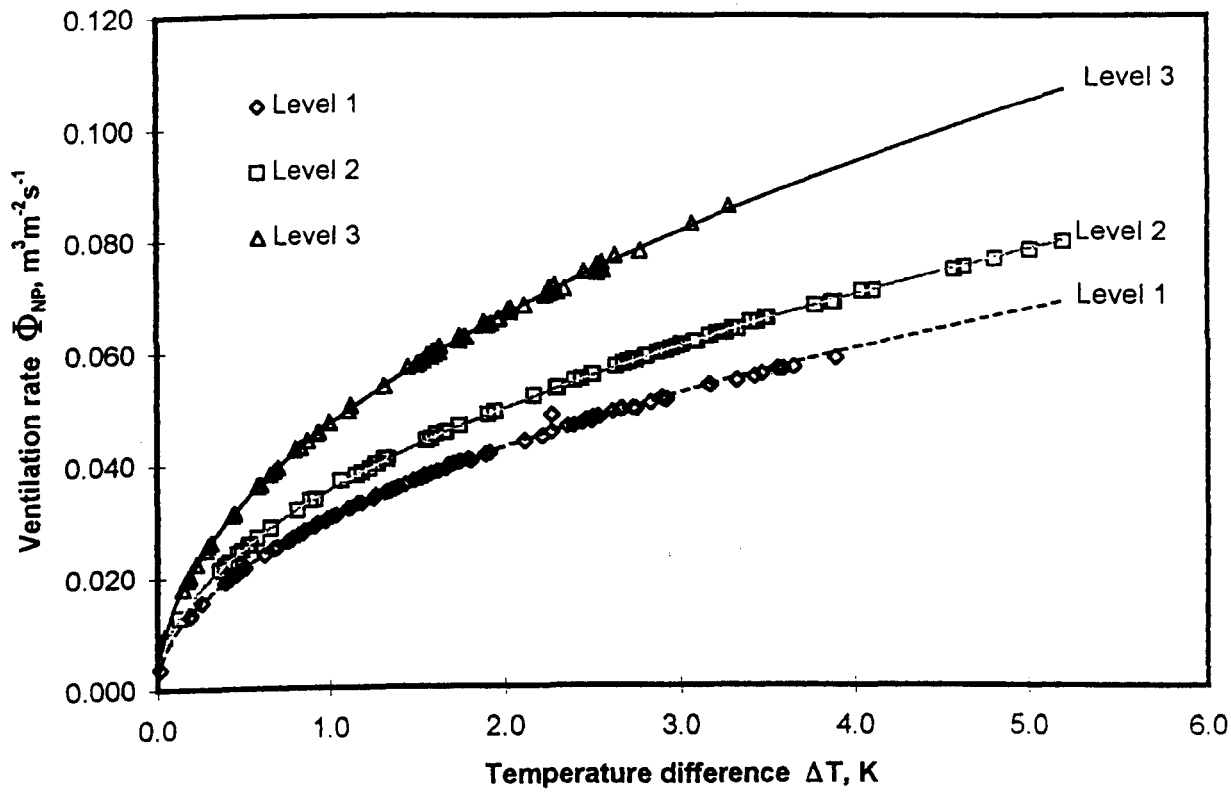

Figure 4.11 (a) Effect of opening level and screen N50 on natural ventilation rate by the stack effect using the neutral plane method

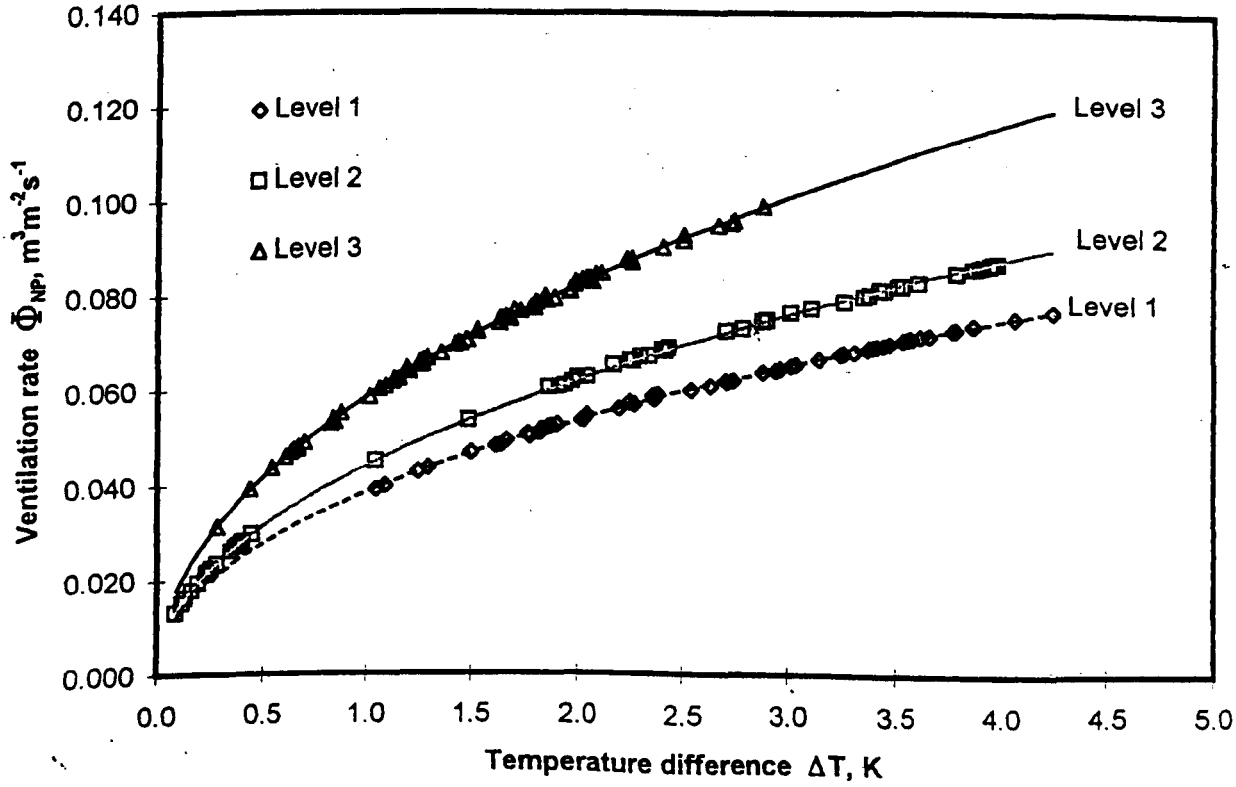

Figure 4.11 (b) Effect of opening level and screen N32 on natural ventilation rate by the stack effect using the neutral plane method

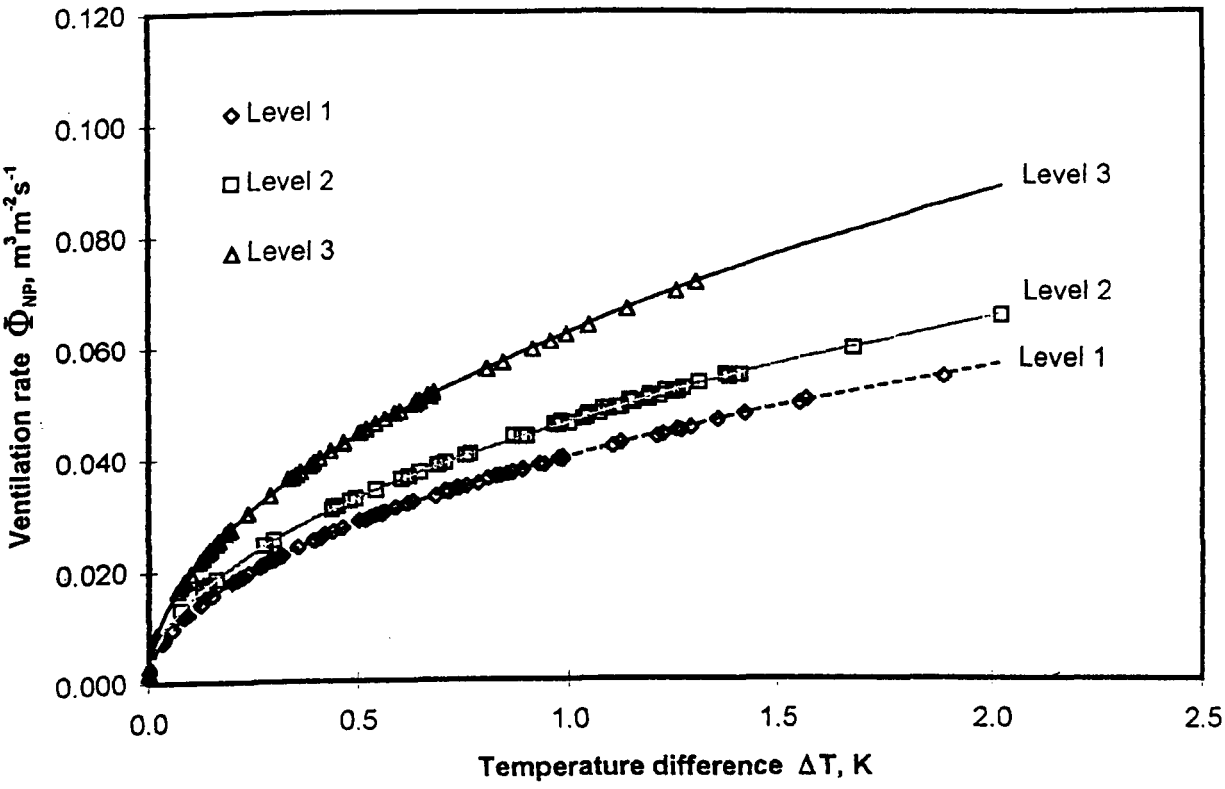

Figure 4.11 (c) Effect of opening level and screen N24 on natural ventilation rate by the stack effect using the neutral plane method

A summary of regression equations of the ventilation rates from Figure 4.11 is presented in Table 4.9.

Table 4.9 Regression equations of natural ventilation rate by the stack effect for the Crop Protection Structure using the neutral plane method.

Screen/level	Level 1	Level 2	Level 3
Screen N24	$\Phi_{NP} = 0.0401\Delta T^{0.4949}$ Adj. $R^2 = 0.9999$ n = 82 $S.E._C = 0.000013$ $S.E._\lambda = 0.000596$	$\Phi_{NP} = 0.0464\Delta T^{0.4945}$ Adj. $R^2 = 0.9998$ n = 56 $S.E._C = 0.000016$ $S.E._\lambda = 0.001000$	$\Phi_{NP} = 0.0577\ \Delta T^{0.4983}$ Adj. $R^2 = 1.0000$ n = 63 $S.E._C = 0.000018$ $S.E._\lambda = 0.000360$
Screen N32	$\Phi_{NP} = 0.0386\ \Delta T^{0.4724}$ Adj. $R^2 = 0.9992$ n = 61 $S.E._C = 0.000028$ $S.E._\lambda = 0.001710$	$\Phi_{NP} = 0.0442\ \Delta T^{0.4903}$ Adj. $R^2 = 0.9999$ n = 62 $S.E._C = 0.000012$ $S.E._\lambda = 0.000530$	$\Phi_{NP} = 0.0588\Delta T^{0.4888}$ Adj. $R^2 = 0.9994$ n = 74 $S.E._C = 0.000021$ $S.E._\lambda = 0.001450$
Screen N50	$\Phi_{NP} = 0.0305\ \Delta T^{0.4947}$ Adj. $R^2 = 0.9951$ n = 97 $S.E._C = 0.000043$ $S.E._\lambda = 0.003600$	$\Phi_{NP} = 0.0354\Delta T^{0.4930}$ Adj. $R^2 = 0.9999$ n = 80 $S.E._C = 0.000008$ $S.E._\lambda = 0.000570$	$\Phi_{NP} = 0.0473\Delta T^{0.4957}$ Adj. $R^2 = 0.9998$ n = 87 $S.E._C = 0.000014$ $S.E._\lambda = 0.000780$

Note: Φ_{NP} is the ventilation rate by tracer gas method, ΔT is the temperature difference between inside and outside, n is the number of observation, Adj. R^2 is the adjusted of coefficient of determination , $S.E._C$ and $S.E._\lambda$ are the standard of error of the ventilation coefficient (C) and power curve (λ) respectively.

The neutral plane positions were observed by using a smoke generator. Even though the exact position of the neutral plane was difficult to see, the neutral plane was seen close to be to the calculated one. For the calculated neutral plane $\bar{h}$ intersects the side opening, and an air flow transition was observed where the smoke was drawn into the structure below $\bar{h}$ and exhausted above $\bar{h}$. Strong eddies were observed at the boundary between the air inlet and outlet. However, air was clearly seen entering the side openings and leaving at the roof openings when $\bar{h}$ lay between the side and roof openings. These observations agree with the observation of Down et al. (1990). A typical airflow observation using the smoke generator is shown in Figure 4.12.

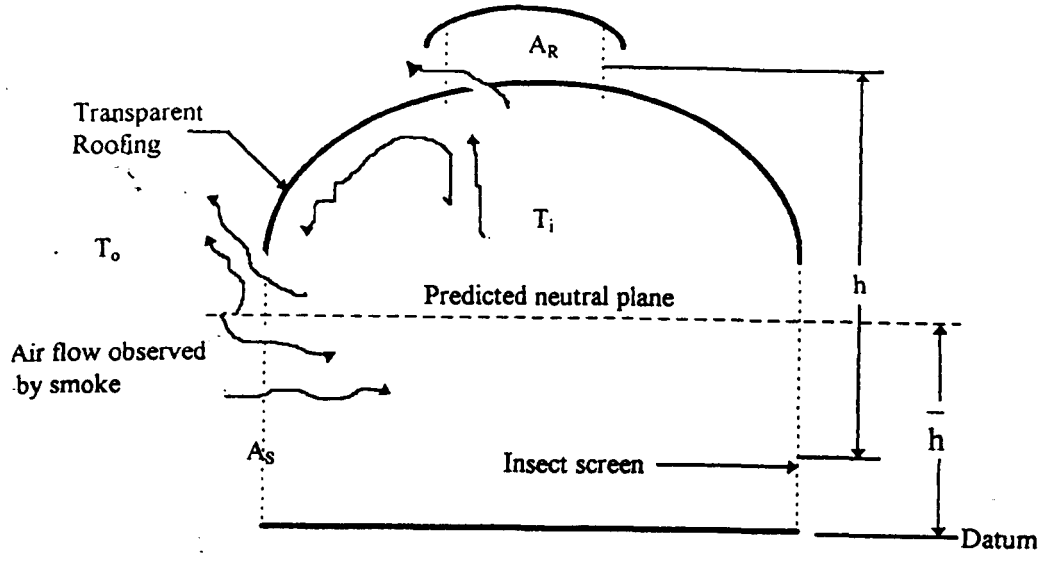

Figure 4.12 Comparison between predicted and observed plane height from the datum

4.4.5 Comparison of ventilation by different methods

In order to validate the estimations of natural ventilation rates, comparisons between the methods have been made. In this study the tracer gas method was used the control method and others as calculated methods. Figures 4.13 (a) - (i), Figures 4.13 (a) - (i) and Table 4.10 show the comparison of results between measured and calculated ventilation rates.

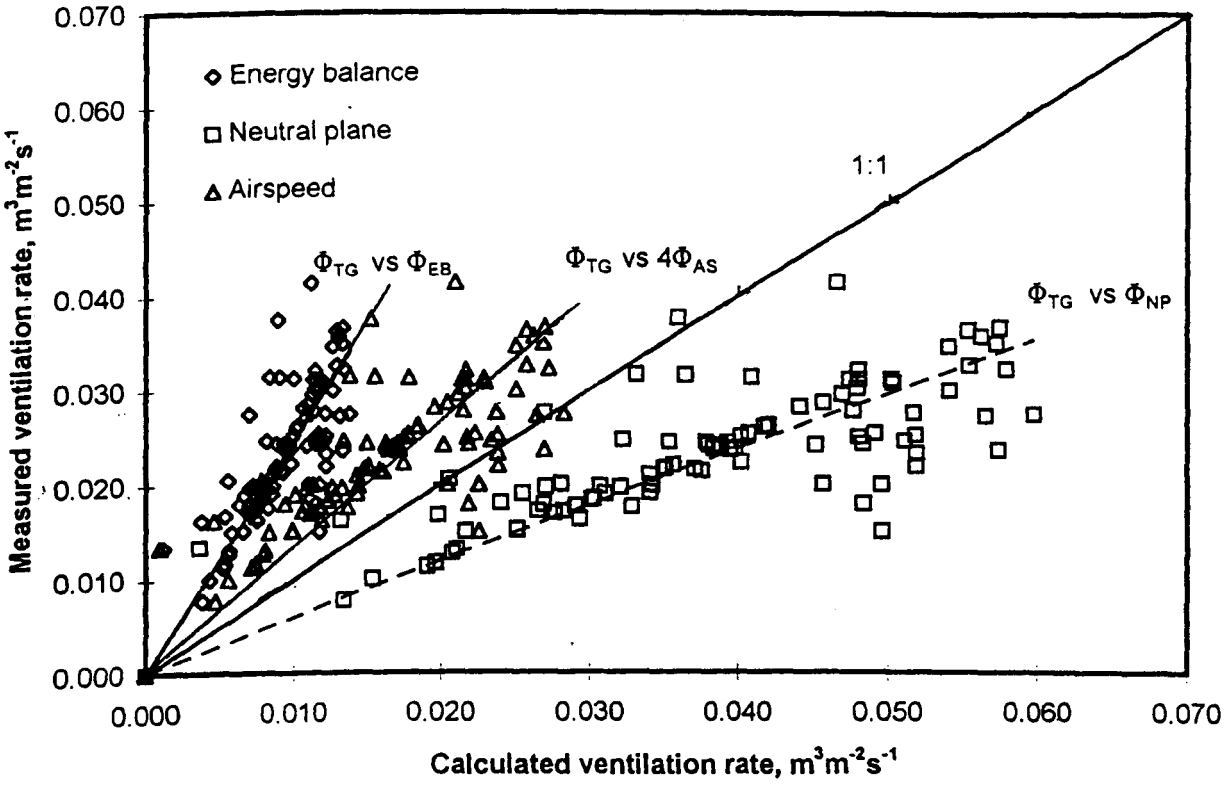

Figure 4.13 (a) Comparison between measured and calculated ventilation rates for screen N50 at opening level 1

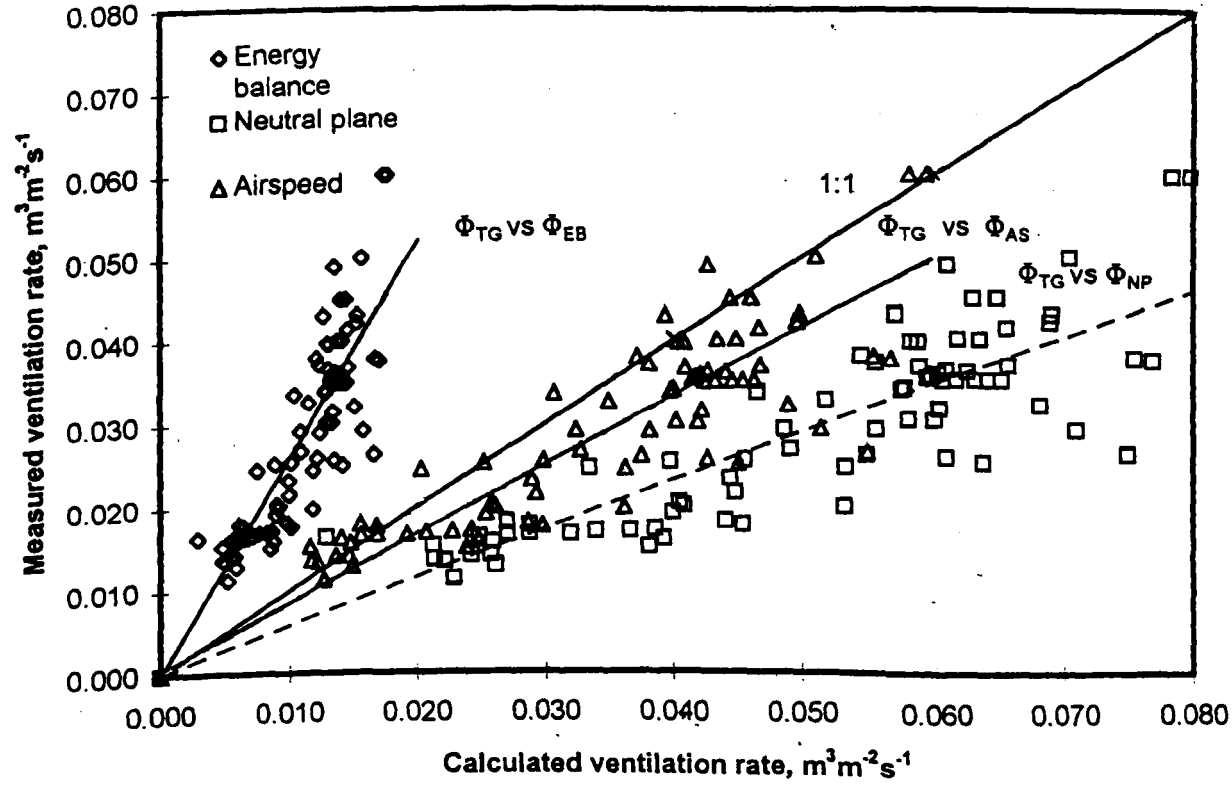

Figure 4.13 (b) Comparison between measured and calculated ventilation rates for screen N50 at opening level 2

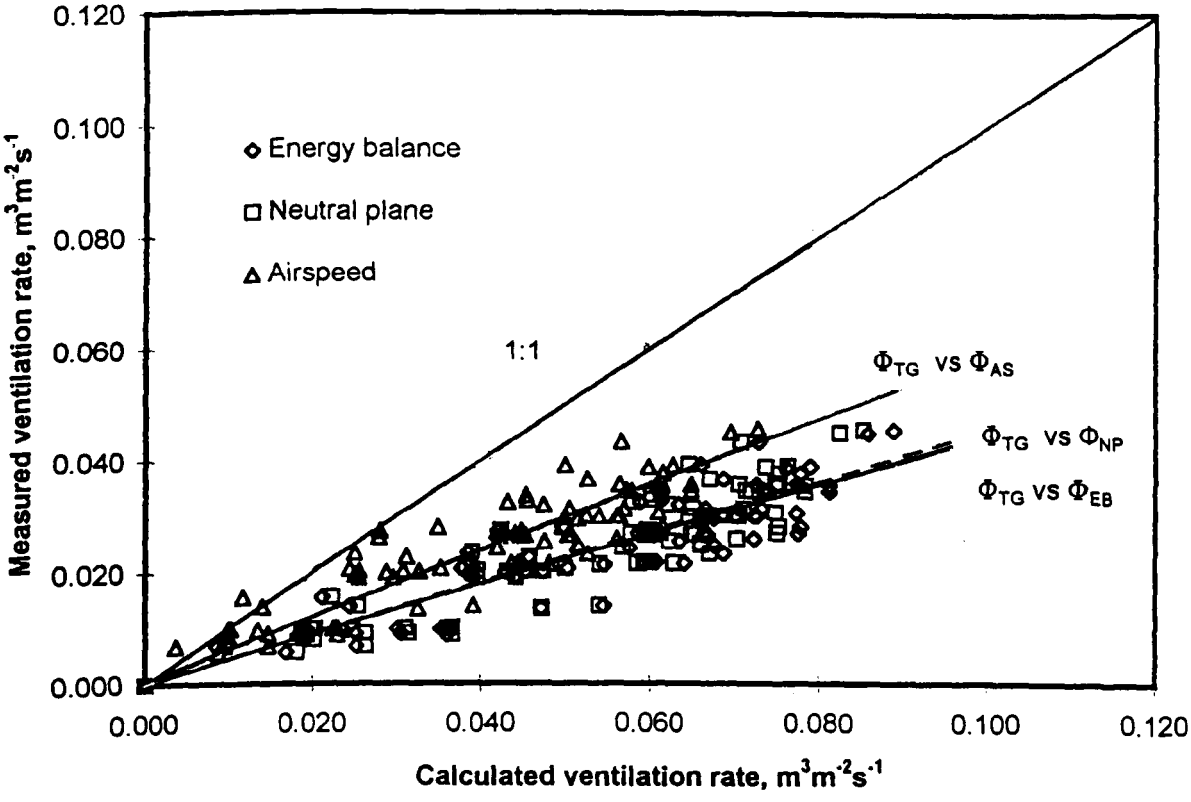

Figure 4.13 (c) Comparison between measured and calculated ventilation rates for screen N50 at opening level 3

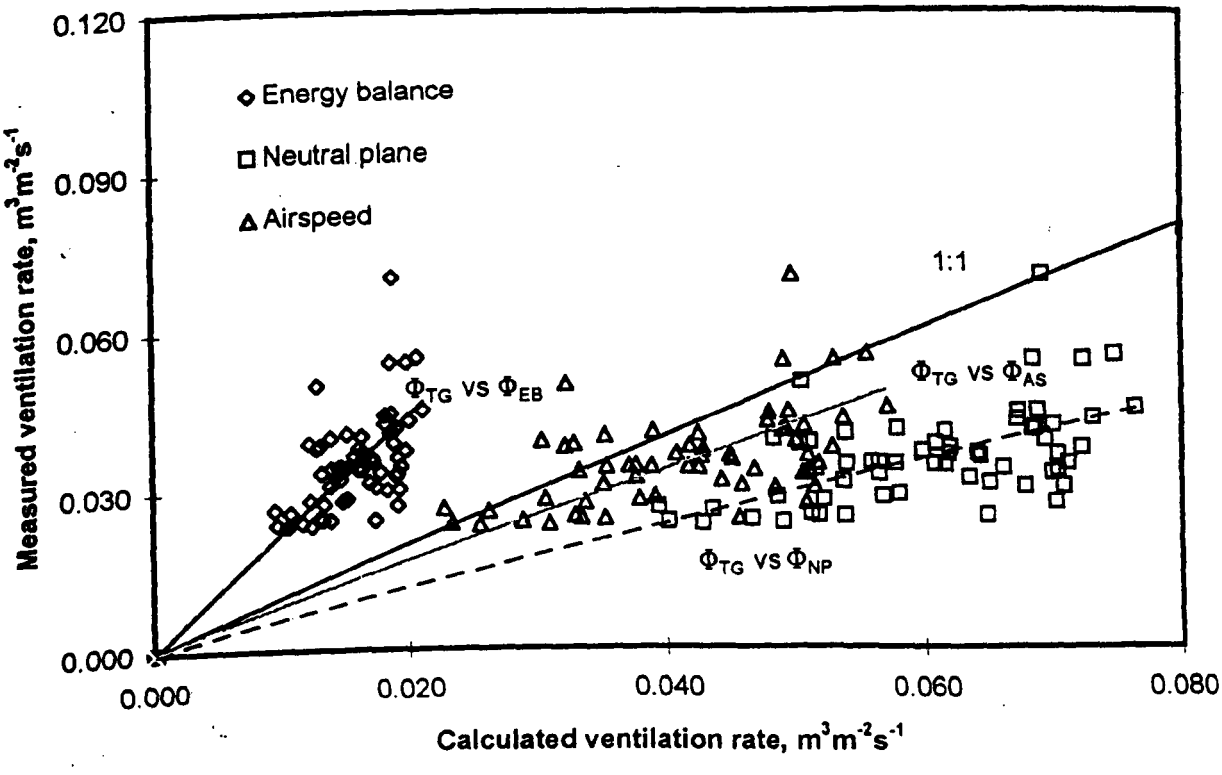

Figure 4.13 (d) Comparison between measured and calculated ventilation rates for screen N32 at opening level 1

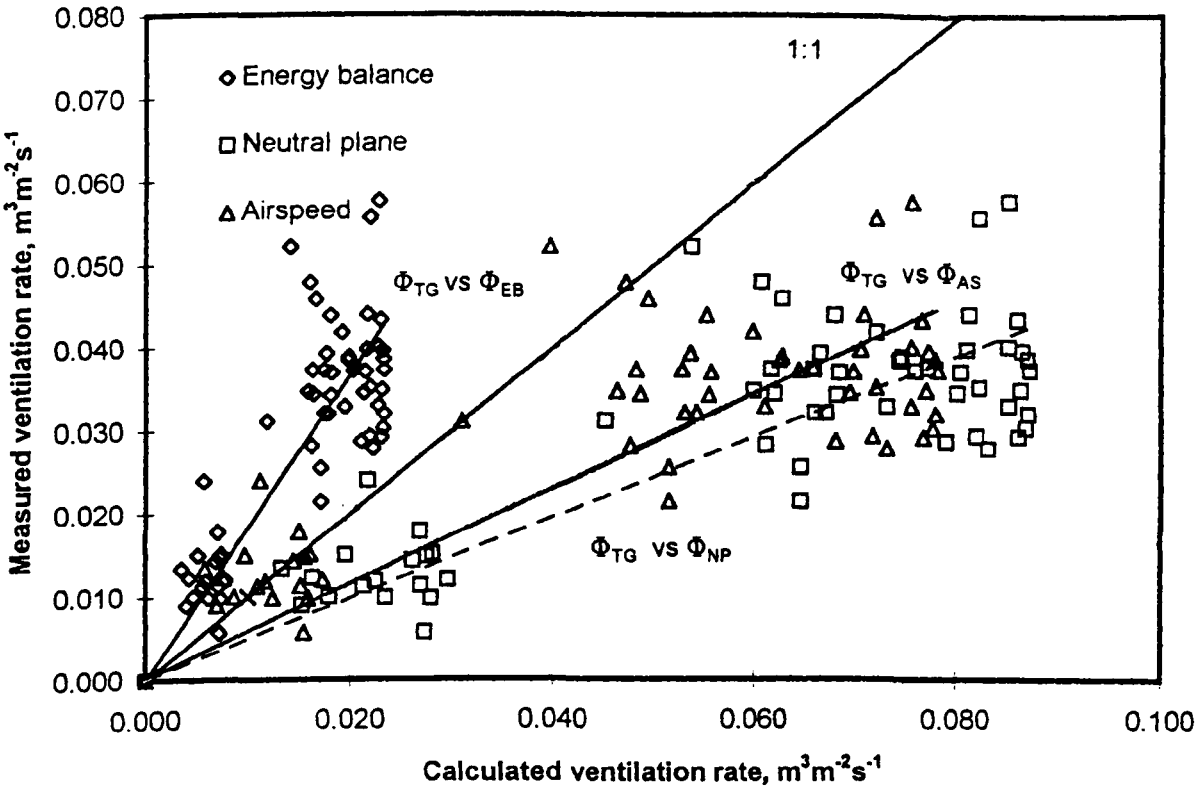

Figure 4.13 (e) Comparison between measured and calculated ventilation rates for screen N32 at opening level 2

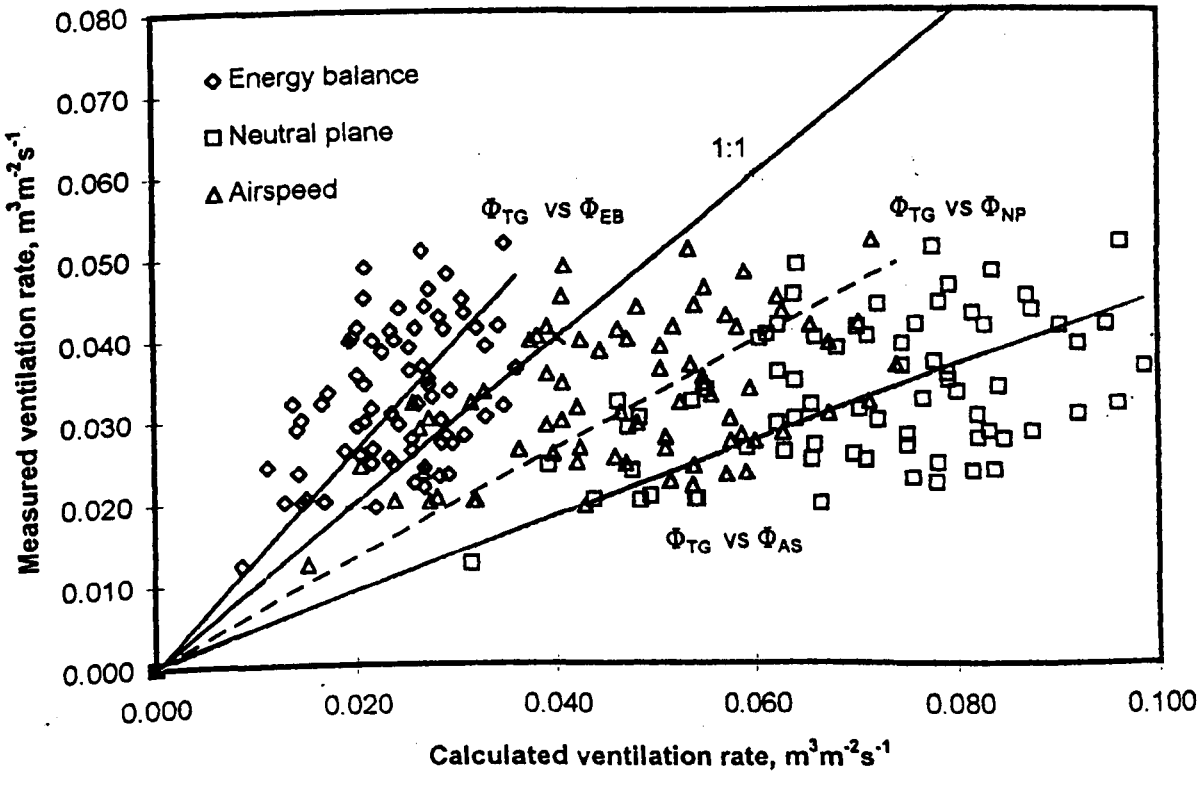

Figure 4.13 (f) Comparison between measured and calculated ventilation rates for screen N32 at opening level 3

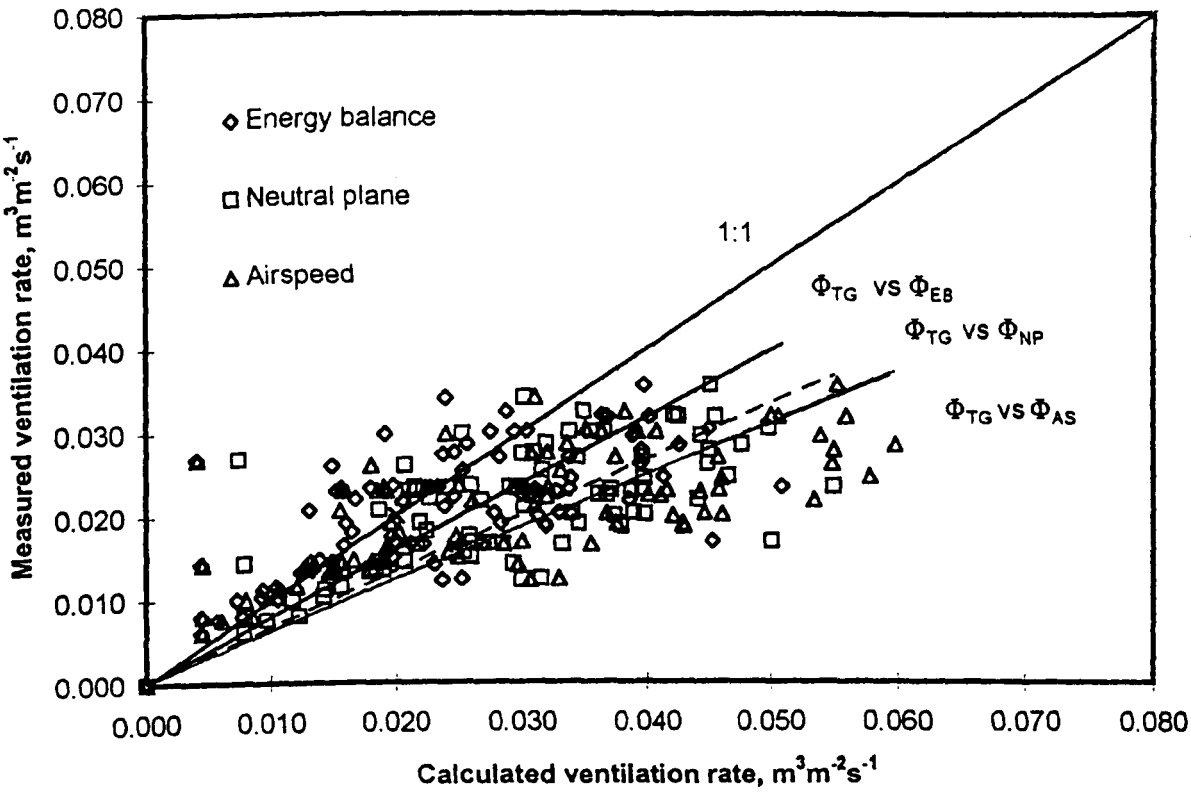

Figure 4.13 (g) Comparison between measured and calculated ventilation rates for screen N24 at opening level 1

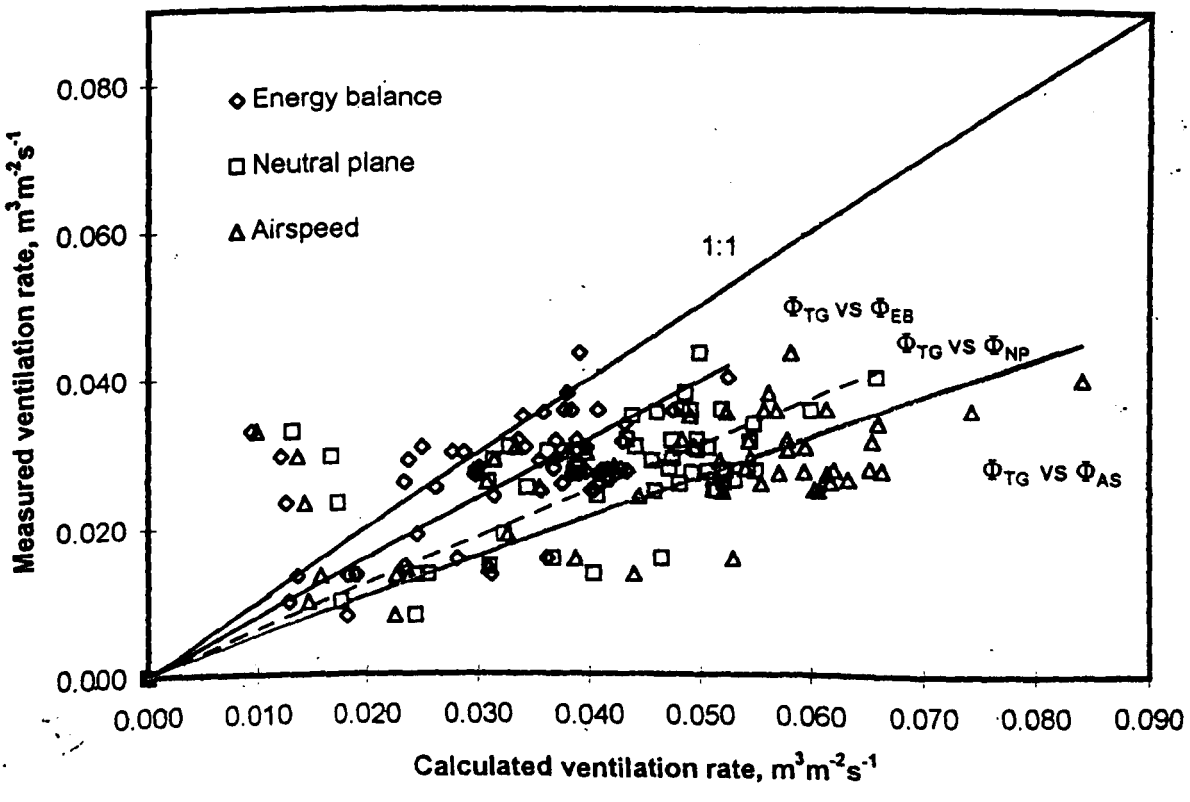

Figure 4.13 (h) Comparison between measured and calculated ventilation rates for screen N24 at opening level 2

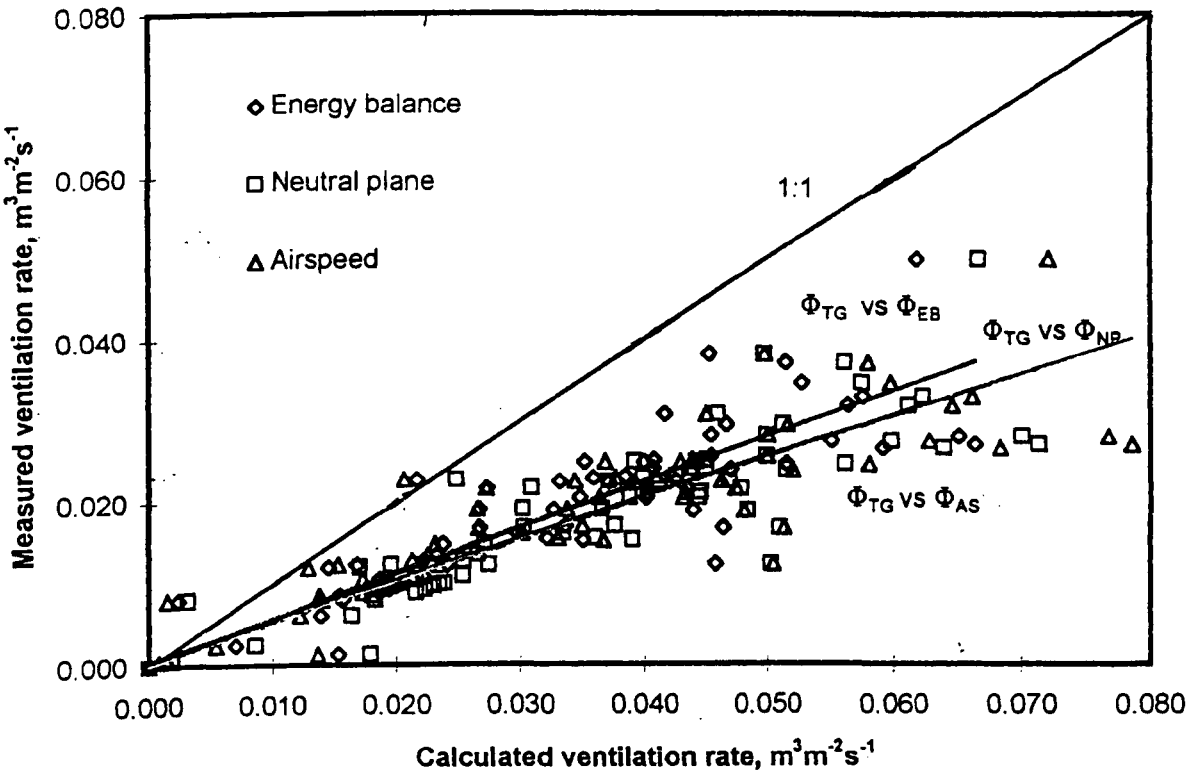

Figure 4.13 (i) Comparison between measured and calculated ventilation rates for screen N50 at opening level 3

Figure 4.13 (a)-(i) shows the linear relationship is observed between the measured and all calculated ventilation rates. The regression equations, correlation coefficients and standard error are presented in Table 4.8. The equations show the gradients of the calculated methods compared to the measured method. The closer the gradient to the 1:1 line means a stronger correlation between the calculated and the measured methods. Figure 4.14(a)-(i) show the residuals between the calculated and measured methods. If the scattered points are close to zero that means the calculated value is closer to the measured ventilation.

Table 4.10 Comparison results between measured and calculated values of natural ventilation rates by stack effect.

Screen	Level	Φ_{TG} vs Φ_{EB}	Φ_{TG} vs Φ_{NP}	Φ_{TG} vs Φ_{AS}
Screen 50	Level 1	$\Phi_{TG} = 2.4681\Phi_{EB}$ n = 96 Adj. $R^2 = 0.5687$ S.E. = 0.04934	$\Phi_{TG} = 0.5940\Phi_{NP}$ n = 96 Adj. $R^2 = 0.5140$ S.E. = 0.01265	$\Phi_{TG} = 1.3314\Phi_{AS}$ n = 30 Adj. $R^2 = 0.3881$ S.E. = 0.03227
	Level 2	$\Phi_{TG} = 2.5948\Phi_{EB}$ n = 80 Adj. $R^2 = 0.7341$ S.E.= 0.05628	$\Phi_{TG} = 0.5763\Phi_{NP}$ n = 80 Adj. $R^2 = 0.7349$ S.E. = 0.01248	$\Phi_{TG} = 0.8305\Phi_{AS}$ n = 41 Adj. $R^2 = 0.7281$ S.E. = 0.01823
	Level 3	$\Phi_{TG} = 0.4459\Phi_{EB}$ n = 87 Adj. $R^2 = 0.7887$ S.E.= 0.00838	$\Phi_{TG} = 0.4552\Phi_{NP}$ n = 87 Adj. $R^2 = 0.7876$ S.E. = 0.00858	$\Phi_{TG} = 0.5920\Phi_{AS}$ n = 45 Adj. $R^2 = 0.7697$ S.E. = 0.01167
Screen 32	Level 1	$\Phi_{TG} = 2.2043\Phi_{EB}$ n = 61 Adj. $R^2 = 0.3833$ S.E.= 0.06116	$\Phi_{TG} = 0.5854\Phi_{NP}$ n = 61 Adj. $R^2 = 0.4065$ S.E.= 0.01591	$\Phi_{TG} = 0.8430\Phi_{AS}$ n = 46 Adj. $R^2 = 0.3412$ S.E.= 0.02424
	Level 2	$\Phi_{TG} = 1.7908\Phi_{EB}$ n = 62 Adj. $R^2 = 0.1804$ S.E.= 0.08891	$\Phi_{TG} = 0.4893\Phi_{NP}$ n = 62 Adj. $R^2 = 0.6333$ S.E.= 0.01540	$\Phi_{TG} = 0.5716\Phi_{AS}$ n = 32 Adj. $R^2 = 0.4932$ S.E.= 0.02155
	Level 3	$\Phi_{TG} = 1.3199\Phi_{EB}$ n = 74 Adj. $R^2 = 0.0946$ S.E.= 0.04236	$\Phi_{TG} = 0.4517\Phi_{NP}$ n = 74 Adj. $R^2 = 0.2284$ S.E.= 0.01329	$\Phi_{TG} = 0.6595\Phi_{AS}$ n = 42 Adj. $R^2 = 0.0141$ S.E.= 0.02217
Screen 24	Level 1	$\Phi_{TG} = 0.7947\Phi_{EB}$ n = 82 Adj. $R^2 = 0.01137$ S.E.=0.03030	$\Phi_{TG} = 0.6702\Phi_{NP}$ n = 82 Adj. $R^2 = 0.2590$ S.E.=0.02176	$\Phi_{TG} = 0.6235\Phi_{AS}$ n = 24 Adj. $R^2 = 0.0206$ S.E.= 0.02364
	Level 2	$\Phi_{TG} = 0.7947\Phi_{EB}$ n = 56 Adj. $R^2 = 0.2204$ S.E.= 0.0289	$\Phi_{TG} = 0.6208\Phi_{NP}$ n = 56 Adj. $R^2 = 0.2609$ S.E.=0.02195	$\Phi_{TG} = 0.5352\Phi_{AS}$ n = 56 Adj. $R^2 = 0.0667$ S.E.= 0.02152
	Level 3	$\Phi_{TG} = 0.5621\Phi_{EB}$ n = 63 Adj. $R^2 = 0.7227$ S.E.= 0.01687	$\Phi_{TG} = 0.5115\Phi_{NP}$ n = 63 Adj. $R^2 = 0.7128$ S.E.= 0.01566	$\Phi_{TG} = 0.5110\Phi_{AS}$ n = 44 Adj.$R^2 = 0.6875$ S.E.= 0.01640

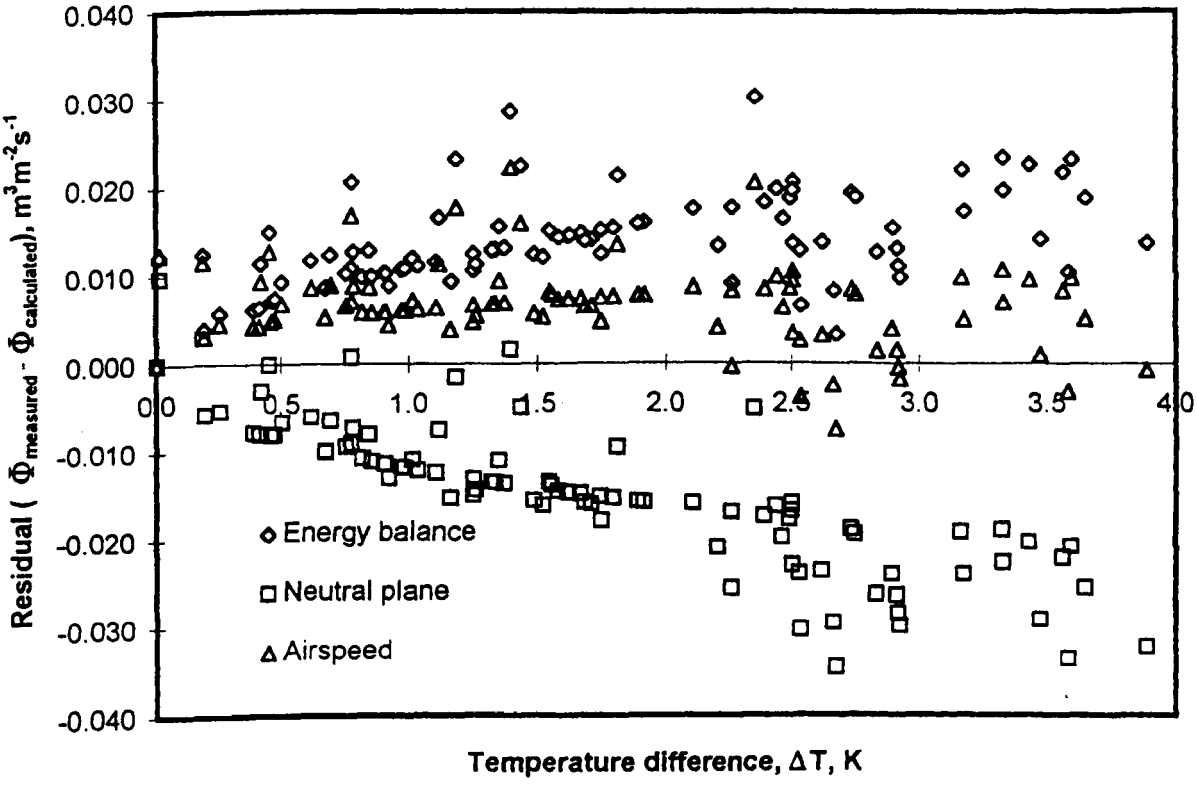

Figure 4.14 (a) Residual of energy balance, neutral plane and airspeed method for screen N50 at opening level 1

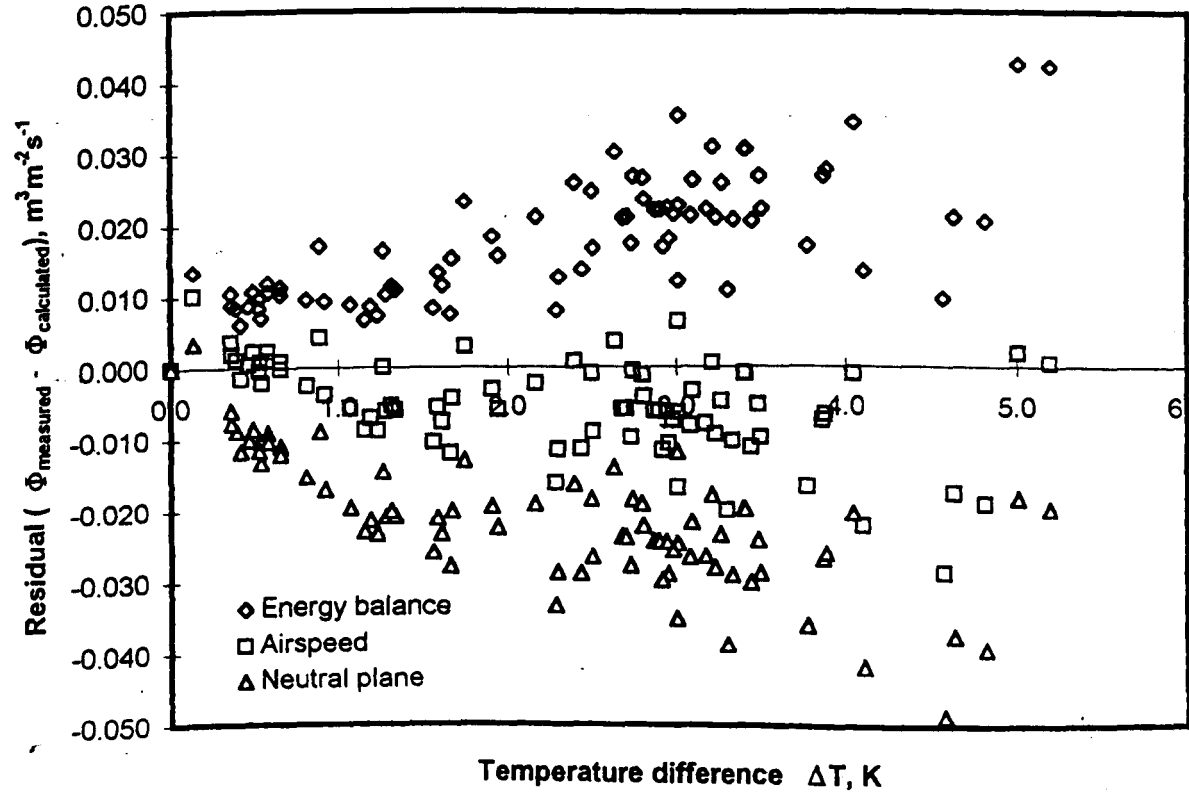

Figure 4.14 (b) Residual of energy balance, neutral plane and airspeed method for screen N50 at opening level 2

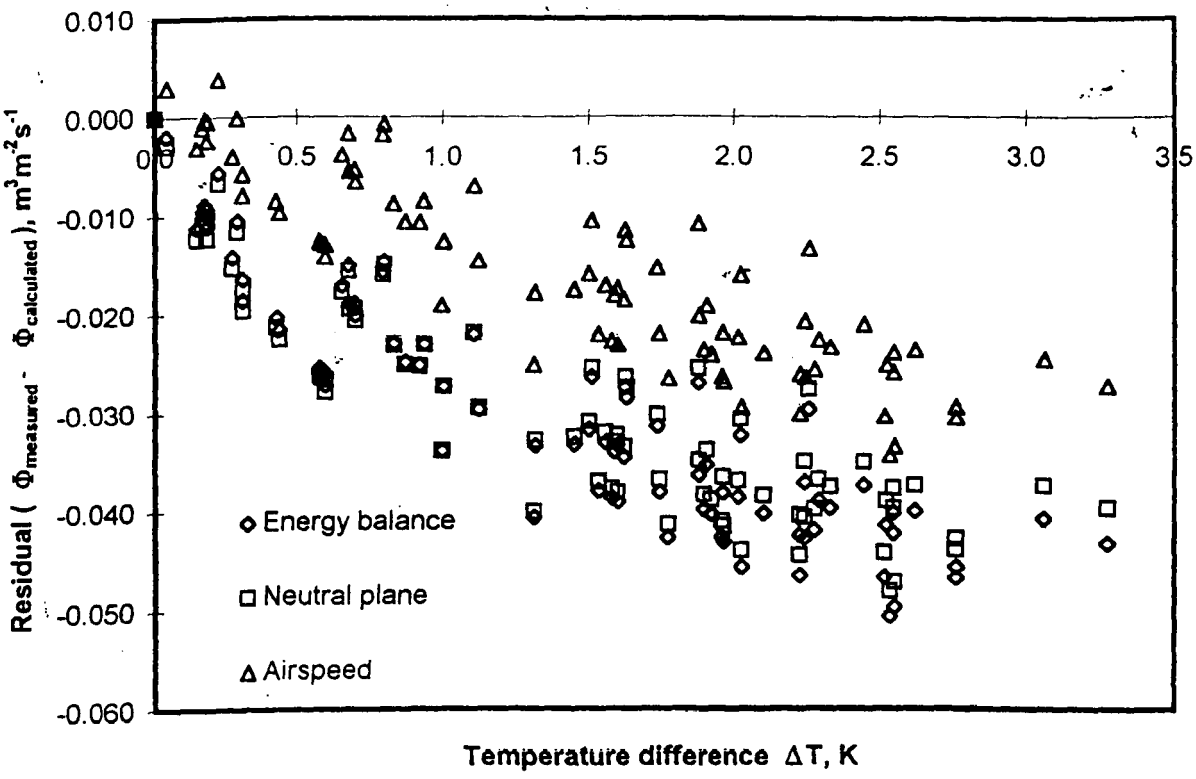

Figure 4.14 (c) Residual of energy balance, neutral plane and airspeed method for screen N50 at opening level 3

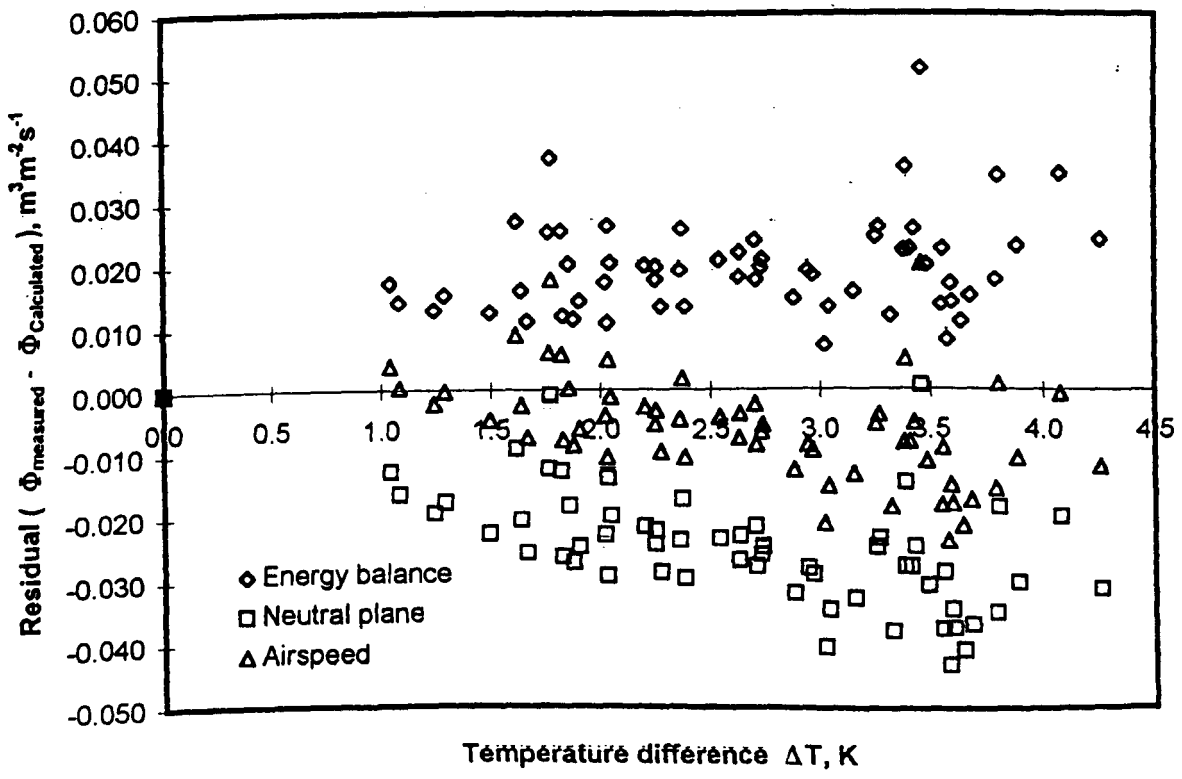

Figure 4.14 (d) Residual of energy balance, neutral plane and airspeed method for screen N32 at opening level 1

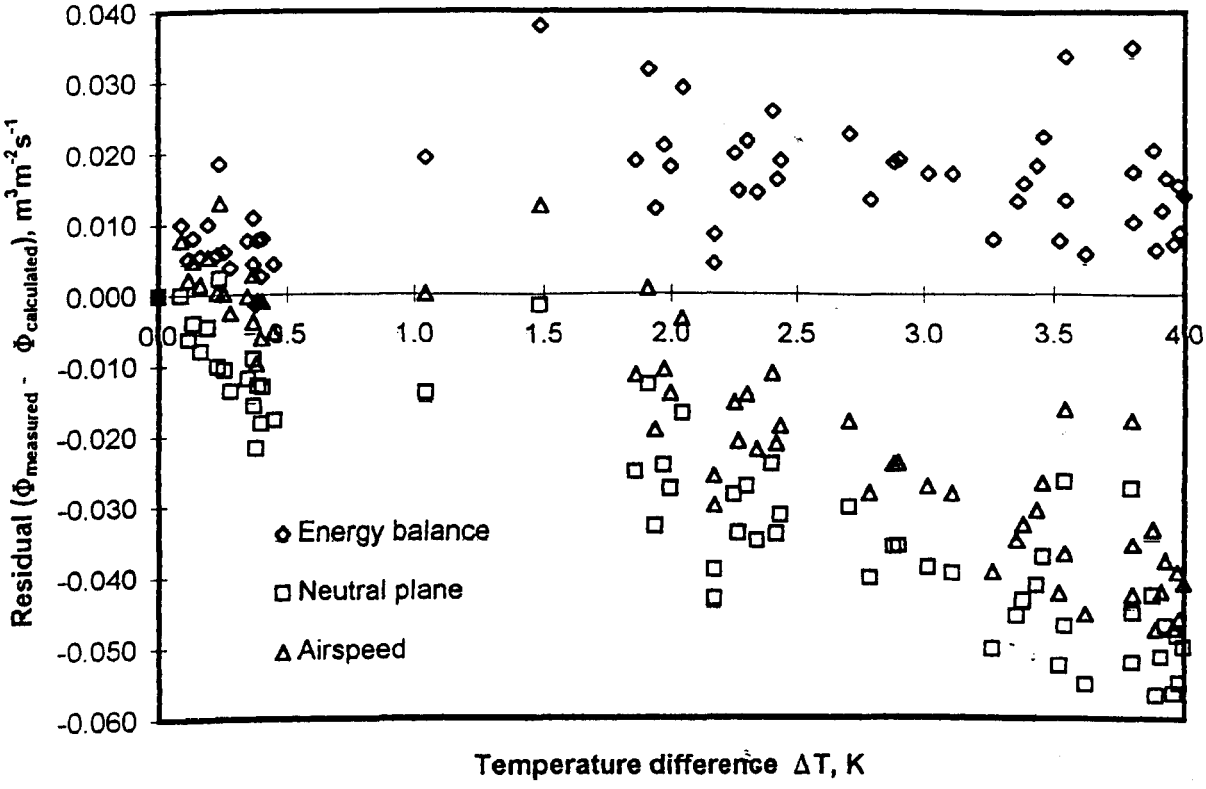

Figure 4.14 (e) Residual of energy balance, neutral plane and airspeed method for screen N32 at opening level 2

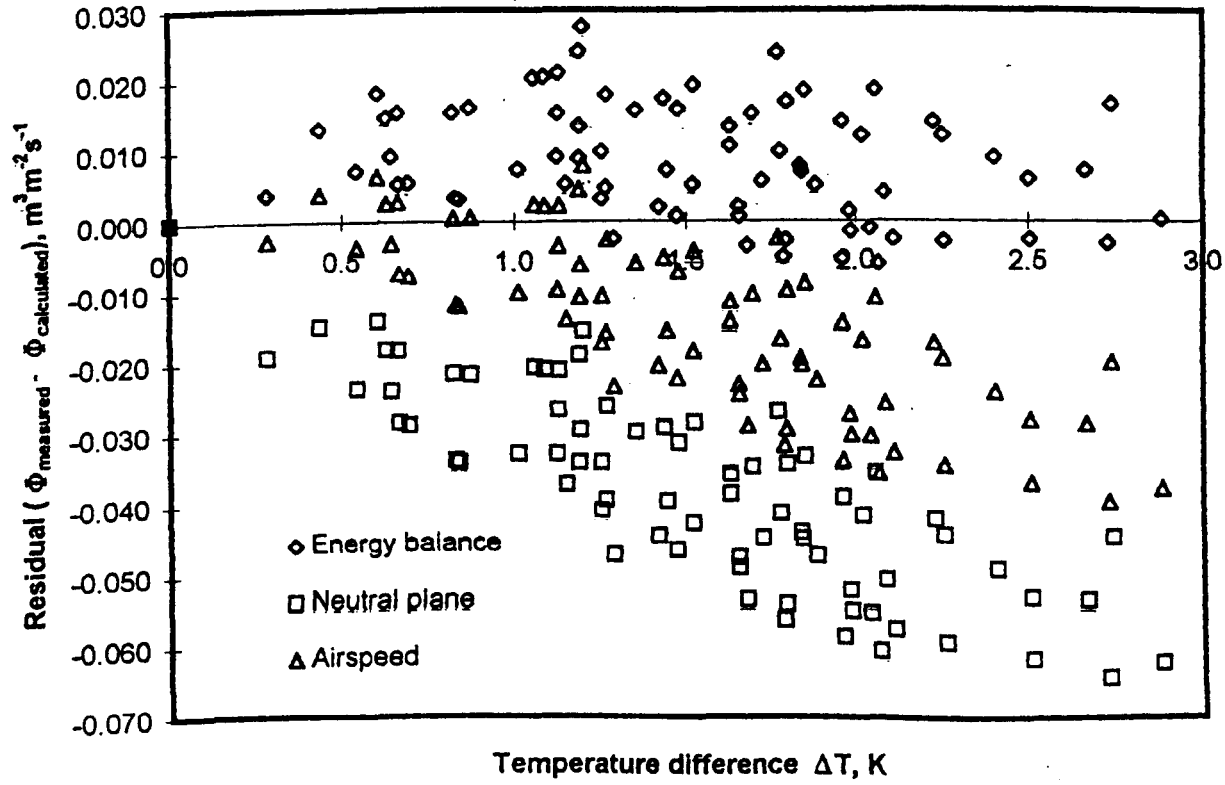

Figure 4.14 (f) Residual of energy balance, neutral plane and airspeed method for screen N32 at opening level 3

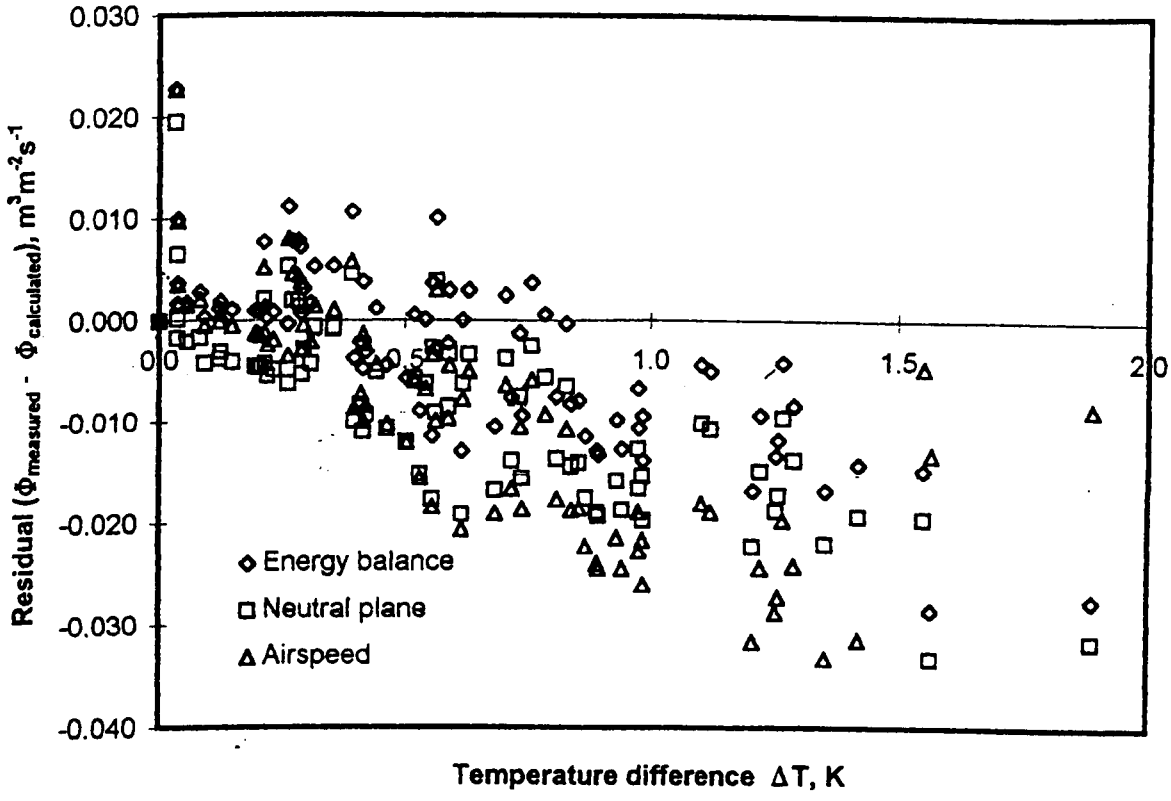

Figure 4.14 (g) Residual of energy balance, neutral plane and airspeed method for screen N24 at opening level 1

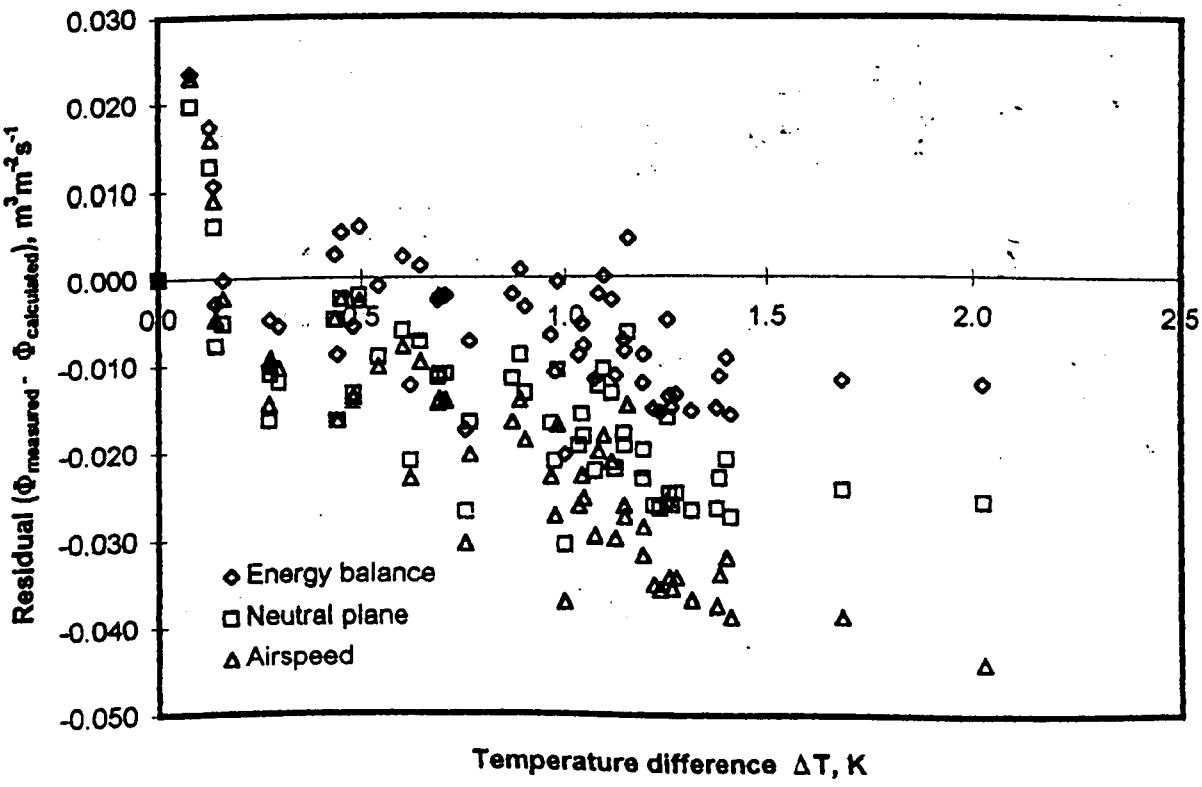

Figure 4.14 (h) Residual of energy balance, neutral plane and airspeed method for screen N24 at opening level 2

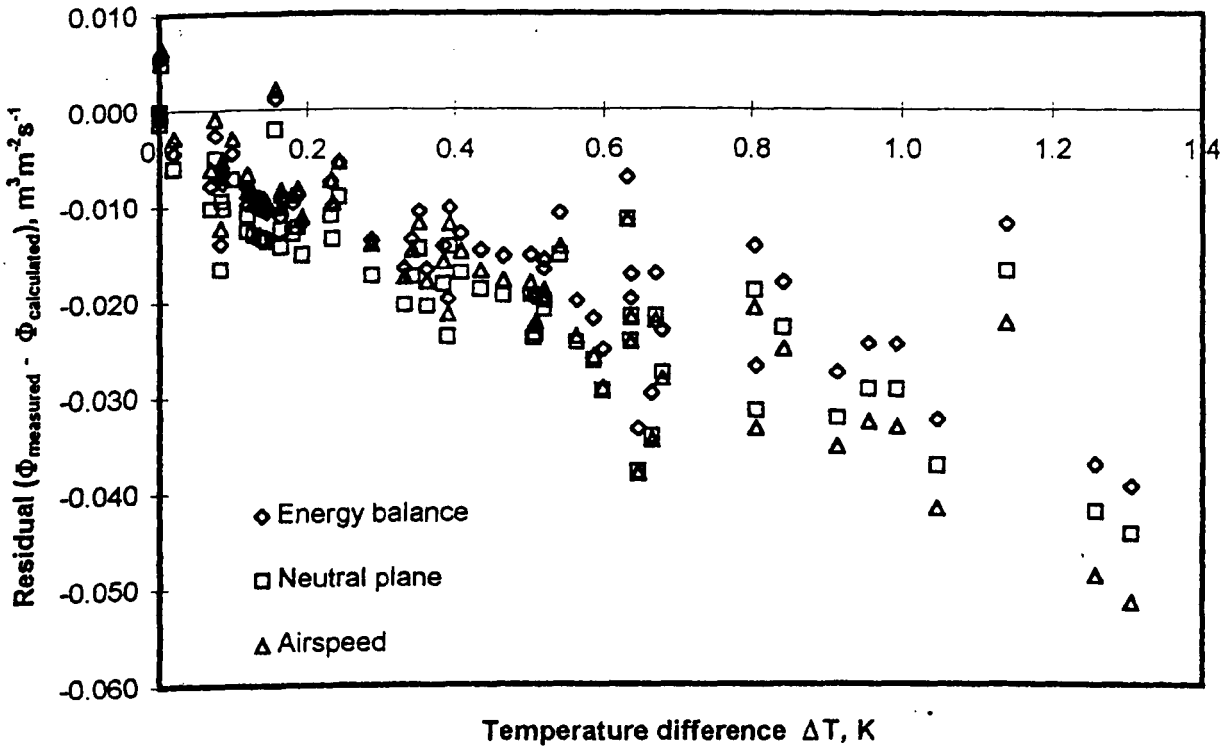

Figure 4.14 (i) Residual of energy balance, neutral plane and airspeed method for screen N24 at opening level 3

In order to determine which method is closest to the measured method, ventilation rate comparisons in terms of percentages is presented in Table 4.11. From the means of nine sets of data the energy balance, neutral plane and airspeed ventilation rates differ by 63 %, 45 % and 35 % from the tracer gas method respectively. This means that the direct airspeed measurement gives the closest result, followed by the neutral plane and energy balance methods. In addition, the mean adjusted correlation of these methods is 0.412, 0.504 and 0.390 respectively. That means in general all methods have a strong correlation with the measured method, about 66 % of the data lie on the regression line as shown in Table 4.11.

Even though the energy balance method has the biggest difference, more than half of the data sets are closer to the tracer gas method. This trend is similar to that was found by Fernandez and Bailey. (1992). They found that the variation was

between 1 - 24%. The differences in this method were attributed to uncontrolled errors in data measurement and in various parameters included in the calculation. Data were taken from averages over 8 to 15 minutes concurrently with the tracer gas measurements. Within that period the solar radiation frequently changed which affected light transmission, temperature difference and sensible heat formation. These errors also affected the calculation of the neutral plane and airspeed ventilation rates.

Table 4.11 Ventilation rate comparison between measured and calculated methods in term of percentage (%)

Descriptive statistics	**n**	$\overline{x}$	**max**	**min**	**s**	σ_{n-1}
Tracer gas against energy balance	9	63	160	20	2305	48
Tracer gas against neutral plane	9	45	55	33	60	8
Tracer gas against airspeed	9	35	49	16	142	12

The gradient of the neutral plane method increases consistently with increasing screen size. In this method the biggest screen gives closer estimation of ventilation to the measured method. Furthermore the standard deviation is smallest when compared to other methods. In this comparison the differences were found between 33 - 55 %. This difference is higher than the 8-15% difference reported by De Jong (1990). He did a similar comparison study in a small model with roof windows under restricted accuracy.

Direct airspeed measurement of ventilation is closest to the measured method with difference between 16 - 49%. This difference may be due to the data collection error as mentioned for energy balance error. However, the errors are very difficult to

identify after all necessary procedures have been taken into consideration. Finally, the comparison between methods comes back to the reality that the tracer gas method had a change of only 60-70% of the actual room air Dufton *et al.* (1942), Hitchin *et al.* (1967) and Ducarme *et al.*(1994) If this statement is considered, all methods have no significant difference between them in estimating natural ventilation rate.

4.5 Conclusions

This study has shown that when the outside wind is absence, the outside temperature will increase, then the inside temperature will also increase and at the same time the ventilation decreases. This is due to the low air exchange rate induced by thermal buoyancy or the stack effect. It is found that the ventilation rate will increase with increasing of temperature difference between inside and outside according to the power law. However, the increase of ventilation rate due to temperature difference increases does not avoid the high temperature inside the crop protection structure. In order to solve this problem, this study has revealed that the effects of screen size and ventilator opening area are paramount importance to limit the rise of indoor temperature and in the ventilation system design. The biggest screen and ventilator opening are found to give highest ventilation rates compared to smaller ones, which also give the lowest temperature difference between the inside and outside of the structure.

According to the F-test and T-test, the difference between the measured and calculated methods are found to have statistically significant differences between the control and all the calculated methods at the 5% significance level. Ventilation rate by direct airspeed measurement is closest to the tracer gas method followed by neutral

plane and energy balance methods. Therefore, the direct airspeed method is suggested can be used as a control method. If we consider only 60 - 70% air change in one air exchange by the tracer gas method, there is no significant difference between all the methods. Therefore ventilation rates for crop protection structure in the tropics can be predicted using tracer gas, neutral plane, airspeed or energy balance method. This can be made by gas decay measurement, temperature difference between inside and outside, direct airspeed measurement at the openings or measuring various parameters respectively. The neutral plane method is easier and cheaper for calculating natural ventilation rate compared to the other methods.

Chapter 5

Natural ventilation by wind effect

5.1 Introduction

Ventilation is one of the important components in the environmental control system for the Crop Protection Structure in the tropics. The purpose of the ventilation system is to provide an exchange of fresh environmental air based on climatic conditions and the environmental requirements of the crop in the structure. The driving force for natural ventilation is the pressure difference across openings in the structure caused by the wind, temperature difference or the combination of both. Usually, the wind effect is considered in the ventilation system if the temperature difference between inside and outside the structure is relatively low and the wind speed is adequately high. In this chapter, discussion is specifically focused on natural ventilation by the wind effect.

The relationship between ventilation rate and wind speed in a closed greenhouse has been presented by Whittle and Lawrence (1960). They used the tracer gas technique in their studies and established a formula for leakage ventilation, presuming a linear relationship between the ventilation and the outside wind speed. According to them, the air temperature difference between the greenhouse air and the outside air was not found to be significant in the case of leakage ventilation.

Natural ventilation induced by wind was also studied by Bot (1983) and De Jong (1990) in compartments that were located in a large glasshouse. The tracer gas decay method was used in their studies. They reported that a linear relationship occurred between ventilation flux and outside wind speed. In addition, ventilation flux was not affected by wind direction.

The wind effect dominance was also presented by Bot (1983) and De Jong (1990). Considering the extreme value for temperature difference between inside and outside the greenhouse was about 25 K, they suggested that the wind effect will be the predominant when the wind speed at reference level is higher than 1.67 - 2.0 m s^{-1}.

Natural ventilation rates can also be calculated by computing external and internal wind pressure coefficients based on Bernoulli's equation. Kozai *et al.* (1980), Wiren (1983), Sase *et al.* (1984) and Sase and Nare (1985) have experimentally determined the wind pressure coefficients on scale models in a wind tunnel. Hoxey *et al.* (1981) have measured wind loads on film plastic tunnels. They presented wind pressure coefficients for designing plastic tunnel greenhouses. Other studies on the coefficients of full scale greenhouses were also made by Robertson and Hoxey (1992).

In livestock buildings, ventilation and airflow patterns around and through buildings resulting from wind have been discussed by Bottcher *et al.* (1986), and Brockett and Albright (1987). These authors identified the main factors that affect ventilation rates as being wind speed, wind direction, area of building openings and local obstructions. Their aims were to maximise air exchange rates due to wind forces at the inlet and outlet openings and to site the buildings for maximum exposure to the existing winds.

In glasshouses, direct air speed measurements at ventilator openings by sonic anemometer were made by Boulard *et al.* (1996) and Wang (1998). They revealed that this method allowed understanding of airflow patterns in different openings over the whole greenhouse affected by the external wind and window opening angles.

Air flow driven by wind speed through thermal screens at the greenhouse ceiling was studied by Miguel (1998). He found that the airflow through a porous

screen can be described by the Forchheimer's equation and Darcy's law for the usual range of temperature differences between inside and outside greenhouse. His findings show the theoretical approach agreed reasonable well with the experimental value with differences of less than 20% in general.

Until now, very little information was available on air exchange through porous screens. Ventilation due to the wind effect on a full opening wall covered with a screen has not been studied. Moreover, the wind pressure coefficient method for calculating natural ventilation in this type of structure has also not been used. Therefore, the present study is aimed to contribute some knowledge on how to predict natural ventilation rate by the wind effect. The effects of screen size, ventilator opening, wind speed and direction were also investigated.

5.2 Principal Considerations

A theoretical analysis for ventilation by the wind effect was presented by Bruce (1974,1975,1977) and Redding (1981). As air flows around a building, it is caused to either accelerate or decelerate and so cause decreases and increases in the static pressure on the surfaces of the building. Usually, the pressures on the windward surface are positive and those on the leeward surface are negative.

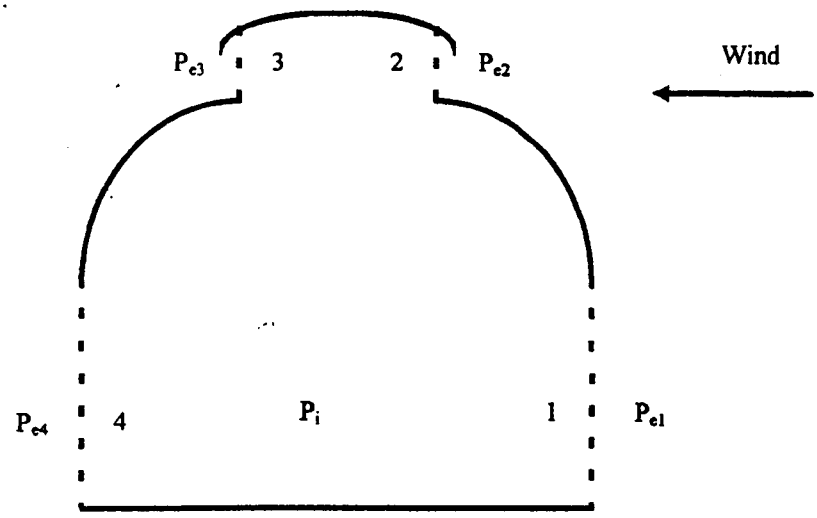

Figure 5.1 Wind pressures caused by wind perpendicular to the structure

Consider the crop protection structure cross section sketched in Figure 5.1. Wind causes the exterior pressures P_{e1}, P_{e2}, P_{e3}, and P_{e4} external to ventilator openings 1, 2, 3 and 4 respectively. There is some internal pressure that is not necessarily equal to the ambient, free stream air pressure. If no heat is added to the structure (wind-induced ventilation only) the outdoor air density applies everywhere. For this condition, Bruce (1977) and Albright (1989) expressed the pressure at any location on the external surface of the structure by;

$$P_e = C_{pe} \frac{1}{2} \rho_e V^2 \tag{5.1}$$

where P_e is the external wind pressure (Pa), C_{pe} is the external wind pressure coefficient (dimensionless), ρ_e is the external air density (kg m^{-3}) and V is the wind speed at eaves level (m s^{-1}). The external pressure coefficient on the building surface is defined as the fraction of the kinetic pressure of free wind acting on the building at that particular location. Bruce (1977) defined an internal pressure coefficient, C_{pi}, which is constant throughout a building if there are no internal partitions. The internal air pressure can be expressed similarly as,

$$P_i = C_{pi} \frac{1}{2} \rho_i V^2 \tag{5.2}$$

where P_i is the internal air pressure (Pa), C_{pi} is the internal wind pressure coefficient (dimensionless), ρ_i is the internal air density (kg m^{-3}) and V is external wind speed at eaves height (m s^{-1}). The internal wind pressure coefficient is defined in a manner similar to the external wind pressure coefficient. It is the ratio between the existing internal gauge pressure and the wind stagnation pressure.

According to Albright (1990), the indoor air pressure differs from the free stream atmospheric pressure and is affected by the external pressure coefficients and the sizes of the ventilators openings. External pressure coefficients are thought not to be affected by the sizes of vents unless the vents are greater than 15 % of the wall area. The value of the indoor pressure coefficient must be bounded by the range defined by the highest and lowest external coefficients. At each nth ventilator opening,

$$\Delta P_n = \left(C_{pe} - C_{pi}\right)\left(\frac{1}{2} \rho_e V^2\right) \tag{5.4}$$

where ΔP_n is the pressure difference between internal and external (Pa). Based on the definitions of the pressure coefficients, wind speed at eaves height and

$$\Delta P = \frac{1}{2}\rho_e V_n^2 \tag{5.5}$$

According to the Bernoulli equation, where V_n is the velocity of air moving through the nth inlet opening. Thus, the two pressure differences are the same and we have an expression as;

$$V_n = V\frac{\left(C_{pe} - C_{pi}\right)}{\sqrt{\left|\left(C_{pe} - C_{pi}\right)\right|}} \tag{5.6}$$

Equation 5.6 is in the form of a vector identity in which positive velocity is defined as flow into the structure and negative is outflow. However, openings 1 and 2 can be inlet or outlet depending on the magnitudes of the pressure coefficients and areas of the openings. Therefore, the ventilation rate of the crop protection structure is given by,

$$\Phi_{WS} = \frac{1}{2A_g}\sum_{i=1}^{n} A_n V_n \tag{5.7}$$

where Φ_{WS} is the ventilation rate by wind effect ($m^3 m^2 s^{-1}$) and A_g is the ground floor area (m^2). Ventilation rates can also be calculated from measuring flow characteristics of screen samples in the laboratory and wind pressure coefficients at the openings of a full scale structure in the field. If we plot a graph of airspeed

against the pressure difference across the screen from the laboratory data, a linear regression equation can be produced as;

$$V = \sqrt{m\Delta P_m} \tag{5.8}$$

where V is the actual air velocity across the screen sample (m s^{-1}), m is the slope gradient ($m^2 s^{-2} Pa^{-1}$) and ΔP_m is the pressure difference between inside and outside of the screen sample. The pressure difference relationship across the screen between full scale and laboratory measurement can be expressed as;

$$\Delta C_p \times \Delta P = \Delta P_m \tag{5.9}$$

where ΔCp is the pressure coefficient difference of the full scale measurements (dimensionless), ΔP is pressure difference across the screen at the full scale structure (Pa) that can be obtained from equation 5.5 and ΔP_m is the pressure difference across the screen sample measured in the laboratory (Pa). The actual air velocity through the full scale screen can be obtained by substituting ΔP_m in equation 5.8. Finally the ventilation rate can be calculated by substituting V in equation 5.7.

5.3 Experimental design

The same crop protection structure as used in the Chapter 4 was transferred to the Silsoe Research Institute's open field as shown in Plate 28. The structure was built on the open lawn which had no surrounding obstructions. The position was perpendicularly oriented to the well exposed prevailing winds. Data was taken in an evening during winter when there was strong winds and low solar radiation. At that

time the outside temperature, solar radiation and wind speed were 5 - 7 °C, 60 - 70 W m^{-2} and 5 - 10 m s^{-1}. This condition was chosen to ensure that there was no stack effect and that the wind effect dominated the ventilation rate.

Plate 28. Crop protection structure for wind effect study

The relationships between ventilation rates and the different screen sizes and opening areas were studied in this chapter. The opening areas of the full scale structure were changed as described in the Chapter 2. In addition, the air flow characteristics in relation to the pressure difference across and air velocity through the screen sample were made at the Fan Test Facilities (in the laboratory) and which been described in Chapter 3.

Pressure tube, windvane and a sonic anemometer instruments were installed at the eaves height of the structure. This was to measure the free stream wind pressure, speed and direction. The windvane has an inherently fast response to the wind variation. In addition, the pitot tube attached horizontally to the windvane measured the kinetic energy of the air as a dynamic pressure. The internal and external wind pressures of the structure were sensed by pressure tapping points distributed over the surface. Each tapping point consisted of a 9.5 mm hole at the centre of a 150 mm diameter transparent acrylic disc, which was designed to be installed at any position on the plastic and screen surfaces. Rainwater entering the hole was drained away by a porous (2 μm) ceramic plug that sealed the lower end of the pressure tapping assembly. Flexible p.v.c. tubing of 6 mm bore in 6 - 10 m length was used to convey all the internal and external pressure signals and were automatically switched in pairs to two transducers, at the same time as measurements of wind pressure and direction, to the data recording and computer system.

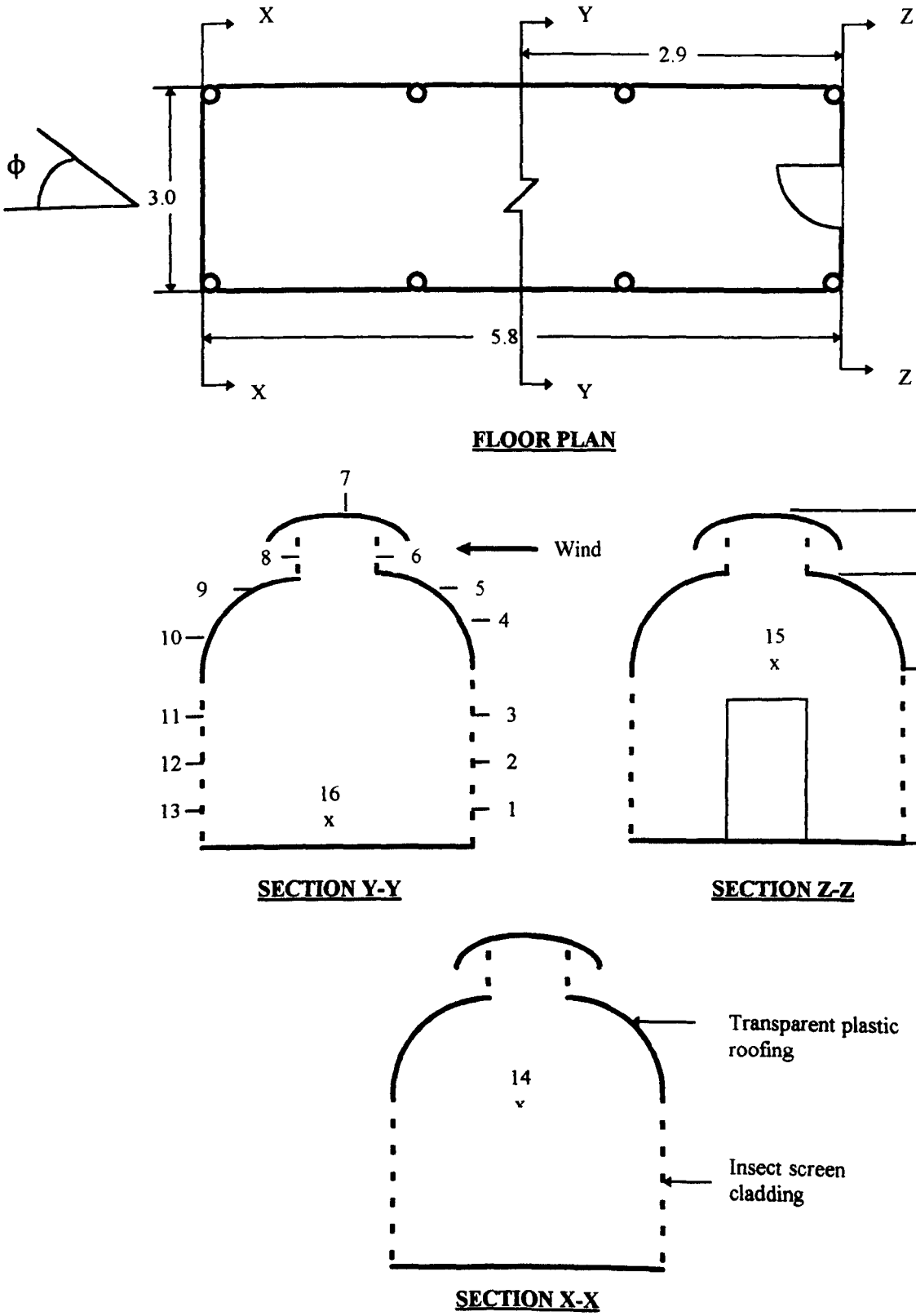

Figure 5.2 Tapping plan for Crop Protection Structure

Generally data were recorded for 16 tapping points (15 external and 1 internal) over a 90° span of wind direction to determine the pressure distribution over the surface of the structure. Recordings of 240 s duration were taken in sequence from pairs of tappings together with continuous wind pressure and direction data. Chart records were also taken during data collection so that an immediate visual check could be maintained. Figure 5.2 and Plates 29 and 30 show the instruments and tapping plan of the study respectively. This instrumentation system was calibrated before being used and developed by Hoxey (1974) at Silsoe Research Institute.

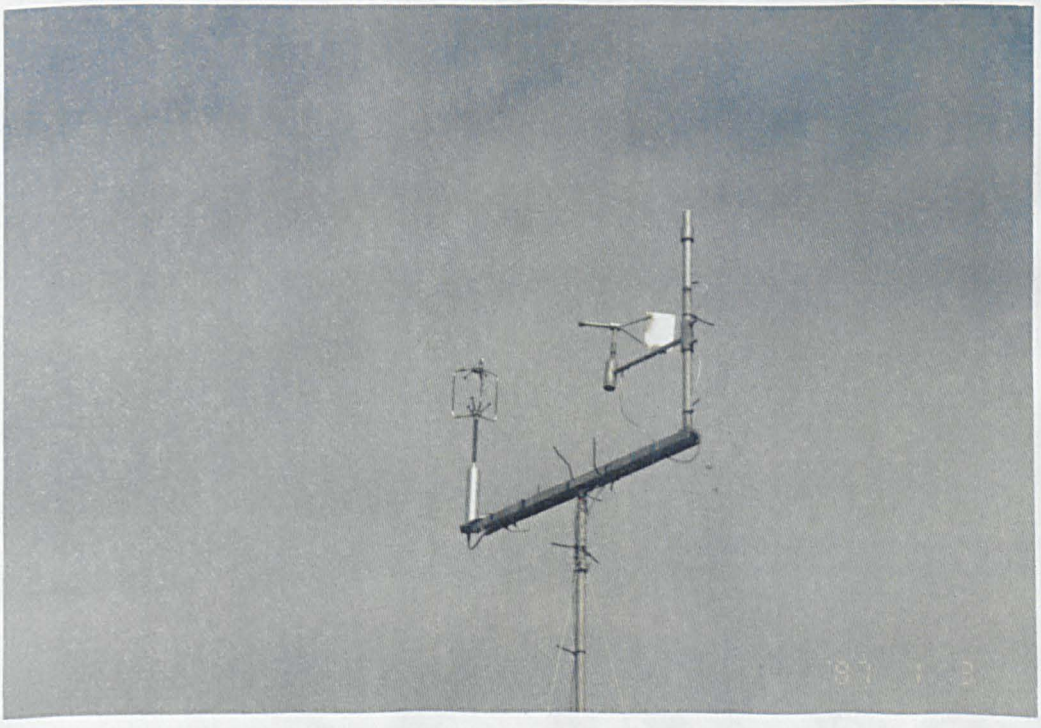

Plate 29. Windvane and sonic anemometer

Plate 30. Pressure tapping transducer and logging system

5.4 Results and discussion

The pressure coefficients for incident wind perpendicular to the structure ($\phi = 90^{\circ}$) are given in Table 5.1 and the reference tapping points are given in Figure 5.2. These results are accordance to the design procedures of CP3, to determine coefficients relating wind loads to wind pressure at ridge height. The results have shown that the internal and external wind pressure coefficients increase with increasing screen opening area (Level 3 > Level 2 > Level 1). Positive and negative pressure coefficients are clearly exhibited at the windward and leeward sides of the structure respectively, which agree with the principle consideration in section 5.2.

Table 5.1 Data of internal and external pressure coefficients of Crop Protection Structure. These coefficients are related to the wind pressure at eaves height and in the direction perpendicular to the roof ridge

Tapping point no.	Height (m)	C_{pe} Level 1	C_{pe} Level 2	C_{pe} level 3
01	0.25	0.46	0.50	0.48
02	0.75	0.00	0.52	0.58
03	1.25	0.00	0.00	0.66
04	1.83	0.48	053	0.60
05	2.50	0.16	0.22	0.29
06	2.98	0.71	0.76	0.84
07	3.12	-0.49	-0.44	-0.42
08	2.98	-0.35	-0.31	-0.30
09	2.50	-0.17	-0.13	-0.13
10	1.83	-0.17	-0.15	-0.12
11	1.25	0.00	0.00	-0.13
12	0.75	0.00	-0.18	-0.14
13	0.25	-0.18	-0.18	-0.14
14	1.50	-0.38	-0.38	-0.32
15	1.50	-0.34	-0.35	-0.19
16 (internal Cpi)	0.50	0.05	0.02	0.18

The pressure coefficients were found to be dependent on wind direction. This can be clearly seen in Table 5.2. An incident angle perpendicular to the structure (90°) gives the highest internal and external wind pressure coefficients compared to other incident angles. If a comparison between 90° and 50° is made, the difference is about 20%. This contradicts the findings of Bot (1983) and De Jong (1990) which claimed that ventilation flux was not affected by wind direction. However, studies by Wang *et al.* (1997) agree with the present studies. These results show that the airspeed and direction at the roof window openings can be changed significantly by the external wind speed and direction.

Table 5.2 Data of internal and external pressure coefficients of Crop Protection Structure. These coefficients are related to wind pressure at eaves height and a range of angles of wind direction (ϕ) for the third level opening.

Tapping point no.	Height (m)	$\phi = 90^o$	$\phi = 80^o$	$\phi = 70^o$	$\phi = 60^o$	$\phi = 50^o$
01	0.25	0.48	0.45	0.41	0.37	0.41
02	0.75	0.58	0.52	0.47	0.44	0.44
03	1.25	0.66	0.60	0.54	0.49	0.50
04	1.83	0.60	0.52	0.47	0.40	0.38
05	2.50	0.29	0.20	0.18	0.12	0.14
06	2.98	0.84	0.74	0.69	0.63	0.64
07	3.12	-0.42	-0.54	-0.53	-0.58	-0.59
08	2.98	-0.30	-0.40	-0.40	-0.42	-0.43
09	2.50	-0.13	-0.20	-0.22	-0.27	-0.27
10	1.83	-0.12	-0.20	-0.20	-0.24	-0.27
11	1.25	-0.13	-0.21	-0.22	-0.26	-0.27
12	0.75	-0.14	-0.23	-0.23	-0.27	-0.28
13	0.25	-0.14	-0.21	-0.22	-0.25	-0.27
14	1.50	-0.32	-0.40	-0.36	-0.34	-0.32
15	1.50	-0.19	-0.06	0.08	0.22	0.39
16 (internal Cpi)	0.50	0.18	0.11	0.10	0.06	0.08

The relationship between airspeed and pressure difference for different screen samples that were measured at the Fan Test Facility are presented in Figure 5.3 (a)-(c).

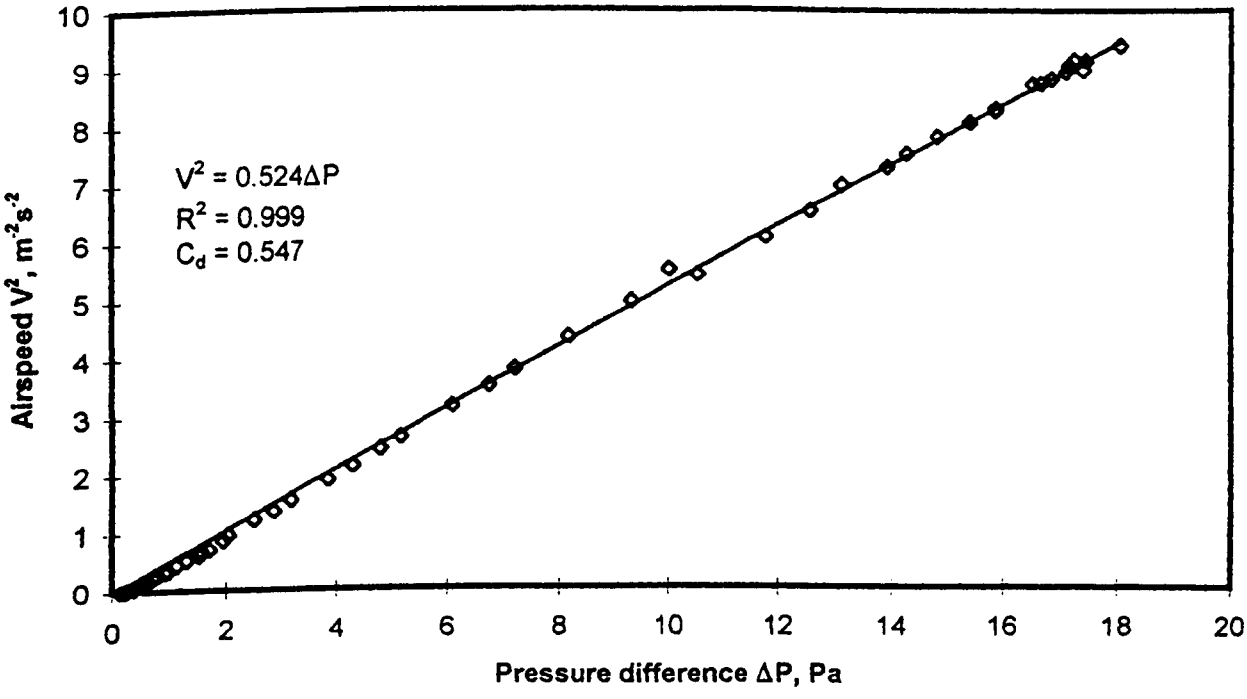

Figure 5.3 (a) Relationship between airspeed and pressure difference across screen N24

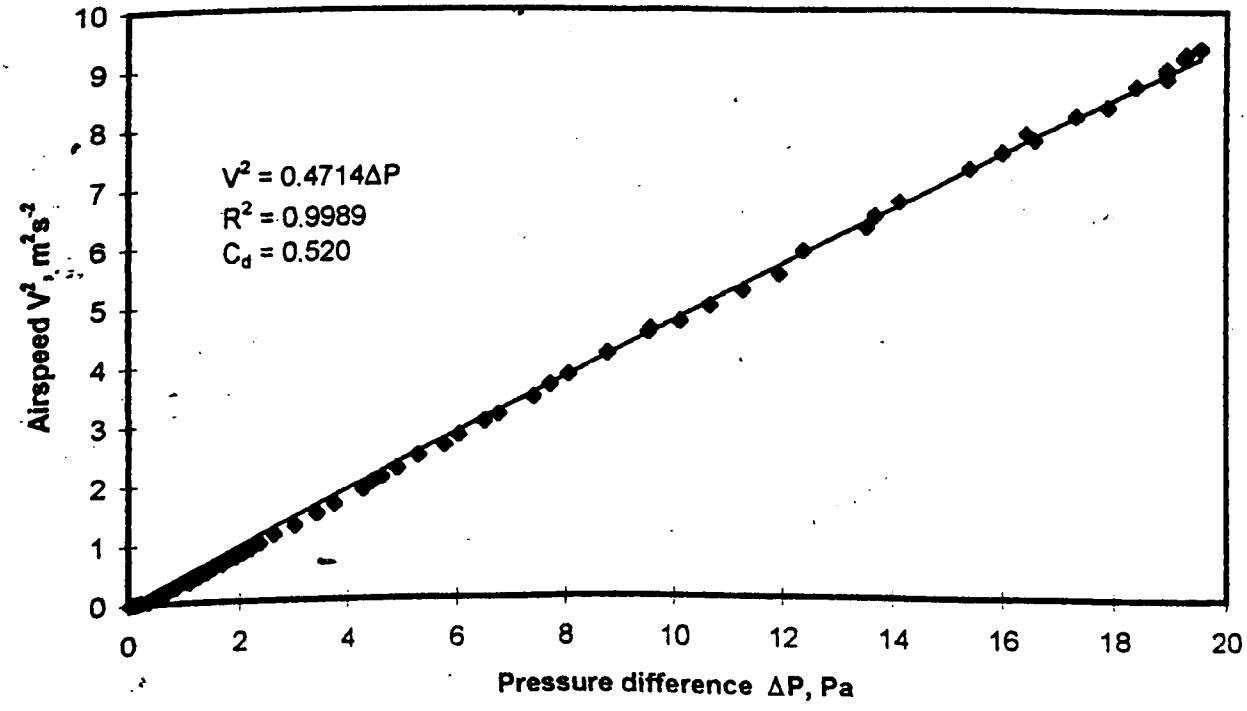

Figure 5.3 (b) Relationship between airspeed and pressure difference across screen N32

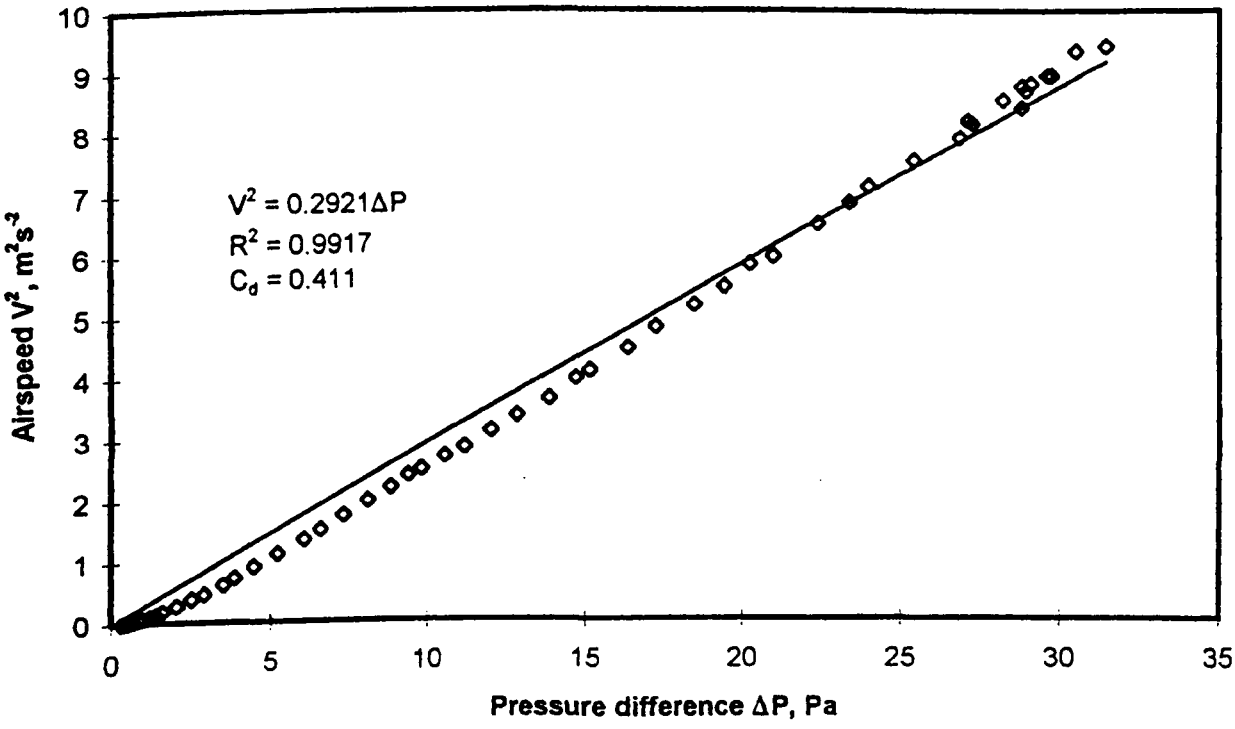

Figure 5.3 (c) Relationship between airspeed and pressure difference across screen N50

The graphs show very strong linear relationships between the square of airspeed (V^2) and pressure difference (ΔP) across the screen which is in agreement with Bernoulli's theory and equation 5.8. The regression equations show the values of the coefficient (C) are 0.524, 0.4714 and 0.2921 for the screen N24, N32 and N50 respectively. That means the biggest screen size gives the highest value of multiple coefficient and the smallest screen gives the lowest value accordingly.

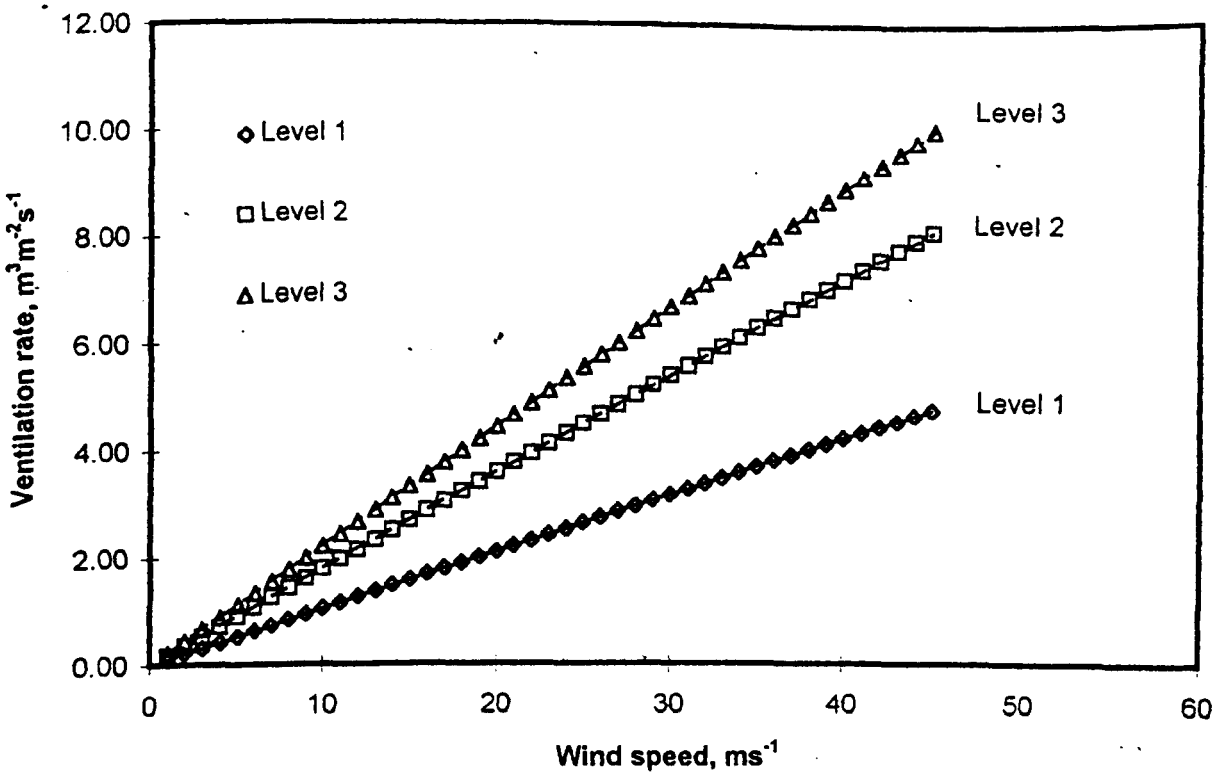

Figure 5.4 (a) Relationship between natural ventilation rate and opening levels for screen N50

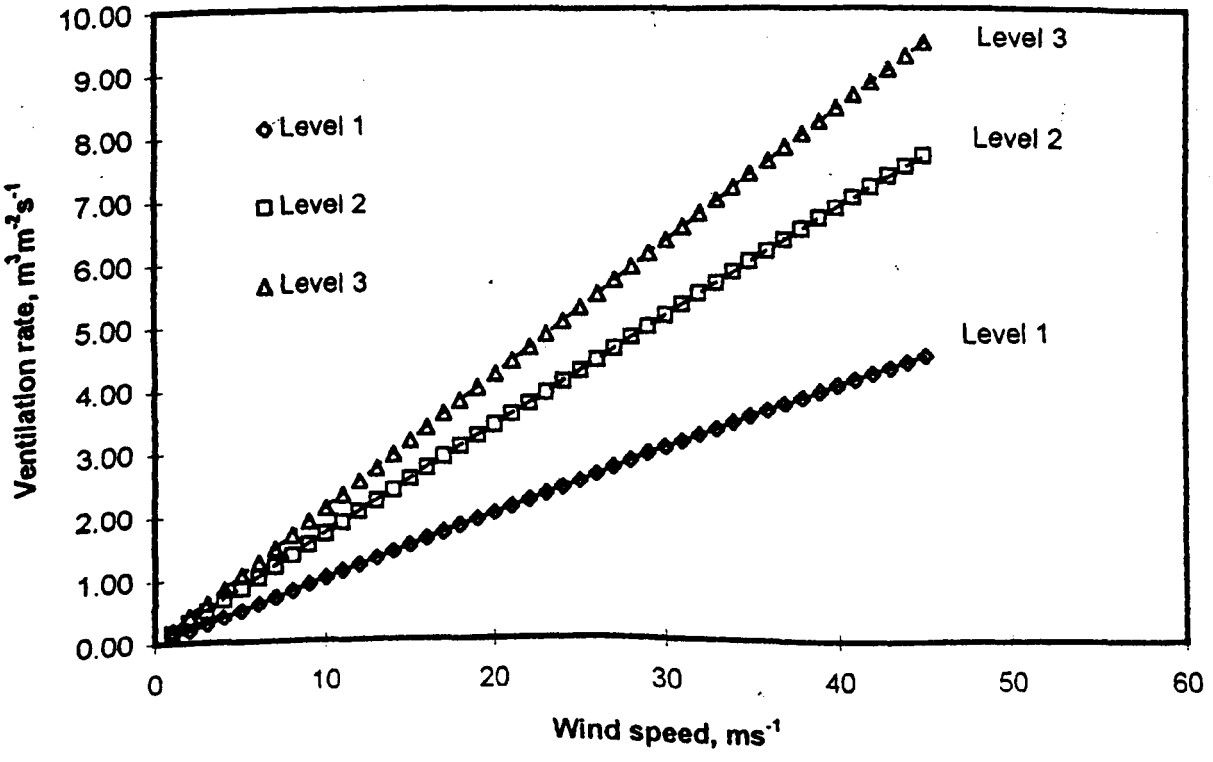

Figure 5.4 (b) Relationship between natural ventilation rate and opening levels for screen N32

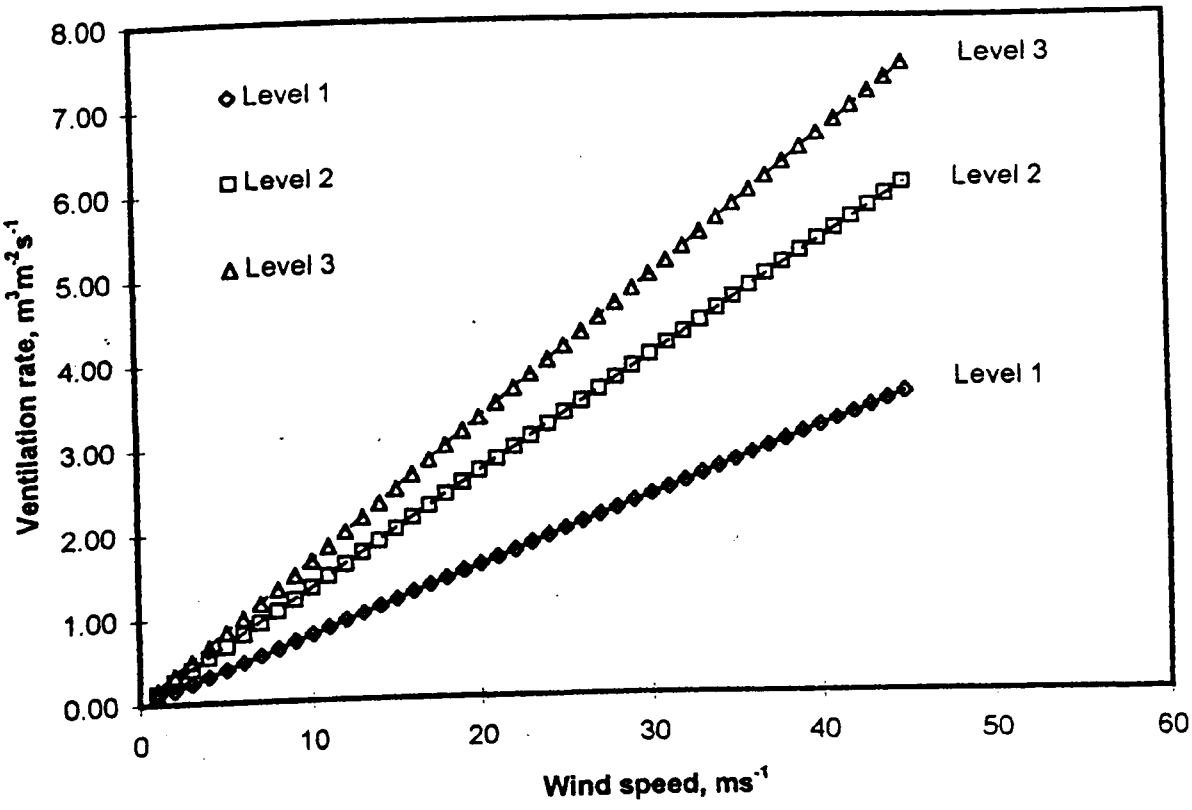

Figure 5.4 (c) Relationship between natural ventilation rate and opening levels for screen N24

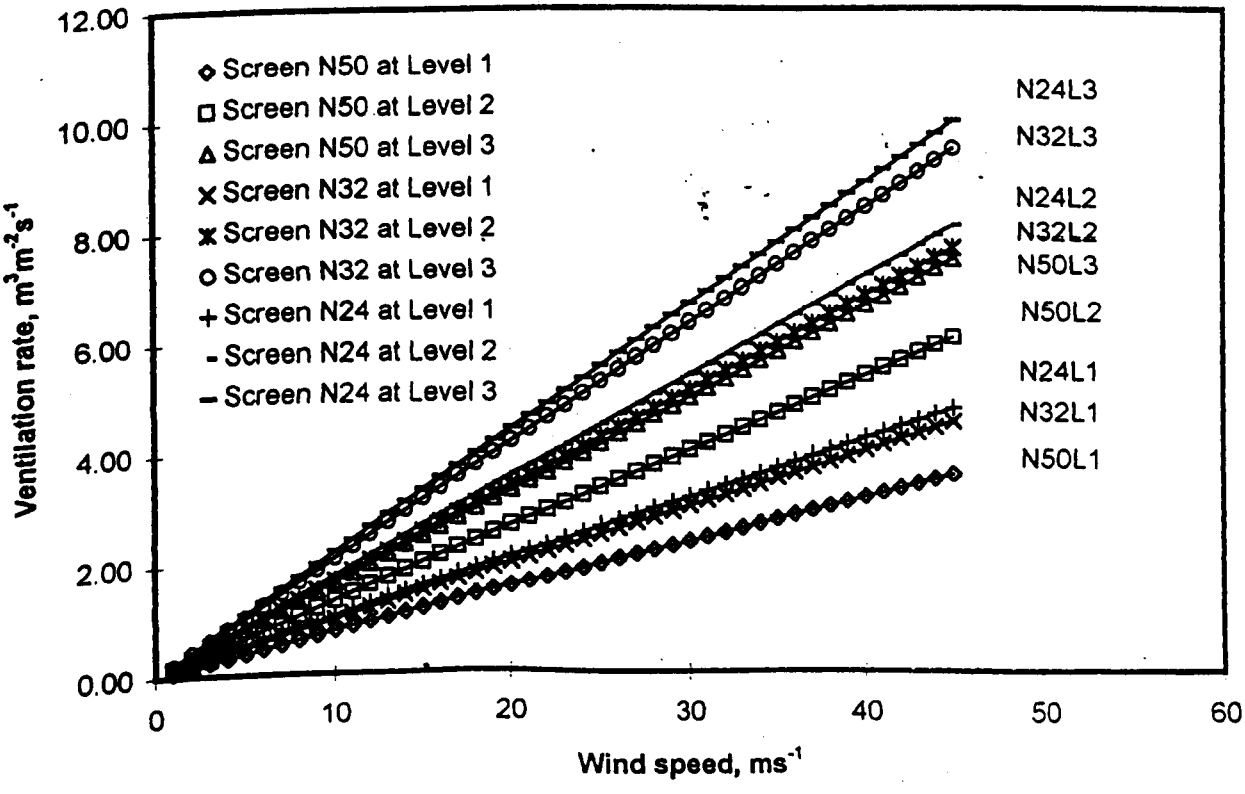

Figure 5.4 (d) Relationship between natural ventilation rates and opening levels for screen sizes N50, N32 and N24

Natural ventilation rate as a function of wind speed and direction is presented in Figure 5.4 (a)-(d). These results were calculated by using equation 5.7 and all winds were perpendicular to the longitudinal axis of the structure. Very strong linear correlation is shown between the natural ventilation rate and wind speed at eaves height. This relationship agrees with the findings of Whittle and Lawrence (1960), Bot (1983) and De Jong (1990). These studies were made using the tracer gas decay method and linear relationships were found between ventilation flux and outside wind speed. The regression equations from Figure 5.4 are summarised in Table 5.3.

Table 5.3 Regression equations for different screen sizes and ventilator opening areas All correlation values of R^2 are equal to 1.0.

Screen	Level	Regression equation
Screen N24	Level 1 Level 2 Level 3	Φ_{WS}=0.1054V Φ_{WS}=0.1791V Φ_{WS}=0.2213V
Screen N32	Level 1 Level 2 Level 3	Φ_{WS}=0.1000V Φ_{WS}=0.1690V Φ_{WS}=0.2099V
Screen N50	Level 1 Level 2 Level 3	Φ_{WS}=0.0787V Φ_{WS}=0.1337V Φ_{WS}=0.1650V

Table 5.3 shows that the ventilation rate increases linearly with wind speed and the ventilation coefficient (C) also increases with increasing screen size or ventilator opening. Therefore, from the table a general regression equation can be formulated as;

$$\Phi_{ws} = CV \tag{5.10}$$

where Φ_{WS} is the ventilation rate by wind effect ($m^3\ m^{-2}\ s^{-1}$), V is the outside wind speed at eaves level ($m\ s^{-1}$) and C is the ventilation coefficient (dimensionless) which is a function of screen size, coefficient of discharge, wind direction and opening area. The values of C for different screen sizes and opening areas (levels) are shown in Figure 5.5.

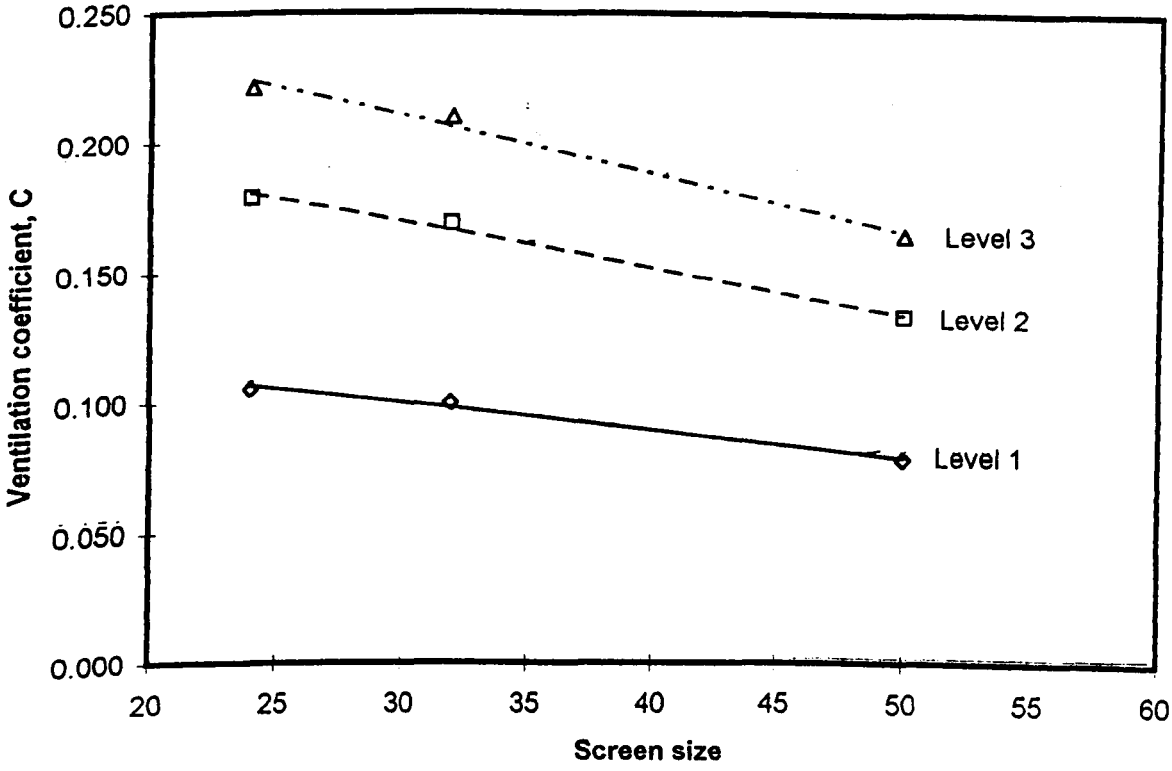

Figure 5.5 Relationship between ventilation coefficient, screen size and area of opening at different levels

Figure 5.5 shows very strong linear correlation between ventilation coefficient and screen size. This relationship can be used for predicting the ventilation coefficient for a range of insect screens between N50 and N24. (N50 means there are 50 holes per inch of that screen).

5.5 Conclusions

The present studies contribute some knowledge on how to predict natural ventilation rates of full side screen ventilators for tropical conditions. The conclusion has shown that there is a very strong linear correlation between natural ventilation rate with outside wind speed at eaves height, which is in agreement with theory and the findings of other researchers. The ventilation rate is also effected by wind direction, insect screen size and ventilator opening area. The flow characteristics of the screen samples show a linear relationship between square of airspeed and pressure difference which is in agreement with the Bernoulli's equation. Finally, the internal and external wind pressure coefficients which are not available in the CP3: Code of Practice, contribute a reference for the structural wind loading design for this type of structure in the tropics.

Chapter 6

Natural ventilation by stack and wind effect

6.1 Introduction

Natural ventilation has the potential for reducing operating and building costs of crop protection structures in the tropics. An understanding of natural ventilation is critical in routine ventilation management because of fluctuations of outside solar radiation, air temperature, and wind speed and direction. Therefore, a suitable mesh screen size in screens covering ventilator openings is crucial to maintain the desired inside climatic conditions for crop production.

Ventilation can be caused by the stack or wind effects or by a combination of both in the naturally ventilated crop protection structure. It is a complicated process to be quantified, and has been under research for a long time. Theories have been developed to predict the ventilation rates for cases where only the stack or wind effect occurs, while few studies have been made on both effects in greenhouses. All of these studies have been conducted in Temperate and Mediterranean regions. However, ventilation studies of both effects in the tropics have not yet been carried out. In the tropics the weather is uniformly hot, humid with heavy rainfall, and the crucial problem of insect and diseases throughout the year. Natural ventilation studies by only stack and wind effects have been separately carried out and presented in Chapters 4 and 5 respectively. However, in this chapter, ventilation caused by the combination of stack and wind effects is discussed in detail.

When there is no wind, the stack effect provides the minimum ventilation rate that is critical in the design of tropical greenhouses. For cases when the wind speed is relatively large, the contribution of the stack effect to the total ventilation rate can

usually be neglected compared to that of the wind effect. However, when both contributions are comparable, both effects must be considered in calculating ventilation rates. ASHRAE (1989) recommends a simple method for estimating the total airflow due to the combined stack and wind effect by quadrature. Sherman *et al.* (1980) have developed an equation to calculate air infiltration in buildings as a function of wind speed and temperature difference between the inside and outside. Its simplicity, combined with the need to measure only a few parameters, make this formula of interest.

Brockett *et al.* (1987) have developed a theoretical description of combined natural ventilation. They used their description to calculate airflow rates in a natural ventilation control model for adjusting side wall openings. A model of combined wind and thermal buoyancy effect was developed by Zhang *et al.* (1989). Their model was developed from established theories. Considering steady state conditions, they found that the measured internal temperatures were close to the predicted temperatures.

Bot (1983) compared ventilation phenomena due to wind or temperature effects in a greenhouse compartment. He found that the measured and theoretical values were in good agreement. The effect of temperature difference could be observed at wind speeds under about 1.0 m s^{-1} and the wind effect dominated when wind speed was higher than 1.7 m s^{-1}. In addition, he revealed that the temperature effect increased with the square root of the temperature difference and the wind effect was linearly proportional to wind speed. No influence of wind direction was observed.

De Jong (1990) made similar observations as Bot. He noted that agreement between the estimated and measured total ventilation was fairly good. The maximum

error was found to be around 20 %. Both authors used the tracer gas method to measure ventilation in their studies.

Natural ventilation by the stack and wind effects was also studied by Fernandez and Bailey (1992) in a glasshouse. They used tracer gas and energy balance methods in their studies and found that wind speed had a strong influence on both leakage and ventilation rates. No influence was observed from either wind direction or temperature difference. In addition, they claimed that good agreement was obtained between values predicted by the energy balance model and measured values for larger openings, but that at low ventilation rate the agreement was poor.

The combined effects have also been studied by Kittas *et al.* (1996) in a plastic greenhouse. They found that the total ventilation flux was linearly dependent on the total area of openings, but that the temperature effect depended also on the ratio of ridge to side openings. The stack and wind effects depended on the ratio between wind speed and the square root of the inside-outside temperature difference. In their case the wind effect predominated over the stack effect when this ratio was greater than 1.0. Ventilation rate was not affected by wind direction in their studies.

The aim of the present studies is to develop a knowledge how to predict natural ventilation rates caused by a combination of wind and stack effects, in a typical crop protection structure in the tropics. The effects of screen mesh size, ventilator opening area, temperature, wind speed and direction on natural ventilation rate were also investigated.

6.2 Principal consideration

Air flow through the ventilator openings can be caused by the stack or wind effects or the combination of both effects. The theories of the stack and wind effects only have been separately discussed in Chapters 4 and 5 respectively. This chapter highlights the theory of the combination of both stack and wind effects.

When there is no wind, buoyancy or stack effect dominates the minimum natural ventilation rate. Fresh air will enter from the lowest openings and exhaust through the upper ventilator openings. The principal of this effect has been discussed in Chapter 4 and can be expressed as;

$$\Phi_{NP} = \frac{4}{3A_g} C_d L X \left[2g \frac{\Delta T}{T_o} \right]^{\frac{1}{2}} \qquad (6.1)$$

where Φ_{NP} is the ventilation rate derived from neutral plane method ($m^3 m^{-2} s^{-1}$), C_d is the coefficient of discharge (dimensionless), A_g is the ground area (m^2), g is the acceleration due to gravity ($m s^{-2}$), ΔT is the air temperature difference between the inside and outside of the structure (K), T_o is the outside air temperature (K), L is the length (m) and X is obtained from an integral (m) over side opening heights of the typical crop protection structure. The heights of side openings from the ground for 1st, 2nd and 3rd ventilator levels are 0.5, 1.0 and 1.5 m respectively. However, the roof opening height is constant at 0.3 m. The integral values of X are as follows;

First level, x = 0.637, if the neutral plane is above the side openings

Second level, x = 0.739, if the neutral plane intersects the openings

Third level, x = 0.993 if the neutral plane intersects the openings

According to Bot (1983), De Jong (1990) and Kittas *et al.* (1996), when the wind speed is relatively large, the contribution of thermal buoyancy to the total ventilation rate can usually be neglected compared to that of the wind effect. If the wind direction is perpendicular to the ventilator openings, the wind ward and leeward openings will become the inlet and outlet respectively. The ventilation of the crop protection structure is given by;

$$\Phi_{WS} = C_d \frac{A_T}{2A_g} V_w \cdot \frac{\left(C_{pe} - C_{pi}\right)}{\sqrt{\left(\left|C_{pe} - C_{pi}\right|\right)}} \qquad (6.2)$$

where Φ_{WS} is the ventilation rate by wind effect ($m^3 m^2 s^{-1}$) and A_g is the ground floor area (m^2). A_T is the area of the total inlet ventilators (m^2), V_w is the air speed perpendicular to the openings at eaves level ($m\ s^{-1}$), C_{pe} and C_{pi} are the wind pressure coefficients at the exterior and interior of the structure respectively.

When both contributions are comparable with each other (e.g., when wind speed is low), both must be considered for calculating the ventilation rate.

According to ASHRAE (1989), Zhang *et al.* (1989) and Albright (1990), the net rate of ventilation is not the sum of the two effects acting independently. Air flow through ventilators is proportional to the square root of the pressure difference. Theoretically, the pressure differences is added but not the flow rates and the total air flow from

combined stack and wind effects is approximated by adding through quadrature as given by;

$$\Phi_{SW} = \sqrt{\left(\Phi^2_{STACK} + \Phi^2_{WIND}\right)} \tag{6.3}$$

where Φ_{SW} is the ventilation rate by the combination of stack and wind effects ($m^3\ s^{-1}$). Φ_{STACK} and Φ_{WIND} are the ventilation rates induced by only stack and effect respectively ($m^3\ s^{-1}$). If equation 6.1 and equation 6.2 are substituted in equation 6.3, we will have the natural ventilation rate of the typical crop protection structure as given by;

$$\Phi_{SW} = \left[\left[\left(\frac{4}{3A_g} C_d L X\right).\left(2g\frac{\Delta T}{T_o}\right)^{\frac{1}{2}}\right]^2 + \left[C_d \frac{A_T}{2A_g} V_w . \frac{\left(C_{pe} - C_{pi}\right)}{\sqrt{\left(\left|C_{pe} - C_{pi}\right|\right)}}\right]^2\right]^{\frac{1}{2}} \tag{6.4}$$

Ventilation rates by the combination of stack and wind effects can also be obtained using the tracer gas and energy balance methods. These methods have been reported in Chapter 4. According to Bot (1983), De Jong (1990), and Fernandez and Bailey (1992), the measured ventilation rate obtained by the tracer gas method (Φ_{TG}) can be easily compared with ventilation rates calculated in the crop protection structure with other characteristics if it is expressed as the dimensionless function $G(\alpha)$;

$$G(\alpha) = \frac{\Phi_{TG}}{UA_S} \tag{6.5}$$

where α is the angle of glasshouse ventilator opening. This parameter gives the relation between Φ_{TG} per unit ventilator area A_S (= L_S x H_S x number of ventilators, (m^2)) and the wind speed U (m s^{-1}) at eaves level.

6.3 Experimental design

Studies on natural ventilation caused by the combination of stack and wind effects have been made in the open in the garden in Silsoe Research Institute, England. This location is suitable for studying of both effects, which is surrounded by wind obstructions to control extreme wind speeds. The naturally ventilated crop protection structure described in Chapter 4 was transferred and erected at this location. Plate 31 shows the structure and the surrounding area for natural ventilation studies caused by combination of stack and wind effects.

The floor of the structure was covered with a polyethylene sheet, a 50 mm thick polycarbonate panel and a black plastic sheet. This was to reduce CO_2 emissions from the ground and to insulate the ground from the solar energy absorbed. The same experimental programme that has been reported in Chapters 4 and 5 were applied here. The effects of screen and opening sizes on natural ventilation were conducted in nine sets of experiments as shown in Table 6.1. For each set of the experiment, the same screen was used to clad both the continuous side and roof openings. There were two side openings 5.8 m long with heights of 0.5 m (level 1), 1.0 m (level 2) and 1.5 m (level 3) from the ground. There were also two fixed roof openings 5.8 m long and

0.3 m high. To change the screen level, the same procedure as described in Chapters 4 and 5 was applied in the present experiment.

Plate 31. Crop protection structure for stack and wind effects

Three methods were used to facilitate the comparison studies in quantifying natural ventilation rates. They were the dynamic tracer gas, energy balance and combination of stack and wind method. The tracer gas as a control method and energy balance method have described in equation 4.2 and 4.22. In addition, the stack and wind method is a combination results of the neutral plane and wind pressure measurement methods that has been described in equation 6.4. Data collection for all methods was carried out simultaneously for each set, for example screen N50 and level 1, and so on. The required parameters of each method are presented in Table 6.1

Table 6.1 Experimental programme for combination of stack and wind effects studies

Screen	N50			N32			N24		
Method/Level	L1	L2	L3	L1	L2	L3	L1	L2	L3
1. Tracer gas	a,b	a,b	a,b	a,b	a,b	a,b	a,b	a,b	a,b
3. Energy balance	a,c,d	a,c,d	a,c,d	a,c,d	a,c,d	a,c,d	a,c,d	a,c,d	a,c,d
3. Stack and wind	a,e,f	a,e,f	a,e,f	a,e,f	a,e,f	a,e,f	a,e,f	a,e,f	a,e,f

Note: N50 means insect screen N50 and L1 means level of one side vent and one roof vent on both sides. a = inside and outside temperature, b = gas decay and time, c = inside and outside solar radiation, d = inside and outside relative humidity, and e = inside and outside wind pressure, f = speed and direction

Sensors to measure the required environmental variables were installed inside and outside the structure. Table 6.2 gives a description of the measured variables and sensors. The readings of all sensors were recorded every 30 s using a data logging computer system. This was made to cater for the rapid and turbulent gas decays which occurred in the structure in the open field. All the sensors had been tested and calibrated by Silsoe Research Institute. However, another calibration was made before they were used.

Table 6.2 Variables measured during the experiments and sensors and instruments

Parameters	Sensors
Solar radiation	Pyranometer, PAR sensor
Total radiation	Pyrradiometer
Air temperature	Aspirated platinum resistance thermometer
Relative humidity	Electronic hygrometer
Dry and wet bulb temperature	Aspirated platinum resistance thermometer
Airspeed	Hot wire anemometer
CO_2 concentration	Infra red gas analyser
Wind speed	Sonic anemometer
Wind direction	Wind vane
Wind pressure	Transducer

Temperature and humidity sensors inside aspirated screens were hung in the middle and outside the crop protection structure. Solar radiation sensors were placed on the structure's floor and on the roof top of a nearby structure.

A pressure tube, wind vane and sonic anemometer were installed at the eaves height of the structure. This was to measure the free stream wind pressure, speed and direction. The internal and external wind pressures of the structure were sensed by pressure tapping points distributed over the surface. The details of the tapping points and data recording that have been described in Chapter 5 were used in the present studies.

CO_2 gas was used as a tracer gas and the gas was injected through perforated pipe. To ensure the gas was uniformly distributed, many holes at different angles were punched in the pipe which lay around inside the structure. A fan was not used for mixing because the structure had highly porous side walls that would disturb the buoyancy force. The side screens were covered with transparent polythene sheets while the tracer gas was injecting. When the desired concentration (1500 ppm) was reached, the supply of CO_2 was stopped, the polythene sheets were removed and then

the inside and outside air was sampled during the period of decreasing CO_2. The air from the 3 positions was mixed and pumped through an infra red gas analyser to measure CO_2 concentration. Plates 26, 27, 29, and 30 show some of the sensors installed inside and outside the crop protection structure.

6.4 Results and discussion

6.4.1 Ventilation by tracer gas method

The results of the natural ventilation rates caused by the stack and wind effects are presented in Table 6.3. In general this shows that all the ventilation rate regression equations are inconsistent as a function of square root of temperature difference, wind speed, opening level and screen size. The adjusted coefficients of determination (R^2) are also inconsistent in the range of positive and negative correlation. The correlations are shown to be a very weak and modest.

Adjusted R^2 is defined as the difference between total mean sum of squares and residual mean sum of squares divided by total mean sum of squares. The equation form is as follow,

$$\text{Adjusted } R^2 = \frac{\text{Total mean sum of squares} - \text{Residual mean sum of squares}}{\text{Total mean sum of squares}}$$

It can be negative if the residual mean sum of squares is greater than the total mean sum of squares (Draper, 1998). Negative adjusted R^2 means there is a weak or no correlation between ventilation rate as a function of square root temperature difference and wind speed.

Table 6.3 Regression equations of natural ventilation rates by combination of stack and wind effects according to the tracer gas method

Screen	Level	Regression equation $\Phi_{TG} = A\Delta T^{1/2} + BU$	n	$S.E._A$	P_A	$S.E._B$	P_B	Adjusted R^2
N50	L 1	$\Phi_{TG} = 0.01301\Delta T^{1/2} + 0.00645U^*$	39	0.00204	1.91×10^{-7}	0.00181	0.001	0.290
	L 2	$\Phi_{TG} = 0.00345\Delta T^{1/2} + 0.00926U^*$	57	0.00160	0.035	0.00075	1.31×10^{-17}	0.093
	L 3	$\Phi_{TG} = 0.00526\Delta T^{1/2} + 0.00683U$	30	0.00590	0.380	0.00204	0.002	-0.729
N32	L 1	$\Phi_{TG} = 0.01809\Delta T^{1/2} + 0.00383U$	44	0.00372	1.68×10^{-5}	0.00136	0.008	-0.500
	L 2	$\Phi_{TG} = 0.05815\Delta T^{1/2} - 0.00494U$	29	0.01491	0.001	0.00378	0.202	-1.902
	L 3	$\Phi_{TG} = 0.01692\Delta T^{1/2} + 0.00574U$	26	0.00812	0.048	0.00199	0.008	-0.619
N24	L 1	$\Phi_{TG} = 0.00656\Delta T^{1/2} + 0.00901U$	37	0.00965	0.501	0.00267	0.008	-0.713
	L 2	$\Phi_{TG} = 0.01698\Delta T^{1/2} + 0.00490U$	27	0.00504	0.002	0.00248	0.060	-0.383
	L 3	$\Phi_{TG} = 0.00959\Delta T^{1/2} + 0.00795U$	27	0.00943	0.319	0.00230	0.002	-1.373

Where A and B are the coefficients of stack and wind effect respectively (dimensionless), S.E. is the standard of error, P is the probability value and * shows regression equation has statistically significant at 5% level of significance.

Among the regression equations only the smallest screens at the two smallest opening levels give statistically significant ventilation rates. These were screen N50 at level 1 and screen N50 at level 2. Their F-significance levels are within the 0.05 level of significance which are 0.0006 and 0.02444 respectively. In addition their standard errors are small and their probability values are less than 0.04. The regression equations show ventilation rate as a function of square root of temperature difference and wind speed. The descriptive statistics of the data are shown in Table 6.4. and the general regression equation of screen N50 at levels 1 and 2 can be written as follows;

$$\Phi_{SWR} = A\Delta T^{\frac{1}{2}} + BU \qquad (6.6)$$

where Φ_{SWR} is the natural ventilation rate by combination of stack and wind effects derived by multiple regression line ($m^3\ m^{-2}\ s^{-1}$), A is the coefficient of the stack effect, ΔT is the temperature difference between the inside and outside of the structure (K), B is the coefficient of the wind speed effect and U is the outside wind speed at eaves

level (m s^{-1}). The values of A and B for the screen N50 at levels 1 and level 2 are shown in Table 6.3. Coefficient A is a function of coefficient of discharge, opening area, height of the two openings and gravitational acceleration. In addition, the B is a function of coefficient of discharge, opening area and, wind speed and direction.

The other regression equations were statistically insignificant. This was because their ventilator opening areas are bigger than 20 % of the ratio of opening area and wall area. The larger ventilator opening gives very rapid air exchange that is very difficult to measure because of the quick and turbulent tracer gas decays.. According to Albright (1990), ventilation is effected by indoor and outdoor air pressures. The indoor pressure differs from free stream atmospheric pressure and is effected by the external pressure coefficients and the size of the openings. The external pressure coefficients are thought not to be affected by the sizes of vents unless the vents are larger than 15% of the wall area.

Table 6.4 Descriptive statistics of screen N50 at level 1 and screen N50 at level 2 by the tracer gas method

Statistics	**Temperature difference (K)**	**Wind speed (m s^{-1})**	**Ventilation rate (m^3 m^{-2} s^{-1})**
Screen N50 at level 1			
Mean	4.4	2.2	0.041
Count	39	39	39.000
Standard Error	0.3	0.1	0.002
Standard deviation	1.6	0. 9	0.013
Maximum	7.5	4.2	0.080
Minimum	1.8	0.1	0.012
Screen N50 at level 2			
Mean	2.1	3.0	0.033
Count	57	57	57.000
Standard Error	0.2	0.1	0.001
Standard deviation	1.6	0.9	0.010
Maximum	5.7	5.1	0.058
Minimum	0.3	1.3	0.002

Table 6.4 shows that the mean wind speed for level 1 and level 2 was 2.2 and 3.0 m s^{-1} respectively. The wind directions associated with wind speeds were observed to be diagonally 70 - 80° from normal to the ventilator openings. These speeds are within the wind speed range of the combined stack and wind effects, which is 1.0 m s^{-1} to 4.0 m s^{-1} according to Bot (1983), De Jong (1990) and Wang (1998). This can clearly be seen in Figure 6.1, if the combined effects are plotted on the same graph.

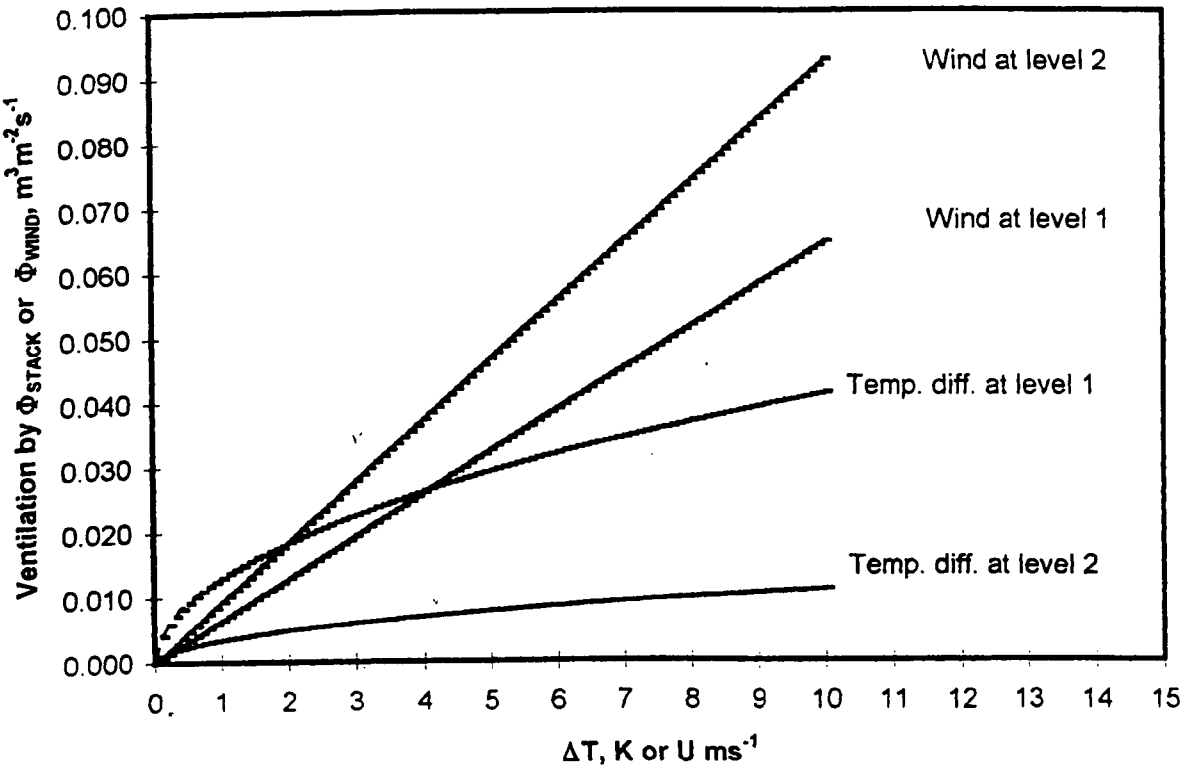

Figure 6.1 Relationship between ventilation rate caused by stack or wind effect using the tracer gas method for screen N50 at level 1 and level 2

According to Bot (1983) and Kittas et al. (1996), the relative influence of the temperature and wind effects on ventilation can be defined from combination of equation 6.4 and measured ventilation rate (Φ_{TG}) and then plotting the measured

values of the reduced flux (Φ_{TG}/A_TU) as a function of the ratio $U/\Delta T^{0.5}$ as shown in Figure 6.2.

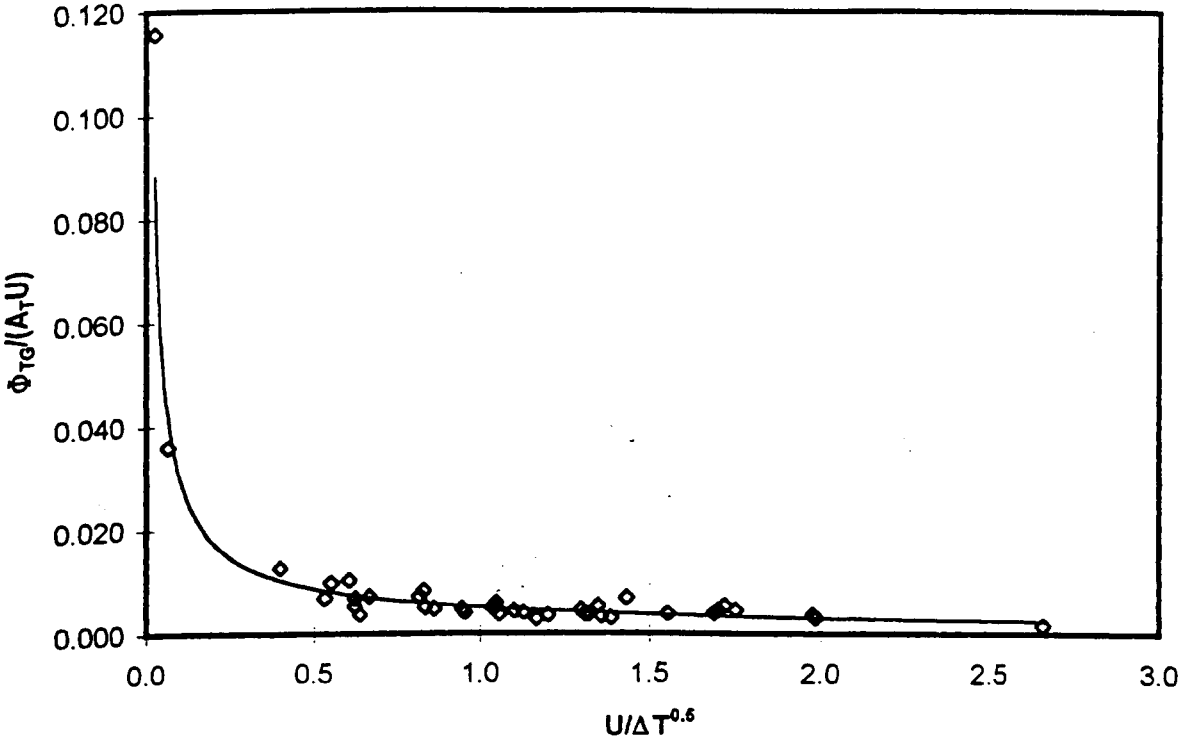

Figure 6.2 Measured values of the reduced flux (Φ_{TG}/A_TU) as a function of the ratio $U/\Delta T^{0.5}$

Figure 6.2 shows the variation of Φ_{TG}/A_TU in relation to $U/\Delta T^{0.5}$ and it allows the determination of when the wind effect predominates over the temperature effect. We can see that, when $U/\Delta T^{0.5} > 0.5$ the wind effect predominates over the

temperature effect. For example, for ΔT = 1.8 K, the wind effect will predominate on ventilation for u > 0. 7 m s^{-1}; while for ΔT = 7.5 K the wind effect will predominate for u > 1.4 m s^{-1}.

Kittas *et al.* (1996) have presented $u/\Delta T^{0.5} > 1$ for a greenhouse equipped with roof and side openings, this ratio is higher than the present finding because their structure had a smaller ratio of vents to covered area, which was 7% . The present structure has a ratio of more than 15 % with screen covering the vent opening area. However, the ratio of 0.333 was revealed by Bot (1983) for the glass house with only roof windows .

6.4.2 Ventilation by energy balance method

The results of natural ventilation rates induced by the combination of stack and wind effects are presented in Table 6.5. These ventilation rates have been calculated according to energy balance equation 4.22 presented in Chapter 4. For comparison purposes, the energy balance parameters were measured simultaneously with the tracer gas data. The regression results show screen N50 at level 1, screen N32 at level 1 and screen N24 at level 2 have statistical significance. That means the natural ventilation rate is a function of square root temperature difference and wind speed. This shows in good agreement with tracer gas regression equation as shown in equation 6.6. In addition, these results agree with the model by Kittas *et al.* (1996).

Table 6.5 Regression equations of natural ventilation rate by the combination of stack and wind effects according to the energy balance method

Screen	Level	Regression equation $\Phi_{EB} = A\Delta T^{1/2} + BU$	n	$S.E._A$	P_A	$S.E._B$	P_B	Adjusted R^2
N50	L 1	$\Phi_{EB} = 0.00490\Delta T^{1/2} + 0.00400U^*$	39	0.00121	0.0002	0.00107	0.001	0.066
	L 2	$\Phi_{EB} = -0.00994\Delta T^{1/2} + 0.01879U^*$	57	0.00278	0.001	0.00129	$1.85x10^{-20}$	0.524
	L 3	$\Phi_{EB} = -0.01508\Delta T^{1/2} + 0.02274U$	30	0.01524	0.331	0.00527	0.00018	-0.324
N32	L 1	$\Phi_{EB} = -0.01344\Delta T^{1/2} + 0.02088U^*$	44	0.00627	0.038	0.00230	$1.74x10^{-11}$	0.352
	L 2	$\Phi_{EB} = 0.06644\Delta T^{1/2} - 0.00100U$	29	0.01643	0.0004	0.00417	0.813	-3.258
	L 3	$\Phi_{EB} = 0.02449\Delta T^{1/2} + 0.01518U$	26	0.02485	0.334	0.00610	0.020	-0.216
N24	L 1	$\Phi_{EB} = 0.00481\Delta T^{1/2} + 0.01279U$	37	0.00640	0.084	0.00326	$4.24 x10^{-7}$	-0.208
	L 2	$\Phi_{EB} = -0.01194\Delta T^{1/2} + 0.02211U^*$	27	0.00663	0.002	0.00248	0.060	0.260
	L 3	$\Phi_{EB} = 0.02697\Delta T^{1/2} + 0.00587U$	27	0.01108	0.022	0.00270	0.0390	-1.496

Where A and B are the coefficients of stack and wind effect respectively (dimensionless), S.E. is the standard of error, P is the probability value and * shows regression equation has statistically significant at 5% level of significance.

In general, the regression equations are inconsistent, the wind speed and temperature difference fluctuate positively or negatively according to which driving force is dominant. Positive value means the positive driving force is dominant and for negative value it is less dominant. Among the regression equations only the result for screen N50 at level 1 shows highly statistical significance that gives a good representation, where both temperature difference and wind speed are accounted. In addition, their coefficients A and B exhibit small standard errors and their P-values are significance at less than 0.05. This equation is also in accordance with the result that has been measured by the tracer gas method in Section 6.4.2., where the ratio of ventilator openings and wall area was less than 15%. Therefore, the energy balance method can be used to calculate natural ventilation rate for this typical structure and the reliability is dependent to the ratio of ventilator openings and wall area.

6.4.3 Ventilation by stack and wind method

The ventilation rate results that have been calculated using equation 6.4 are presented in Table 6.6. The results show all regression equations consistently represent the ventilation as a function of square root of temperature difference and wind speed. Both stack and wind effects are accounted for in these regression equations. However, the coefficients A and B vary inconsistently. This is due to fluctuations of wind speed and temperature difference while the data was being taken.

The test shows all the regression equations are statistically significant at less than the 0.05 level of significance. In addition, the standard error are very small for all coefficients A and B. These good results are attained because of the proven method that has been widely used by many authors in different publications. Therefore, this stack and wind method can be used in the calculation of natural ventilation rate of the present typical structure.

Table 6.6 Regression equations of natural ventilation rates by combination of stack and wind effects according to stack and wind method

Screen	Level	Regression equation $\Phi_{sw} = A\Delta T^{1/2} + BU$	n	$S.E._A$	P_A	$S.E._B$	P_B	Adjusted R^2
N50	L 1	$\Phi_{sw} = 0.02556\Delta T^{1/2} + 0.01049U^*$	39	0.00044	4.94×10^{-38}	0.00039	6.12×10^{-26}	0.932
	L 2	$\Phi_{sw} = 0.01968\Delta T^{1/2} + 0.02636U^*$	57	0.00045	2.04×10^{-44}	0.00021	2.56×10^{-69}	0.959
	L 3	$\Phi_{sw} = 0.01455\Delta T^{1/2} + 0.04768U^*$	30	0.00042	1.73×10^{-24}	0.00015	1.06×10^{-51}	0.964
N32	L 1	$\Phi_{sw} = 0.02009\Delta T^{1/2} + 0.02002U^*$	44	0.00056	5.13×10^{-33}	0.00021	5.01×10^{-51}	0.992
	L 2	$\Phi_{sw} = 0.01711\Delta T^{1/2} + 0.03612U^*$	29	0.00077	2.21×10^{-19}	0.00019	7.79×10^{-45}	0.964
	L 3	$\Phi_{sw} = 0.02408\Delta T^{1/2} + 0.03066U^*$	26	0.00111	9.59×10^{-18}	0.00027	2.33×10^{-35}	0.955
N24	L 1	$\Phi_{sw} = 0.01699\Delta T^{1/2} + 0.01948U^*$	37	0.00038	3.14×10^{-33}	0.00011	2.67×10^{-55}	0.970
	L 2	$\Phi_{sw} = 0.02333\Delta T^{1/2} + 0.03617U^*$	27	0.00074	1.07×10^{-21}	0.00036	4.92×10^{-34}	0.949
	L 3	$\Phi_{sw} = 0.01642\Delta T^{1/2} + 0.06307U^*$	27	0.00107	1.50×10^{-14}	0.00026	3.98×10^{-45}	0.960

Where A and B are the coefficients of stack and wind effect respectively (dimensionless), S.E. is the standard of error, P is the probability value and * shows regression equation has statistically significant at 5% level of significance.

6.4.4 Comparison between measured and calculated method

For comparison purposes, the statistically significant results of the tracer gas method are compared those predicted by the energy balance, and stack and wind methods. Data from screen N50 at level 1 and level 2 that has been taken simultaneously with other methods are compared and presented in the Figures 6.3 and 6.4.

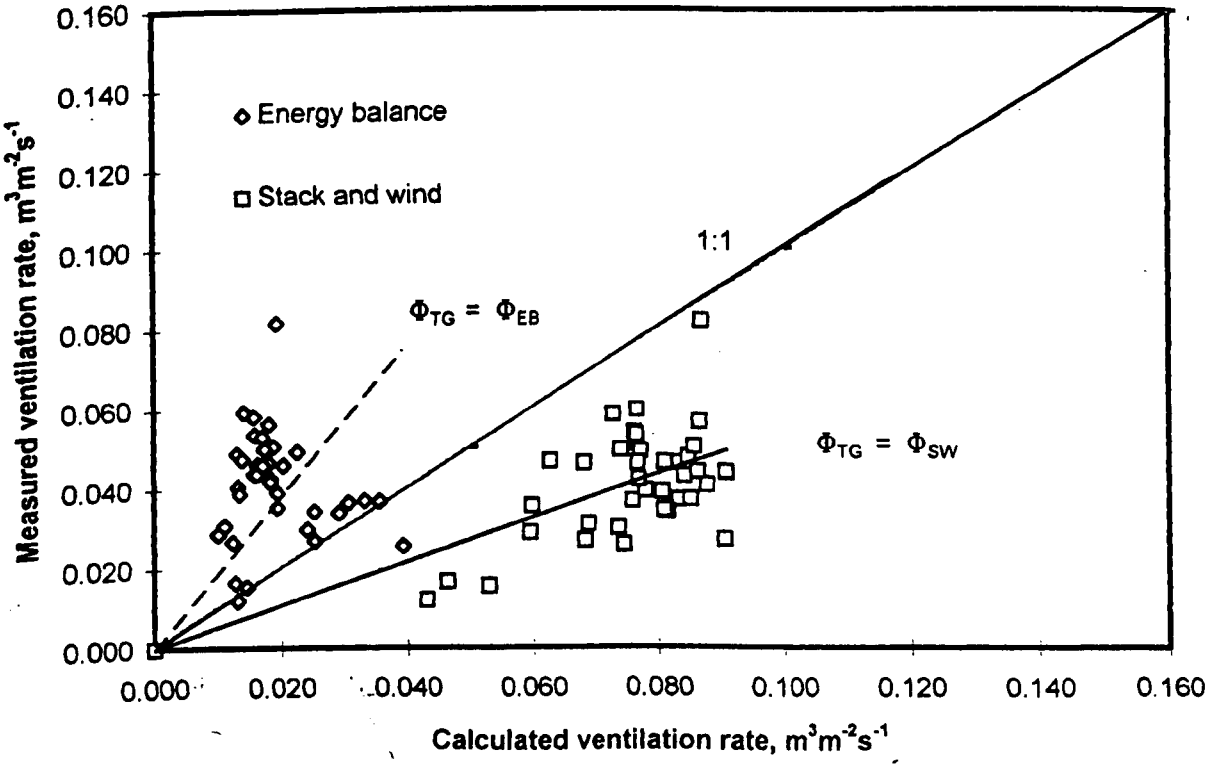

Figure 6.3 Comparison between measured and calculated natural ventilation rates by the stack and wind effects for the screen N50 at level 1

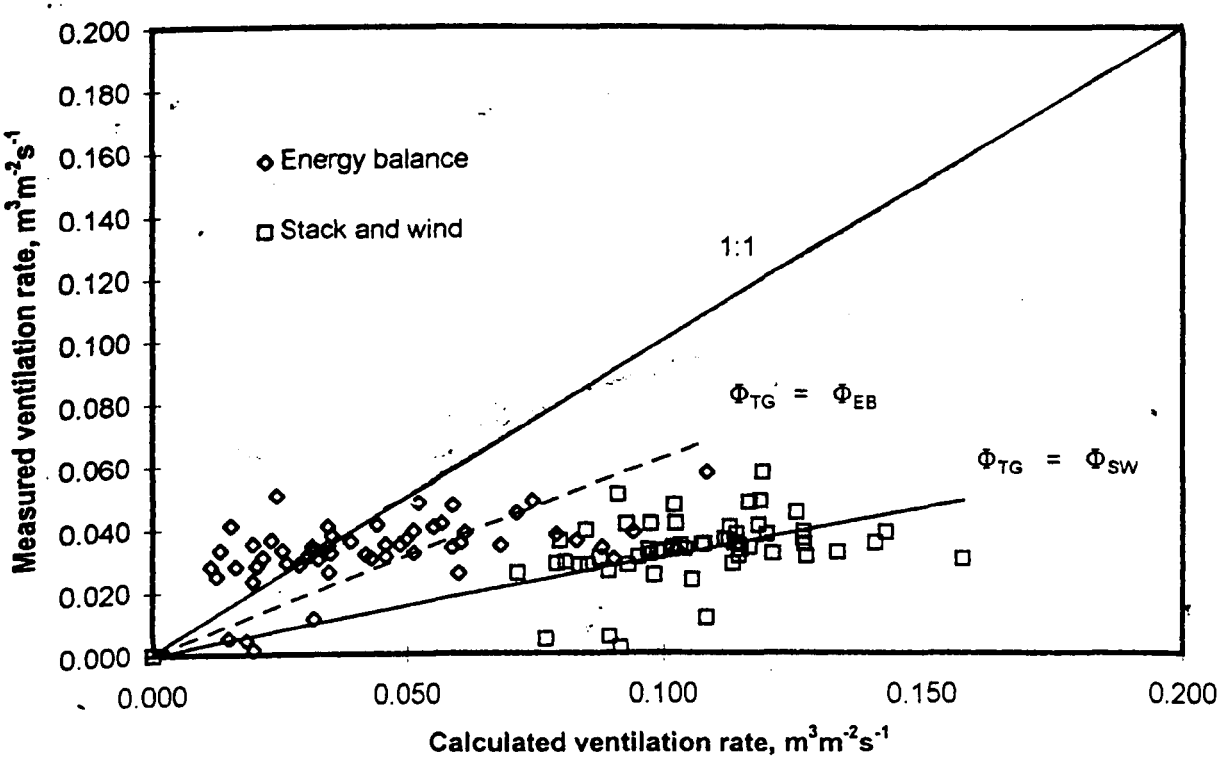

Figure 6.4 Comparison between measured and calculated natural ventilation rates by the stack and wind effects for the screen N50 at level 2

The figures show that the comparison between tracer gas and energy balance methods poor correlation because of negative adjusted R^2, while a modest correlation is found between the tracer gas and the stack and wind method. The deviation of the points from the line increases as the ventilation rates increased. This shows that as the ventilation rate increases, the accuracy of measurement decreases due to the rapid and turbulent of air exchange in the structure. However, some of the energy balance points fall close to the 1:1 line, somewhere in the range 0.02 and 0.05 $m^3 m^{-2} s^{-1}$. This is due to the negative adjusted R^2 that was shown in the regression equation. The statistics regression results for both sets of data are presented in Table 6.7. as follows;

Table 6.7 Comparison results between measured and calculated of natural ventilation rates caused by combination of stack and wind effects.

Screen	Level	Φ_{TG} vs Φ_{EB}	Φ_{TG} vs Φ_{SW}
Screen N50	Level 1	$\Phi_{TG} = 1.888\Phi_{EB}$ n = 39 Adj. $R^2 = -1.288$ S.E. = 0.157 $P = 1.616 \times 10^{-14}$	$\Phi_{TG} = 0.541\ \Phi_{SW}$ n = 39 Adj. $R^2 = 0.276$ S.E. = 0.023 $P = 2.970 \times 10^{-24}$
Screen N50	Level 2	$\Phi_{TG} = 0.625\ \Phi_{EB}$ n = 57 Adj. $R^2 = -1.216$ S.E. = 0.040 $P = 3.280 \times 10^{-22}$	$\Phi_{TG} = 0.310\ \Phi_{SW}$ n = 57 Adj. $R^2 = 0.060$ S.E. = 0.012 $P = 8.468 \times 10^{-33}$

From the ANOVA results, the relationship between the tracer gas results with stack and wind method is statistically significant. The F significance is shown less than 0.05 and the errors are fairly good. However, the strengths of the adjusted coefficients of determinations are in modest correlation between them. Therefore, this method can be used to calculate natural ventilation rates caused by the stack and wind effects.

Based on Table 6.7, the average ventilation rates by the energy balance and stack and wind methods give the same difference of 60 % higher than the tracer gas method. For the energy balance, the difference is higher than the finding of Fernandez and Bailey (1992), which was 16-25% difference measured for a glasshouse with only roof ventilator openings. A comparison study of tracer gas and combination of stack and wind methods was made by Kittas *et al.* (1996), in a plastic greenhouse with side and roof ventilators. They have found that the measured and calculated results were close to each other. However, their plastic house had a smaller ratio of vents to wall compared to the present studies. If the tracer gas method only measures 60-70% of

the actual air exchange (Dufton *et al.* (1942), Hitchin *et al.* (1967) and Ducarme *et al.* (1994)) and some error may occur in the measurements, then both calculated methods give results which are fairly close to the measured method.

6.5 Conclusions

In conclusion all methods have their limitations and their scale of accuracy. In general all methods show natural ventilation as a function of the square root of temperature difference between the inside and outside of the structure, and the outside wind speed at eaves level. The accuracy of the results is based on the effort taken to minimise the experimental errors and on the ratio of ventilator opening to the total wall area which should be less than 20 %. In general, whether the stack or wind effect predominate in the ventilation rate depends on the ratio between wind velocity and the root of inside-outside temperature difference. In these studies the wind effect predominates when the ratio becomes greater than 0.5.

All methods can be used to calculate the natural ventilation rate for a typical crop protection structure in the tropics. Preference is given to the tracer gas method which gives direct ventilation measurement. The energy balance method has some advantages because of important climatic parameters for crop production and the structure interactions with environment are accounted in calculation. In addition, the stack and wind method is easier to be used if the temperature difference and wind parameters are already known. If the calculated methods are used because of their simplicity, the difference of 60% compared to the measured method have to be resolved. However, if the tracer gas method only measures less than the actual ventilation rate, then other calculated methods give results which are fairly close to the measured method.

Chapter 7

Final discussion, conclusions and recommendations

Introduction

Natural ventilation is an important process in controlling the air temperature, humidity and CO_2 concentration inside a crop protection structure. It also can save operational costs on in-house climatic control compared to forced ventilation. This study has focused on natural ventilation of a crop protection structure with insect screen side walls for tropical conditions. No studies previously have been made on natural ventilation in tropical greenhouses, except for the measurement of temperature difference in imported temperate greenhouses adapted for the tropics.

The important driving forces that induce natural ventilation have been studied. The forces are caused by the stack effect, wind effect and a combination of both stack and wind effects. In order to quantify ventilation rates by the different effects, physical properties and airflow characteristics of covering materials are also investigated. The conclusions of the studies are;

[1] Light transmission of covering materials

The direct light transmission of polyethyelene insect screens N50, N32, N24 and transparent polyethylene film were found to be 91.0, 93.3, 96.0 and 91.3 % respectively. The film transmission was close to the screen transmissions. That means the combination of both materials for covering the structure does not affect the light transmission inside the structure. It was found that the direct light transmissions did not follow the cosine law. The biggest screen gave a higher light transmission compared to the smallest one. In addition, the diffuse light transmission of the screens

N50, N32, N24 and film were less than the direct light transmission. They were 75.0, 78.9, 83.2 and 82.0 % respectively.

[2] Coefficients of discharges for insect screens

Coefficient of discharges of polyethylene insect screens N50, N32 and N24 were 0.411, 0.520 and 0.547 respectively. The biggest screen gave the highest value of coefficient of discharge compared to the smallest one. This trend is similar to the finding of Sase *et al.* (1990). He found that the coefficients of discharges of Chicoppee 52 Mesh and Chicoppee 32 Mesh were 0.375 and 0.478 respectively. Coefficient of discharge was found to be one of the dominant parameters in calculating the natural ventilation rate induced by the stack effect, wind effect and the combination of both effects.

[3] Airflow characteristics through insect screens

It was found that when air flows through a screen, the pressure drop increased linearly with the square of the approach air speed. This relationship is in good agreement with the findings of Sase (1990), Baker (1995) and Brundrett (1995). In addition, the pressure drop increased with approach air speed according to the quadratic curve. This trend is similar to the finding of Miguel (1988). Wind pressure and static pressure drop have been found to be greatly affected by the size of the screen. The smallest screen gave the highest pressure drop compared to the biggest screen. This was because the smallest mesh gave the highest airflow resistance when the air flows across the screen.

[4] Natural ventilation by stack effect

It was found that if the outside wind is absent or less than 1.0 m s^{-1}, the inside temperature was increased and at the same time the ventilation was decreased. This was due to the low air exchange rate induced by thermal buoyancy or the stack effect. This study has shown that the measured ventilation rate increased with increasing of temperature difference between inside and outside according to the power law. The power index was found to be 0.5 which agrees with the theoretical ventilation rate. This trend was in good agreement with the findings of Bruce (1978) and De Jong (1990). However, the increase in ventilation rate due to the increasing temperature difference does not avoid high temperatures inside the crop protection structure. To solve this problem, this study revealed that the effects of screen size and ventilator opening area are of paramount importance in reducing the inside temperature rise and increasing the ventilation rate. The biggest screen and ventilator opening were found to give higher ventilation rates than smaller ones, and also give the lowest temperature difference between the inside and outside of the structure. This trend agrees with the finding of Bailey (1978) and Miguel (1998).

[5] Natural ventilation by wind effect

It was found that ventilation induced by the wind effect increased linearly with the wind speed at eaves level and the ventilation rate induced by the stack effect decreased slowly. The inside temperature decreased with increasing wind speed. As the wind direction deviates from perpendicular to the upwind side wall, ventilation due to the wind effect will decrease and that due to stack effect will increase. This trend is in good agreement with Zhang *et al.* (1989).

Ventilation induced by the wind effect was found to be affected by wind speed and direction. This finding was in contradiction with the conclusions of Bot (1983), De Jong (1990) and Fernandez and Bailey (1992), who claimed that the importance of wind direction was insignificance.

The internal and external wind pressure coefficients measured in this study contribute some information for the designer, in calculating the ventilation rate and also for crop protection structure design. Wind pressure coefficients for this kind of structure are not available from the CP3: Standard Codes of Practice .

[6] Natural ventilation by combination of stack and wind effects

This study has revealed that the ventilation rate can be predicted as functions of temperature difference, wind speed and direction, coefficient of discharge, ventilator opening area and the height between the ventilators. For the stack effect, the ventilation rate was found to increase with increasing temperature difference between inside and outside of the crop protection structure according to a power law. The wind effect ventilation rate was found to increase linearly with increasing outside wind speed at the eaves level. A combination of both stack and wind effects can be calculated by the vectorial sum or quadrature ($\Phi_{SW} = (\Phi_{stack}^2 + \Phi_{wind}^2)^{0.5}$) of both effects. However, the result of the wind effect in the combined effects was insignificant when the ratio of ventilator opening to the total wall area is higher than 20 %.

The relative importance of the stack and wind effects is dependent on the ratio between wind speed and the square root of the inside-outside temperature difference ($u/\Delta T^{0.5}$). In this study, the wind effect dominates over the stack effect when the ratio

$u/\Delta T^{0.5}$ becomes greater than 0.5. Kittas *et al.* (1996) have presented $u/\Delta T^{0.5}$ as greater than one for a greenhouse equipped with roof and side openings, this ratio is higher than the present finding because their structure had a smaller ratio (7%) of vent to covered area.

[7] Comparison between different methods of quantifying ventilation rates

Different methods have been used for measuring natural ventilation rates in this study. Comparisons between the methods have shown that the dynamic tracer gas (measured), direct airspeed, energy balance and neutral plane methods can be used to predict ventilation induced by the stack effect. Direct airspeed and air pressure field measurements can be used to quantify ventilation induced by wind effect. In addition, the dynamic tracer gas (measured), energy balance and stack and wind methods can be used to predict ventilation induced by the combined effects

Comparison study of the measured and calculated methods have shown that they were statistically significant differences, but if we consider the measured method only 60 - 70 % air change in one air exchange (Dufton *et al.* (1942), Hitchin *et al.* (1967) and Ducarme *et al.* (1994)), there is no significant difference between all the methods.

The neutral plane method is suggested to be used to calculate ventilation rate induced by stack effect in the tropics. This is because the method is simplest and cheapest, requiring only measuring the internal and external temperature. The energy balance method has advantages which providing many climatic and structure parameters that are important for crop production. In addition, the dynamic tracer gas gives direct measurement which is always referred by researchers. Apart from the tracer gas method, the direct air measurement can be used as a control method as it is

cheaper and easier to operate. However, the energy balance and tracer gas methods require extra instruments and costs.

Ventilation rate induced by the wind effect can be measured using the wind pressure transducers in the full scale structure and it requires some information on airflow characteristics that must be measured in the laboratory. However, direct measurement of airspeed at openings using air speed anemometers is more practical and easier than this approach.

The tracer gas method is preferred for calculating ventilation rate induced by the combination of stack and wind effects. However, when the wind speed is high, the rate of gas decay is also high and a special technique must be designed. The energy balance, and stack and wind methods can also be used provided the extra instruments are available.

[8] Experimental technique for control method

Natural ventilation rates induced by stack effect, wind effect, and combination of stack and wind effects for totally porous side wall structures have been difficult to quantify. This study has revealed a novel technique to set up the experiments by developing a full scale crop protection structure. This structure can be erected, dismantled and transferred to different sites according to the requirements of ventilation. In addition, a novel technique to overcome rapid tracer gas decay measurement for different insect screen opening areas was introduced. This has been done by covering the insect screen using a transparent polyethylene film while tracer gas was injected and then removed the film when gas was decaying. Tracer gas measurement in the highly porous structure is very difficult to measure because of the high air exchange rates and turbulent airflow.

[9] Airflow patterns inside the crop protection structure

The airflow patterns inside the crop protection structure caused by the stack and wind effects were also determined in this study. For the stack effect, it was found that the air entered through the bottom opening and left through the top opening. Some of the flow left above the neutral plane in the bottom opening if the neutral plane intersected this opening. However, for the wind effect, when the wind direction was perpendicular to the side wall, the windward and leeward of the structure became the air inlet and outlet respectively. For the top and bottom openings the air flowed straight from the inlet to the outlet and there was an anti-clockwise air circulation at intermediate levels. This information enhances the knowledge of natural ventilation in the crop protection structure. These patterns gives guidance to the designer on the location of ventilators in the structure to provide the optimum ventilation rate.

Recommendations for future research

It is suggested that future work should be carried out in actual tropical conditions to be more representative. The addition of extra spans may affect the present findings that are limited to a single span structure. The effect of a crop in the structure on the natural ventilation should be investigated because of the uncertain results found in the present study. The usage of screens for cladding the whole structure may be useful for leafy vegetable production in the tropics.

Final remarks

Finally, this thesis presents theoretical and experimental studies of a naturally ventilated crop protection structure for tropical conditions. It brings forward the existing natural ventilation knowledge that can be used to quantify natural ventilation

in the screened greenhouse. The objective of this study has been achieved with contribution of the knowledge on how to calculate natural ventilation induced by the stack effect, wind effect and combination of both stack and wind effects. In addition, the important parameters for ventilation rate calculation have been presented.

REFERENCES

Albright, L.D. (1978). Airflow through baffled, centre-ceiling and slotted inlets. *Transactions of the American Society of Agricultural Engineers*, 21(5), 944-952.

Albright, L.D. (1990). *Environment Control for animals and plants.* The American Society of Agricultural Engineers. An ASAE text book No 4, pp319-345.

Albright, L.D., Adre, N. and Rousseau, A. (1992). System characteristics graph as a basis for ventilation system. *American Society of Agricultural Engineers*, ASAE No. 92-4045.

Aldrich, R.A., Downs, R.J., Krizek, D.T. and Campbell, L.E. (1983). The effect of environment on plant growth. Ventilation of agricultural structures. *The American Society of Agricultural Engineers*, An ASAE text book No 6, 217-248.

ASHRAE (1985). *Natural ventilation and infiltration.* ASHRAE Handbook of Fundamentals, Chapter 22.

ASHRAE (1989). *Handbook of fundamentals. American Society of Heating and Air Conditioning Engineers.* Atlanta, GA.

Bailey, B. J. (1978*). Glasshouse thermal screens: air flow through permeable materials.* National Institute of Agricultural Engineering, England. Departmental Note No: DN/G/859/04013.

Bailey, B. J. (1981). The reduction of thermal radiation in glasshouses by thermal screen. *Journal of Agricultural Engineering Research*, 26, 215-222.

Bailey, B.J. (1978). *Glasshouse thermal screens: air flow through permeable materials.* National Institute of Agricultural Engineering, England. Departmental Note No: DN/G/859/04013. pp6.

Bailey, B.J. (1981). The reduction of thermal radiation in glasshouses by thermal screens. *Journal of Agricultural Engineering Research*, 26, 215-224.

Bailey, B.J., Graves, C.J. and Cockshull, K.E. (1993). Influence of wind speed and direction on the natural ventilation of a single span glasshouse. *Paper presented on the International Workshop on Cooling Systems for Greenhouses, Tel-Aviv, Israel, May 1993.*

Baker, J.R. and Shearin, E.A. (1994*). An update on screening for the exclusion of insect pests.* N.C. Flower Growers Bulletin, 39(2), 6-11.

Balemans, L (1988*). Assessment of criteria for energetic effectiveness of greenhouse screens.* Ph.D. Thesis, Ghent University, Belgium.

Bear J., and Bachmat, Y. (1990). *Theory and applications of transport phenomena in porous media*. Kluwer Academic Publishers, New York.

Benseman, R.F. and Hart, H.R. (1959). A thermocouple anemometer. *Journal of Scientific Instrumentation*, 32,145.

Berlinger, M., Mordechai, J.S. and Leeper, A. (1991). *Application of screens to prevent whitefly penetration into greenhouses in the Mediterranean basin*. Bull. IOBC/WPRS XIV (5), 105-110.

Boon, C.R. (1973). *Some aspects of the light transmission of glass and acrylic greenhouses*. National Institute of Agricultural Engineering, England. Departmental Note No: DN/C/388/1021.

Bot, G.P.A (1983). *Greenhouse climatic: from physical process to a dynamic model*. Ph. D. Thesis, Agricultural University of Wageningen, The Netherlands. pp 240.

Bot, G.P.A. and Van de Braak, (1995). *Greenhouse climate control: Physics of greenhouse climate*. Wageningen Pers. The Netherlands.

Bottcher, R.W. and Willits, D.H. (1987). Numerical computation of a two dimensional flow around and through a peaked-roof building. *Transactions of American Society of Agricultural Engineering*, 30(2), 469-475.

Bottcher, R.W., Willits, D.H. and Baughman, G.R. (1986). Experimental analysis of wind ventilation of poultry buildings. *Transactions of American Society of Agricultural Engineering*, 29(2), 571-578.

Boulard, T. and Baille, A. (1993). A simple greenhouse climate control model incorporating effects of ventilation and evaporative cooling. *Agricultural and Forest Meteorology*, 65, 145-157.

Boulard, T. and Baille, A. (1994). A simple greenhouse climate control model incorporating effects of ventilation and evaporative cooling. *Agricultural and Forest Meteorology*, 79, 61-77.

Boulard, T. and Baille, A. (1995). Modelling of air exchange rate in a greenhouse equipped with continuous roof vents. *Journal of Agricultural Engineering Research*, 61, 37-48.

Boulard, T. and Draoui, B. (1995). Natural ventilation of a greenhouse with continuous roof vents: measurements and data analysis. *Journal of Agricultural Engineering Research*, 61, 26-36.

Boulard, T., Kittas, C., Papadakis, G. and Mermier, M. (1998). Pressure field and airflow at the opening of a naturally ventilated greenhouse. *Journal of Agricultural Engineering Research*, 71, 93-102.

Boulard, T., Meneses, J.F., Mermier, M. and Papadakis, G. (1996). The mechanisms involved in the natural ventilation of greenhouses. *Agricultural and Forest Meteorology*, 79, 61-77.

Boulard, T., Meneses, J.F., Mermier, M. and Papadakis, G. (1997). *Characterising and modelling the air flow and temperature profiles in a closed greenhouse in diurnal conditions*. To be published.

Boulard, T., Papadakis, G. Kittas, C. and Mermier, M. (1997). Airflow and associated sensible heat exchanges in a naturally ventilated greenhouse. *Agricultural and Forest Meteorology*, 88, 111-119.

Boulard, T., Baille, A. and Draoui, B. (1993). Greenhouse natural ventilation measurements and modelling. *Acta Horticulture*. (in press) Special issue of the international workshop on cooling systems for greenhouses, Tel Aviv, 2-5 May 1993.

Bravo, F. P. and Morales, J.J. (1995). *Studies on a quonset type greenhouse in a tropical environment*. Instituto de Botanica Agricola, Facultad de Agronomia, Universidad Central de Venezuela, Apdo. 4579 Maracay, 21001 Aragua, Venezuela.

Breuur, J.J.G. and Short, T.H. (1985). Greenhouse energy demand comparisons for the Netherlands and OHIO, USA. *Acta Horticulturae*, 174, 145-153.

Brockett, B.L. and Albright, L.D. (1987). Natural ventilation in single airspace buildings. *Journal of Agricultural Engineering Research*, 37, 141-154.

Brown, W.G. (1962). Natural convection through rectangular openings in partitions. *International Journal of Heat and Mass Transfer*, 5, 869-878.

Brown, W.G. and Solvason, K.R. (1962).,Natural convection through rectangular openings in partitions. *International Journal of Heat Mass Transfer*, 5, 859-868.

Bruce, J.M. (1973). Natural ventilation by stack effect. *Farm Building Progress*, 32, 23-28.

Bruce, J.M. (1974/75). Natural ventilation of cattle buildings. *Journal of Farm Building Association*, 18, 48-55.

Bruce, J.M. (1975a). *A computer program for the calculation of natural ventilation due to wind*. Farm Building Research and Development Studies, Scottish, No. 7.

Bruce, J.M. (1975b). Natural Ventilation of cattle buildings by thermal buoyancy. *Farm Building Progress*, 42, 17-20.

Bruce, J.M. (1977a). *Natural ventilation - its role and application in the bio-climate system*. Farm Building Research and Development Studies, 8, 1-8.

Bruce, J.M. (1977b). *Natural ventilation. Farm Building Research and Development Studies*, 8,1-8.

Bruce, J.M. (1977c). *Thermal buoyancy.* Farm Building Research and Development Studies, 47: 23-25.

Bruce, J.M. (1982). Ventilation of a model livestock building by thermal buoyancy. *Transaction of the American Society of Agricultural Engineers*, 25(6), 1724-1726.

Bruce, J.M. (1978). Natural ventilation through openings and its application to cattle building ventilation. *Journal of Agricultural Engineering Research*, 23, 151-167.

Brundrett, E. (1993). Predication of pressure drop for incompressible flow through screens. *Journal of Fluids Engineering*, 115, 239-242.

Businger, J.A. (1963). *The glasshouse (greenhouse) climate.* Physics of plant Environment, North-Holland, Amsterdam, 277-318.

Campbell, G.S. and Unsworth, M.H. (1970). An inexpensive sonic anemometer for eddy correlation. *Journal of Applied Meteorology*, 18, 1027-1077.

Carpenter, G.A., Moulsley, L.J. and Boothroyd, D.N. (1973*). The resistance to airflow of some materials used for ventilation in agriculture.* National Institute of Agricultural Engineering, England. Departmental Note: DN/FB/235/3020.

Carpenter, G.A., Moulsley, L.J. and Boothroyd, D.N. (1973*). The resistance to airflow of some materials used for ventilation in agriculture.* National Institute of Agricultural Engineering, England. Departmental Note, DN/FB/235/3020.

Chiapale J.P., Kittas, C. and De Villele, O. (1981). Estimation regionale des besoins de chauffage des serres . *Acta Horticulturae*, 115, 493-502.

Coppin, P.A. and Taylor, K.J. (1983). A three-component sonic anemometer/thermometer system for general micro meteorological research. *Boundry-Layer Meteorol.*, 27, 27-42.

CP 3: Basic data for the design of buildings, Ch V: Loading, Part 2. Wind loads. British Standards Institution London 1972. pp55.

Dalziel, S.B. (1993). Rayleigh-Taylor instability: experiments with image analysis: *Dyn. Atmos. Occans.*, 20, 127-153.

De Halleux, D. (1989). *Modele dynamique des echanges energetiques des serres: etude theorique et experimentale.* Ph. D. Dissertation, Faculte des Sciences Agronomiques de Gembloux, Belgique. pp278.

De Jong, T. (1990). *Natural ventilation of large multi-span greenhouses.* Ph. D. Thesis, Agricultural University of Wageningen, The Netherlands, pp116.

De Jong, T. and Bot, G.P.A. (1992). Flow characteristics of one-side-mounted windows. *Energy and Building*, 19, 105-112.

Deltour, J., De Halleux, D., Nijskens, J., Coutisse, S. and Nisen, A. (1985). Dynamic modelling of heat and mass transfer in greenhouses. *Acta Horticulturae*, 174, 119-126.

Down, M. J., Foster, M.P. and McMohan, T.A. (1990). Experimental verification of a theory for ventilation of livestock buildings by natural convection. *Journal of Agricultural Engineering Research*, 45, 269-279.

Draper, N.R. (1998). *Applied regression analysis*. 3rd ed, John Wiley and Sons, USA, pp 726.

Ducarme, D., Vandaele, L. and Wouters, P. (1994*). Single sided ventilation: a comparison of the measured air change rates with tracer gas and with the heat balance approach.* Documentation for BAG meeting on ventilation related aspects in buildings, 26-35.

Dufton, A.F. and Marley, W.G. (1942). The comparison of heating systems. *J. Instn Heat. Vent. Engrs*, 10, 17.

Dufton, A.F. and Marley, W.G. (1942). The comparison of heating systems. *JIHVE*, 10, 17-64.

Duncan, G.A. and Hamilton, H.E. (1969). *Ventilating farm buildings part III; Systems types and features*. Kentucy Agricultural Engineers, pp 8-10.

Emswiler, J.E. (1962). The natural zone in ventilation. ASHVE Trans., 32: 59-74.
Ergun S. (1952). Fluid flow through packed columns. *Chemical Engineering Progress*, 48, 89-94.

Fernandez, J.E. and Bailey, B.J. (1992). Measurement and prediction of greenhouse ventilation rates. *Agricultural and Forest Meteorology*, 58, 229-245.

Fernandez, J.E. and Bailey, B.J. (1993). Predicting greenhouse ventilation rates. *Acta Horticulturae*, 328, 107-114.

Feuilloley P., Mekikdjian, C.H. and Lagier, J. (1994*). Natural ventilation of plastics tunnels greenhouses in the Mediterranean.* Plasticulture, No:104, 33-46.

Garzoli, K.V. and Blackwell, J. (1981). An analysis of the nocturnal heat loss from a single skin plastic house. *Journal of Agricultural Engineering Research*, 26(39), 204-214.

Geodhart, M., Nederhoff, E.M., Udink Ten Cate, A.J. and Bot, G.P.A (1984). Methods and instruments for ventilation rate measurements. *Acta Horticulturae*, 148, 393-400.

Hawa, J. and Rezuwan, K. (1990). Performance and feasibility of high value vegetable cultivation under rainshelters. *Special report presented at MARDI scientific Council Meeting, No. 66, 17 Dec. 1990. Serdang. Malaysia.* pp40.

Hawa, J., Embi, Y. and Rezuwan, K. (1992). *Vegetable Cultivation under simple rainshelters in Malaysia.* Food and Fertiliser Technology Centre. Teipei City, Republic of China on Taiwan. Extension Bulletin No. 350.

Hitchin, E.R. and Wilson, C.B. (1967). A review of experimental techniques for the investigation of natural ventilation in buildings. *Build. Sci.*, 2(1), 59-82.

Hoxey, R.P. and Richardson, G.M. (1981). *Full-scale measurements of the wind loads on film plastic clad greenhouses: single span 6.3 m x 24.4 m semi-circular 'tunnel' greenhouse.* National Institute of Agricultural Engineering, England. Departmental Note No: DN 1073.

Hoxey, R.P. and Richardson, G.M. (1984). Measurements of wind loads on full-scale film plastics clad greenhouse. *Journal of Wind Engineering and Industrial Aerodynamics*, 16,57-83.

Hoxey, R.P. and Wells, D.A. (1974). Instrumentation for full-scale wind load measurement on glasshouses. Research notes. *Journal of Agricultural Engineering Research*, 19, 435-438.

Hoxey, R.P and Moran, P. (1991). *Full-scale wind pressure and load experiments - Multispan 167x111 m glasshouse (venlo).* National Institute of Agricultural Engineering, England. Departmental Note No: DN 1594. pp11.

Hsu, C. and Cheng, P. (1990). Thermal dispersion in a porous medium. International *Journal of Heat and Mass Transfer*, 33, 1587-1597.

Hunt, G.R. and Linden, P.F. (1997a) *The fluid mechanics of natural ventilation-displacement ventilation by buoyancy-driven flows assisted by wind.* A paper produced by Department of applied Mathematics and Theoretical Physics, University of Cambridge, Silver Street, Cambridge, CB3 9EW, UK. Building and Environment (in press).

Hunt, G.R. and Linden, P.F. (1997b). Laboratory modelling of natural ventilation flows driven by the combined forces of buoyancy and wind. *CIBSE National Conference 1997*, 101-107.

Hurd, R.G. and Sheard, G.F. (1981*). Fuel saving in greenhouses: the biological effects.* Guide No. 22, Grower Books, London, 1-53.

Illias, M.K., Ramli, M.N. and Hawa, J. (1990*). Rainshelters for vegetables. Vegetables Technology.* MARDI 6: 1-6. (In Bahasa Malaysia with English abstract).

Illias, M.K., Rezuwan, K. and Tengku Ariff, T.A. (1994). *Production of temperate vegetable under insect-proofed rainshelter in the lowlands.* MARDI Technology, Kuala Lumpur, Malaysia.

Illias, M.K., Rezuwan, K., Hawa, J. and Mohd Khairol, M.A. (1992). High-value vegetable production under rainshelter. *Presented at MARDI Senior Staff Conference, Hilton Kuala Lumpur. Malaysia.*

Izumi, Y. and Barad, M.L. (1970). Wind speeds as measured by cup and sonic anemometers and influenced by tower structure. *Journal of Applied Meteorology*, 9, 851-856.

Jolliet, O.J., Gay, J. B., Bourgeois, M., Danloy, L., Brelton, J., Mantilleri, S., Resist A. and Moncousi C. (1985). Solar gains and thermal rejects by ventilation. *Acta Horticulturae*, 174,127-134.

Jolliet, O. (1991). HORTICERN: a model for predicting and optimising humidity and transpiration in greenhouses. *Journal of Agricultural Engineering Research*, 57, 23-37.

Jolliet, O. (1991). Horticern: An improved static model for predicting the energy consumption of a greenhouse. *Agricultural and Forest Meteorology*, 55, 265-294.

Jolliet, O. and Bailey, B.J. (1994) The effect of climate on tomato transpiration in greenhouses: measurements and models comparison. *Agricultural and Forest Meteorology*, 58,43-62.

Kaimal, J.C. and Businger, J.A. (1963). A continuous wave sonic anemometer-thermometer. *Journal of Applied Meteorology*, 2, 156-164.

Kelly, T.G., Dodd, V.A. and Ruane, D.J. (1986). Ventilation and air flow patterns in climatic calf houses. *Journal of Agricultural Engineering Research*, 33, 187-203.

Kinddelan, H. (1980). Dynamic modelling of greenhouse environment. *Transaction of the American Society of Agricultural Engineers*, 23, 1232-1231.

Kittas, C., Boulard, T. and Papadakis, G. (1996). Natural ventilation of a greenhouse with ridge and side openings: Sensitivity to temperature and wind effects. *Transaction of the American Society of Agricultural Engineers*, 40(2), 415-425.

Kittas, C., Boulard, T., Mermier, M. and Papadakis, G. (1996).Wind induced air exchanges rates in a greenhouse tunnel with continuous side openings. *Journal of Agricultural Engineering*, 65, 37-49.

Kittas, C., Draoui, B. and Boulard, T. (1995). Quantification of the ventilation of a greenhouse with a roof opening. *Agricultural and Forest Meteorology*, 77, 95-111.

Kittas, C. and Baille, A. (1998). Determination of the spectral properties of several greenhouse cover materials and evaluation of specific parameters related to plant response. *Journal of Agricultural Engineering Research*, 71, 193-202.

Kosmos, S.R., Riskowski, G.L. and Christianson, L.L. (1993). Force and static pressure resulting from airflow through screens. *Transactions of the American Society of Agricultural Engineers*, 36(5), 146-1472.

Kozai, T. and Sase, S. (1978). A simulation of natural ventilation for a multi-span greenhouse. *Acta Horticulturae*, 87, 339-349.

Kozai, T., Sase, S. and Nara, M. (1980). A modelling approach to greenhouse ventilation control. *Acta Horticulturae*, 106, 125-136.

Krishnasswamy, N. (1963) A hot-wire micro anemometer. *J. appl. Physiol.*, 20, 297.

Lane-Serff, G.F. (1989). *Heat flow and air movements in buildings*. Ph.D. Thesis, University of Cambridge, United Kingdom.

Lawrence, W.J.C. (1948). *Science and the glasshouse*. Oliver & Boyd, Edinb., 2nd Edition.

Lebon, G. and Cloot, A. (1986). A thermodynamically modelling of fluid flows through porous media: application to natural convection. *International Journal of Heat and Mass Transfer*, 29, 381-390.

Lee, K. B. (1986). *Heat and mass transfer in highly porous media*. Ph.D. Thesis, University of Texas at Austin, USA,

Malaysian Meteorology Department (1996). *Weather forecast report*, Kuala Lumpur, Malaysia.

Miguel, A.F., Van de Braak, N.J., Silva, A.M. and Bot, G.P.A. (1998). Free-convection heat transfer in screened greenhouses. *Journal of Agricultural Engineering Research*, 69, 133-139.

Miguel, A F., Van de Braak, N. J., Silva, A. M. and Bot, G. P. A. (1997) *Forced fluid motion through openings and pores*. Building and Environment (in press).

Miguel, A. F., Van de Braak, N. J. and Bot, G. P. A. (1997). Analysis of the airflow characteristic of greenhouse screening Materials. *Journal of Agricultural Engineering Research*, 67, 105-112.

Miguel, A.A.F. (1998). *Transport Phenomena through porous screens and openings: from theory to greenhouse practice*. Ph. D. Thesis. Agricultural University of Wageningen, The Netherlands. pp129.

Mistriotis, A., Bot, G.P.A., Picuno, P. and Scarascia, G. (1997). Analysis of the efficiency of greenhouse ventilation using computational fluid dynamics. *Agricultural and Forest Meteorology*, 85, 217-228.

Mistriotis, A., De Jong T.M., Wagemans, M.J.M. and Bot, G.P.A. (1997). Computational Fluid Dynamics (CFD) as a tool for the analysis of ventilation and

indoor microclimate in agricultural buildings. *Netherlands Journal of Agricultural Sciences*, 45, 81-96.

Mitsuta, Y. (1966). Sonic anemometer thermometer for general use. *Journal of. Meteorology Society*, Japan, 44, 12-24.

Montero, J.I., Munoz, P. and Anton, A. (1997). Discharge coefficients of greenhouse windows with insect-proof screens. *Acta Horticulturae*, 443, 71-77.

Montero, J.I. (1998). *Personal communication and unpublished diagram of airflow distribution inside the crop protection model induced by stack effect.*

Montero, J.I. and Bailey, B.J. (1998*) Personal communication and unpublished diagram of airflow distribution inside the crop protection structure induced by wind effect.*

Morris, L.G. (1964). *The heating and ventilation of greenhouses.* National Institute of Agricultural Engineering, Wrest Park, Silsoe, England.

Morris, L.G and Neale, F.E. (1954). *The infrared carbon dioxide gas analyser and its use in glasshouse research.* National Institute of Agricultural Engineering, Wrest Park, Silsoe, England.

Mousley, L.J., Randall, J.M., Hartshorn, R.L., Houghton, C.J. and Randle, D.G. (1987). *Facilities for measuring fan performance.* DN 1408 AFRC Institute of Engineering Research, WrestPark, Silsoe, Bedford. England.

Nederhoff, E.M., Van De Vooren, J. and Udink Ten Cate, A.J. (1984). A method to determine ventilation in greenhouse. *Acta Horticulturae*,148, 345-350.

Nederhoff, E.M., Van de Vooren, J. and Udink Ten Cate, A.J. (1985). A practical tracer gas method to determine ventilation in greenhouses. *Journal of Agricultural Engineering Research*, 31, 309-319.

Nijskens, J., Deltour, J., Coustisse, S., and Nisen, A. (1985). Radiation transfer through covering materials, solar and thermal screens of greenhouses. *Agricultural and forest Meteorology*, 35, 229-242.

Oca, J., Montero, J.I., Anton, A. and Crespo, D. (1998). *A method for studying natural ventilation by thermal effects in a tunnel greenhouse using laboratory scale models.* A paper produced by Escola Superior d'Agricultura de Barcelona.c/Urgell 187. 08036 Barcelona. Spain. pp27.

Okada, M. and Takakura, T. (1973). Guide and data for greenhouse air conditioning: 3. Heat loss due to air infiltration of heated greenhouses. *Journal of Agricultural Meteorology*, 28(4), 223-230.

Papadakis, G., Mermier, M., Meneses, J.F. and Boulard T. (1996). Measurement and analysis of air axchange rates in a greenhouse with continuous roof and side openings. *Journal of Agricultural Engineering Research*, 63, 219-228.

Pieters, J. G., Deltour, J. M. and Debruyckere, M.J. (1994) Condensation and static heat transfer through greenhouse covers during night. *Transaction of the American Society of Agricultural Engineers*, 37(6), 1965-1972.

Pieters, J.G., Deltour, J.M. and Debruyckere, M.J. (1996). Condensation and Dynamic Heat Transfer in Greenhouses. Part 11: Results for a Standard Glasshouse. *International Agricultural Engineering Journal*, 5(3/4), 135-148.

Pieters, J.G., Deltour, J.M. and Debruyckere, M.J. (1996). Condensation and Dynamic Heat Transfer in Greenhouses. Part 1: Theoretical Model. *International Agricultural Engineering Journal*, 5(3/4), 119-133.

Randall, J.M. (1973*). Air distribution in a full scale section of a livestock building - Part 1.* National Institute of Agricultural Engineering, England. Departmental Note: DN/FB/319/3020.

Rault, P.A. (1990). A tunnel greenhouse adapted to the tropical lowland climate. Second workshop on greenhouse construction and design. *Acta Horticulturae*. 281, 95-103.

Redding, G.I. (1981). *Functional Design Handbook for Australian Farm Buildings*. Univ. of Melbourne. pp 72-77.

Rezuwan, K. (1995). Insect-proofed rainshelter structures for temperate vegetables production in the lowlands. *Presented at Malaysian Sciences and Technology Congress, Kuala Lumpur, Malaysia.*

Roberts, W.J., Vasvary, L. and Kania, S. (1995). Screening for insect control in mechanically ventilated greenhouses. American Society of the Agricultural Engineers, Paper No. 95-4541. *St. Joseph, Michigan. International Conference, June 1-4, 1995, Uppsala, Sweden.*

Robertson, A.P. and Hoxey, R.P. (1992). *Structural design of greenhouses with an emphasis on wind loading.* REUR Technical Series 25 (FAO). pp 17-41.

Ross, D.S. and Gill, S.A. (1994). *Insect screening for greenhouses.* Information Facrs. Facts 186. College Park, Md., University of Maryland.

Russell, R. W. J. (1985). An analysis of the light transmittance of twin-walled materials. *Journal of Agricultural Engineering Research*, 31, 31-53

Ruther, M. (1985). Natural ventilation rates of closed greenhouses. *Acta Horticulturae*, 170, 185-191.

Sakurai, K., Nara, M., Sase, S. and Murakami, L. (1985). Wind pressure and velocity on windbreak screens (In Japanese). *In Abstracts of Annual Meeting of the Japanese Society of Irrigation, Drainage and Reclamation.* pp 338-339.

Sase, S and Christianson, L.L. (1990). *Screening greenhouses - Some engineering considerations.* American Society of the Agricultural Engineering. Paper No. NABEC 90-201.

Sase, S. and Nara, M. (1985). A control algorithm for natural ventilation based on tunnel testing. *Acta Horticulturae*, 174, 75-80.

Sase, S., Takakura, T. and Nara, M. (1984). Wind tunnel testing on airflow and temperature distribution of a naturally ventilated greenhouse. *Acta Horticulturae*, 148, 329-336.

Seginer, I. (1994). Tranpirational cooling of a greenhouse crop with partial ground cover. *Agricultural and Forest Meteorology*, 71, 265-281.

Seginer, I. and Kantz, D. (1989). Night-time use of dehumidifiers in greenhouses: an analysis. *Journal of Agricultural Engineering Research*, 39, 19-37.

Seginer, I., Boulard, T. and Bailey, B.J. (1993). Neural network models of the greenhouse climate. Paper No. 93 4578, *American Society of the Agricultural Engineers, Winter Meeting, December 11-14, Chicago, USA.*

Shaw, B.H. (1971). Heat and mass transfer by natural convection and combined natural convection and forced air flow through large rectangular openings in a vertical partition. I. Mech. Eng. *Symposium on Heat and Mass Transfer by combined forced and natural convection, 15 September 1971*, pp31-39.

Shaw, B.H. and Whyte, W. (1974). Air movement through doorways-the influence of temperature and its control by forced airflow. *Building Services Engineer.* 42, 210-218.

Sherman, M.H. and Grimsrud, D.T. (1980). Infiltration-pressurisation correlation: simplified physical modelling. *Transactions of the American Society of Agricultural Engineers*, 86, 778-807.

Sherman, M.H. (1990). Tracer-gas techniques for measuring ventilation in a single zone. *Building and Environment*, 25(4), 365-374.

Sherman, M.H. and Grimsurd, D.T., (1980). Infiltration-pressurisation correlation: simplified physical modelling. American Society of Heating, Refrigerating and Air-Conditioning Engineers, *Transaction ASHRAE*, 86(2), 778-807.

Simmons, L.F.G. (1949). A shielded hot-wire anemometer for low speeds. *J. Sci. Instr.* 26, 407-411.

Smith, S.D. (1980). Evaluation of the mark 8 thrust anemometer-thermometer for measurement of boundry-layer turbulence. *Boundry-Layer Meteorol.*, 19, 273-292.

Stone, G.E. (1913). *The relation of light to greenhouse culture.* Bull. 144, Mass. Agric. Exp. Sta..

Suomi, V.E. (1957). *Energy budget studies and development of the sonic anemometer for spectrum analysis.* AFCRC Tech. Rep. 56-274, Univ. Wisconsin, Dept. Meteorol., pp91.

Takakura, T., Jordan, K.A. and Boyd, L.L. (1971). Dynamic simulation of plant growth and environment in the greenhouse. *Transaction of the American Society of Agricultural Engineers*, 14, 955-964.

Tanner, C.B. (1963). *Basic instrumentation and measurements for plant environmental micrometeorology.* Univ. of Wisconsin., Madison, Dep. of Soil Science. Soil Bull. No. 6.

Teitel, M. and Shklyar, A. (1998). Pressure drop across insect-proof screens. *Transaction of the American Society of the Agricultural Engineers*, 41(6), 1829-1834.

Timmons, M.B., Bottcher, R.W. and Baughman, G.R. (1984). Monographs for predicting ventilation by thermal buoyancy. *Transactions of the American Society of Agricultural Engineers*, 1891-1893.

Timmons, M.B. and Baughmam, G.R. (1981). Similitude analysis of ventilation by the stack effect from an opening ridge livestock structure. *Transactions of the American Society of Agricultural Engineers*, 24(4), 1030-1034

Van Bavel, C.H.M., Damagnez, J. and Sadler, E.J. (1981). The fluid-roof solar greenhouse: energy budget analysis by simulation. *Agricultural Meteorology*, 23, 61-76.

Van de Braak, N.J. (1995). Heating equipment, in: Bakker J.C., Bot G.P.A., Challa H. and Van de Braak N.J. (Eds.), *Greenhouse Climate Control.* Wageningen Press, Wageningen. pp. 171-179.

Vladimirova, S. V., Bucklin, R. A. and Mc Connel, D. B. (1996). Influence of shade level, wind velocity, and wind direction on interior air temperature of model shade structures. *American Society of the Agricultural Engineers*, 39(5), 1825-1830.

Walker, J.N. (1965). Predicting temperatures in ventilated greenhouses. *Transactions of the American Society of Agricultural Engineers*, 8, 445-448.

Walker, J.N., Aldrich, R.A. and Short, T.H. (1983). *Quantity air flow for greenhouse structures. Ventilation of agricultural structures.* An ASAE monograph number 6. The American Society of Agricultural Engineers, 257-276.

Wang, S. (1998). *Measurement and modelling of natural ventilation in a large venlo-type greenhouse*. Ph. D. Thesis. Faculte Universitaires Des Sciences, Agronomiques De Gembloux. pp208.

Wang, S. and Deltour, J.M. (1996). An Experimental Ventilation Function for Large Greenhouses Based on a Dynamic Energy Balance Model. *International Agricultural Engineering Journal*. 5(3/4), 102-112.

Wang, S. and Deltour, J.M. (1997) Natural ventilation induced airflow patterns measured by an ultrasonic anemometer in venlo-type greenhouse openings. *International Agricultural Engineering Journal*, 6(3&4), 186-196.

Wang, S., Cui, S., Deltour, J. and Nijskens, J. (1993). Dynamic simulation of temperatures and fluxes in greenhouse. *Journal of Zhejiang Agricultural University*, 19(2), 159-162.

Wang, S., Deltour, J., Nijskens, J. and De Wergifosse, P.H. (1990). *Exact analytical solution of a linear dynamic model of greenhouse climate: the direct cover case*. Bull. Rech. Agron. Gemblux, 25 (4), 489-518.

Whittle, R.M. and Lawrence, W.J.C. (1959). The climatology of glasshouse. *Journal of Agricultural Engineering Research*, 4(4).

Whittle, R.M. and Lawrence, W.J.C. (1960).The climatology of glasshouses:II. Ventilation. *Journal of Agricultural Engineering Research*, 5: 36-41

Winspear, K.W. (1977). Vertical temperature gradients and greenhouse energy economy. *Acta Horticulturae*, 76, 97-103.

Wiren, B.G. (1983). Effects of surrounding buildings on wind pressure distributions and ventilate heat losses for a single family house. *Journal of Wind Engineering and Industrial Aerodynamics*, 15, 15-26.

Wolfe, J.S., Winspear, K.W. and Cotton, R.F. (1972). *Studies of air flow in glasshouses with fan ventilation*. National Institute of Agricultural Engineering, England. Departmental Note: DN/G/223/2102.

Wyngaard, J.C. (1981). Cup, propeller, vane and sonic anemometer in turbulence research, *Rev. Fluid Mech.*, 13, 399-423.

Yeoh, K.C. (1992). *Design and construction of rainshelters*. Taipei City Centre. Teipei City, Republic of China on Taiwan. Extension Bulletin No. 350.

Zhang, J.S., Janni, K.A. and Jacobson, L.D. (1989). Modelling natural ventilation induced by combined thermal buoyancy and wind. *Transactions of the American Society of Agricultural Engineers*. 32 (6), 2165-2174.